RELATIONSHIP BETWEEN FROTH BEHAVIOUR AND THE PROPERTIES OF PARTICLES

A THESIS SUBMITTED

TO THE UNIVERSITY OF CAPE TOWN IN FULFILLMENT OF THE REQUIREMENTS FOR THE DEGREE OF

MASTER OF SCIENCE IN ENGINEERING (CHEMICAL ENGINEERING)

BY

DITEND KANYIK TESH

B. Eng Metallurgical Engineering (University of Lubumbashi)
B-Phil: Sustainable dev. Plan & Management (Stellenbosch University)

UNIVERSITY OF CAPE TOWN
CENTRE FOR MINERALS RESEARCH

DEPARTMENT OF CHEMICAL ENGINEERING

December 2011

DECLARATION

I hereby certify that this thesis is the result of my own work and has not been submitted prior to this for any higher degree to any other university or institution. I know the meaning of plagiarism and declare that all the work in the document, save for that which is properly acknowledged, is my own.

_____

Ditend K Tesh

ACKNOWLEDGEMENT

I would like to thank my supervisors, Professor Jean-Paul Franzidis and Mr. Martin Harris, for their patience and invaluable guidance throughout this project.

My sincere gratefulness to the following people and institutions:

- The AMIRA P90 project and the CMR deserve special mention as without their funding and assistance this project would have not been possible.
- Dr Victor Ross and Mr Allen Hemphill from Lonmin PLC. Without their help, access to site and the completion of important tasks of this project would have been difficult.
- Mr. Roger Amelunxen and Professors Janusz Laskowski and Tim Napier-Munn for assistance during interpretation of the results.
- Messrs Bill Randall, Peter Dobias and Kenneth Maseko for their assistance in the modifications of the experimental apparatus used in this project.
- Drs Sam Morar and Megan Becker for their unconditional willingness to give assistance when required.
- My parents, Pastor Kanyik Tesh and Mankand A Ditend for being always there for me.
- George Phiri, Isabelle and Martin Tshipuk, Astrid and Chiyey Tesh, Kamij Nicole, Heidi and Muzemb Kanyik, Nkongal Tesh, Kalong Tesh, Kaj Tesh, Rachel and Jeff Nguza Kakoma, Papy Kona, Matoto Lenge... for their support and encouragement.
- Last but not least my wife Nadine A Mwez and my children for their patience, love and encouragement. Your love and support gave me the strength to go until the end!

ABSTRACT

The aim of this project was to gain an insight into how the properties of particles entering the froth affect the performance of the froth phase. In platinum group mineral (PGM) flotation, gangue minerals are known to have a stabilizing effect on the froth phase; in this project, their hydrophobicity was changed by the addition of depressant and the performance of the froth phase was measured in terms of froth recovery. A column cell was used in all the tests, because columns can be run continuously, allowing a wider range of froth depths to be investigated and allowing for enhanced detection of froth effects.

The first part of the experimental work was performed in the laboratory at UCT, using Merensky ore. An experimental procedure was developed which allows the study of the interaction between the froth and the pulp phases. In this procedure, the column is run continuously while changing the flotation conditions. The procedure allows the study of the effect of any flotation parameter (e.g. collector type and dosage, depressant type, feed size...) on flotation performance. The results showed that the UCT method can be used on a continuously run column flotation cell. The UCT method allows the contribution to the concentrate of selectively attached (true flotation) and entrained particles to be determined separately. This procedure was initially developed for batch flotation tests.

The site tests were carried out on a UG2 ore at the Lonmin Karee K3 flotation plant, to investigate the effect of depressant dosage on the froth performance on the gangue and the PGMs. The UCT method was used to predict recovery by entrainment. A second technique using Cr2O3 as a tracer confirmed the accuracy of the UCT entrainment predictions. This is a significant finding as, previously, the UCT method had not been applied on a continuously-run column flotation cell.

The results showed that as the depressant dosage or the froth height was increased, water and total solids recoveries in the concentrates decreased. This could be attributed mostly to a decrease in recovery by entrainment, especially of gangue minerals, although PGM recovery by entrainment also decreased. For the runs operated at constant froth height more PGM were recovered by true flotation when the depressant dosage increased. For the runs operated in the absence of depressant PGM recoveries by true flotation remained fairly constant, indicating that the froth was stable even at the highest froth height used (12 cm).

An important outcome of this project is the remarkable difference in the recoveries of the gangue minerals and the PGMs, at the different conditions studied. The combined effect of increasing the depressant dosage and the froth height caused the recoveries of the gangue minerals to drop to below 1%, while the PGM recoveries remained high, even at 500 g/t depressant dosage and 12 cm froth height.

One of the more significant findings to emerge from this study is that froth recovery of both gangue minerals and PGMs is linearly proportional to froth height. Froth zone recovery Rf was found to be strongly linked to particle properties entering the froth: when the depressant dosage was increased, froth recoveries of both gangue minerals and PGM were affected negatively. This confirms that particle properties (depressant) critically affect froth stability, which was found to be proportional to floatable solids content in the froth phase.

In froth flotation, an increase in grade is generally known to result in loss in recovery. This project showed that working at moderate air rate resulted in very high PGMs grade, while avoiding a loss in recovery. A possible reason for this is the low air flow rates employed in these tests, because of the phenomenon of pulp/froth interface vanishing observed during site tests. This result is useful and should be investigated further in future tests.

GLOSSARY

SIBX	Sodium-isobutyl-xanthate supplied by Senmin
Depramin 267	a commercial carboxy-methyl cellulose supplied by Akzo Nobel
PGM	Platinum Group Minerals
PGE	Platinum Group Elements
SIBX	Sodium-isobutyl-xanthate supplied by Senmin
SNPX	Sodium Normal Propyl Xanthate
Sasfroth 200	A commercial frother supplied by Senmin
UG-2	Upper Group 2
Sendep 369	A guar gum depressant supplied by Senmin
CMR	Centre for Mineral Research
k_c	Zone rate constant
k	First order rate constant
R_f	Froth recovery
UCT	University of Cape Town
CMR	Centre for Minerals Research

TABLE OF CONTENTS

LIST OF TABLES

LIST OF FIGURES AND PICTURES

CHAPTER ONE: INTRODUCTION

1.1 BACKGROUND

Froth performance in flotation is affected by many parameters. One of the most important of these is the hydrophobicity of particles. Past researchers (Klassen and Mokrousov, 1963; Dippenaar, 1982 a, b; Johansson and Pugh, 1992; Schwarz, 2004; Aktas et al., 2008) have recognized that moderately hydrophobic particles (both gangue and valuable minerals) stabilize froths, while highly hydrophobic particles have a destabilizing effect instead. The hydrophobicity of particles can be changed by the addition of collectors or depressants. The first are used to increase the hydrophobicity of valuable minerals, while the second are used to decrease the hydrophobicity of floatable gangue minerals.

The aim of this thesis is to develop a strategy to study the interaction between the froth performance and the properties of the particles entering the froth zone. The strategy will be developed in the laboratory and then trialed on an operating flotation plant. The study will be applied to the flotation of PGM ores: the work arises from the concern in the PGM industry that the use of high depressant dosage will destabilize the froth phase, leading eventually to loss of PGMs.

In platinum flotation, the concentration of platinum group minerals (PGMs) is low; most of the particles in the froth are naturally floatable gangue minerals, which have a stabilizing effect on the froth (Martinovic et al., 2005). The addition of *depressant* to improve the concentrate grade by removing these particles from the froth has the unwanted side effect of making the froth less stable, potentially impacting severely on the recovery of PGMs (Bradshaw et al., 2005b). The choice of *collector* also affects the stability of the froth phase: adding a strongly hydrophobic collector such as sodium isobutyl xanthate (SIBX) has been found to have a destabilizing effect on the froth (Bradshaw et al., 2005a; Wiese et al., 2006a). Thus platinum ore is a good case study of the interaction between the pulp and the froth phases in flotation.

It should be remembered that, in froth flotation, mineral particles are recovered into the concentrate in two ways: by true flotation and by entrainment. True flotation is the desired mode of separation, whereas entrainment is unwanted, because it is non-selective and reduces the concentrate grade. True flotation involves the recovery of particles attached selectively to bubbles, while entrainment is the recovery of unattached particles that report to the concentrate in the water trapped between the bubbles. Hydrophobic and hydrophilic particles are affected equally by entrainment, but for gangue minerals, entrainment is usually the more important method of recovery, because of the greater proportion of gangue in the ore.

Thus, any attempt to improve the understanding of the effect of particle properties on flotation froths or to study the interaction between the pulp and the froth phases in flotation, particularly in the flotation of PGMs ores, should include the determination of the *separate* contributions made to the concentrate by true flotation and entrainment. In the past this has been difficult to do, and has required the presence (or addition) of a non-floatable tracer mineral in the feed to measure entrainment (Lynch et al., 1981; Savassi et al., 1998). Recently, however, the Centre for Minerals Research (CMR) at the University of Cape Town (UCT) has developed a technique, based on laboratory batch flotation cells, which allows the contribution to the concentrate of selectively attached (true flotation) and entrained particles to be determined separately (Oostendorp et al., 2005a, b; Wiese et al., 2005). This method is ideally suited to the study of the interaction between the pulp and the froth phases in flotation.

In the UCT method, batch tests are performed at increasing depressant dosages. When the mass recovery drops no further with increasing depressant dosage, and is related linearly with water recovery, it is assumed that all the gangue recovered to the concentrate is by entrainment only. This is used as a calibration, and means that the amount of floatable gangue can be found at any depressant dosage by subtracting the entrained gangue recovery from the total gangue

recovery (see Chapter 2 for more details). It should be noted that to date this method has been applied only to batch laboratory flotation cells and not to column cells.

Froth performance is an important contributor to overall flotation performance, because the froth determines the amount of material that goes to the concentrate (recovery) and its quality (grade). Historically, froth performance has been measured in several ways. The most common indicators include concentrate recovery, grade and enrichment ratio; froth stability; water recovery; froth structure and froth recovery. Concentrate recovery, grade and enrichment ratio are the most used indicators of froth performance, probably because they are easy to measure. Other indicators are more difficult to measure but provide insights into froth performance.

Froth stability is known to play an important role in flotation performance although its measurement remains a major challenge. Bikerman (1973) made the first attempt in measuring foam stability by observing the rate of foam breakdown from an equilibrium height in a sparged column. Since then, various types of froth stability measurement have been developed based on the Bikerman approach (e.g. Barbian et al., 2003; Tsatouhas et al., 2006). Some of these methods have been used to measure the froth stability during plant operations (e.g. Barbian et al. 2005, Ventura-Medina et al., 2003, Barbian et al., 2006). However, they will not be considered for this thesis because they have the potential to interfere with small scale flotation tests.

Water flow rate in the concentrate can also be used as an indicator of froth stability; this is justified by the fact that the stability of the froth phase is determined by the stability of the liquid lamellae between gas bubbles, which in turn affects the froth water content (Ekmekci et al., 2006). Various workers have used water recovery to quantify froth stability (e.g. Tao et al., 2000; Wiese et al.,

2005; Oostendorp et al., 2005a, b; Bradshaw et al., 2005 b), and it will be one of the measures used in this thesis.

Froth surface structure is emerging as a useful descriptor of froth performance, as measured using machine vision systems (Banford et al., 1998; Barbian et al., 2006, Sweet, 2000, Francis, 2001; Hatfield et al., 2003). A machine vision system for froth flotation typically consists of a light pointing directly at the froth surface and a video camera capturing footage of the top of the froth. The video footage is processed using image analysis software and returns a variety of measurements. In the case of the SmartFroth® system developed at UCT (Forbes, 2005) these measurements include the surface bubble size distribution, described by the mean, median, minimum, maximum, 20^{th} and 80^{th} percentiles of the distribution, as well as by the area weighted bubble size; and a number of froth stability factors (such as the *stability correlation peak*). There are currently some machine vision systems being used on flotation plants, e.g. the Metso system at Kennecott and JKFrothCam (JKMRC) at Escondida, (Heinrich, 2003). The UCT SmartFroth® system will be used in this thesis as one of the measures of froth performance.

Froth recovery is defined as the fraction of the particles entering the froth attached to bubbles that is recovered in the concentrate (Vera et al., 1999b). Froth recovery is therefore an expression of the performance of the froth zone in recovering particles by true flotation. Several techniques have been used to evaluate froth recovery. Following the work of Feteris et al. (1987), Vera et al. (1999b) developed a technique based on determining the first order rate constant at several froth depths, and extrapolating the linear relationship between k and froth depth to zero froth depth to obtain the collection zone rate constant, k_c. The froth recovery at any froth depth is then given by k/k_c. This method has proved to be very useful in the laboratory, in batch and continuous modes (Vianna, 2004; Welsby et al., 2010), and will be employed in this thesis.

Seaman et al. (2004) proposed the use of a bubble load device for measuring froth recovery. This device provides direct measurement of particles entering the froth zone from the pulp zone and allows the identification of selective processes occurring across the pulp-froth interface. Seaman et al. (2006) have noted that there is a discrepancy when measuring R_f using the bubble load device, as R_f includes the particles lost when crossing the pulp/froth interface. However, the bubble load device would be very difficult to use in a small column and so was not employed in this thesis.

Seaman et al. (2006) also reported that the froth recovery was not the same for all minerals in their work: differences were noted between the R_f values for chalcopyrite, galena, sphalerite, pyrite and non-floatable gangue at different froth depths. In this thesis, froth recovery values will be calculated and reported for both PGM and gangue minerals.

Another method for measuring froth recovery was proposed by Alexander et al. (2000). This method involves solving the mass balance equations across the froth, and measuring the grade at the very top of the froth and the gas holdup below the pulp/froth interface. This technique is currently used to measure froth recovery in large industrial flotation cells (Wills and Napier-Munn, 2006), but is considered too complicated for use in this thesis.

Three major types of flotation cell design are currently used in industry: mechanically agitated sub-aerated cells, sparged column cells and pneumatically driven (e.g. Jameson type) cells. In the laboratory, mechanically agitated batch cells are in universal use while column flotation cells are also employed. Column flotation cells allow a deeper froth depth to be obtained and can be run continuously with much greater ease allowing them to be operated under steady state, which is useful for this study of particle effects on froth performance.

In summary, several measurements will be made in this thesis to describe froth performance, while the properties of particles will be changed by varying the

depressant dosage. A column cell will be used as it can be run in a continuous mode, allows a wider range of froth depths to be investigated and allows for enhanced detection of froth effects. To enable the calculation of froth recovery as a measure of froth performance, the UCT method will be used to determine the separate recovery of particles by true flotation and entrainment. This method will first need to be extended to columns, as to date it has only been used in laboratory batch flotation cells.

1.2 RESEARCH OBJECTIVES

The aim of this thesis is to develop a strategy to study the interaction between the pulp and the froth phases in flotation, in particular the relationship between froth performance and the properties of the particles entering the froth zone.

The specific objectives of this project are:

1. To establish and validate the UCT methodology for a continuously-run column flotation cell. This is important because this methodology has never been applied to a column flotation cell before.
2. To develop an experimental procedure to study the interaction between the pulp and froth phases, using the UCT methodology to distinguish between true flotation and entrainment.
3. To investigate the relationship between the froth performance (froth stability, froth recovery, concentrate recovery and grade) and the properties of particles entering the froth. The depressant dosage change will be used to change the particle properties.

1.3 THESIS SCOPE

The test work for this project will be carried out in two stages; a procedure/strategy will be developed in laboratory tests which will be followed by site tests. Operating parameters such as superficial feed and air rates (the latter is linked to bubble size) which are critical for the performance of the flotation

process will be optimized during the preliminary tests. They will then be kept constant during all the experiments. Froth recovery will be evaluated using *the fitting technique* developed by Vera et al., (1999b). The froth depth will be varied by the use of different lengths of column above the pulp froth interface.

Froth stability will be evaluated using water recovery measurement. An attempt will also be made to adapt and use a machine vision system (UCT SmartFroth®) as an indicator of froth stability.

Changing frother and collector dosages is beyond the scope of this project. Frother and collector dosages will be optimized during the commissioning and preliminary tests.

1.4 STRUCTURE OF THE THESIS

The structure of this thesis is presented in Figure 1.1; the following paragraphs provide an overview of each chapter.

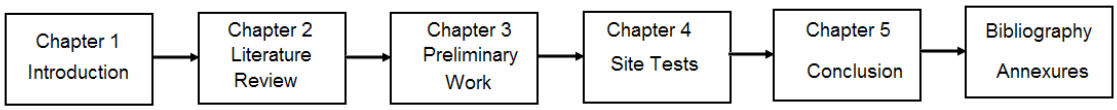

Figure 1.1: Structure of the Thesis

Chapter 2 presents a review of the relevant literature for the work presented in this thesis.

Chapter 3 describes the experimental rig used in this project, the materials used and the preliminary work carried out to validate the UCT methodology on column cells and to establish the methodology to study the interaction between pulp and froth phases in flotation.

Chapter 4 describes the site work that was carried out using the column on an operating PGM plant and presents the results obtained.

Chapter 5 provides a summary of the work that was performed followed by the recommendations for future work.

CHAPTER TWO: LITERATURE REVIEW

2.1 INTRODUCTION

While many studies in flotation have been devoted to the pulp phase, it is only recently that attention had shifted to the froth phase, although froth behaviour has long been recognized as the key driver of flotation performance. This project aims to contribute to the understanding of the effect of particle properties on froth performance. Particle properties will be changed by changing the depressant dosage in the flotation of PGM ore. Froth performance will be measured using the froth varying technique and true flotation will be decoupled from entrainment using the UCT methodology.

The present chapter reviews the literature relevant to this study. It begins with a brief introduction to the flotation process, followed by a discussion of various methods for quantifying froth recovery and entrainment. This is followed by a review of froth stability, some techniques to measure it and the factors affecting it. A review of column flotation technology follows with an emphasis on why a column flotation cell is indicated for this study. The chapter ends with a brief overview of platinum flotation.

2.2 PRINCIPLE OF FROTH FLOTATION

Froth flotation is a widely used process, and is a primary concentration step in mineral beneficiation. It is based on the difference in hydrophobicity between valuable minerals and gangue. However, very few minerals are naturally hydrophobic (Fuerstenau, 2007). In most cases, during or after size reduction (crushing and milling), the ore is conditioned with flotation reagents, which create and/or enhance differences in surface properties (hydrophobicity) between valuable minerals and gangue. The slurry is then introduced into a flotation cell where it is mixed with air.

In the flotation cell, valuable minerals become attached to rising air bubbles and are recovered in the concentrate stream, while gangue minerals are report to the tailings stream. In practice, the process is more complex than this, e.g. during the flotation process, there is always some gangue material that is recovered in the concentrate along with the valuable minerals. Figure 2.1 is a schematic representation of the flotation process.

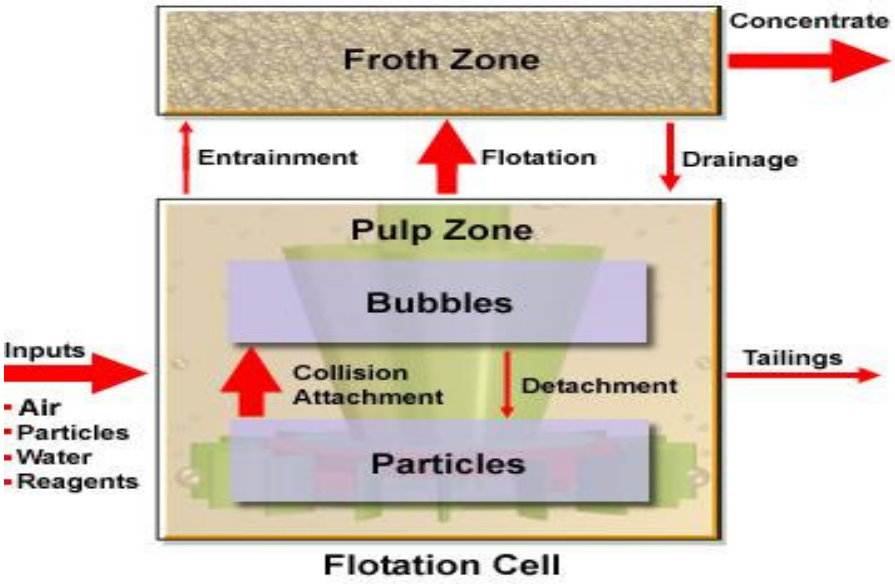

Figure 2. 1: Froth flotation process (Bradshaw, 2009)

As can be seen in Figure 2.1, there are two distinct zones in a flotation cell: the pulp zone in which mineral particles collide with and become attached to bubbles, and the froth zone, in which the particle-bubble aggregates are transported into the concentrate launder. The froth zone is important because allows upgrading of the concentrate by gravity drainage of water back to the pulp phase (Nguyen and Schulze, 2004).

Figure 2.1 also shows the second mode of particle recovery into the concentrate: entrainment. This is the recovery of unattached particles, trapped in the water between the bubbles. Unlike true flotation, entrainment is unwanted because it reduces the grade of the concentrate. The choice of flotation cell can reduce entrainment.

Mechanical flotation cells are widely used in the flotation industry. They are characterized by a mechanically driven impeller, which provides the necessary agitation to keep the particles in suspension, disperses the air into small bubbles and promotes bubble-particle collision and attachment (Wills and Napier-Munn, 2006). A schematic of a mechanical flotation cell is shown in Figure 2.2.

Figure 2. 2: Mechanical flotation cells (Wills and Napier-Munn, 2006)

Column cells were introduced into flotation to reduce entrainment. In column flotation cells, air is introduced at the bottom of the column and feed is introduced counter currently near the top of the column (Gupta and Yan, 2005). The ability to produce deep froths and the use of wash water allow column cells to produce far higher grades than their mechanically agitated counterparts. Additionally, columns have been found to improve the separation performance of fines materials (Wills and Napier-Munn, 2006).

In many flotation plants, mechanically agitated flotation cells are used as roughers, while column cells are used as cleaners. The choice of the type of flotation cell is driven mainly by the metallurgical performance (recovery and grade), the capacity (tons produced per hour), the operating costs and the ease of operation (Kelly and Spottiswood, 1989). In the PGM industry in South Africa mechanically driven cells are used exclusively, both in roughing and cleaning

applications; however there has been renewed interest recently in column flotation, due to the concern over the level of chromite in the smelters.

2.2.1 Particle recovery

In froth flotation, there are two main ways that a particle can reach the concentrate launder: It can be recovered either by true flotation or entrainment. The AMIRA P9 flotation model (equation 2.1; JKMRC/Amira International, 2004) is a good representation of the duality of particle recovery; distinguishing between true flotation (left hand side) and entrainment (right hand side):

$$R = \frac{P \cdot S_b \cdot \tau \cdot R_f \cdot (1 - R_w) + ENT \cdot R_w}{(1 + P \cdot S_b \cdot \tau \cdot R_f) \cdot (1 - R_w) + ENT \cdot R_w} \quad \textbf{(2. 1)}$$

where:

- R = recovery
- P = floatability
- S_b = bubble surface area flux
- τ = residence time
- R_f = froth recovery
- R_w = water recovery
- ENT = degree of entrainment

The degree of entrainment is defined by (Savassi et al., 1998):

$$ENT = \frac{R_{Entrainment}}{R_W} \quad \textbf{(2. 2)}$$

where:

- R_E is the recovery of entrained material
- R_{water} is the recovery of water

Equation 2.2 can be rewritten as

$$R_{Entrainment} = R_{Water} \bullet ENT \quad \textbf{(2. 3)}$$

It can be seen from Equation 2.1 that true flotation is affected by particle properties (represented by P, the floatability) and operating parameters (residence time, bubble surface area flux, froth recovery and water recovery). Equation 2.3 shows that entrainment changes linearly with water recovery, which is in agreement with the findings of previous studies on entrainment (Johnson et al., 1974; Engelbrecht and Woodburn, 1975; Bisshop, 1976).

Some of the terms in Equation 2.1 can be measured or calculated from mass balance surveys; these include (Naik and Van Drunick, 2005; JKMRC/Amira International, 2004; Yianatos et al., 2009):

- Operating parameters: bubble surface area flux, residence time
- Water and overall recovery

The determination of the remaining terms (entrainment and froth recovery) in equation 2.1 has been recognized as important for a better evaluation of the flotation performance (Engelbrecht and Woodburn, 1988; Mathe et al, 1998; JKMRC/Amira International, 2004). Over the past few decades, a number of different methods have been developed to evaluate froth recovery and entrainment in flotation. These are reviewed briefly in the sections that follow.

2.3 MEASURES OF FROTH PERFORMANCE

2.3.2 Froth recovery

Not all particles transferred from the pulp zone to the froth zone will be recovered in the concentrate launder. Froth recovery refers to the successful transfer to the concentrate launder of ore particles entering the froth zone attached to bubbles (Mathe et al., 1998). Figure 2.3 shows the mass transfer between the collection zone and the froth zone for particles that are recovered by true flotation (Vera et al., 2002). R_c is the recovery of the collection zone and R_f is the froth recovery.

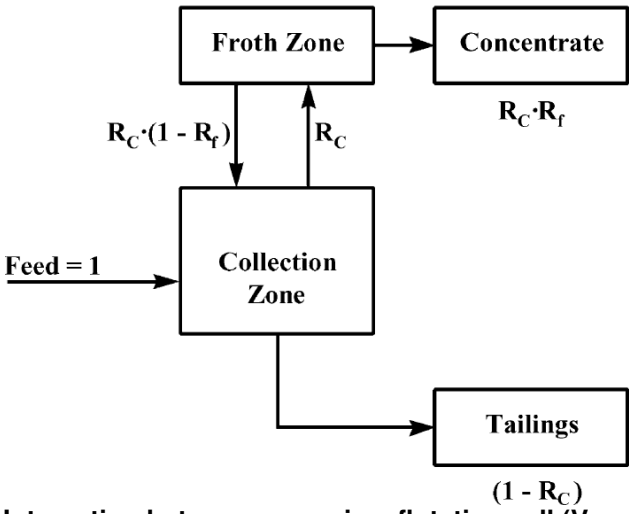

Figure 2. 3: Interaction between zones in a flotation cell (Vera et al., 2002)

The overall recovery R (Falutsu and Dobby, 1989) due to true flotation can be derived from Figure 2.3:

$$R = \frac{R_c R_f}{R_c R_f + (1 - R_c)} \qquad \textbf{(2. 4)}$$

It can be seen from equation 2.4 that the overall recovery is a function of both the collection zone recovery (R_c) and the froth zone recovery (R_f); the latter is clearly the most limiting factor of the overall recovery R. This is shown graphically in Figure 2.4 which is a 3D-plot of R as a function of R_f and R_c (equation 2.4).

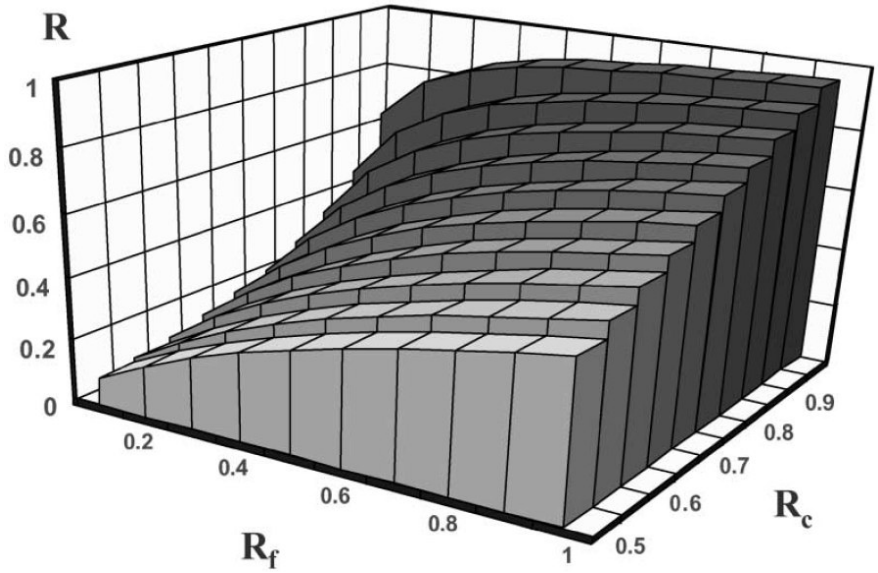

Figure 2. 4: Overall recovery as function of R_c and R_f (Vera et al., 2002)

Froth recovery R_f is the total rate of transfer from the pulp to the concentrate divided by the rate of transfer from the pulp to the froth phase (Vera et al., 1999b; Vera et al., 2002):

$$R_f = \frac{k}{k_c} \quad \textbf{(2. 5)}$$

Various techniques have been used in the past to measure froth recovery. In the next section a brief review is provided of the *fitting technique* which will be used during the experimental work. More details of the method can be found elsewhere (Vera et al., 1999b; Vera et al., 2002).

2.3.2.1 The fitting technique (Vera et al., 1999b)

Following the work of Feteris et al. (1987), Vera et al. (1999b) developed a technique for froth recovery measurement based on determining the first order rate constant k in a flotation cell at several froth depths. The collection zone rate constant k_c is obtained by extrapolating the linear relationship between k and the froth depth to zero froth depth (Figure 2.5). This is based on a well known relationship that exists between flotation rate constant k and froth depth FD:

$$k = a - b(FD) \quad \textbf{(2. 6)}$$

where a and b are constants

The constants a and b can be calculated as follows (refer to Figure 2.5):

1. When FD = 0 the intercept of the straight line (equation 2.6) on the rate constant axis is the collection zone rate k_c. Therefore a = k_c
2. $(FD)_{k=0}$ is the intercept of the straight line (equation 2.6) with the X-axis. At this point, the froth depth is so high that there is no material transferred from the froth zone to the concentrate launder, i.e. k = zero. This condition put into equation 2.6 gives

$$0 = a - b(FD)_{k=0} \quad \textbf{(2. 7)}$$

With the value of “a” found previously;

$$b = \frac{k_c}{(FD)_{k=0}} \qquad \textbf{(2. 8)}$$

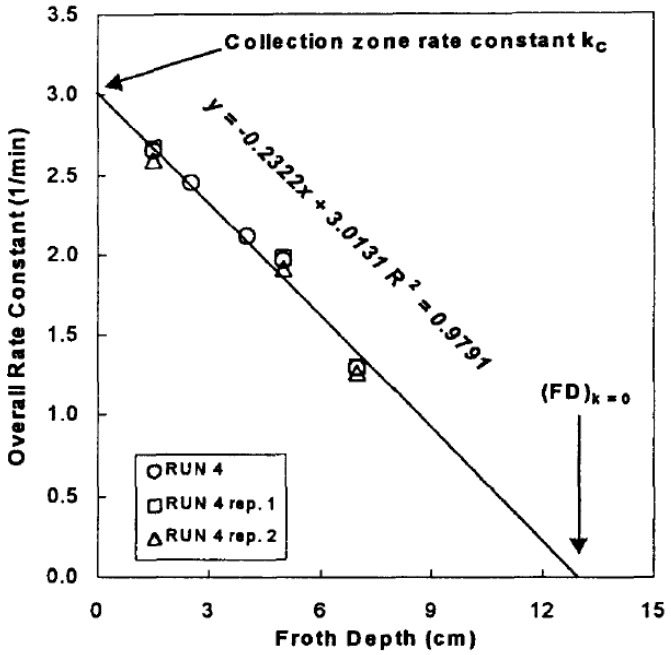

Figure 2. 5: Fitting technique for determining froth zone recovery (Vera et al., 2002)

Substituting a and b into equation 2.6 gives

$$k = k_c\left[1 - \frac{(FD)}{(FD)_{k=0}}\right] \qquad \textbf{(2. 9)}$$

and substituting equation 2.5 into equation 2.9 gives

$$R_f = \left[1 - \frac{(FD)}{(FD)_{k=0}}\right] \qquad \textbf{(2. 10)}$$

Equation 2.10 shows how the froth recovery may be estimated at any froth depth. However this relationship should not be used for conditions outside the experimental ranges.

The advantage of the *fitting technique* is that it is simple and can be applied to various cell sizes, types and duties (Alexander et al., 2003). The main limitation of the fitting technique is the fact that the maximum froth recovery is assumed to be 100% at zero froth depth, which is true only in an ideal situation (Yianatos, 2007). It should be noted that the fitting technique provides only information

about what is happening in the froth phase; it does not include any pulp zone effects and entrainment is not taken into account.

2.3.2 Entrainment

Entrainment needs to be measured in this thesis because of the need to distinguish between gangue recovered in the concentrate by entrainment and by true flotation: the latter only is used to calculate froth recovery which is used as a measure of froth performance in this thesis. Previous experimental studies of entrainment have focused mainly on hydrophilic minerals and their relationship with water recovery (Johnson et al., 1974; Engelbrecht and Woodburn, 1975; Bisshop, 1976). There have been a few experimental studies focused on finding separately the contribution of true flotation and entrainment to the overall flotation recovery. These include, but are not limited to, the *method of Trahar* (Trahar and Warren, 1976), the *method of Warren* (Warren, 1985), the *method of Ross and Van Deventer* (Ross, 1990), *the hydrophobic-hydrophilic method* (George et al., 2004) and more recently *the UCT method* (Oostendorp et al., 2005a, 2005b). The majority of these studies were conducted in ideal systems, which are not representative of the industrial environment.

A brief critical analysis of some of these methods is provided in the following sections. The assumptions used to develop each method are highlighted and an emphasis is put on the UCT method which will be used in this thesis.

2.3.2.1 Method of Johnson (Johnson et al., 1974)

One of the earliest studies of entrainment was performed by Johnson and co-workers. Plant and laboratory tests were conducted on five different chalcopyrite ores. The typical composition was:

- Sulphide (less than 10%)
- Variable amounts of quartz, magnetite, dolomite and chlorite.

A linear relationship between gangue recovery and water recovery was observed. Gangue minerals were subjected to hydraulic classification, according to the following classification function (CF_i),

$$CF_i = \frac{\text{mass of free gangue in the ith size interval per unit of water in the concentrate}}{\text{mass of free gangue in the ith size interval per unit of water in the pulp}} \quad \textbf{(2. 11)}$$

The classification function expresses the efficiency of the water in transporting the various size fractions of the free non-sulphide gangue from the pulp into the concentrate launder (Lynch et al., 1974). Figure 2.6 shows the variation of the classification factor (CF_i) with particle size. It can be seen that for very fine particles the classification factor is close to unity, but as the particle size increases, the classification function decreases (less entrainment).

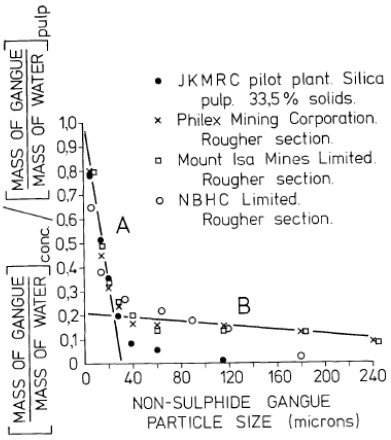

Figure 2. 6: Classification function vs. particle size (Lynch et al., 1974)

Unlike other entrainment quantification techniques, the Johnson method was developed on true systems (using real ores) which is good for modelling purposes. However the method does not account for gangue material recovered by true flotation. This case arises when an ore contains some gangue minerals that are hydrophobic and others that are hydrophilic (as in South African platinum ores). Therefore this method will not be considered for use in this thesis.

2.3.2.2 Method of Trahar (Trahar and Warren, 1976)

Two separate batch flotation tests are performed in this method; frother is used in both experiments but one of the experiments is done without collector. The recovery by true flotation is calculated as the difference between the solids recovered in the collector and non-collector tests as a function of water recovery. Figure 2.7 is an illustration of this method.

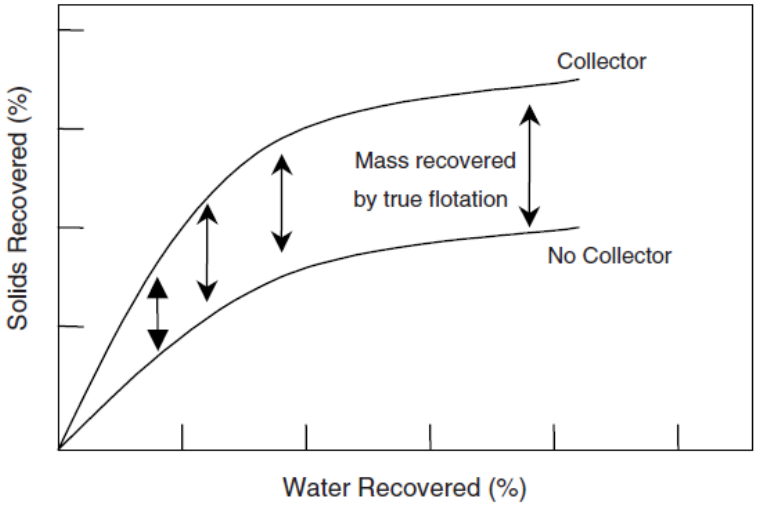

Figure 2. 7: True flotation and entrainment by Trahar Method (George et al., 2004)

The following assumptions were made in the development of this method:

i. All the particles captured in the froth with no collector used, are recovered by entrainment only.
ii. The degree of entrainment is the same in the presence and absence of collector.

As highlighted by Ross (1991) the application of this method is questionable when dealing with an ore containing naturally hydrophobic gangue minerals which will float even when no collector is added. In addition, collector addition is known to affect froth stability profoundly (Bradshaw et al., 2005; Wiese et al., 2006a**)** which will affect water recovery and consequently entrainment. Hence this method will not be considered for use in this thesis.

2.3.2.3 Method of Warren (Warren, 1985)

This method is based on a simple correlation between the recovery of hydrophilic particles and water recovery. Laboratory batch flotation tests were performed on a deslimed (+ 6 μm) sulphide-rich cassiterite ore, an ultrafine fraction (- 6 μm) of a cassiterite ore and a bituminous coal. Chemical conditions were kept constant; recovery was monitored as the froth height and the rate of froth removal were changed during different tests.

It was found that the recovery of the mineral (floatable) in each system was linearly related to the mass of water recovered. The intercept of the regression line on the mineral recovery axis, where water recovery is zero, was interpreted as the recovery due to true flotation. The entrainment contribution was taken to be proportional to the slope of the line. In this way the contributions of entrainment and true flotation to the overall recovery could be separated. The Warren method is illustrated in Figure 2.8.

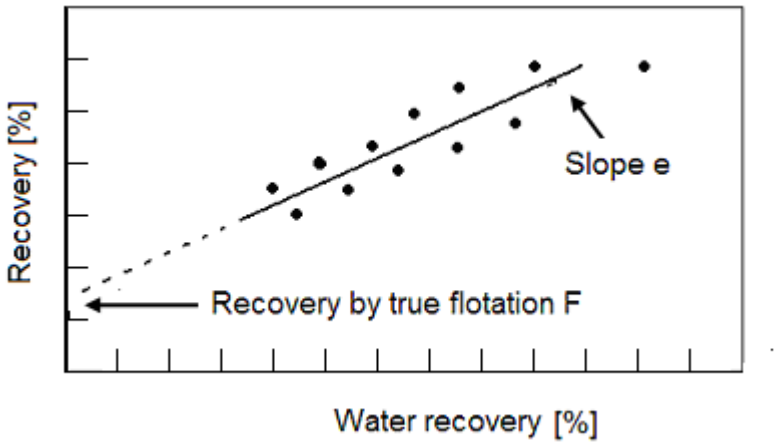

Figure 2. 8: True flotation and entrainment by the method of Warren

The following equations have been proposed to describe the behaviour of entrained and floated particles:

$$R(t) = F + eW(t) \quad \textbf{(2. 12)}$$

$$R_G = eW(t) \quad \textbf{(2. 13)}$$

where:

R (t) and R_G are the cumulative recoveries of valuable and gangue minerals ,respectively

F is the recovery by true flotation

W(t) is water recovery

eW(t) is the recovery by entrainment

e is the degree of entrainment, which is equal to the slope of R(t) versus W(t)

Because fast floating particles are recovered first, Ross (1991) recommended that the Warren method be applied just long enough to recover the most easily floatable solids, because longer flotation time will lead to a change of froth structure.

2.3.2.4 Method of Ross and Van Deventer (Ross, 1990, 1991; Ross and Van Deventer, 1988)

In this method, tests were conducted in a Leeds open-top laboratory flotation cell. The feed was a mixture of pure pyrite and gangue material from different sources.

The main assumption is that the concentration of entrained particles in the froth and in the concentrate is identical to the concentration of particles in the pulp. As the flotation test goes on, the recovery of floatable particles decreases, so that toward the end the test, the particles are recovered by entrainment only. Therefore, water recovery and solids concentration in the pulp can be used to evaluate recovery by entrainment. Recovery by true flotation can then be calculated,

$$m_{fi}(t) = m_{ti}(t) - m_{ei}(t) \quad \textbf{(2. 14)}$$

where $m_{fi}(t), m_{ti}(t)$ and $m_{ei}(t)$ are the recovery by true flotation, the total recovery and the recovery by entrainment, respectively.

The advantage of this method is that a single flotation test suffices to estimate the rate of flotation; therefore errors due to differences in the composition and conditioning of the feed are minimized. However the assumption that the concentration of entrained particles in the froth and concentrate is identical to the concentration of particles in the pulp needs to be verified when dealing with an

ore containing a large amount of floatable (hydrophobic) gangue minerals. It has been shown that hydrophobic particles have the potential to increase froth stability (Dippenaar, 1982a) therefore increasing recovery by entrainment.

2.3.2.5 Hydrophobic-hydrophilic method (George et al., 2004)

In this method two separate flotation tests are performed using different colloidal species of equal size (silica and alumina). Tests were conducted in a one litre column-type cell of internal diameter 70 mm and of variable height in the range 305 - 405 mm.

Because silica is naturally negatively charged and alumina carries positive charges, the conditioning of these species with a cationic collector will produce two different behaviours: The silica will be recovered by true flotation only and alumina will be recovered by entrainment only. Thus the difference in recovery between the two experiments gives a measure of true flotation of the hydrophobic species (e.g. silica). This method is illustrated in Figure 2.9.

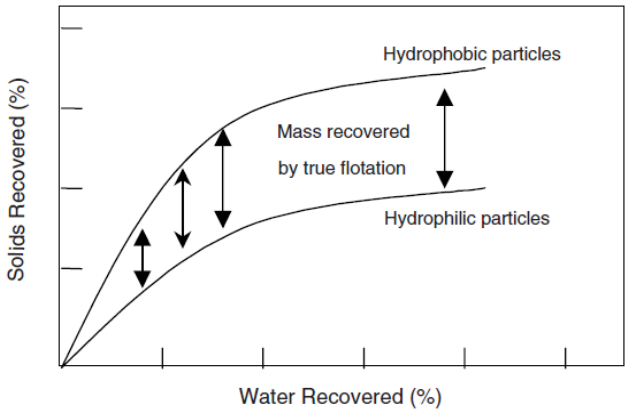

Figure 2. 9: True flotation and entrainment by the hydrophobic-hydrophilic method (George et al., 2004)

A limitation of this method is the fact that it is based on the use of an ideal system which is not representative of industrial conditions, where one has to deal with real ores (of various surface properties). Furthermore the assumption that silica is recovered by true flotation only is questionable, as entrainment is known to affect both hydrophilic and hydrophobic particles. Another weakness is the fact that the

method was developed to evaluate the entrainment of submicron particles; the question arises whether or not this method can be used for normal particle size ranges.

2.3.2.6 JKMRC method (Savassi et al., 1998)

This method which was developed at the Julius Kruttschnitt Mineral Research Centre (JKMRC) at the University of Queensland, aimed to develop a model that can be used to predict entrainment of gangue minerals into the concentrate. In this method a tracer or a fully liberated hydrophilic mineral in the feed is required. Savassi et al. (1998) proposed the following equation, to calculate the degree of entrainment:

$$ENT_i = \frac{\text{Mass transfer of entrained particles of the ith size interval to the concentrate}}{\text{Mass transfer of water to the concentrate}} \quad \textbf{(2. 15)}$$

where i indicates the particle size interval.

Equation 2.15 is similar to the classification factor shown earlier (see section 2.3.2.1). The mass transfer to the concentrate (in units of mass per time) is calculated on the basis of pulp, feed or tailings.

The following empirical partition curve was used to describe the variation of the degree of entrainment (similar to the classification factor) with the particle size in a flotation cell operated at fixed conditions:

$$ENT_i = \frac{2}{\exp\left(2.292\left(\frac{d_i}{\xi}\right)^{adj}\right) + \exp\left(-2.292\left(\frac{d_i}{\xi}\right)^{adj}\right)} \quad \textbf{(2. 16)}$$

$$adj = 1 - \frac{\ln(1/\delta)}{\exp(d_i/\xi)} \quad \textbf{(2. 17)}$$

where d_i is the particle size [μm]

ξ is the entrainment parameter [μm], given by the particle size for which. the degree of entrainment is 20%.

δ is the drainage parameter (dimensionless), related to the preferential. drainage of coarse particles.

Figure 2.10 is a graphical representation of Equation 2.16, which shows that the following boundary conditions are applicable to these equations:

$d_i \to \infty \Rightarrow \quad ENT_i \to 0$

$d_i = 0 \Rightarrow \quad ENT_i = 1$

$d_i = \xi \Rightarrow \quad ENT_i = 0.20$

In this method entrainment is linked only to particle size. Although Savassi et al. (1998) recognized other parameters affecting entrainment; they were not taken into account in the model.

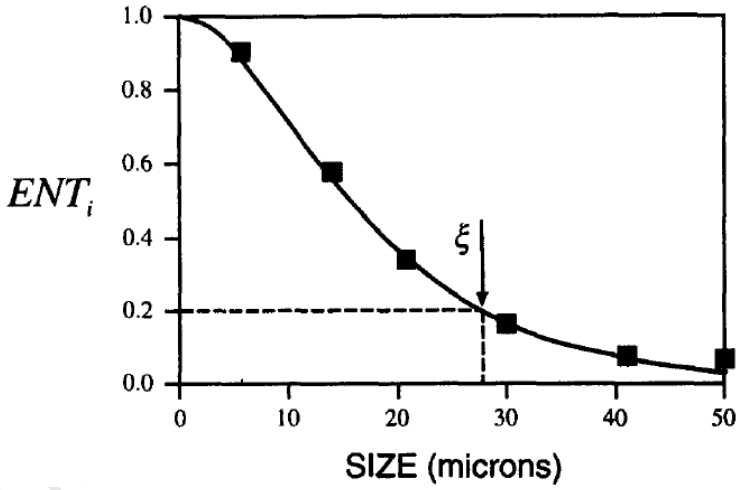

Figure 2. 10: The variation of the degree of entrainment with the particle size

The empirical partition curve (equation 2.16) was used to fit a number of data sets published previously in the literature. All the data fitted well, even though they were from various researchers, using different minerals and were collected under different experimental conditions (Figure 2.11).

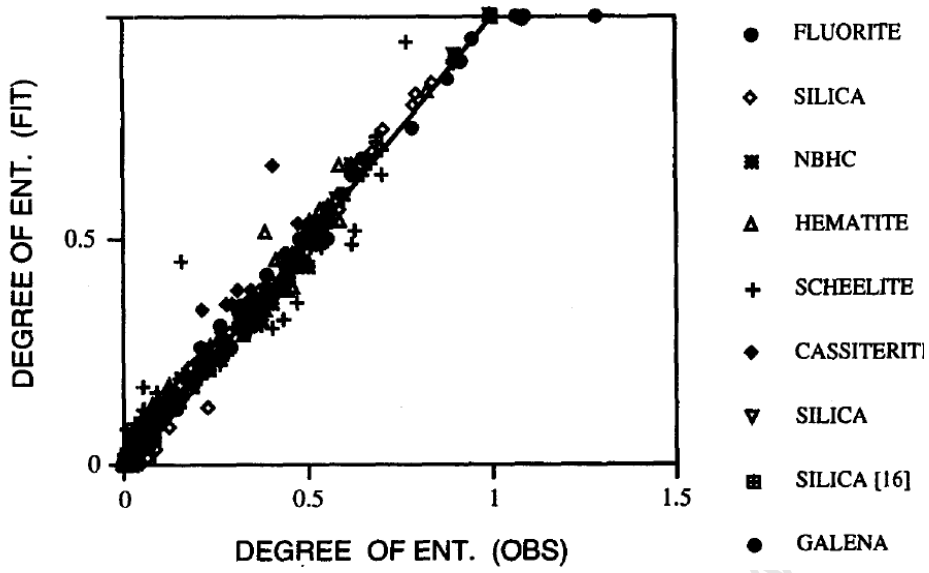

Figure 2. 11: Fitting data from various sources (Savassi et al., 1998)

Entrainment is affected by many factors, which include but are not limited to particle size, solids percentage, particle density, the chemistry of the solution and rheology of the pulp. The JKMRC method is limited in the fact that it fails to include any other factors affecting entrainment apart from particle size.

Anderson (2008) established that entrainment can be calculated, using a version of the Savassi method (Savassi et al., 1998) where an entrainment factor is defined as:

$$ENT = \frac{\left(m_{Entr,i} / m_w\right)_{Conc}}{\left(m_i / m_w\right)_{pulp}} \qquad \textbf{(2. 18)}$$

where $m_{Entr,\,i}$ is the mass flow rate of particles recovered by entrainment.

$m_{w,Conc}$ is the mass flow rate of water in the concentrate.

$m_{i,\,pulp}/m_{w,\,pulp}$ is the concentration of particles of class "i" in the pulp just below the pulp-froth interface.

Anderson rearranged Equation 2.18 to yield Equation 2.19 below:

$$m_{Entr,i} = ENT_i \; x \left(\frac{m_i}{m_w} \right)_{Feed} \; x \; (m_w)_{Conc} \qquad \textbf{(2. 19)}$$

Equation 2.19 is a useful representation of the recovery by entrainment, because the solid and water content of the feed are taken into account. Solids percentage in the feed had been found to be one of the important factors of solids entrainment (Lynch et al., 1981, Savassi et al., 1998).

2.3.2.7 The UCT method (Oostendorp et al., 2005a, 2005b)

The "UCT method" was developed at the laboratory batch scale, in an attempt to find separately the amount of gangue recovered by true flotation and entrainment in the flotation of PGM ores. Merensky ore, which contains a large amount of floatable gangue, was used during the development of the UCT method.

The main assumption in this method is that at high depressant dosage, all the gangue recovered is by entrainment only. This is shown graphically in Figure 2.12, which shows results obtained by Oostendorp et al. (2005a). With increase in depressant addition, the recovery of gangue (as well as the water recovery) decreased and at 300 g/t the gradient of the gangue recovery versus water recovery curve is linear, with the line passing through the origin. Further addition of depressant did not decrease the gangue recovery any further. It was concluded that the 300g/t line represents the recovery by entrainment only.

Because entrainment recovery is related directly to water recovery, the relationship between gangue and water recoveries at high depressant dosage is then used as a calibration that maybe applied to all depressant dosages: This is done by subtracting the entrained gangue recovery curve from the total gangue recovery curve for each depressant addition. The floatable gangue recovery is obtained as a function of water recovery (Figure 2.13).

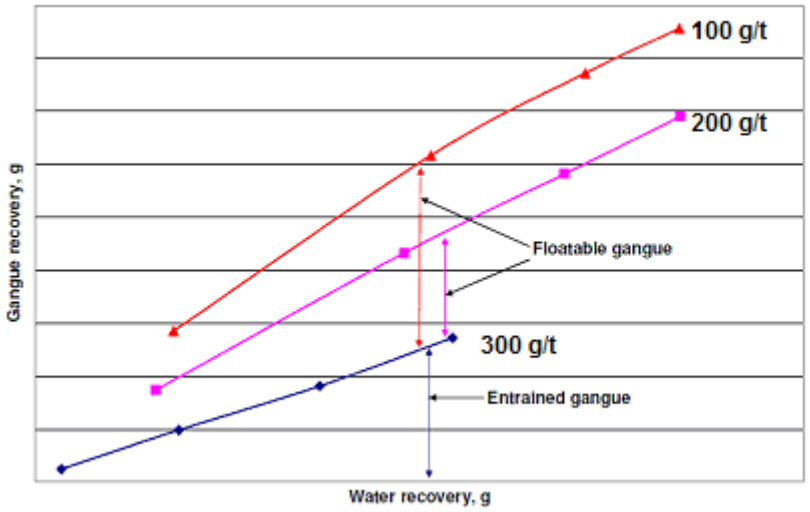

Figure 2. 12: The UCT method (Oostendorp et al., 2005a)

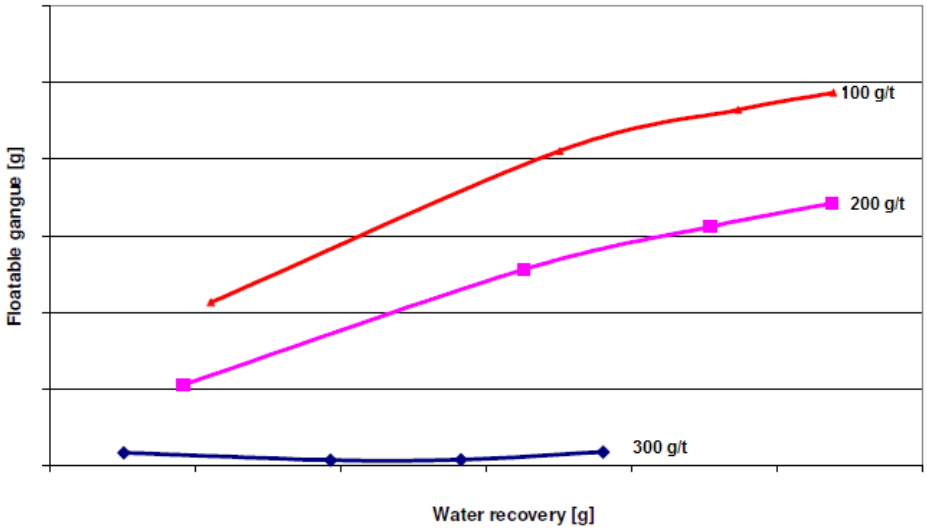

Figure 2. 13: UCT method; Floatable gangue recovery vs. water recovery

The UCT method has been used extensively to estimate the amount of gangue recovered by true flotation and entrainment in platinum ores (Oostendorp et al., 2005a,b; Wiese et al., 2006a,b; 2007). It has been shown to be accurate by the concurrent use of a small amount of manganese oxide, which is a non-floatable tracer (Oostendorp et al., 2005b)

To date, the UCT method has been used only on small laboratory scale, batch flotation cells. This thesis will attempt to establish the method on a continuous

column cell. Apart from being a continuous system, a column cell has an added advantage, as it is possible to have deeper froth than in a conventional laboratory-scale batch flotation cell, to investigate better the effect of particle properties on the froth phase (see section 2.4 below).

2.4 FROTH STABILITY

Slurry feed into a flotation process comprises liquids and solids. Solids can be characterized by their size, shape, density and hydrophobicity. The latter is the chief requisite of a successful flotation process: Hydrophobic particles will attach to bubbles and be carried into the froth phase. Hydrophilic particles are primarily recovered by entrainment in the water between the bubbles. As the laden bubbles in the upper levels of the froth are being transported toward the concentrate launder, coalescence and bursting may occur, releasing hydrophobic particles which may also drain back into the pulp. In the lower levels of the froth, water drains by gravity, returning entrained hydrophilic particles to the pulp.

These processes are illustrated in Figure 2.14. For the successful separation of valuable minerals by froth flotation, the froth phase requires some degree of stability to recover the hydrophobic particles while allowing the entrained particles to drain back into the pulp. Froth stability is important in the flotation process, because it is a key driver of froth performance. Understanding froth stability requires little more knowledge of the structure of a froth.

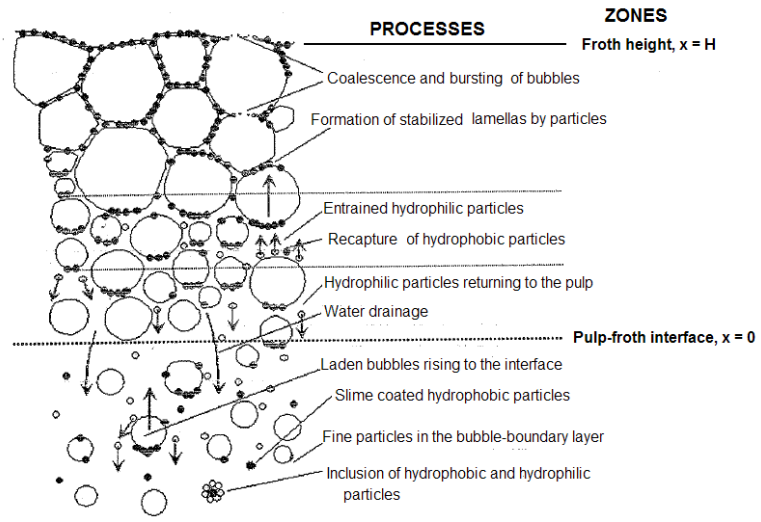

Figure 2. 14: Processes in the froth (Nguyen and Schulze, 2004)

Froth comprises bubbles which are separated by thin liquid films known as lamellae. Plateau borders are channels formed where three lamellae meet. Four Plateau borders meet in a vertex. The Plateau borders and vertices contain most of the liquid in the froth; only a small fraction of the liquid in the froth resides in the lamellae. Plateau borders and vertices form an interconnected web of drainage channels along which liquid and solids flow, as shown in Figure 2.15 below (Neethling et al., 2003).

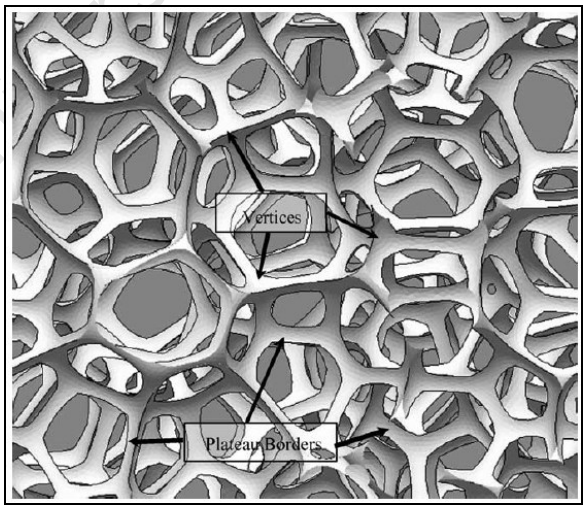

Figure 2. 15: Froth structure (Neethling et al., 2003)

Froth destabilization involves the draining of the liquid film to a critical thickness, where rupture (bubble coalescence or bursting) occurs (Pugh, 2005). Figure 2.16

shows the structure of foam in a column. It can be seen that in the lowest part of the foam, the bubbles are round and wet. But as the bubbles move toward the interface, the foam is significantly drier due to coalescence and drainage of liquid from the foam.

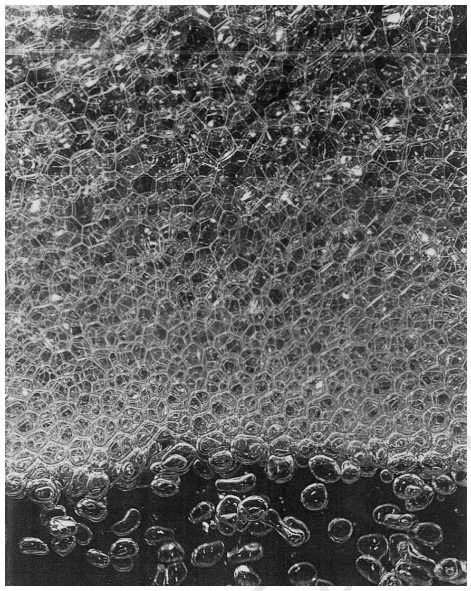

Figure 2. 16: Cross-section through flowing foam (Cilliers, 2006)

Froth stability implies the non-destruction of the boundary between bubbles, until the valuable minerals are collected in the concentrate launder. Selectivity in flotation is achieved by finding a compromise between a stable and unstable froth (Harris, 1982). A very stable froth is not desirable, because more materials are collected (increased recovery) at the expense of the grade (which decreases). An unstable froth, on the other hand, is not recommended, because the froth will collapse before most of the valuable minerals are recovered. The ideal froth should (Hatfield et al., 2003):

- Not be destroyed before its removal from the cell, but collapse in the launders.
- Be mobile or runny enough to withstand the shear stresses encountered during transport to the weir.
- Persist long enough to achieve sufficient froth residence time to allow for drainage.

The study of froth stability, therefore, involves finding an optimal combination of physical, chemical and hydrodynamic conditions that will allow enough material to be recovered, at an acceptable grade.

2.4.1 Measurement of froth stability

The quantitative measurement of froth stability, both at laboratory and industrial scales, remains a significant challenge. Several methods have been developed to assess the stability of froth. Bikerman (1973) made the first attempt, defining the "dynamic foam stability factor" as:

$$\Sigma = \frac{V_f}{Q} = \frac{H_{max}.A}{Q} \qquad \textbf{(2. 20)}$$

where V_f: The foam volume.

Q: The gas volumetric flow rate.

H_{max}: foam height at equilibrium.

A: the cross-sectional area of the vessel.

The measurement involves observing the rate of breakdown of froth from the equilibrium height attained (H_{max}) in a specially designed foam column. Various froth stability measurements have been developed based on Bikerman's work (see e.g. Barbian et al. 2005, Ventura-Medina et al., 2003; Ventura-Medina et al., 2002). These methods will not be considered for use in this thesis, because they have the potential to interfere with the flotation tests. An attempt will be made instead to use water recovery and the UCT SmartFroth system® to measure froth stability.

The stability of a froth is determined by the stability of the lamellae: a rupture of a lamella will cause coalescence between neighbouring bubbles, releasing their water and solids content (Banford et al., 1998). This explains why water recovery at fixed froth height is widely used as a stability measure of the froth (see e.g. Tao et al., 2000; Bradshaw et al., 2005a,b; Oostendorp et al., 2005a; Wiese et

al., 2006a,b). Water recovery as a measure of froth stability is useful because it is easy to measure and does not interfere with the flotation tests.

The UCT SmartFroth system® performs an analysis of the froth surface appearance in order to generate various output measurements that are termed froth surface descriptors, such as froth surface area, bubble size, velocity and burst rate; and cross correlation peak. The latter can be used as a measure of froth stability (Forbes, 2005). In estimating the value of "cross correlation peak", two consecutive images are compared in order to find the relative alignment that maximises their correlation with each other (de Jager *et* al, 2004). The resultant value of "cross correlation peak" varies between zero and unity. A value of unity would represent no changes in the image, and would be indicative of a stable froth, while a value of zero would represent a very unstable froth (Morar et al., 2006).

Froth stability arises from the operating parameters in a cell (air rate, froth height), the system chemistry and the properties of solid particles in the froth. The system chemistry is determined largely by the addition of frothers, while the properties of the solid particles can be either natural or modified by collectors or depressants. The effect of some of these parameters on froth stability will be analyzed briefly in the following sections.

2.4.2 Effect of air flow rate on froth stability

Increasing air flow rate is generally thought to increase froth stability and therefore the overall recovery. Tao et al. (2000) investigated the effect of air rate in a column flotation cell. They conducted their experiments on run-of-mine high-sulphur bituminous Illinois coal, using a 5 cm diameter microbubble flotation column with a height of 170 cm. They found that the froth stability increased with increasing superficial air rate. This is shown in Figure 2.17. It is apparent that the water recovery increased considerably with the increase in the gas flow rate, indicating that the froth was stabilized. Concurrently, combustible and ash recoveries increased as the air rate increased.

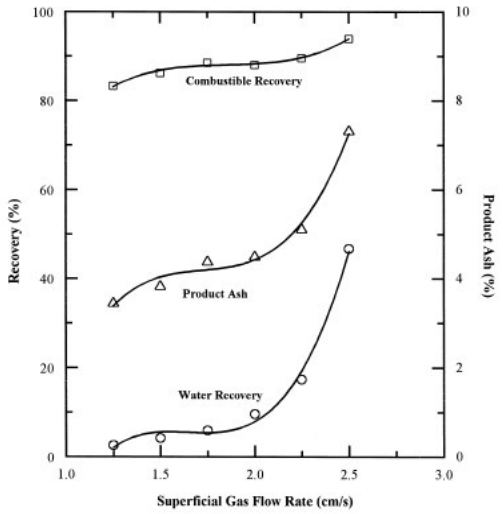

Figure 2. 17: Effect of superficial air rate on flotation performance (Tao et al., 2000)

The effect of air rate on flotation performance was also studied by Hadler et al. (2010). In a study of an operating PGM flotation plant, they found that there was a maximum air rate (which they called the "Peak Air Rate") which allowed optimum flotation performance. This is shown in Figure 2.18. Increasing the air rate toward the PAR (Peak Air Rate), led to an increase in mass pull and recovery, while the concentrate grade decreased. At the same time, decreasing the air rate to obtain PAR (Peak Air Rate) conditions resulted in higher grade and recovery, while the mass pull decreased.

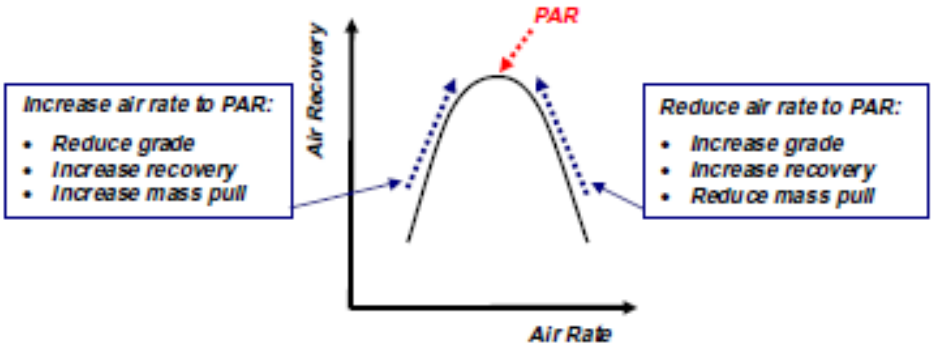

Figure 2. 18: Air recovery optimization and flotation performance (Hadler et al., 2010)

Ventura-Medina et al. (2004) studied the effect of operational variables on the solids loading in bubble lamellae on the surface of flotation froths, in a copper concentrator. They showed that air rate was one of the main parameters which affected the solids bubble loading. The average solids loading on froth surface

bubbles as a function of the superficial gas velocity for different froth depths at standard frother concentration is shown in Figure 2.19. It is apparent that the average solids loading decreased as the superficial gas velocity increased, while the bubble load increased when increasing the froth depth at constant air flow rate.

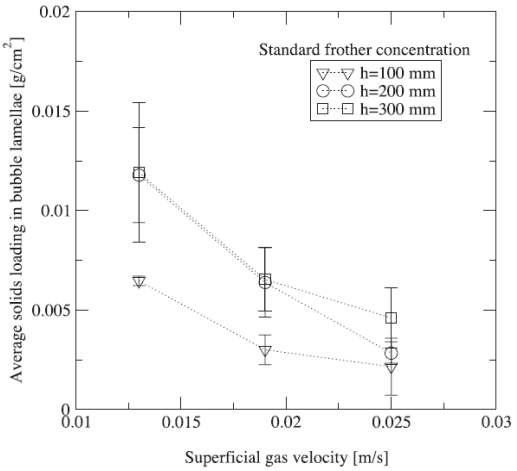

Figure 2. 19: Effect of air rate on bubble loading (Ventura-Medina et al. 2004)

The main implication of these observations is that low superficial air rates generate high bubble loading. This needs to be taken into account when analyzing any flotation result: as Barbian et al. (2005) noted, on a copper flotation plant, higher loadings were found to be associated with higher froth bursting rates, which are indicative of more selectivity in attachment and therefore a higher mineral grade in the concentrate.

2.4.3 Effect of solid particles on froth stability

Froth can be stabilized or destabilized by solids. The mechanism of froth stabilization/destabilization by solids has been investigated thoroughly in the past. In groundbreaking research, Dippenaar (1982a) used high-speed cinematography to record the interactions of particles of different shapes and degrees of hydrophobicity with an artificially thinned film of water. He used single films that could be thinned at will. The particles used were quartz, glass and galena. Prior to the experiments, these particles were endowed with different

degrees of hydrophobicity. This study shed a new light into the mechanism of film rupture by particles. The following results were obtained:

- Any smooth spherical particles with contact angle >90˚ ruptured the film. In the absence of particles, the film survived much longer.
- Smooth orthorhombic particles (xanthated galena) with contact angle of 80° ± 8˚ bridged and ruptured the film.
- Rough particles with a contact angle > 90º could or could not break the liquid, depending on factors relating to their specific shape or their surface roughness. For those with a contact angle = 98˚ the film was broken.

Dippenaar (1982b) also found that with constant agitation, the rate of froth destruction equals the rate of froth production. He concluded that the natural thinning of films is the rate-determining step in particle-induced froth destabilization. He also realized that viscosity change did not seem to affect froth stability, when hydrophobic quartz was used. With a mixture of larger (25 - 37 µm) and smaller (4 - 6 µm) particles, the larger particles partially destroyed the froth. The smaller ones had no effect until they outnumbered the larger ones by more than 50 to 1.

More recently, Johansson and Pugh (1992) studied the influence of particle size and hydrophobicity on froth stability. Their experiments were an advance on Dippenaar's. They used a Hallimond tube in which they could study the behaviour of multiple films. The mechanisms of froth stabilization and destabilization by particle hydrophobicity are illustrated in Figure 2.20. As can be seen in Figure 2.20 (a) particles with a low degree of hydrophobicity have little effect on froth stability. Moderately hydrophobic particles (Figure 2.20 (b)) stabilize froth by preventing the froth films from thinning and draining. Very hydrophobic particles (Figure 2.20 (c)) destabilize froth by bridging the liquid films and collapsing the bubbles.

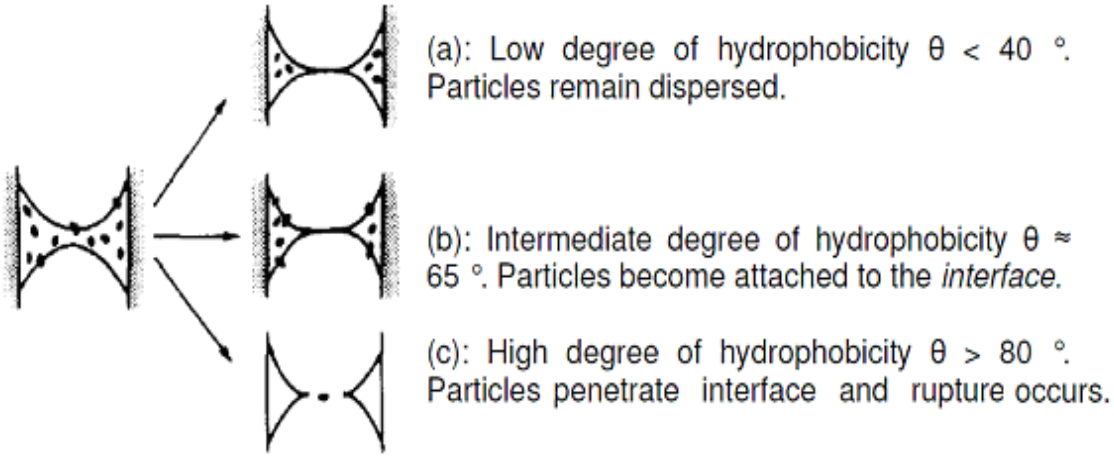

Figure 2. 20: Summary of particles effect on froth stability (Johansson and Pugh 1992)

Johansson and Pugh also studied the combined effect of particle hydrophobicity and size. They found that small particles (26 - 44 µm) affected froth stability as follows:

- When moderately hydrophobic particles (θ = 65°) were present, they maximized the static as well as the dynamic froth stability (both at low and high frother concentration range).
- The more hydrophilic particles did not affect froth stability.
- The more hydrophobic particles quenched the froth.

For coarser particles (74 - 106 µm), on the other hand, these effects were found to be much less pronounced. For a mixture of particles with different degrees of hydrophobicity (θ = 20°, θ = 65° and θ = 80°) the most hydrophobic fraction dominated the mixture and acted as the foam breaker. Fine hydrophobic particles had a stronger stabilizing effect on the froth.

From the previous analysis we see that froth stability is closely related to the size and hydrophobicity of particles. The combined effect of size and hydrophobicity of particles on froth stability is summarized in Table 2.1 (Dippenaar, 1982a, 1982b; Johansson and Pugh, 1992; Pugh, 2005).

Table 2. 1: Summary of particle hydrophobicity effect on froth stability

Size	Degree of Hydrophobicity	Effect on Froth
Smaller than the film thickness	Intermediate critical θ ≈ 45°- 90°	Stabilizing
	θ > 90°	Destabilizing
	θ < 90°	No effect
Larger than the film thickness	θ ≈ 45°- 90°	No effect
	θ > 90°	No effect
	θ < 90°	No effect

The destabilization of froth by hydrophobic particles was also studied by Schwarz (2004) and Ata et al. (2004). Conducting their separate investigations with methylated quartz, they found that there was a critical contact angle where further increase of hydrophobicity decreased froth recovery of both particles and water. This was in agreement with the findings of the previous studies, as discussed above.

The main limitation of Dippenaar's work is the framework of his experimental set-up. The use of cells that produced single films is far from the reality of flotation practice. Another major limitation is that the particles he used were well controlled from the point of view of hydrophobicity, which is not always the case in reality. Furthermore, in practice; flotation froths are subjected to strong hydrodynamic conditions; Dippenaar did not take this fact into account.

In fact the conclusions reached by all the previous workers (Dippenaar, 1982; Johansson and Pugh, 1992; Schwarz, 2004; Ata et al., 2004) require more testing at experimental conditions closer to a true system, as most of the previous studies were performed in ideal systems. However, although these experiments were far from reality in the practice of mineral flotation, the findings provide a basis for improving the understanding of froth behaviour.

2.4.4 Effect of frothers on froth stability

Froth stability in flotation is also affected by the pulp chemistry, which is regulated by flotation reagents. The chemicals in a flotation slurry or pulp include the added reagents (including collectors, depressants, activators, pH regulators and frothers), the soluble components of the ore and the ions in the water (Bulatovic, 2007).

Frothers are surface-active, in most cases non-ionic, molecules whose role in the flotation system is to provide a large air-water interface of sufficient stability to ensure that attached particles will not fall back into the flotation pulp before they can be recovered (Laskowski, 2008). Frothers adsorb at the interface of water and air bubbles forming an envelope around the bubbles which is believed to prevent coalescence (Bulatovic, 2007).

It can therefore be seen that the main role of frothers is to produce a stable froth, although the action of frothers is not limited to this. It has been established that frothers are also involved in (Klassen and Mokrousov, 1963):

- Making air bubbles finer, i.e. they improve the dispersion of air in flotation machines.
- Preventing coalescence of separate bubbles. Coalescence reduces the available surface for minerals collection.
- Decreasing the rate at which air bubbles rise to the surface of the pulp, improving the probability of bubble-particle collision.
- Contributing to the effectiveness of the collector's action.

Various types of frothers are currently used in flotation e.g. alcohol, alkoxy-type and polyglycol-type frothers. In PGM flotation, polyglycols are widely used. Some examples include DOW200, DOW250, SK 700 and SENFROTH frothers. The typical plant concentration used is around 60 g/t (Sweet et al., 1997).

The dosage of frother needs to be selected carefully, as increasing the frother dosage will result in more material being collected which results in grade being affected negatively. Figure 2.21 shows the effect of frother dosage on the water and mass recoveries in the laboratory batch flotation of a Merensky ore (Wiese et al., 2010). It is apparent that irrespective of the depressant type and dosage, an increase in frother dosage resulted in a more stable froth, which resulted in more mass and water being recovered The increases were quite significant with no depressant added: Water increased from 380 to 960 g in the concentrate and solids increased from 620 to 980 g, upon increasing the frother dosage from 40 to 70 g/t. The increase was less marked when depressant was added: the addition of depressant severely reduced the recovery of both water and solids (see section 2.4.6 below). However, even at 500 g/t depressant dosage, increasing the frother concentration increased froth stability and the recovery of water and solids.

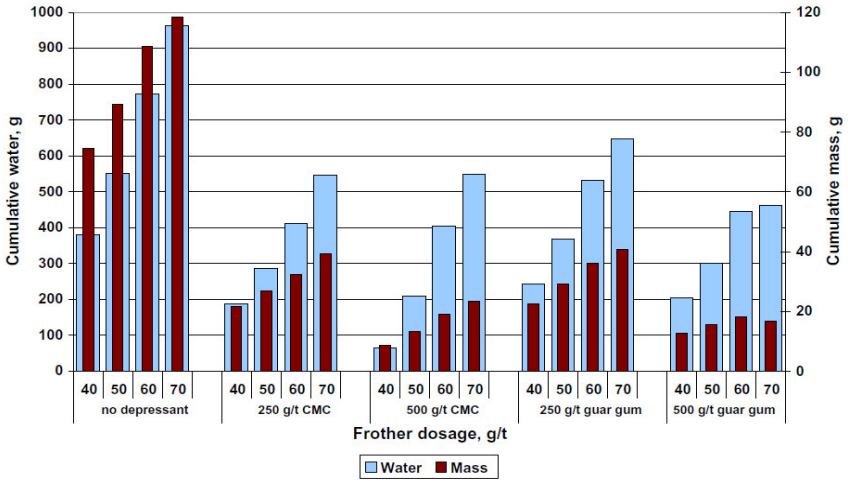

Figure 2. 21: Effect of frother addition on mass and water recoveries in a flotation of a Merensky ore (Wiese et al., 2010)

In the study of the effectiveness of frothers on froth stability, their molecular structure should not be neglected. Schwarz (2004) investigated the effect of molecular weight and concentration of a family of polypropylene glycol frothers and an industrial frother (DF400) in the flotation of methylated quartz. She found that the highest froth recovery was obtained with the frother of the lowest molecular weight, and found also that for each frother there was an optimum dosage where froth recovery was at a maximum.

In this thesis an attempt will be made to optimize frother dosage during the preliminary tests in the laboratory. The optimum frother dosage will then be kept constant during the site experiments.

2.4.5 Effect of Collectors on Froth Stability

Very few minerals are naturally floatable; collectors are used to enhance their floatability by making them hydrophobic (water-repellent) thus increasing their chances of reporting to the froth phase (Bradshaw et al., 2005a). Various collectors are currently available on the market. The typical collectors used in the PGM industry are thiols, the most common of which are the xanthates (SEX, SNPX, PNBX, PAX...), in some cases with co-collectors dithiophosphate or dithiocarbamate (Wills and Napier-Munn, 2006). The collectors have a polar group that adsorbs on the mineral interface and a non-polar group that remains in the liquid and becomes attached to an air bubble.

Increasing the collector chain length has long been recognized to increase hydrophobicity and recovery (Havre, 1952). However the unwanted effect on froth stability needs to be taken into account[1]. For instance it has been found in batch flotation tests of Merensky ore that contrary to expectations a shorter chain length molecule (SEX chemical formula: C_2H_5OCSNa) led to the production of more water and mass and a greater recovery of base metals than a longer chain molecule (SIBX chemical formula: C_4H_9OCSNa) irrespective of the depressant type or dosage (Bradshaw et al., 2005a). This is illustrated in Figure 2.22. An explanation of this behaviour can be offered based on the fact that the stronger collector SIBX led to increased hydrophobicity of sulphide particles which ultimately destabilized the froth phase leading to a decline in water and solids recovery (Bradshaw et al., 2005a).

[1] Refer to section 2.4.3 of the effect of increased particle hydrophobicity on froth stability

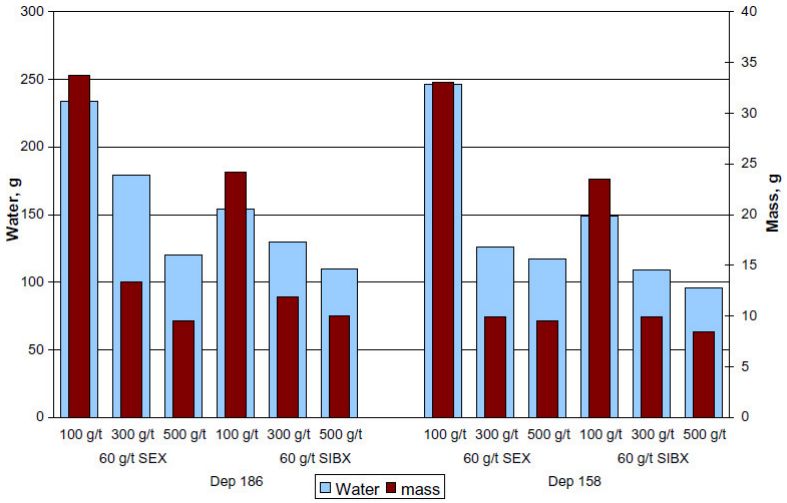

Figure 2. 22: Effect of collector type on mass and water recovery in a flotation of a Merensky ore (Bradshaw et al., 2005)

Therefore any collector addition must take into account the unintended impact on the froth phase e.g. if stronger collectors are being trialed on an industrial plant, they need to be tested at conditions that compensate for the effect on the froth stability, such as suitable frothers or weaker or lower dosage of depressants (Bradshaw et al., 2004; 2005a).

2.4.6 Effect of modifiers on froth stability

The separation of valuable minerals from gangue by flotation is realized by selectively enhancing or hindering the hydrophobicity of selected minerals. Reagents used to enhance the hydrophobicity of slow floating minerals are called activators, while reagents used to hinder the natural hydrophobicity of selected unwanted minerals (gangue) are called depressants (Somasundaran and Moudgil, 1988). The modes of action of depressants include blocking or blinding of the gangue surface, thus preventing collector adsorption onto hydrophobic minerals and rendering them hydrophilic (Pearse, 2004).

Although the proportion of floatable gangue in the PGM ores is small, it has a froth stabilizing effect that causes significant entrainment of other non floatable

gangue minerals (pyroxene; feldspar and chromite)[2]. Consequently, depressants are added into the flotation cell to suppress the recovery of gangue minerals. In South Africa, polymeric depressants such as carboxymethyl cellulose (CMC) and guar are widely used in PGM flotation to depress talcaeous gangue minerals (Wills and Napier-Munn, 2006).

It was shown in Figure 2.21 and 2.22 that the depression of gangue minerals had an adverse effect on the froth phase: froth destabilization, which led to loss in recovery. Figure 2.23 is a further illustration of the effect of depressant and frother dosage on the recoveries and grades of copper and nickel in a Merensky ore. It can be seen that high depressant dosages resulted in an increase in copper and nickel grades but always at the expense of recovery, presumably because of the drop in froth recovery but also as a result of the depression of partially liberated sulphide/gangue particles (Wiese et al., 2010). This observation is valid irrespective of the type of depressant used (CMC or guar gum).

[2] For a review of PGM ore mineralogy refer to section 2.7

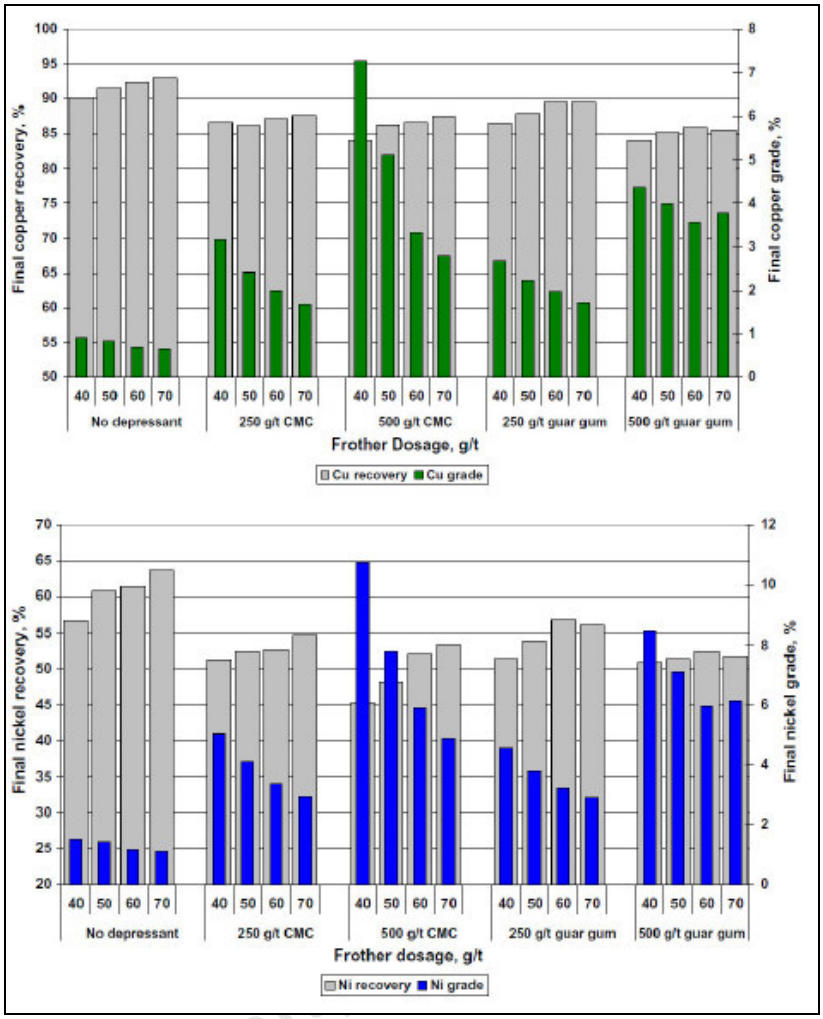

Figure 2. 23: Combined effect of depressant and frother on copper and nickel recovery and grade in the flotation of a Merensky ore (Wiese et al., 2010)

It has been shown above that while depressants are important in achieving good selectivity and having high grade, too much depressant dosage can affect recovery severely. In this project froth stability and froth recovery will be monitored as depressant dosage and froth depth are varied in the column cell testwork.

2.5 COLUMN FLOTATION

The main aim of this thesis is to study the interaction between the froth and the pulp phases; it was decided that a column flotation cell would be used

throughout. This section reviews some of the most important features of a column flotation cell.

2.5.1 Description of a column flotation cell

In industry, a column flotation cell is a vertical vessel typically 12 – 15 m in height and 0.5 – 3.0 m in diameter (Yianatos, 1989). A schematic representation of a column flotation cell is shown in the Figure 2.24. The feed slurry is fed at the top of the recovery zone and flows down to collide with rising bubbles generated at the bottom of the cell. After collision, hydrophobic particles attached to air bubbles rise into the froth zone (Dobby and Finch, 1985), while unattached particles are collected at the bottom of the column (tails).

The most distinctive features of the column flotation cell are the bubble generation system, the ability to generate a deep froth and the use of the wash water (Finch and Dobby, 1990). Unlike conventional flotation cells, bubble generation is achieved through the use of spargers, which can be internal or external.

Wash water is used for the following reasons (Nguyen and Schulze, 2004):

i. To provide a positive bias (downward flow): the net downward flow of water is bigger than in the concentrate flow. This action is believed to decrease the recovery of fine particles by entrainment.
ii. To replace the water which drains away from the froth layer, which is believed to increase froth stability.

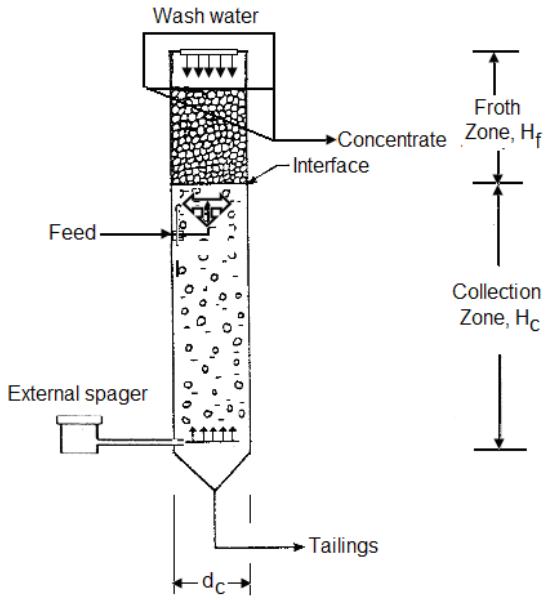

Figure 2. 24: General schematic of a conventional flotation column

2.5.2 Column flotation flow regimes

Volumetric flow rates in column flotation cells are generally converted to superficial velocities which are obtained by dividing the volumetric flow rate by the column cross-sectional area. This is believed to make possible any comparison between columns of different diameters (Finch and Dobby., 1990). As the gas is introduced into the column, there is displacement of the slurry. The volume generated is called the gas holdup (ε_g). The relationship between the gas holdup and the superficial gas rate (J_g) is widely used to characterize the flow regime of flotation cells and determine the operating gas rate range (Finch et al., 2007; Dahlke et al., 2005).

It has been found that the performance of a column flotation cell depends strongly on the prevailing flow regime; the following flow regimes were identified (Shah et al., 1982):

– Bubbly flow regime: This regime is characterized by uniformly sized bubbles with equal radial distribution,

– Churn turbulent regime: As the superficial air rate increases the homogeneity of the mixture can no more be maintained and large bubbles take the form of spherical caps with a very mobile and flexible interface.
– Slug flow: At high superficial air rate large bubbles are formed.

These regimes are shown in Figure 2.25. Column flotation cells have been found to operate efficiently under bubbly flow regimes (Finch and Dobby, 1990).

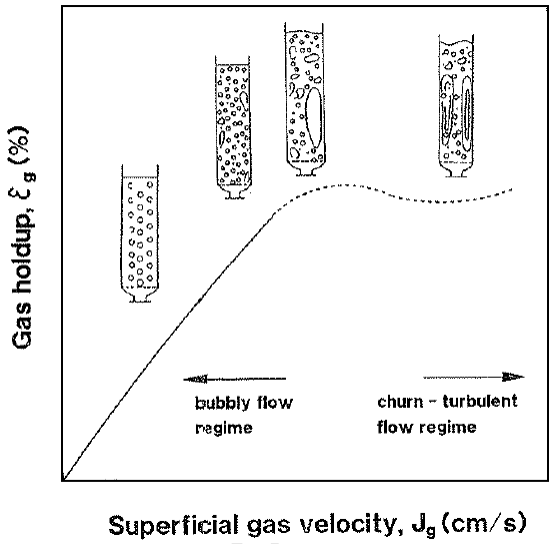

Figure 2. 25: Gas holdup as a function of gas rate (Finch and Dobby, 1990)

From Figure 2.25 it is apparent that for each column flotation cell, there is a superficial gas rate above which the flow regime will move away from the bubbly flow regime. In the following sections the effect of some parameters on performance of column flotation cells is reviewed.

2.5.3 Effect of air rate and frother dosage[3]

Air rate and frother dosage in a flotation column are important parameters, as they have a pronounced effect on the flotation performance.

The effect of increasing frother dosage and superficial gas rate is shown in Figure 2.26 (Finch et al., 1989). It can be seen that increasing the frother dosage is equivalent to increasing the superficial air rate, as it has similar effect on the

[3] Most of the variables discussed in section 2.4 are valid for the column flotation cell

gas hold-up. The very first increase of frother dosage or superficial gas rate will lead to the production of small bubbles. A further increase of frother dosage or superficial gas rate will result in the froth zone being depleted of gas, while the gas hold-up in the pulp zone increases. Increasing the frother dosage or superficial gas rate even more will lead to the loss of interface, because the gas hold up in the froth and the pulp zones will become equal. Following the loss of the interface, selectivity will be severely affected; this is the consequence of the gas hold-up being the same in the collection and froth zones.

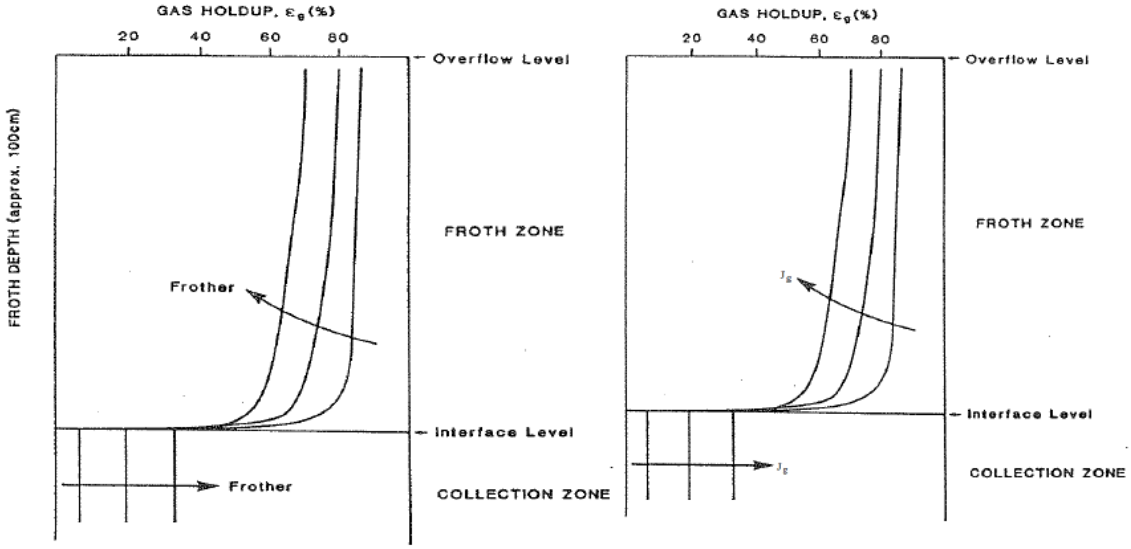

Figure 2. 26: Frother and superficial gas rate on gas hold up (Finch et al., 1989)

The upper limit of these parameters is specific to each flotation system. As pointed out by Xu et al. (1989) for each frother dosage there is an upper limit of air rate, over which the performance of the column flotation cell deteriorates.

2.5.4 Effect of superficial feed rate

An increase in superficial feed rate at fixed solids percentage increases the volume of solids into the column, which result in a decrease in the residence time of the solids in the froth phase (Goodall and O'Connor, 1991). The effect of the feed solids rate (superficial feed rate) is shown in Figure 2.27. It is apparent that as the feed rate is increased, the concentrate solids flow rate will increase until it

reaches a peak, after which it will drop, even though the feed solids rate continues to increase (Del Villar et al., 1989; Xu et al., 1996).

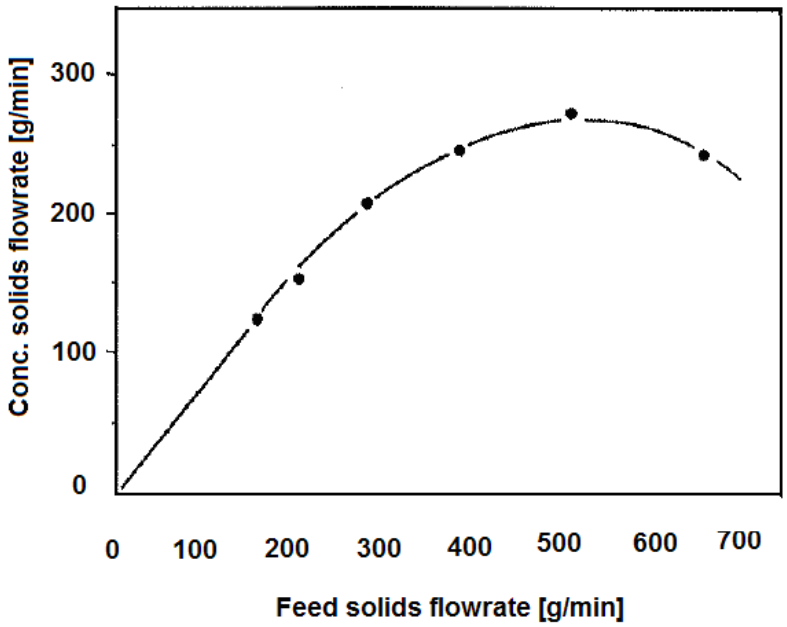

Figure 2. 27: Effect of feed solids flow rate on concentrate solids flow rate (Del Villar et al., 1989)

2.5.5 Effect of froth height

The combined action of wash water and deep froth allow column flotation cells to reduce considerably the recovery of fine particles by entrainment (Finch et al., 1989, 1995). This enables column flotation cells to have recovery by entrainment close to nil and hence produce much higher grades than conventional cells. This is illustrated in Figure 2.28 which shows tests performed to separate copper and nickel (Huls et al., 1989). It can be seen that, with an increase in froth depth, copper recovery decreased and the grade increased, due the rejection of nickel, which is unwanted in copper concentrate.

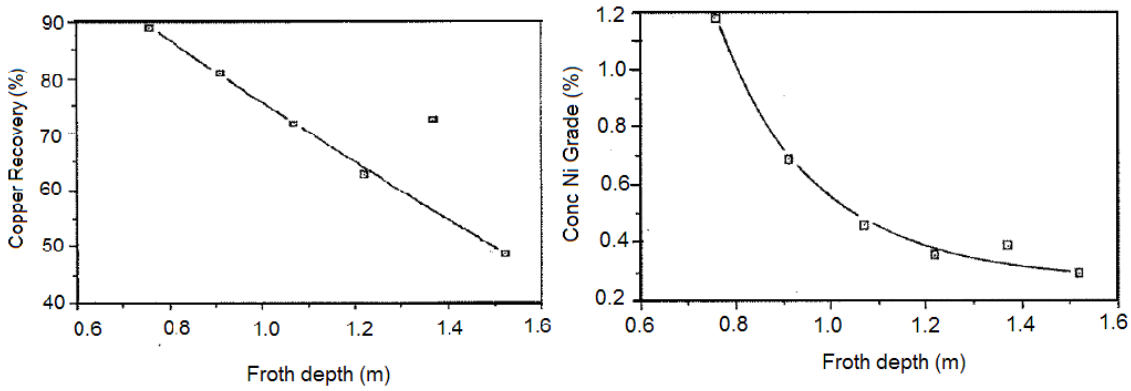

Figure 2. 28: Effect of froth depth on recovery and grade (Huls et al., 1989)

Even though increasing froth height is known to increases grades, too high froth height can result in a poor concentrate grade and the reverse situation can give rise to a reduced recovery due to decreased residence time of particles in the pulp (Tao et al., 2000).

2.5.6 Using a column flotation cell in this project

The key objectives of this study are to find separately the amount of gangue recovered by true flotation and entrainment in the flotation of a platinum ore, using the UCT methodology, and to find out how froth performance is affected by the depressant dosage. The use of a column flotation cell for this project offers the following advantages:

i. Deep froth is likely to make the froth effect easy to monitor and to minimise the recovery by entrainment.
ii. The column is run continuously, which allows the column to be operated under steady state.

In order to achieve the thesis objectives, the froth height and the depressant dosage will be varied independently. Unlike the batch flotation test, in a column flotation cell the froth is not scraped. Therefore it is expected that the implementation of the UCT methodology on a continuously-run column cell might hinder the flowing of the concentrate into the launder. Table 2.2 highlights the differences between batch flotation test and continuously-run column cell tests.

Table 2. 2: Batch flotation test vs. column continuous flotation test

Characteristics	Batch flotation	Continuous column cell
Concentrate collection mode	Scraping	Free Flowing
Feed grade	Being depleted	Remains constant during testing
Froth depth	Shallow	Deeper than in a conventional batch system
Froth characteristic	Changing	Steady state

From Table 2.2 it can be seen that the main constraint in increasing the depressant dosage on a continuously-run column cell is the ability to maintain a steady concentrate flow rate. Any increase of the depressant dosage has the potential to destabilize the froth phase (Bradshaw et al., 2005a) and severely affect the concentrate flow. Consequently the maximum depressant dosage attainable on a continuous column flotation cell needs to comply with the free flowing of the concentrate.

2.6 PLATINUM FLOTATION

In South Africa, platinum ores are extracted from the Bushveld Igneous Complex, the world's largest source of Platinum Group Metals. Several ore bodies are being mined for PGMs, but the most prominent are Merensky and UG2 ores.

The rock-forming minerals of the Merensky reef, which varies in composition according to its location, are comprised of roughly equal amounts of dark ferromagnesium silicate minerals and lighter aluminosilicate minerals (feldspathic pyroxene) and some chromite (Schouwstra and Kilnoch., 2000). The UG2 reef consists predominantly of chromite (60 to 90%), with lesser silicate minerals (5 to 30% pyroxene, and 1 to 10% plagioclase). Other minerals present in minor concentrations include phlogopite, biotite and the oxides (ilmenite, rutile and magnetite). Base metals make up a small percentage, with chalcopyrite, pyrrhotite, pyrite, pentlandite and less frequently millerite representing less than 0.1% (Schouwstra and Kilnoch, 2000; Penberthy et al, 2000).

Table 2.4 presents a mineralogical composition of UG2 and Merensky ores from Lonmin (Solomon, 2010). It can be seen that both ores contain less than 1 %

talc. But even in small percentage, the latter has been found to affect froth stability profoundly. It is evident that chromite is the most abundant mineral in UG2 ore while it represents only a small percentage in Merensky ore. It can also be seen that Merensky ore is characterized by higher base metal (sulphide minerals) content than UG2 ore.

The PGE (not shown in Table 2.3) are distributed unevenly throughout the Merensky and UG2 reefs in the Bushveld complex (Cawthorn, 2011). Due to their small percentage, they are usually expressed in parts per million (g/t). In Merensky and UG2 platinum ores, the PGE represent 3 to 11 g/t and 4 to 10 g/t respectively (Liddell et al, 1986).

Table 2. 3: Mineralogy composition of UG 2 ore (Solomon, 2010)

Mineral	Merensky Reef	UG2 Reef
	Composition [wt %]	
Pentlandite:$(Fe,Ni)_9S_8$	0.6	< 0.1
Pyrrhotite: $Fe_{0.95}S$	0.4	< 0.1
Pyrite: FeS_2	0.2	< 0.1
Chalcopyrite: $CuFeS_2$	0.3	< 0.1
Other sulphide	< 0.01	< 0.01
Orthopyroxyne: (Mg, Fe) SiO_3	45.9	12.8
Clinopyroxene	7.8	0.9
Olivine	0.6	0.2
Talc: $Mg_3Si4O_{11}(OH)_2$	0.1	0.3
Serpentine	1.2	1.6
Amphibole	0.7	0.2
Chlorite	1.5	2.8
Plagioclase: (Na, Ca) $(Si, Al)_4O_8$	33.4	14.5
Mica	0.7	0.74
Chromite: $FeO.Cr_2O_3$	5.03	62.1
Quartz	0.5	0.3
Oxides	0.6	1.1
Calcite	0.2	0.2
Other	0.6	2.3

In the flotation of PGM ores, the choice of reagents depends on many factors, but the determining factors are the downstream operations and the types of ore that are being processed. Typical reagent suites in PGMs flotation include thiol collectors (xanthates, sometimes with co-collectors dithiophosphate or dithiocarbamate); in some cases, copper sulphate is added as an activator; and polymeric depressants such as guar gum or carboxymethyl cellulose are added

to inhibit recovery of naturally floatable talcaceous gangue (Wills and Napier-Munn, 2006).

The flotation behaviour of platinum ore minerals is strongly linked to their mineralogical composition. In Merensky ore, for instance, talc and orthopyroxene have been identified as froth stabilizing components (Becker et al., 2009). Therefore the depression of gangue needs to be conducted carefully, as this has an adverse effect on valuable minerals recovery.

The high chromite content in the UG2 ore has the potential to cause serious metallurgical problems and only 3% of chromite is tolerated in the final concentrate (Ekmekçi et al., 2003). Therefore in processing UG2 Platinum ore, the main target is to keep the chrome grade compatible with downstream processes. Being an oxide mineral and naturally hydrophilic, chromite has low floatability and its passage into the concentrate is almost entirely by entrainment e.g. in the water between the bubbles. This was confirmed by Hay and Roy (2010 a, b) who found that chromite recovery could be described by a linear function and was strongly correlated with water and mass recovery. They found also that there was a similarity between the relationships of Cr_2O_3/water, Cr_2O_3/mass and water/ mass in laboratory flotation tests.

Although chromite has been recognized as hydrophilic its recovery by true flotation is possible under two conditions:

i. Copper sulphate could inadvertently activate chromite and the subsequent addition of collector could result in high recoveries of chromite in contrast to the low recoveries obtained in the absence of copper sulphate (Wesseldijk et al, 1999).

ii. The presence of hydrophobic talc residual layers, similar to those found on orthopyroxene surfaces, probably from partial alteration, could change the surface properties (hydrophobicity) of chromite totally (Jasieniak and Smart, 2010; Opobou-Lando, 2010).

This thesis will investigate the effect of depressant dosage and froth depth on the froth performance in the flotation of PGM ores.

2.7 SUMMARY

Various methods can be used to quantify separately the amount of gangue recovered by true flotation and entrainment. Because of the nature of platinum bearing ores[4], only a few of the methods reviewed in this chapter can be consider for this purpose. The UCT method (Oostendorp et al., 2005) is of particular interest as it is based on the use of high depressant dosage. This is important for platinum ores which contain a significant proportion of floatable gangue minerals. In this method it is assumed that at high depressant dosage, the floatable gangue minerals are totally depressed, consequently the recovery of gangue minerals can be consider to be by entrainment only.

The JKMRC method (Savassi et al., 1998) is also of interest as it requires the presence of a non-floatable tracer. Due to its hydrophilic properties, chromite could be potentially used as a tracer in the flotation of the UG2 ore, on the condition that chromite is proved to be recovered solely by entrainment.

Froth stability is a key driver of flotation performance. Previous workers (Dippenaar 1982 a, b; Johansson and Pugh, 1992, Schwartz, 2004; Ata et al., 2004) have found that particle hydrophobicity is one of the important factors affecting froth stability. Hydrophobicity can be natural or induced via flotation reagents (collectors or depressant). Most of previous work reviewed in this chapter was performed on synthetic systems (i.e. not using real ores) or on a batch scale. In this thesis the effect of depressant dosage on froth performance will be monitored using an experimental set-up closer to a true system; e.g. using real ore and a continuously-run column flotation cell.

[4] Refer to section 2.7 for details about platinum ores

This review has shown that froth stability measurement is not a straightforward exercise. Various techniques can be used for this purpose, but in this thesis “water recovery” and the “UCT SmartFroth® system” will be employed. These techniques are of particular interest as they are not invasive.

This review showed also that froth recovery is an important measure of froth performance, as it affects the overall flotation performance. This thesis will seek to unravel how froth recovery is affected by depressant dosage. The froth depth varying technique will be used to evaluate froth recovery (Vera et al., 1999b).

CHAPTER THREE: PRELIMINARY WORK

3.1 INTRODUCTION

The first two objectives of this thesis were to establish the "UCT method" on a continuously operated column cell, and to develop a strategy using the UCT method for studying the relationship between froth performance and the properties of particles in the pulp phase. These two objectives were addressed during preliminary tests done in the laboratory at UCT. This chapter describes the equipment and materials used in the preliminary work, the experimental methodology that was developed and the results obtained. The experiments were mostly concerned with the determination of the appropriate operating parameters of the column e.g. air flow rate, feed flow rate, froth depth and reagent (frother and depressant) dosages for the PGM ore that was used in the tests.

The aims of the laboratory preliminary work were the following:

- To commission the column cell and determine suitable operating parameters (air and feed flow rates, froth depth, reagent dosages) for the PGM ore being used in the tests.
- To determine the highest depressant dosage attainable during the operation of the continuous column flotation cell, while maintaining a steady froth depth. This was necessary because depressant dosage is a key parameter of the experimental methodology used in this project (UCT method).
- To establish the UCT method on the continuously operated column cell.
- To use the UCT machine vision system (UCT SmartFroth®) as a froth stability indicator, in addition to water recovery measurement.
- To establish a procedure/strategy for studying the relationship between froth performance and the properties of particles in the pulp phase.

The work was complicated by the fact that milling had to be carried out at Stellenbosch University (60 km from UCT), as there was no big mill at UCT. This meant that the flotation tests had to be carried out at a lower pulp density than might otherwise have been the case. Nevertheless the work proceeded successfully as described in the remainder of this Chapter.

3.2 EQUIPMENT

This thesis used much of the same equipment as used by Anderson et al. (2009) in their study of an oscillatory baffled flotation column. The main items were the 100 mm diameter PVC column cell, a 550 L feed tank and a 500 L tailings tank, two peristaltic pumps, a centrifugal pump and an in-line mixer. These items are described in the following sections, followed by a brief description of the ancillary equipment (crusher, mill) used to prepare the feed for the column tests.

3.2.1 Process Flow Diagram

A flow diagram of the rig is shown in Figure 3.1. The rig was set up for continuous operation, to allow steady-state operation of the column cell. This meant that a single set of froth performance measurements could be made for each set of operating conditions. Operating the column in a batch mode would have made it very difficult to measure the froth performance, which would have been changing all the time.

Peristaltic pumps were used to introduce the feed into the column and to withdraw the tails. The tails were withdrawn from the base of the column and were collected in a 500 L tank. Air was added using a static in-line mixer through which part of the tails was pumped using a centrifugal pump. The level control of the pulp was achieved through a potentiometric level controller (L/C) which measured the difference in conductivity between the froth and the pulp phases. A 200 A halogen light and a video camera were used to capture froth images for analysis using the UCT SmartFroth® system.

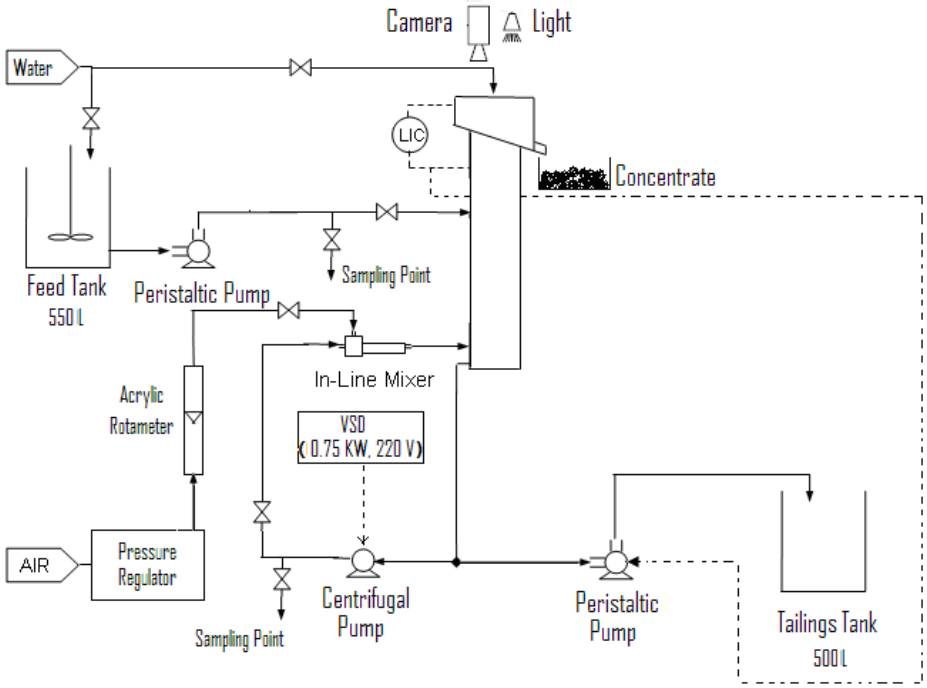

Figure 3. 1: Flow diagram of experimental apparatus

3.2.2 Column Cell

A schematic of the 10 cm diameter flotation column is shown in Figure 3.2. The column was made of a clear PVC section, through which the position of the pulp-froth interface could be distinguished visually during column operation. The feed point was situated 45 cm below the top of the column. The distance from the feed point to the air inlet (in-line mixer), termed the collection zone, was kept constant during the column operation. The air inlet was positioned 10 cm above the column base. The concentrate was allowed to overflow freely into the launder.

Removable extension parts (Figure 3.3) could be placed at the top of the column as required, to increase the froth height without changing the volume of the pulp. The extension parts of the column were not used during the preliminary tests in the laboratory; they were used only during the site tests (see Chapter 4 below).

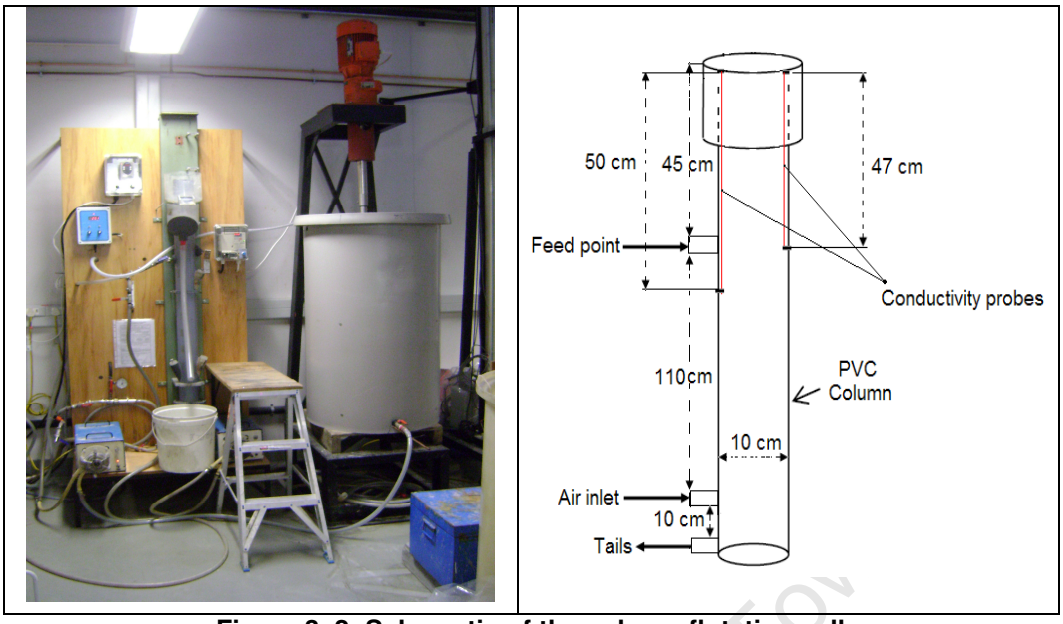

Figure 3. 2: Schematic of the column flotation cell

Figure 3. 3: Removable extensions for the column cell

3.2.3 Feed and Tails Tanks

A 550 L plastic tank with a mixer was used for holding and conditioning the feed slurry. Mixing was provided by a 2.2 kW three phase motor coupled to a variable speed drive, as shown in Figure 3.4.

Figure 3. 4: Mixing tank

A similar but slightly smaller plastic tank was used to collect the tailings from the column.

3.2.4 Feeds and Tails Pumps

Two single phase Masterflex peristaltic pumps (Figure 3.5) were used for feed and tails (pumping capacity 0 – 10 L/min). The feed rate was fixed to around 2.5 L/min and the tails rate was adjusted automatically by the level controller.

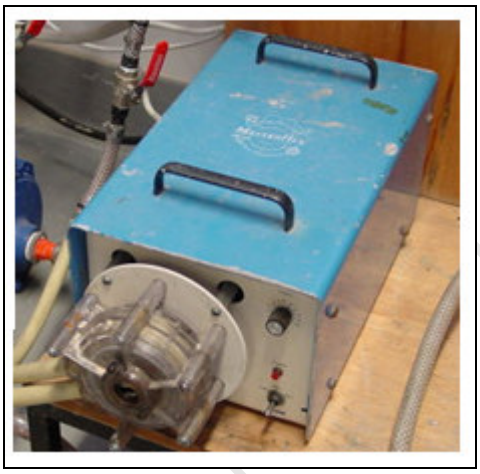

Figure 3. 5: Peristaltic pumps used for feed and tails

3.2.5 Bubble Generation System

The bubbles for flotation were generated outside of the column using a static in-line mixer (shown in Figure 3.6) similar to the one used in the JKMRC High Bubble Surface Area Flux Flotation Cell (Vera et al.,1999a). A centrifugal pump was used to pump a part of the tailings slurry through the in-line mixer at high pressure, and into the base of the column.

The inline mixer was made of two concentric steel tubes; a larger outer tube carrying the slurry and a smaller inner tube carrying the air. The inner tube was perforated and covered tightly by a porous rubber tube. The in-line mixer produced bubbles by mixing air with slurry drawn from the tail line. The resulting air-slurry mixture was introduced to the base of the column through a distribution nozzle. The air flow rate could be adjusted by means of a valve upstream of the static mixer while the slurry rate was controlled by the variable speed drive

coupled to the centrifugal pump. The resulting bubble size distribution was a function of the air flow rate, the slurry flow rate and the frother concentration in the pulp (Vera et al., 1999a).

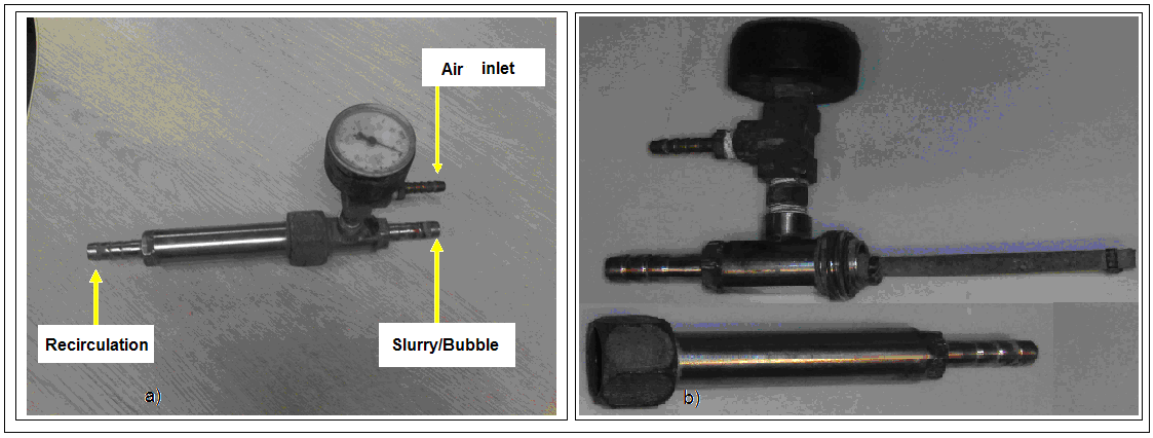

Figure 3. 6: In-line mixer-a) Fully assembled-b) Dismantled

3.2.6 Level Controller

The level of pulp in the column was controlled utilizing the difference in conductivity between the pulp (strong electrolyte) and the froth (weak electrolyte) phases. The level control system consisted of a potentiometric level measurement device and a PI controller. The conductivities were measured by two nickel-chrome electrodes installed inside the column walls. This system produced a linear output (0 to 4 V) proportional to the position of the pulp along the chrome/nickel electrodes. This signal was sent to the PI controller which adjusted the speed of the tails pump to maintain the desired set point. Even though the output could in theory be affected by the pH and the conductivity of the solution, in practice the system was found to maintain the pulp level at the desired value over extended periods of time.

3.2.7 UCT SmartFroth ® System

The UCT SmartFroth ® system was used as a complement to the measurement of froth stability provided by water flow rate measurement. The UCT SmartFroth ® system consists of a video camera and a 200 A halogen light. The camera records the image of froth surface, which is illuminated by the halogen light. The recorded images were analysed off-line using SmartFroth ® software. The

analysis of the footage provides the *Stability Correlation Peak* which is an indication of the stability of the froth phase.

3.2.8 Sampling Points

Samples were collected in 5 L buckets. The feed sample was collected from the feed tank while the slurry was being conditioned; the concentrate samples were collected from the froth launder; and the tails samples were collected just before being diverted into the tailings tank.

3.2.9 Crusher

A Sturtevant jaw crusher (shown in Figure 3.7) in the Department of Geology (University of Cape Town) was used to crush the ore sample as received at UCT from ± 70 mm to ± 10 mm. A spade was used to mix and split the product manually into 60 kg plastic bags. A total of 33 bags were obtained.

Figure 3. 7: Jaw crusher

3.2.10 Mill

After crushing, samples were milled in the laboratory of the Department of Process Engineering at the University of Stellenbosch. A 0.42 m internal diameter ball mill of 1.04 m length was operated continuously in closed circuit with a 106 micron screen (Figure 3.8). Five sets of mild steel balls, 20, 30, 40, 50

and 60 mm in diameter, were used. The mass of balls in each set was 8, 23, 68, 75 and 90 kg respectively.

The mill was operated at 60 % critical speed (45 rpm). The feed rate was set initially to 50 kg/h and progressively adjusted such that the recirculation rate was approximately 2 to 3 times the feed rate. For each flotation run, 60 kg of ore were fed, but only 40 kg were collected. The loss was due to the time (30 min) allowed for the mill to reach steady state.

After steady state was attained, the under flow of the screen was collected in 20 L buckets, while the overflow was recirculated into the mill; this procedure was continued until there was very little material on the screen. Twenty-five buckets of slurry were collected for each flotation run, which was conducted the on the following day at UCT.

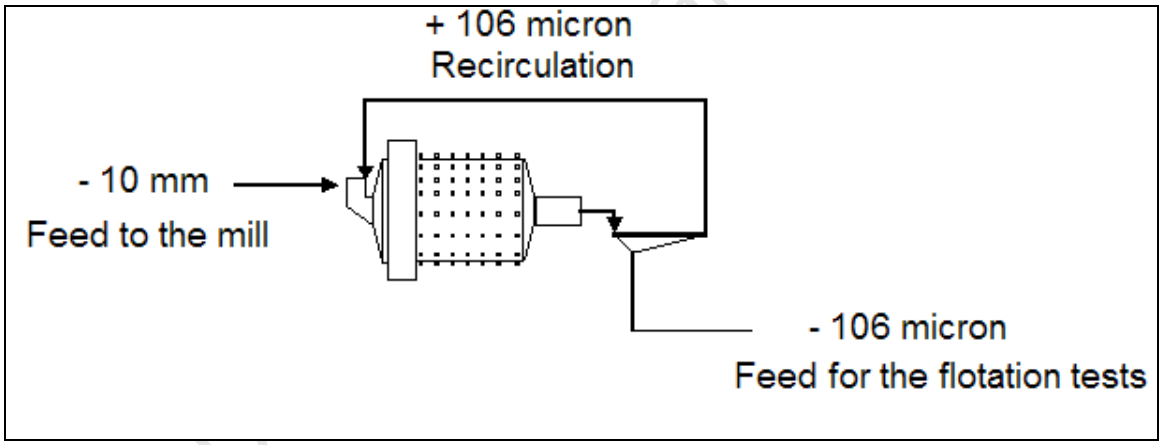

Figure 3. 8: Ball Mill circuit used during preliminary tests

3.3 MATERIALS

3.3.1 Feed Ore

Merensky ore from the Rowland shaft (Lonmin PLC/Rustenburg, South Africa) was used throughout the preliminary tests. Two tons of ore was received from Lonmin, of particle size ± 70 mm diameter. The ore sample was transported to

Cape Town by truck in four plastic drums which protected it from any kind of contamination.

3.3.2 Mineralogy

Merensky ore contains approximately 1% sulphide minerals in the form of chalcopyrite, pentlandite and pyrrhotite; the PGEs are believed to be associated with these sulphide minerals (Wiese et al., 2007). The remainder of the ore is comprised of gangue minerals. A typical QEMSCAN analysis of the Lonmin Merensky ore used in the preliminary tests is shown in Table 2.3 (Chapter 2). It is clear that the ore is dominated by the silicate minerals: 87.2% of the ore is made up of siliceous minerals (i.e. orthopyroxene, plagioclase, clinopyroxene and talc). It is known that talcaceous minerals (orthopyroxene and talc) are naturally floating (Becker et al., 2009), which makes their depression problematic since they contribute to the stability of the froth phase.

3.3.3 Reagents

Cape Town tap water was used in all the preliminary laboratory flotation tests. The following flotation reagents were used:

- Collector: Sodium ethyl xanthate (SEX) supplied as powder by Senmin. 1% solutions of the xanthate collector were prepared using distilled water. The required amount of collector was delivered to the feed tank using a 500 mL syringe.
- Depressant: Carboxyl methyl cellulose (CMC) supplied by Senmin as powder (Dep 267). 1% solutions of depressant were prepared by hydrating the required amount of powder in distilled water for two hours, using a magnetic stirrer. A 2000 mL beaker was used to deliver the depressant to the feed tank.
- Frother: Dowfroth 250 supplied by Senmin was used as received; preparation was not required. Frother was added using a 10 mL syringe.

NB: Collector and depressant were prepared daily.

3.4 OPERATING PROCEDURE

3.4.1 Commissioning Tests

The first stage of commissioning the rig was done using water; to detect any leakage and to ensure that the column was running perfectly. Ore was used only in the second and third stages, to find acceptable levels for the operating parameters of the column: volumetric feed rate, volumetric air rate and froth depth. The starting points for the operating parameters were the values used on the same equipment by Anderson et al. (2009). After commissioning, the parameters listed in Table 3.1 were kept constant for the remainder of the tests.

Table 3. 1: Column tests fixed parameters

Fixed Parameters	Value or Type
Froth Depth	100 mm
Feed solids percentage	10 %
Collector Dosage [SEX]	100 g/t
Water	Tap water
Volumetric air rate	3 L/min
Volumetric feed rate	4 L/min

The parameters showed in Table 3.2 were changed.

Table 3. 2: Column operating variables

Operating variables	Value
Frother Dosage [DowFroth 250]	16, 20, 25 ppm
Depressant Dosage [CMC Dep 267]	0, 100, 300,500 g/t

3.4.2 Initial Runs

In developing the methodology for studying the relationship between the froth performance and the properties of the pulp phase, two procedures were trialled. The first runs were performed as follows.

For each run, twenty-five buckets each containing 20 L of pulp were poured into the 550 L feed tank, while mixing to avoid settling. Tap water was added to make up the final solids content to 10% using a densimeter to evaluate the solids percentage. The tests were performed at this low pulp density because the samples had to be milled at University of Stellenbosch; operating at a high pulp

density would have meant several trips to Stellenbosch in a day. Reagents were added to the feed tank in the following order: first 100 g/t of collector, after which the slurry was allowed to condition for 20 min; secondly 16 ppm of Dowfroth 250, after which the slurry was conditioned for a further 5 min before flotation testing began. The tests were started without any depressant addition.

While the slurry was being conditioned, the column cell was filled with water and the air flow and recycle pump were turned on. The level controller was set so as to have 100 mm froth height. The pulp was introduced into the column after sampling the feed off-line. After the first froth overflowed in the launder, the rig was allowed to operate for 2.5 residence times (≈ 13 min) in order to achieve steady state before samples were taken.

Full-stream samples of tails and concentrate were taken simultaneously. Five samples of each stream were collected. The time between sample collections was two minutes. The concentrate samples were collected over 2.5 min and the tails samples over 45 seconds.

The first feed sample was collected off-line (before the pulp was fed into the column) and the second feed sample was collected at the end of the flotation test. Feed samples were collected over 45 seconds.

When sampling was completed the column was emptied and flushed with water, while the contents of the feed tank continued to be mixed to avoid settling. Depressant was then added to the feed tank to make up a dosage of 100 g/t after which the procedure described above was repeated; and then again for the remaining depressant dosages (300 and 500 g/t).

This procedure was long and consumed a lot of slurry. It was decided to adopt the procedure that is described below instead.

3.4.3 Final Procedure

Unlike the initial procedure (section 3.4.2), each run was continued without shutting down the column after the collection of the first set of samples (test with no depressant added).

After the first set of samples had been collected, the volume and % solids of the slurry remaining in the feed tank were measured, and depressant was added to the feed tank to make the dosage up to 100 g/t. The column was allowed to reach steady state for 2.5 residence times (≈ 13 min), after which samples were again collected as described above. More depressant was added to the feed tank to make the dosage up to 300 g/t and the procedure was repeated; and then again for 500 g/t. This technique allowed 4 different operational conditions (tests) to be carried out for one feed tank (one run).

At the end of the final condition, the feed to the column was switched off and a second feed sample was collected. The circuit was then flushed with water in order to remove any solids from the recycle line before the column was emptied and shut down.

All samples were weighed, filtered, dried and weighed again in the UCT laboratory. Dried samples were assayed for nickel and copper using Atomic Absorption Spectroscopy (AA) and sulfur using a LECO Sulfur Analyser; all in the Department of Chemical Engineering at UCT.

A total of 10 runs and 40 tests were performed over a period of six months. Various air rates, froth heights, frother dosages and recycle rates were tested in the laboratory at UCT during this time. These changes were pursued until the column operation was satisfactory. In this Chapter the results of only four runs and 15 flotation conditions (tests) judged as satisfactory are presented. Table 3.3 below summarizes the values of the operating variables during these tests.

Table 3. 3: Summary of the preliminary tests

Test	Run	Frother Dosage [ppm]	Depressant Dosage [g/t]	Solids Percentage [%]
1	A	5	0	10
2	A	5	100	10
3	A	5	300	10
4	B	16	0	10
5	B	16	100	10
6	B	16	300	10
7	B	16	500	10
8	C	20	0	10
9	C	20	100	10
10	C	20	300	10
11	C	20	500	10
12	C	25	0	10
13	D	25	100	10
14	D	25	300	10
15	D	25	500	10

3.5 RESULTS AND DISCUSSION

3.5.1 Feed characteristics

Feed samples collected from the 550 L feed tank prior to each run were weighed wet and dry, and split into sub samples. Randomly selected sub-samples were sent to the laboratory for assay while others were combined and split into seven size fractions, namely + 214 µm, - 212 µm + 150 µm, - 150 µm + 106 µm, -106 + 75 µm, -75 + 53 µm, - 53 µm + 38 µm and – 38 µm. Because the flotation tests were conducted on different days, every effort was made to keep the milling conditions (dilution, recirculation, ball charge…) constant; however, differences in the milled product were noted. A typical size distribution of the ball mill discharge is presented in Table 3.4. It can be seen that all particles were smaller than 212 µm and that the particles finer than 38 µm represented the most abundant size fraction; this is an indication that the feed was fine (65 % -75 µm).

Table 3. 4: Typical size distribution of the ball mill discharge

Feed size fraction i	% mass size i
+ 212 µm	0.00
- 212 + 150 µm	1.97
- 150 + 106 µm	10.03
- 106 + 75 µm	22.91
- 75 + 53 µm	16.14
- 53 + 38 µm	10.89
- 38 µm	38.06
Total	**100**

The fineness of the feed is further confirmed by Figure 3.9 which presents the cumulative percent passing versus screen size. It is apparent that P_{60} = 60 µm is slightly finer than the P_{60} = 75 µm used in most PGM flotation plants.

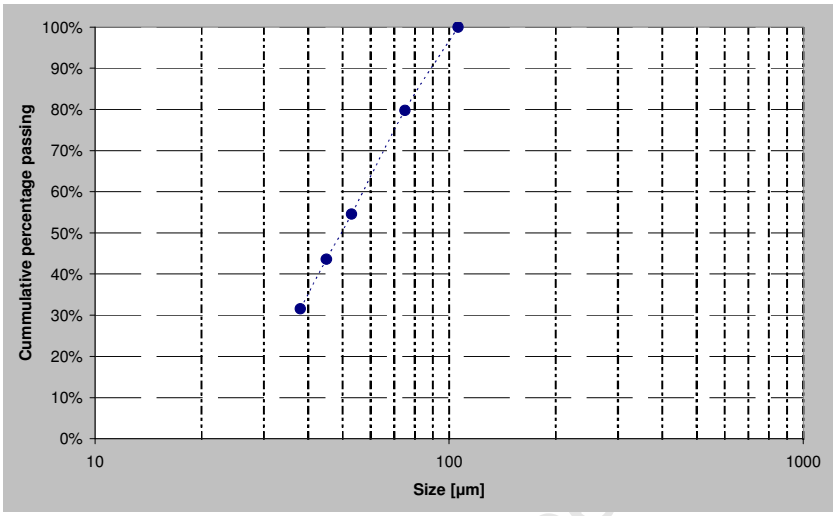

Figure 3. 9: Cumulative percentage passing as function of particle size

3.5.2 Flotation test results

3.5.2.1 Validation of flotation test procedure

Figures 3.10 to 3.13 show the results of the four runs carried out as part of the preliminary work, in which the 15 different reagent combinations listed in Table 3.3 were investigated. The X-axis represents the run time, the Y-axis represents the solids and the water flow rates and the depressant dosages (g/t) are indicated at the top of each plot parallel to the X-axis. Frother dosages of 5, 16, 20 and 25 ppm were tested and the depressant dosages investigated were 0, 100, 300 and 500 g/t. A spreadsheet of the results can be found in Appendix A.

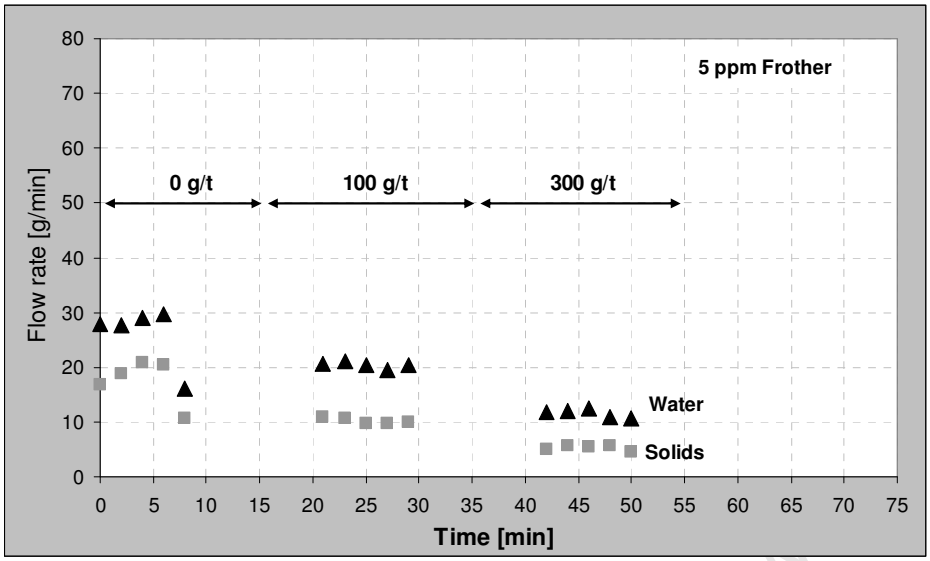

Figure 3. 10: Effect of CMC depressant on concentrate mass and water flow rates at 5 ppm of frother

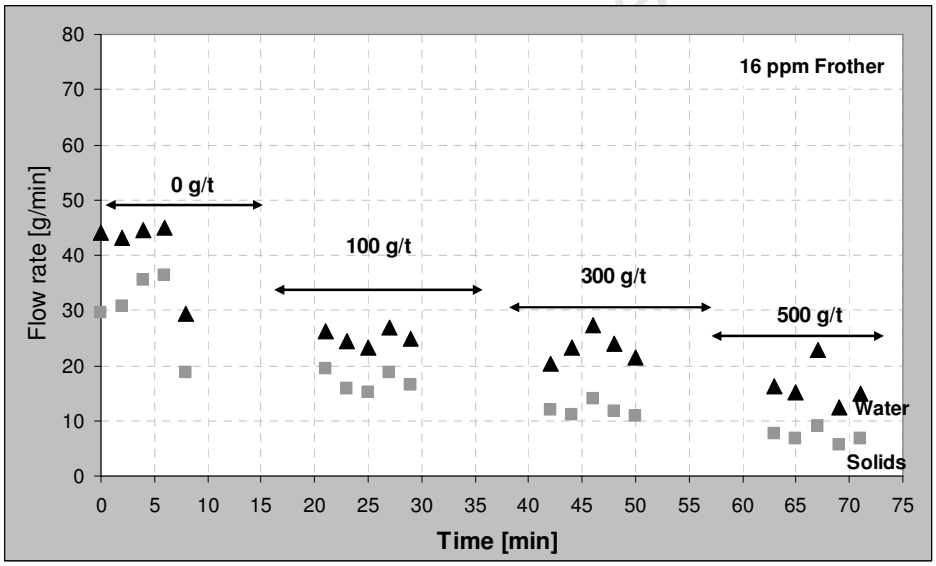

Figure 3. 11: Effect of CMC depressant on concentrate mass and water flow rates at 16 ppm of frother

Increasing the frother dosage (from 5 to 25 ppm) resulted in an increase in water recovery, particularly at low depressant dosage, with a corresponding increase in mass recovery. This indicates a more stable froth, which is consistent with previous work on the effect of frother dosage on water and mass recovery (see section 2.3.2).

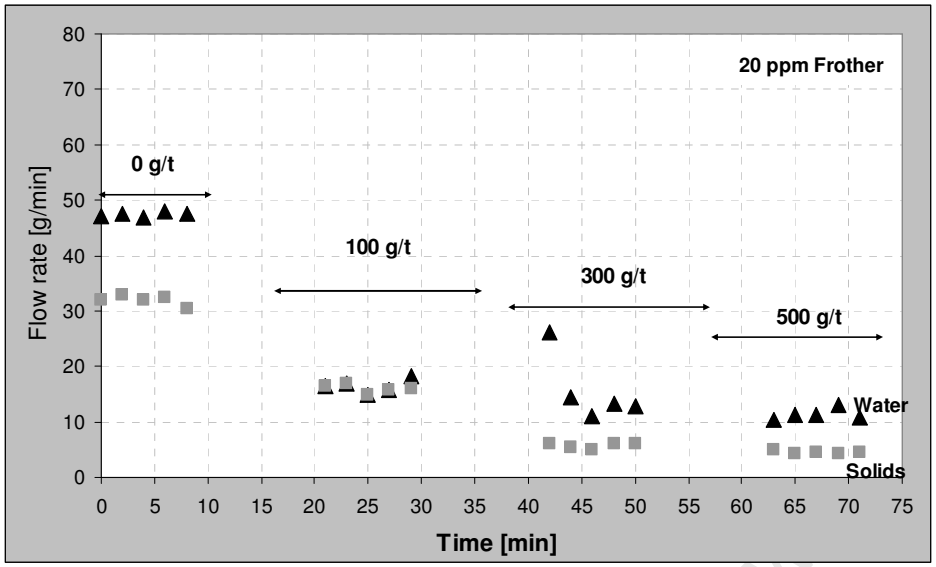

Figure 3. 12: Effect of CMC depressant on concentrate mass and water flow rates at 20 ppm of frother

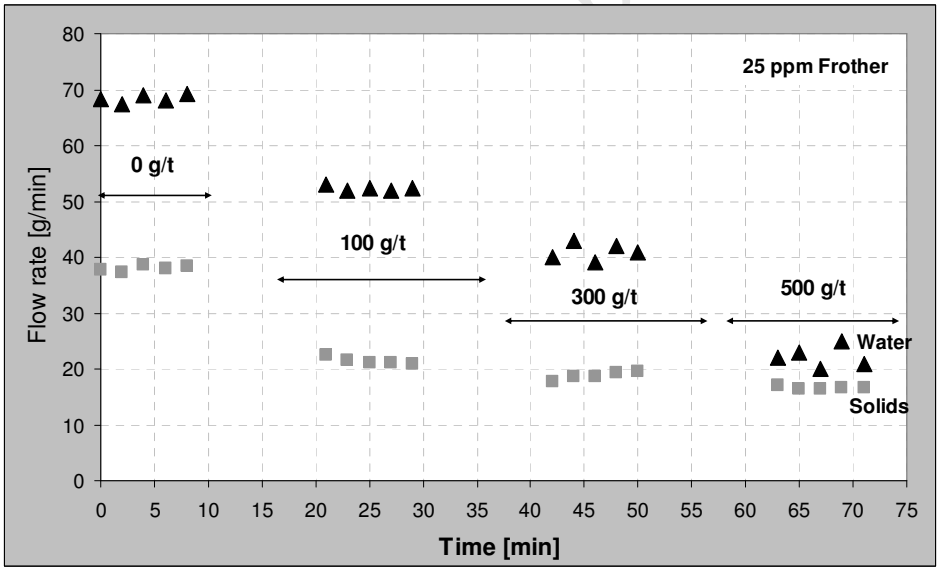

Figure 3. 13: Effect of CMC depressant on concentrate mass and water flow rates at 25 ppm of frother

When carrying out these tests, the major concern was whether or not the froth would survive at high depressant dosage. It was found that the test operated at 5 ppm (Figure 3.10) could not sustain 500 g/t of depressant as this led to the froth ceasing to overflow freely into the concentrate launder.

Concurrently with water and solids recovery measurement, the UCT SmartFroth® system was used to monitor the froth stability during each run as the depressant dosage was increased. The results are shown in Figure 3.14. The 'correlation peak' information can be used as an indication of froth stability: *as the 'correlation peak' rises, the froth gets more stable* (Morar et al., 2005). The X-axis represents the time during which pictures were sampled for analysis using the UCT SmartFroth® software. The graph represents the stability correlation peak of the points (sampled pictures) and pink line represents their average.

It is evident that for all the tests, irrespective of the frother dosage, there was a sharp decrease in the correlation peak on going from 0 to 100 g/t of depressant. There was a smaller drop in going from 300 to 500 g/t depressant dosage. It can also be seen that the stability correlation peaks are related to frother dosage: they are the higher at 20 and 25 ppm than at 5 and 16 ppm. This is consistent with the froth stability measurement indicated by the water recoveries.

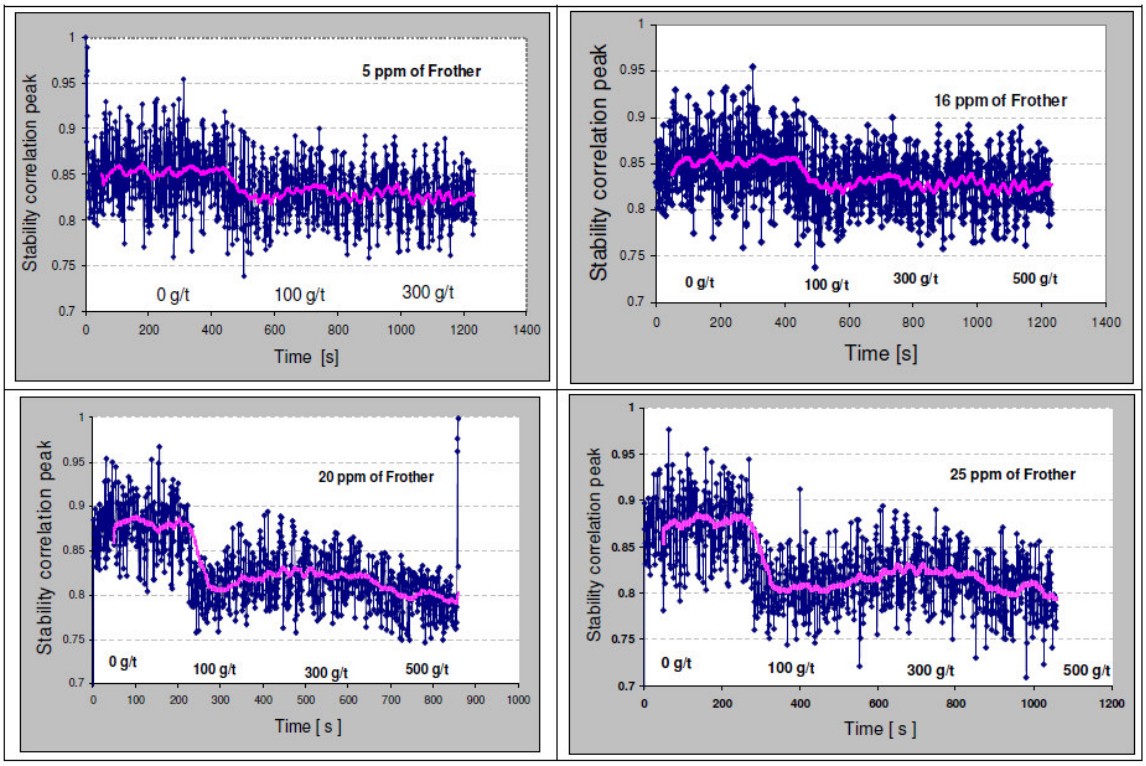

Figure 3. 14: Effect of depressant dosage on froth stability at different frother dosages: output of UCT SmartFroth software

Figure 3.15 shows the structure of the froth at 16 ppm frother dosage as captured from the video footage taken by the UCT SmartFroth® system (Points a, b, c and d) correspond 0, 100, 300 and 500 g/t of depressant respectively, it is clear that froth shed particles as the depressant dosage was increased.

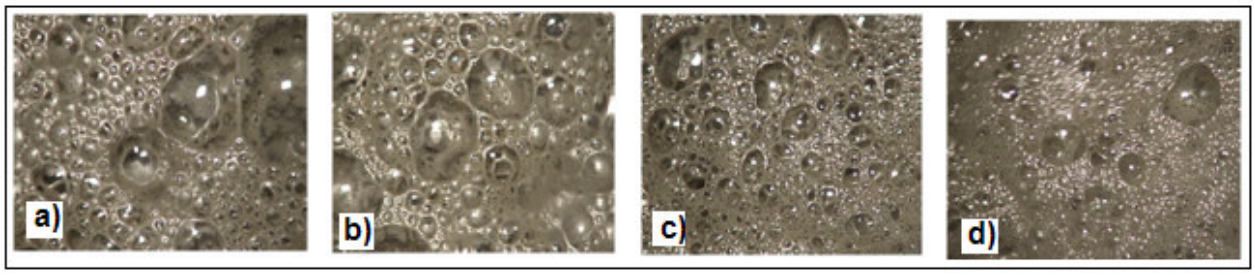

Figure 3. 15: Froth structure at different CMC depressant dosages : a) 0 g/t, b) 100 g/t, c) 300 g/t and d) 500 g/t

3.5.2.2 Effect of depressant dosage on flotation performance

Figures 3.16 and 3.17 present the effect of depressant dosage on water and solids flow rates at different frother dosages. Each point is the average of the five points shown in Figures 3.10 to 3.13. It is clear that at each frother dosage tested, the mass and water flow rates decreased as the depressant dosage was increased; irrespective of the actual frother dosage. This result was expected because previous researchers found similar results on the same ore in a 3L batch flotation cell (Bradshaw et al., 2005 a, b; Wiese et al., 2005, Wiese et al., 2010). In this sample of Merensky ore, 87.20 % of the material is floatable gangue minerals (see section 2.7 for more details), and depression (i.e. removal) of the floatable gangue particles from the froth phase would make the froth phase less stable, resulting in less solids and water being recovered.

The maximum depressant dosage (500 g/t) was determined by the ability of the concentrate to overflow freely into the launder. It was observed that with more than 500 g/t of depressant (not shown) the mobility of the froth was severely reduced: this led to the selection of 500 g/t of depressant as the maximum depressant dosage. In previous work using batch cells, the depressant dosage

was able to be increased without any froth mobility consideration, as the concentrate was scraped manually. However Oostendorp et al. (2005a, b)[5] found that 300 g/t was enough to depress all the floatable gangue minerals.

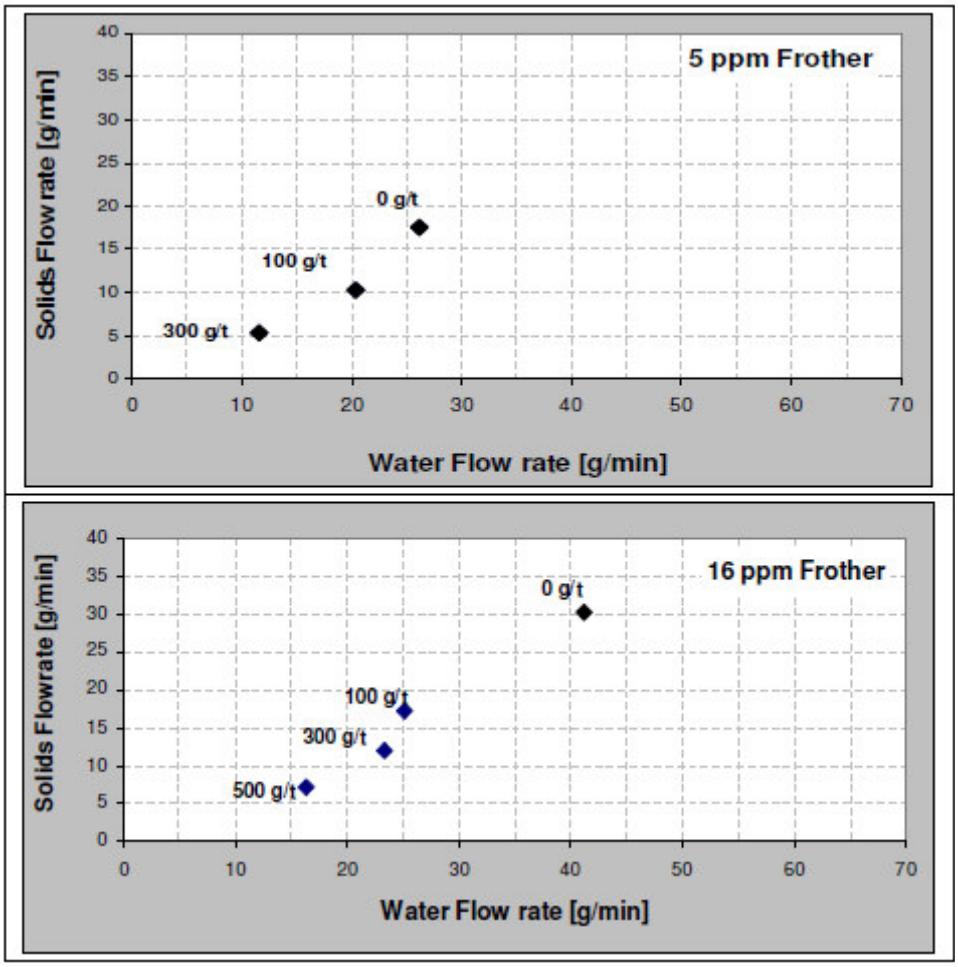

Figure 3. 16: Effect of depressant dosage on solids and water flow rates at 5 and 16 ppm frother dosage

Figure 3.18 plots the solids vs. water flow rate for all fifteen tests described above. Each depressant dosage is represented by four points (corresponding to four frother dosages), except for the 500 g/t of depressant which has only 3 points, because the froth failed to survive at 5 ppm of frother.

[5] For more details refer to section 2.4.1.7

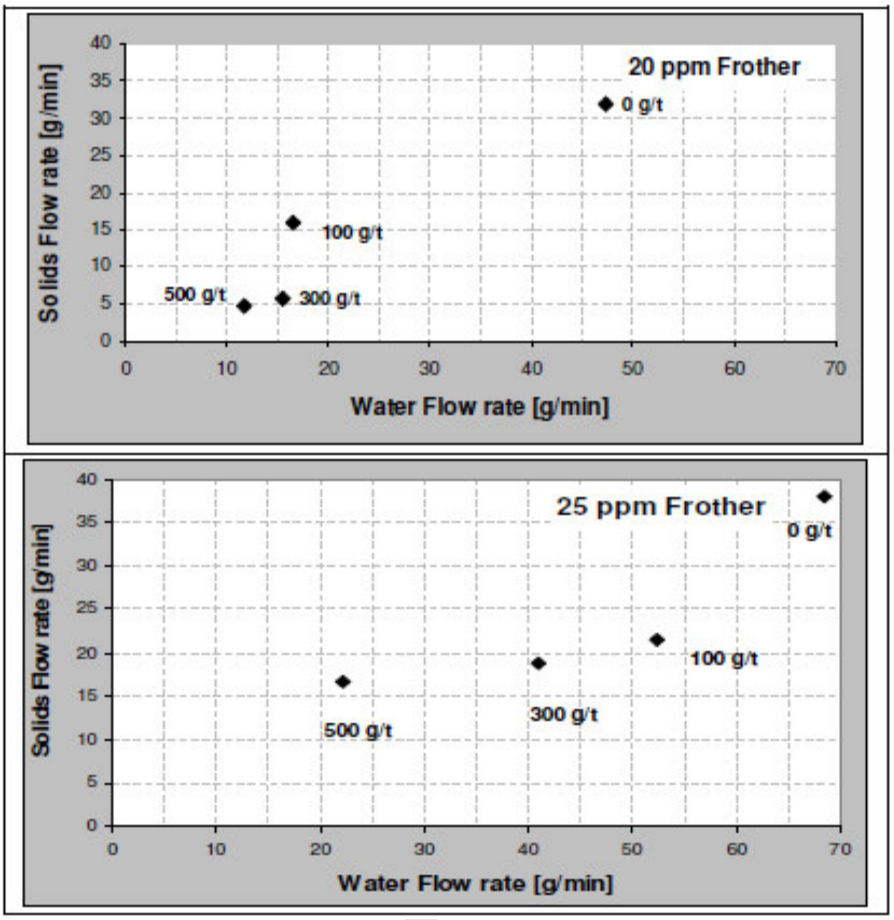

Figure 3. 17: Effect of depressant dosage on solids and water flow rates at 20 and 25 ppm frother dosage

It can be seen that with an increase in depressant dosage from 0 to 500 g/t at any fixed water flow rate, solids recovery decreases. It can also be seen that two of the three points at 500 g/t of depressant, are well aligned with the series of points at 300 g/t depressant (dotted line). This observation leads to the possible conclusion that 300 and 500 g/t depressant dosage gave similar results. The coefficient of correlation between these points was found to be close to unity, confirming the linearity between water and mass flow rates at 300 g/t (and 500 g/t); in addition the equation obtained passes very close to the origin, suggesting that the gangue is recovered by entrainment only.

Comparison between Figure 3.18 and Figure 2.12 (Chapter 2) shows that the two sets of results are in agreement. It can be inferred that the UCT methodology has

been established and can be applied on a continuously-run column flotation cell. No attempt was made to calculate separately the amount of gangue recovered by true flotation and entrainment. This was done during the next phase of the tests in which the column was operated on a mine site (Chapter 4).

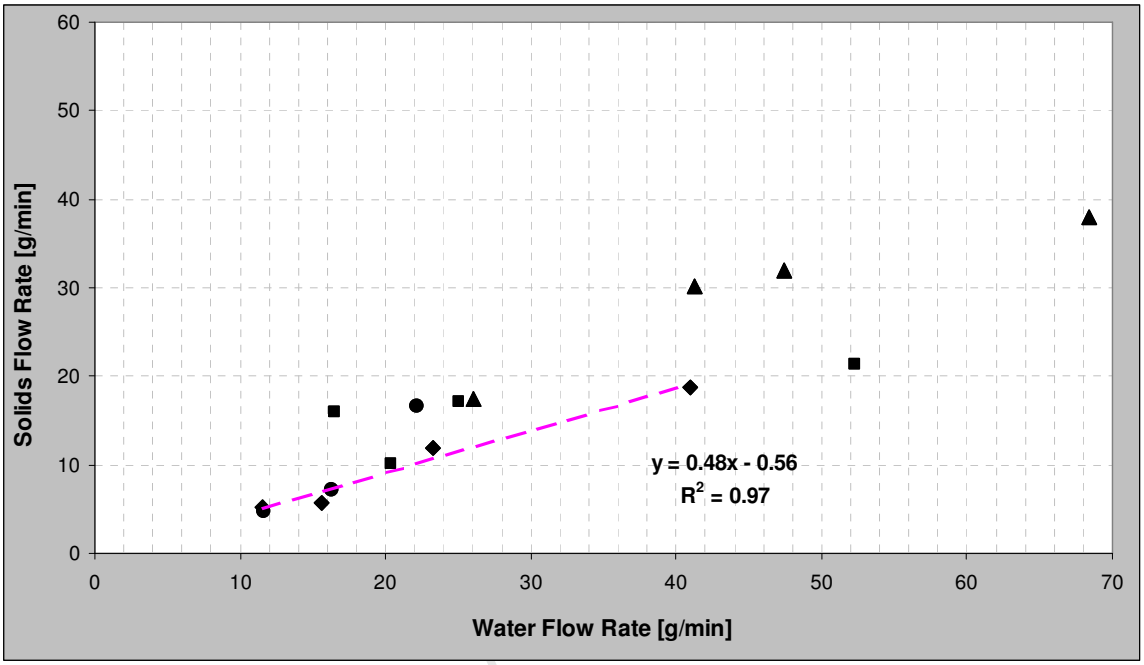

Figure 3. 18: Effect of depressant dosage on water and solids flow rates at 0, 100, 300 and 500 g/t depressant (▲ = 0 g/t, ■ = 100 g/t, ♦= 300 g/t, ● = 500 g/t)

3.5.3 Effect of depressant dosage on recovery and grade of copper and nickel

Figures 3.19 to 3.22 plot the recoveries of copper and nickel during each of the runs reported above. The X-axis represents the run time and the Y-axis represents the recoveries of the base metals. It can be seen that the recoveries of copper remained higher than the recoveries of nickel for all the tests. This was expected as the flotation rate of chalcopyrite is known to be very rapid and pentlandite is considered to be a slow floating sulphide (Wiese et al., 2006a).

It can be also seen that increasing the depressant dosage did not affect the recoveries of base metals negatively for all the frother dosages tested. On the

other hand, the grade of copper and nickel increased as the depressant dosage was increased, as shown in Figures 3.23 to 3.26.

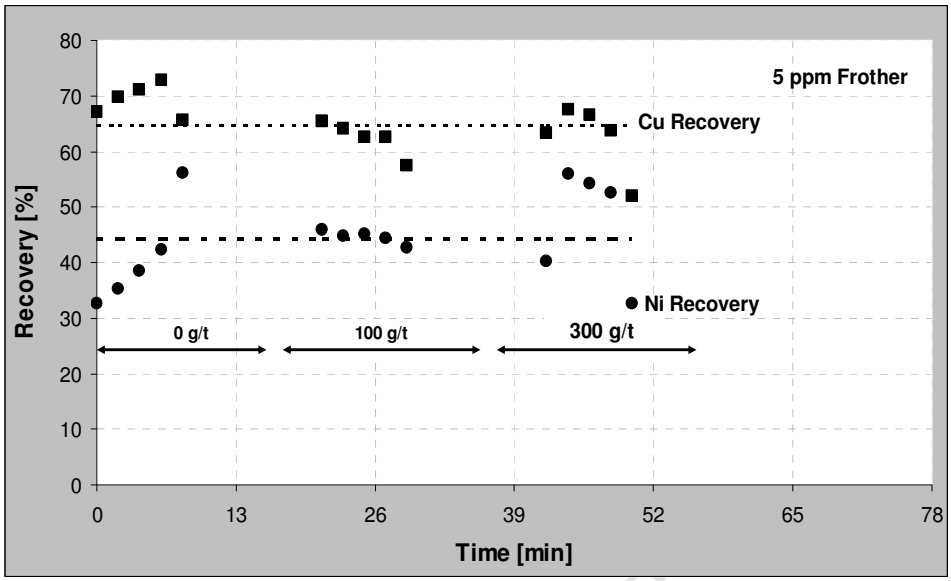

Figure 3. 19: Effect of depressant dosage on base metals recovery at 5 ppm frother dosage (dashed lines = Mean Cu and Ni recoveries)

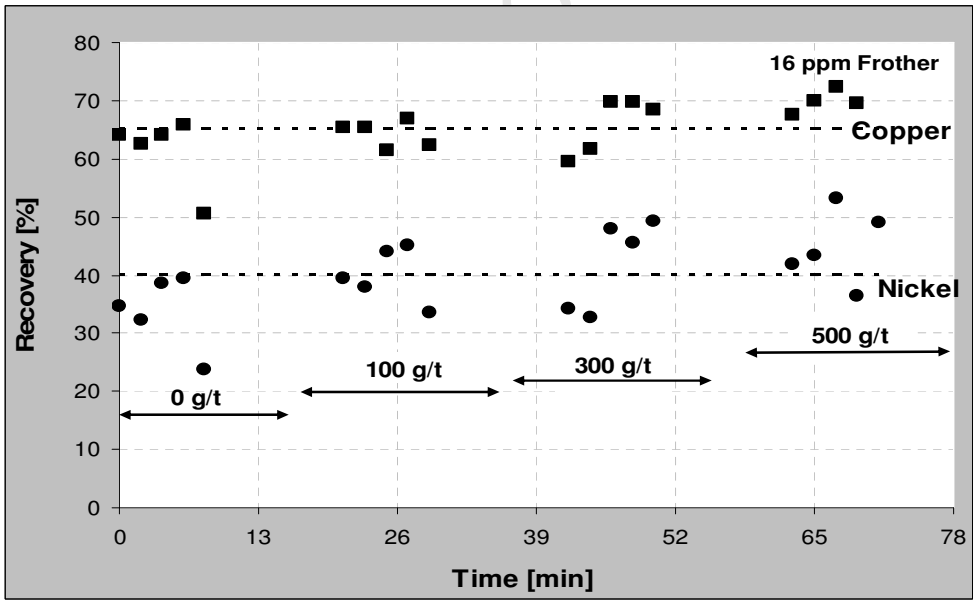

Figure 3. 20: Effect of depressant dosage on base metals recovery at 16 ppm frother dosage (dashed lines = Mean Cu and Ni recoveries)

This outcome is predictable as, upon addition of depressant, gangue particles were being removed from the concentrate. It can be seen however that the grade increased more upon addition of depressant in the runs done at 5 and 16 ppm of frother than in the runs at 20 and 25 ppm of frother. This may be explained by the

fact that as the frother dosage increased, the froth became more stable leading to more material being recovered by entrainment. This would lead to a decrease in grade in the tests done at higher frother dosage (20 and 25 ppm). This result is consistent with the findings of previous workers as discussed section 2.3.5.

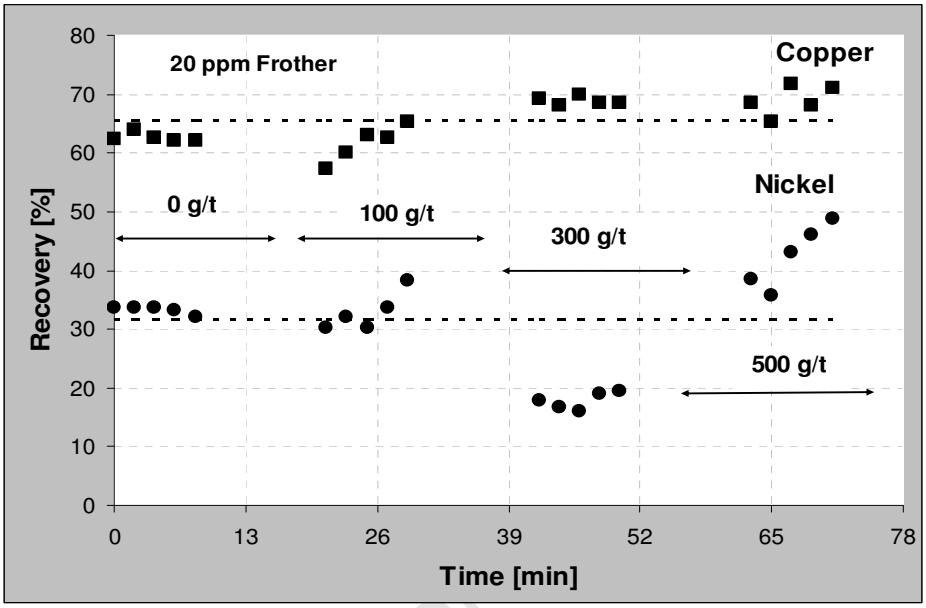

Figure 3. 21: Effect of depressant dosage on base metals recovery at 20 ppm frother dosage (dashed lines = Mean Cu and Ni recoveries)

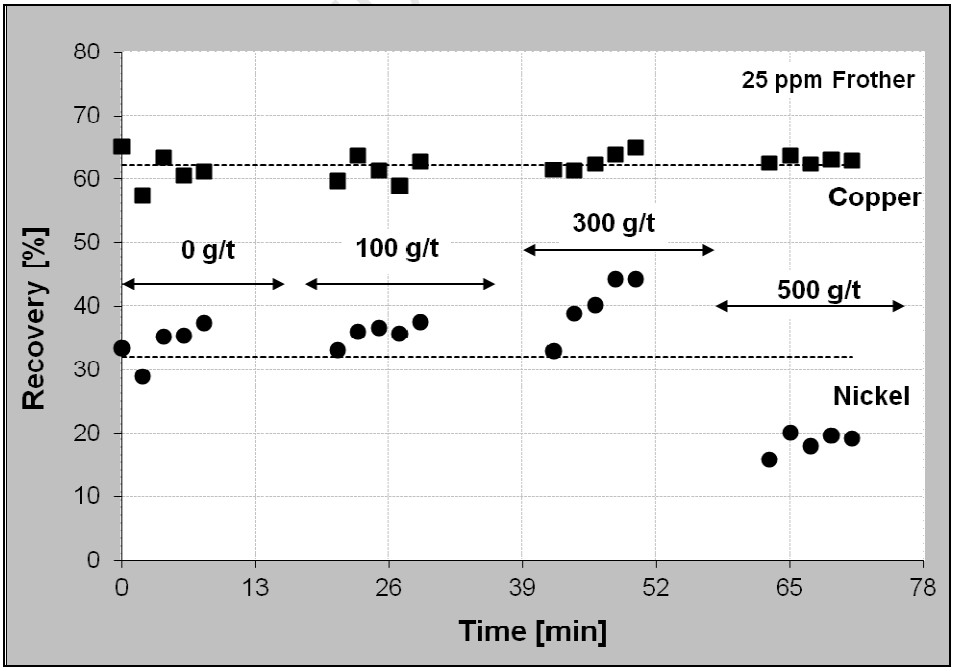

Figure 3. 22: Effect of depressant dosage on base metals recovery at 25 ppm frother dosage (dashed lines = Mean Cu and Ni recoveries)

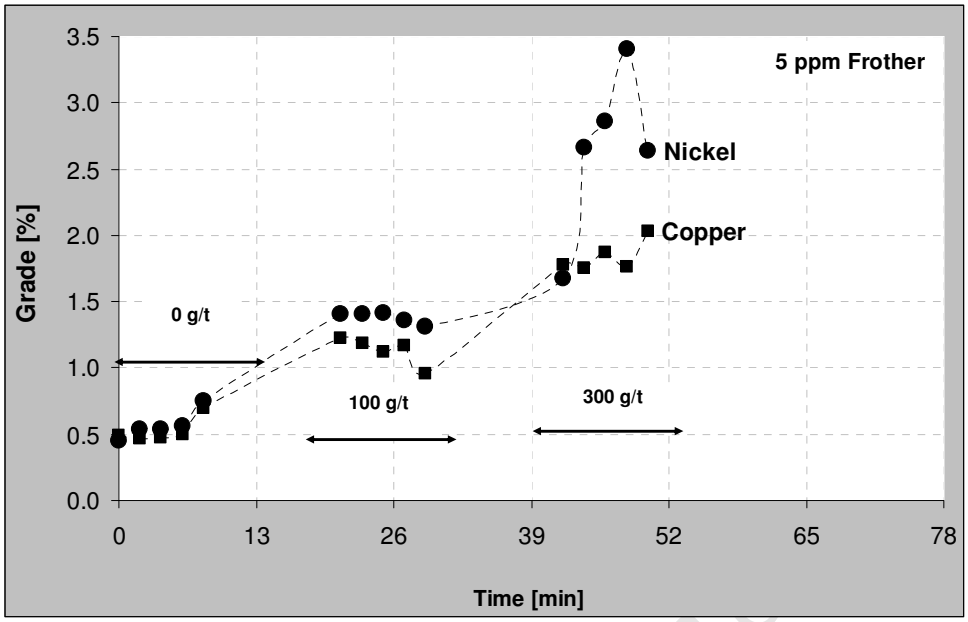

Figure 3. 23: Effect of depressant dosage on base metals grade at 5 ppm frother dosage

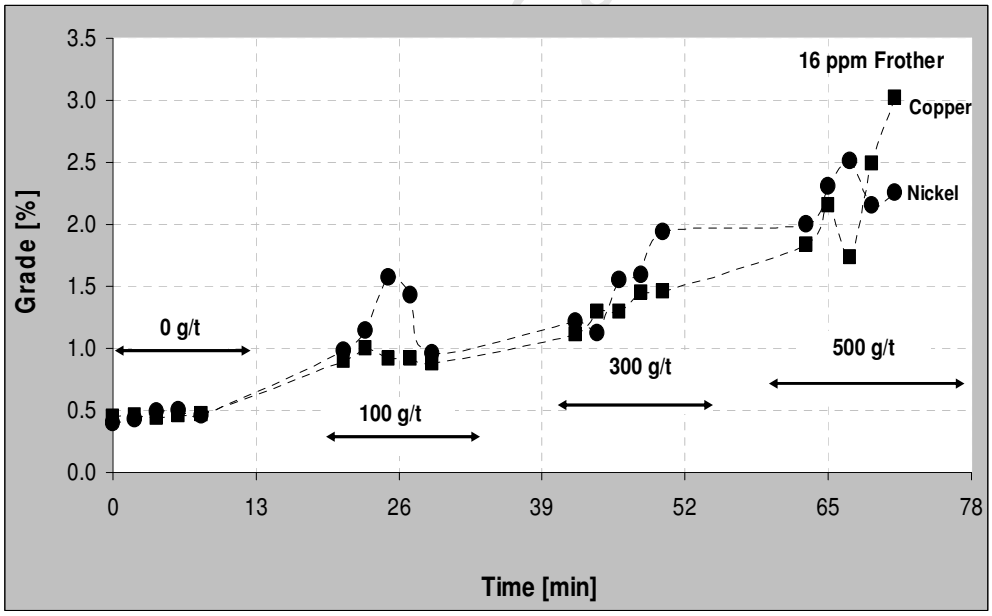

Figure 3. 24: Effect of depressant dosage on base metals grade at 16 ppm frother dosage

Due to cost constraints, platinum assays were not conducted, so the influence of depressant dosage on PGM recoveries and grades is not known.

Of the frother dosages tested, 16 ppm was considered to be optimum, as it produced the highest recovery and grade of copper and nickel. This frother dosage was therefore selected for future tests.

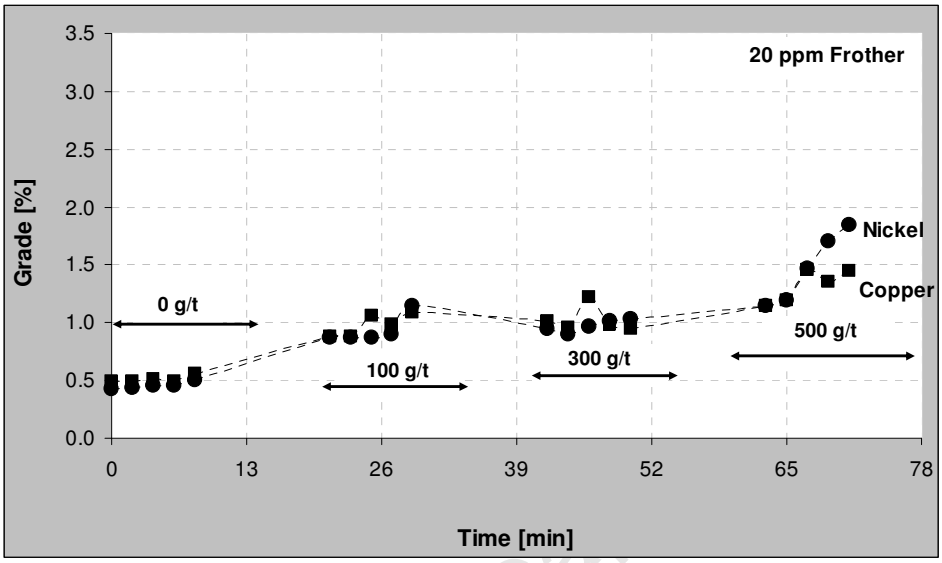

Figure 3. 25: Depressant dosage on base metals grade at 20 ppm Frother

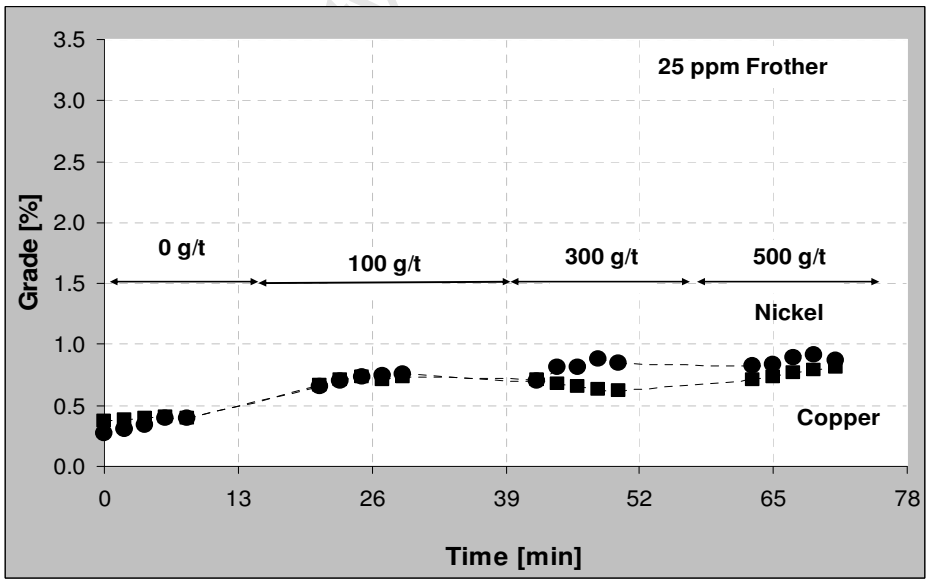

Figure 3. 26: Depressant dosage on base metals grade at 25 ppm Frother dosage

3.6 CONCLUSIONS OF THE PRELIMINARY WORK

The column flotation cell was commissioned successfully. The procedure to study the interaction between the pulp and froth phases was established.

The UCT method was tested successfully. The results showed that 10 cm froth depth can survive a high depressant dosage of 500 g/t, which is expected to make possible the use of the UCT method on a continuously-run column flotation cell, during the next stage of the tests.

The test work at UCT was performed at low pulp density (10% solids) due to the fact that the ore had to be milled at Stellenbosch University (60 km from UCT), making the transportation of slurry a challenging task. The site tests (Chapter 4 below) provided the opportunity to work at high solids percentage.

The recoveries of copper and nickel were not affected negatively with the increase in the depressant dosage, while the grades of both base metals increased steadily. Unfortunately no assays of the PGMs were possible, to determine whether the PGMs were affected negatively by the poor froth stability (upon adding extra depressant). PGMs assays were done in the next phase of work (Chapter 4).

The UCT SmartFroth® system was adapted and tested as a complement to water recovery measurement of froth stability. The froth stability measured with SmartFroth® corresponded well with froth stability measurements provided by water recovery.

Based on the preliminary tests, a frother dosage of 16 ppm was selected for the site tests. Dosages of 20 and 25 ppm were not considered because of the poor upgrade of the base metals and at 5 ppm of frother, the froth could not survive at 500 g/t of depressant.

CHAPTER FOUR: COLUMN FLOTATION TESTS AT K3 FLOTATION PLANT (LONMIN PLC)

4.1 INTRODUCTION

This chapter presents the results of the site tests, which were performed at the Karee K3 flotation plant at Lonmin PLC. The Karee K3 flotation plant is situated in the Rustenburg area (North West Province) and has two streams: the first stream processes mainly the Merensky ore and the second processes the UG2 Platinum ore. Tests in this project were performed on the UG2 stream. The column was used in the final cleaning application: the feed was the concentrate from the primary cleaner second stage.

The aims of the site tests were two fold: firstly, to determine separately the recovery of minerals by true flotation and entrainment and, secondly, to evaluate the effect of depressant dosage on froth performance (recovery and grade of PGM and Cr_2O_3, froth recovery of PGM). The mass recovered by entrainment was determined by the UCT method, which was established in Chapter 3. Froth recovery was measured using the varying froth depth technique; hence, at each depressant dosage, the column was operated and sampled at three different froth depths. Every test was conducted twice under similar experimental conditions (same feed location, same column settings). Changes in the feed characteristics were outside of the control of the experiments.

This chapter begins with a description of the column operation, the flotation conditions and the data analysis technique. The test results are then presented, beginning with the feed characteristics (particle size distribution, composition and percentage solids), the mass and water recoveries and an evaluation of entrainment by the UCT methodology. An alternative entrainment methodology is presented, which allows assessing the accuracy of the UCT methodology. The chapter ends with the study of the effect of depressant dosage and the froth height on the froth recovery, and on the overall recovery and grade of PGMs.

The most significant operational change from the preliminary tests (see Chapter 3) was the use of column removable parts, which allowed the change of the froth height without changing the pulp volume, as discussed in section 2.2.2.

4.2 TESTWORK AND DATA ANALYSIS

4.2.1 Column flotation equipment

The equipment used during the site tests was almost identical to that used during the preliminary tests[1]: the same PVC column cell, the same centrifugal pump and in-line mixer, and the same potentiometric level controller (L/C).

During the site tests, a 235 L feed tank coupled with a mixer replaced the 550 L feed tank which was used during the preliminary tests, and two new Watson Marlow pumps (620S and 620U) were used for the feed and tailings respectively. The tailings tank was not required as the tails were disposed into the plant tailings stream. An attempt to use UCT SmartFroth® during the site tests failed because the tests were performed in the open air, which severely affected the quality of the pictures (see Chapter 2 for information on SmartFroth). The final set-up of the equipment at K3 flotation plant is shown in Figure 4.1; the operating parameters of the column are shown in Table 4.1.

Table 4. 1: Column parameters

Column variables	Values
Diameter [cm]	10
Total Height [cm]	3, 9, 12
Wash water [L/min]	Nil
Air flow rate [L/min]	1.0
Feed rate [L/min]	2.5

Before tests were carried out, scoping tests were done, in order to find the most appropriate running conditions of the column cell (reagent dosage, air flow rate and froth height).

[1]Refer to Chapter 3

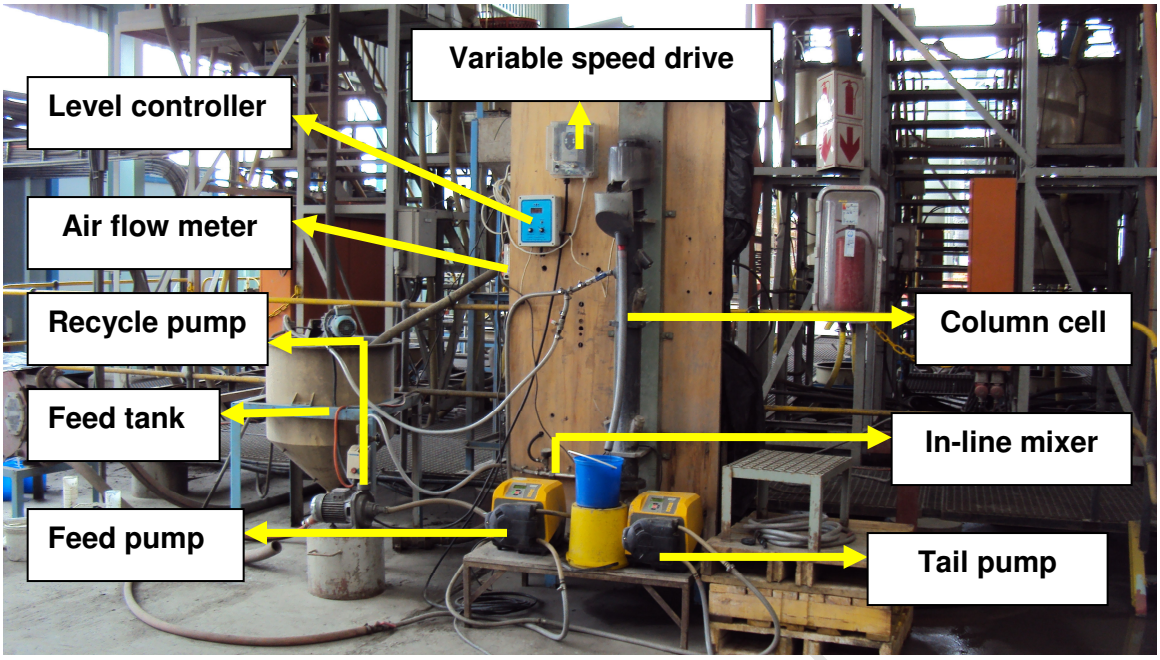

Figure 4. 1: Experimental apparatus on site at the Karee 3 flotation plant

4.2.2 Column flotation, operation and sampling

The feeds used in the site-work tests comprised samples of primary cleaner second stage concentrate, taken by hand and poured into the column feed tank while mixing to avoid settling. The feeds were collected from the plant on different days, just before a run was to be carried out. For each run enough feed material was collected to allow three conditions to be tested (depressant dosage or froth height change).

The air was taken from the plant circuit and all the reagents used during the site work were those in use on the plant. Guar gum (Sendep 369) was used as depressant in all the tests. SNPX collector was used for all the tests, at a dosage of 60 g/t, while frother was not added for the reasons provided below. The reagent dosages used are summarized in Table 4.2.

Table 4. 2: Reagent dosages

Reagents	Value [g/t]
Frother Dosage	Not added
Depressant Dosage [Sendep 369]	0, 100, 500
Collector Dosage [SNPX]	60

At the beginning of each scoping test the pulp/froth interface could be observed but as the test went on, the interface practically disappeared. This phenomenon was detected over many tests, which led to the conclusion that there was a “loss of interface” as described by Finch et al. (1989) and discussed in section 2.6.2.1. This phenomenon was observed previously in coal flotation (Tao et al., 2000). Nothing could be done to change the frother content of the pulp as frother was added upstream in the plant; the only option was to decrease the volumetric air rate. This led to the use of a much lower volumetric air rate than used previously in the laboratory tests. The air flow rate was decreased from 3 L/min (0.64 cm/s) to 1 L/min (0.21 cm/s); this would be expected to produce lower recoveries.

The same flotation procedure was used as that developed for the preliminary tests (section 3.4.3). The reagents were added to the feed tank in the following order: collector first after which the slurry was allowed to condition for 15 min before adding the depressant. The slurry was conditioned for a further 15 min before flotation testing began. While the feed was conditioning the column cell was filled with water and the air and recycle pump turned on and set to the appropriate levels. The pulp was introduced into the column, after sampling the feed off-line. Feed samples were taken at the beginning and at the end of each run. After the first froth overflowed and after any change of variable (depressant dosage or froth height), the rig was allowed to operate for three residence times in order to achieve steady state before samples were taken. Timed samples of concentrate and tail were taken simultaneously. At 0 and 100 g/t of depressant, the concentrate was collected over 3 min; at 500 g/t of depressant, the concentrate was collected over 15 min. The tails as well as the feed were sampled over 2 min.

All samples were weighed, filtered, dried in an oven and weighed again. They were sent to the Lonmin analytical laboratory to be assayed for platinum group elements (PGE), Cr_2O_3 and other mineralogical species (SiO_2, Al_2O_3). A total of

eight runs were performed; in each run three different conditions were tested; and 192 samples of feed, concentrate and tail were generated.

Table 4.3 summarizes the conditions that were varied in the tests. It can be seen that each test was done twice (A and B) under similar experimental conditions. In Runs 1A and 1B the depressant dosage was varied while all other parameters were kept constant. The other tests were conducted at constant depressant dosage with froth height being varied.

Table 4. 3: Experimental conditions

Test	Run	Froth Height [cm]	Depressant Dosage [g/t]	Date
1	1A	9	0	24 June 2010
2	1A	9	100	24 June 2010
3	1A	9	500	24 June 2010
4	1B	9	0	25 June 2010
5	1B	9	100	25 June 2010
6	1B	9	500	25 June 2010
7	2A	3	0	2 July 2010
8	2A	9	0	2 July 2010
9	2A	12	0	2 July 2010
10	2B	3	0	3 July 2010
11	2B	9	0	3 July 2010
12	2B	12	0	3 July 2010
13	3A	3	100	5 July 2010
14	3A	9	100	5 July 2010
15	3A	12	100	5 July 2010
16	3B	3	100	7 July 2010
17	3B	9	100	7 July 2010
18	3B	12	100	7 July2010
19	4A	3	500	8 July 2010
20	4A	9	500	8 July 2010
21	4A	12	500	8 July 2010
22	4B	3	500	10 July 2010
23	4B	9	500	10 July 2010
24	4B	12	500	10 July 2010

4.2.3 Data analysis (mass-balancing)

Raw data from sampling continuous processes always contain errors. A common solution to this problem is to adjust the measured assays and solids flow rates, and create a new consistent data set that satisfies all the mass balance equations (Luttrell, 2010). In order to mass balance correctly, two criteria must be met: all the mass balance equations must be valid, and the total adjustments to the data set must be minimized (Wills and Napier-Munn, 2006).

The TECHBAL (Luttrell, 2010) program was chosen to adjust the raw data in this project. This program was developed at Virginia Tech and was chosen because it is user-friendly and flexible. It is based on the use of the Solver function which is part of the Microsoft Excel spreadsheet program. The Solver function minimizes the error between the raw data and the balanced data, subject to the standard deviation of the raw data points.

TECHBAL utilizes a connection matrix, which is a mathematical representation of the flow sheet. Within the matrix defined by the nodes and the streams, the flows are indicated by the presence of (+1), (-1) and (0). A (+1) indicates an inflow e.g. feed; a (-1) indicates an out flow e.g. tail; and a (0) shows that the stream is not connected to the node (Kohmuench, 1998). The flow sheet used in this project is rather simple; it can be seen in Figure 4.2, where F, C, T are the feed, the concentrate and the tail flow rates, respectively, and f, c, t are their assays.

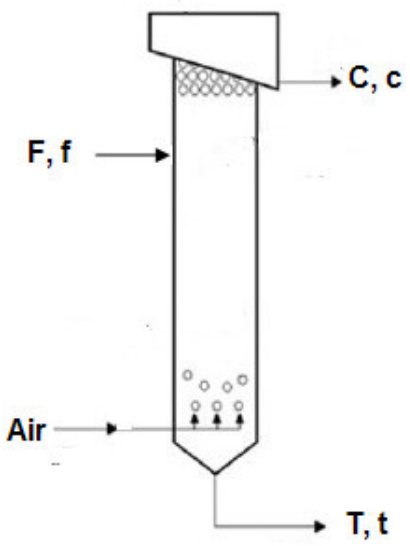

Figure 4. 2: Flow sheet used in this project

The generalized mass balance equations for the circuit are given by:

$$\sum_{i=1}^{m} C_{ij} M_i = 0 \qquad \textbf{(4. 1)}$$

$$\sum_{i=1}^{m} C_{ij} A_i^k M_i = 0 \qquad \textbf{(4. 2)}$$

where C_{ij} is the connection matrix of component i in the concentrate of unit j

M_i is the mass flow rate of each stream i, and

A_i^k is the assay for each component k in stream i.

The balanced data are estimated through the minimization of the weighted sum-of squares (WWSQ) between the raw data and the balanced data (Kohmuench, 1998). This minimization needs to respect equations 4.1 and 4.2.

The data from each test were mass-balanced separately: one feed sample, one concentrate and one tail. Feed number one was selected because it was less variable than feed two over all the tests. The following data were mass-balanced: solids flow rates; mass fractions of solids; Cr_2O_3, SiO_2 and Al_2O_3 grades (percentages); and PGM grade (g/t). The number of samples to mass balance per test was 3 (feed, concentrate and tail).

Figure 4.3 compares the measured and the balanced solids flow rates [g/min], PGM flow rates [g/h], Cr_2O_3 flow rates [kg/h] and solids percentages [%] for Runs 1A and B.

Figures 4.4 to 4.6 show the same for Runs 2A and B; Runs 3A and B; and Runs 4A and B, respectively.

It can be seen that for all the runs, the agreement between the measured and the balanced data is good. The details of the TECHBAL mass-balancing procedure as well as the Al_2O_3 data not shown in Figures 4.3 to 4.6 can be found in Appendices B, C and D. Only the balanced data (Cr_2O_3, PGM, solids flow rate and solids percentage) will be used in all the calculations that follow.

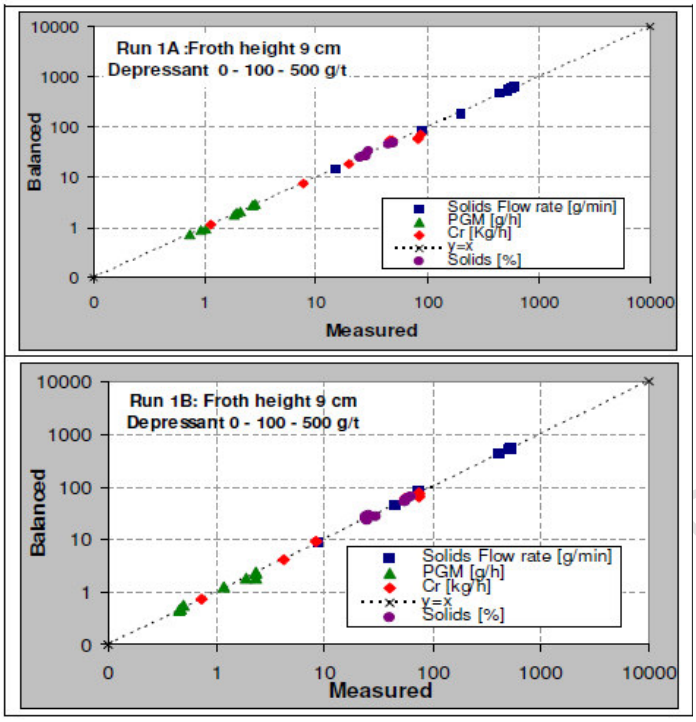

Figure 4. 3: Measured and balanced data for Runs 1A and B (three tests per run)

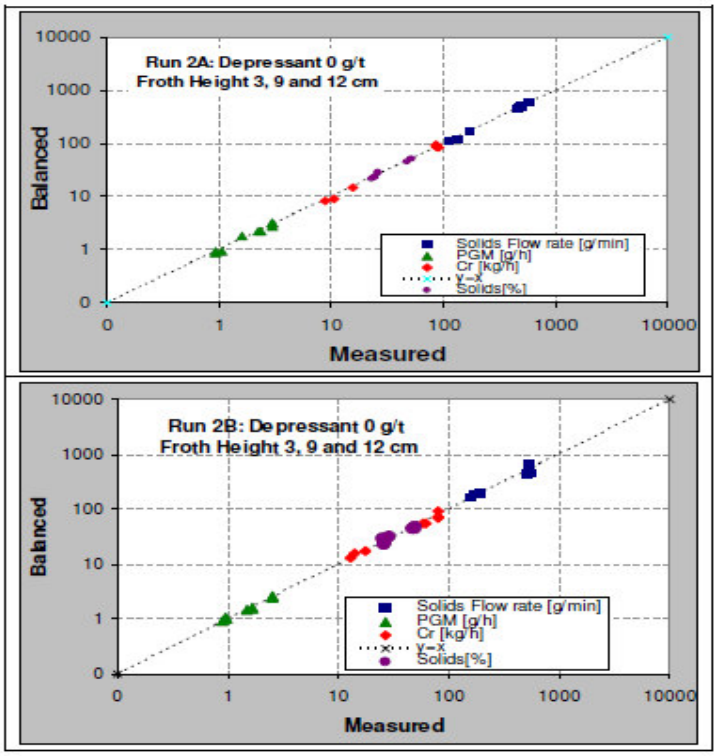

Figure 4. 4: Measured and balanced data for Runs 2A and B (three tests per run)

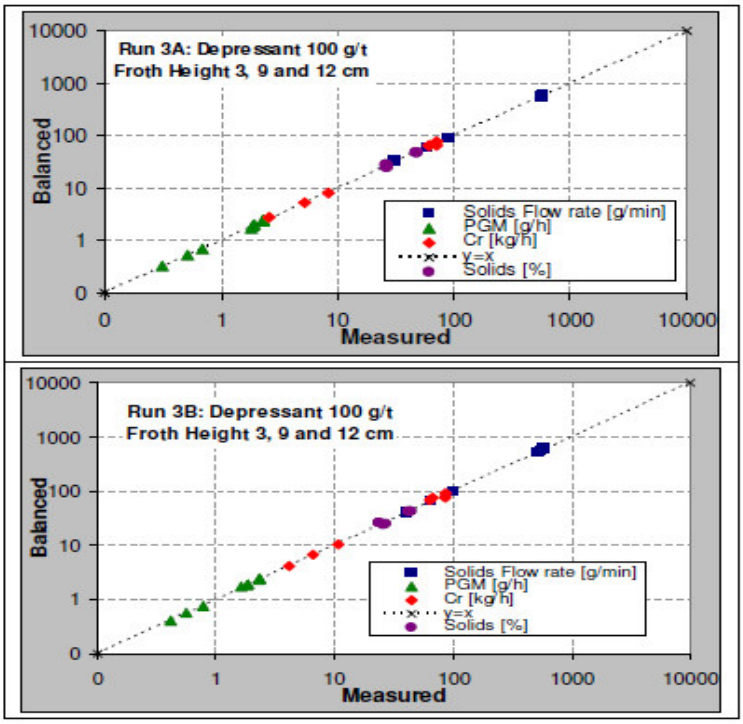

Figure 4. 5: Measured and balanced data for Runs 3A and B (three tests per run)

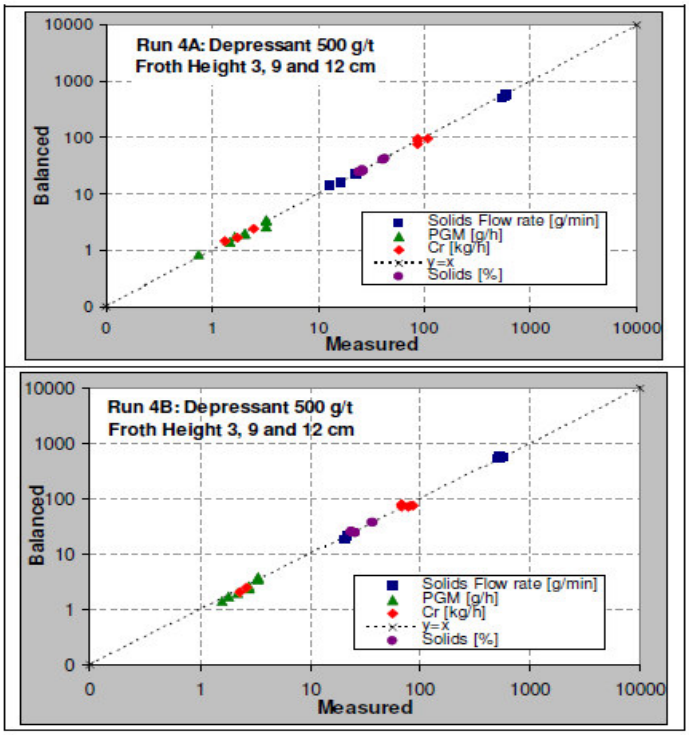

Figure 4. 6: Measured and balanced data for Runs 4A and B (three tests per run)

4.3 RESULTS AND DISCUSSION

4.3.1 Feed characteristics

The feed samples were sized using a Malvern Mastersizer. Figure 4.7 shows the mean d50 of each run, as well as the global mean and standard deviation of all the runs. It is apparent that the feed was changing constantly; this result was expected due to plant variability. The feed was clearly fine, with a global mean d50 of 36.35 µm. It can also be seen that the feeds to Runs 1B, 4A and 4B were finer than the mean of all runs, while the feeds to the remaining runs were coarser than the average. The detailed Malvern Mastersizer results can be found in Appendix E.

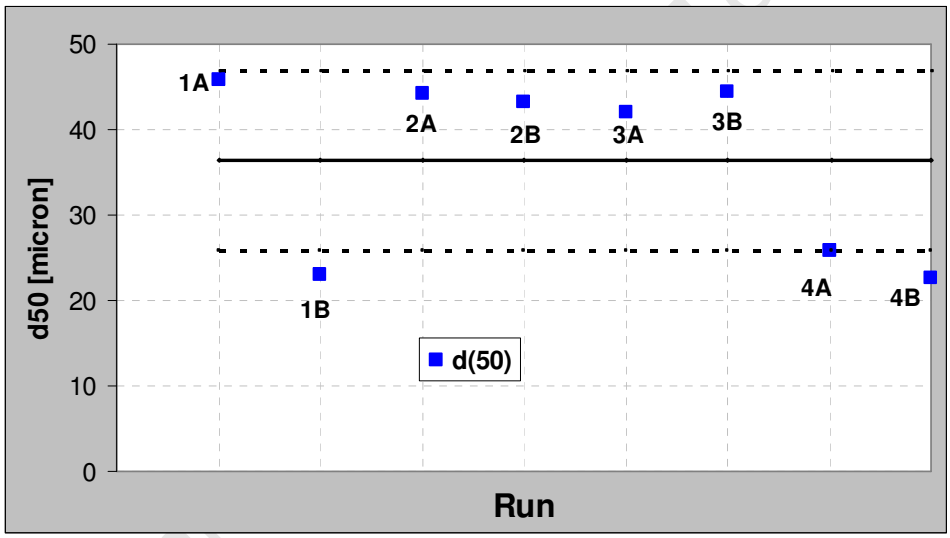

Figure 4. 7: Average feed particle size for all eight runs (solid line = global mean, dashed line = standard deviation)

Figures 4.8 to 4.11 below present the mass balanced values of percentage solids, percentage SiO_2, percentage Cr_2O_3 and PGM grade [g/t] in the feeds for the different runs in the following order: 1A – 1B – 2A – 2B – 3A – 3B – 4A – 4B, as well as the global mean value in each case and the standard deviation. For each run there were three tests and therefore three values: as there were eight runs, the total number of data points is 8 x 3 = 24.

Figure 4.8 shows that the percentage solids in the feed also varied, with an average of 27.79 % and a standard deviation of 2.12 %. It also appears that the solids content decreased *during* the run in some cases, i.e. Run 1A (tests 1, 2 and 3), Run 2B (10, 11, 12), Run 3B (16, 17, 18) and 4A (19, 20, 21). This is an indication of poor mixing in the feed tank. Future tests should try to improve the mixing characteristics of the feed tank.

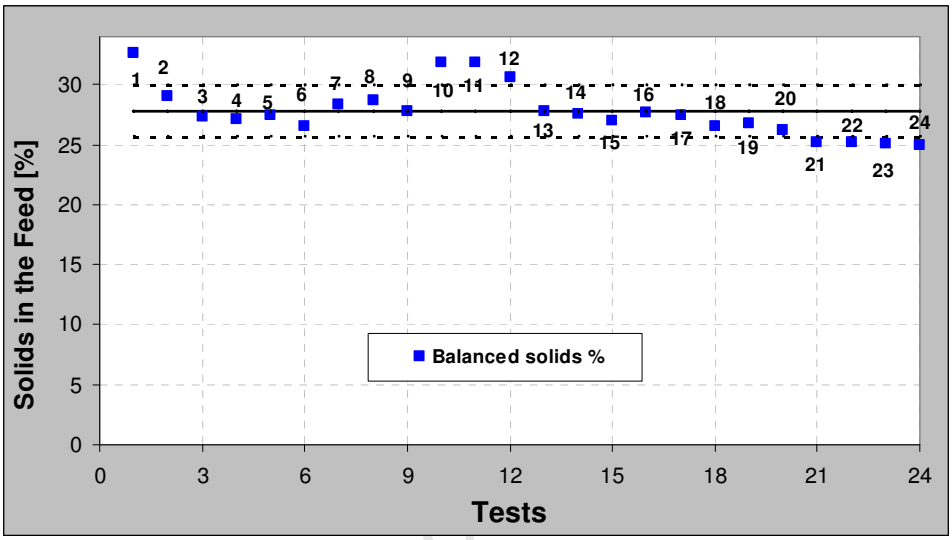

Figure 4. 8: Percentage solids in the feed for all eight runs (solid line = global mean, dashed line = standard deviation)

Figure 4.9 presents the SiO_2 content of the feed during each test. It can be seen that SiO_2 was the most abundant gangue mineral in the feed, with a mean of 51.32 % and low standard deviation. This shows that the silicate content in the feeds was steady.

Figure 4.10 shows the variability of Cr_2O_3 during the site tests. The Cr_2O_3 grade was very low, with a global mean of around 2 % in the feed. This can be compared with the Cr_2O_3 content of the feed to the Karee K3 flotation plant (rougher feed) which is of the order of 62 % (Solomon, 2010). Most of the Cr_2O_3 would have been removed during previous ore processing steps (roughing and first stage of cleaning), so it was expected that the Cr_2O_3 in the feed to these tests would be low. The variability of Cr_2O_3 is a further indication of poor mixing in the feed tank.

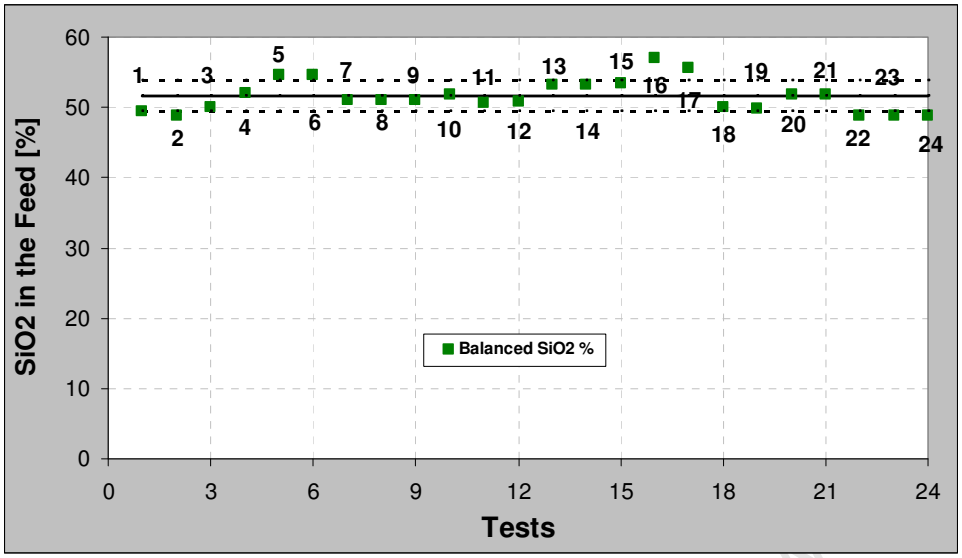

Figure 4. 9: Mass % SiO_2 in the feed for all eight runs (solid line = global mean, dashed line = standard deviation)

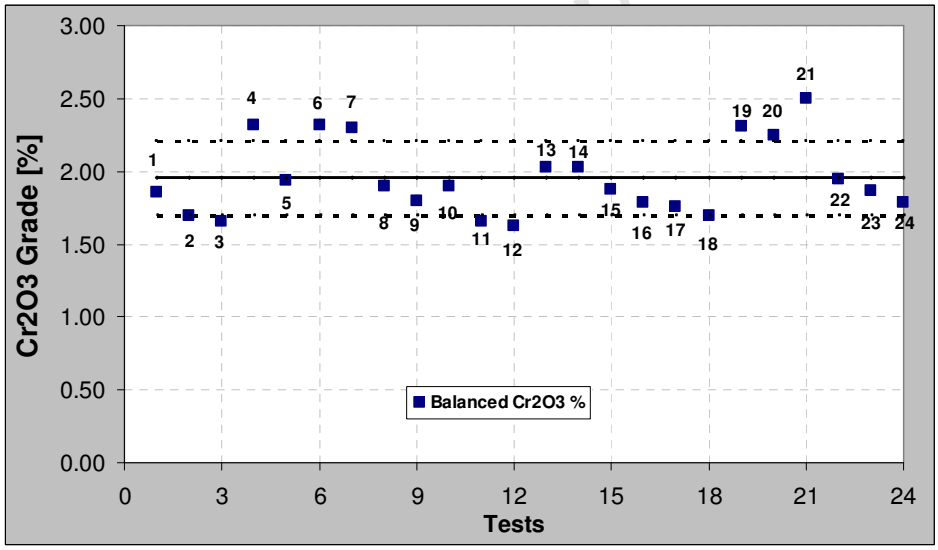

Figure 4. 10: Mass % Cr_2O_3 in the feed for all eight runs (solids line = global mean, dashed line = standard deviation)

Figure 4.11 shows the variability of the PGM grade in the feed during the site tests. The average PGM grade over all the tests was 78.36 g/t but this was highly variable. The most visible change happened in the last six tests (19 to 21 in Figure 4.7), where PGM grade increased by 20 to 30 g/t above the average. This change is attributed to change in upstream plant operations, which could not be controlled.

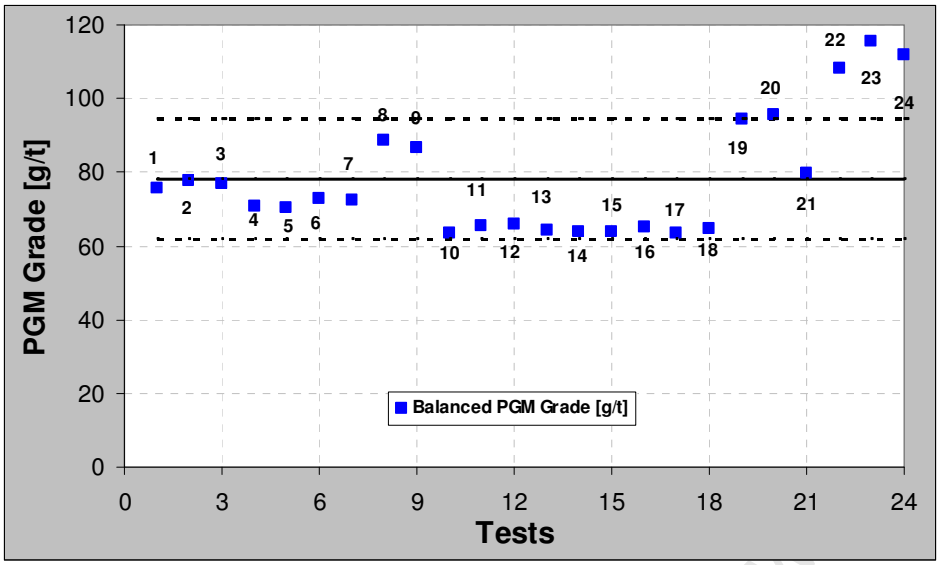

Figure 4. 11: PGM grade (g/t) in the feed for all eight runs (solids line = global mean, dashed line = standard deviation)

Most of feed variability described above was unavoidable, a consequence of drawing feed from an operating plant. This variability can be mineralogical (PGM, SiO_2) or physical (size, solids percentage) in nature. It will be important to take this variability into account when analyzing the flotation results. As pointed out by Napier-Munn (1995), flotation performance is usually correlated with the feed characteristics.

4.3.2 Effect of depressant dosage and froth height on total solids and water recoveries

Figures 4.12 and 4.13 show the effects of depressant dosage (Runs 1 A and B) and froth height (Runs 2 A and B; Runs 3 A and B; and Runs 4 A and B), respectively, on the solids and water flow rates in the concentrates during each of the runs.

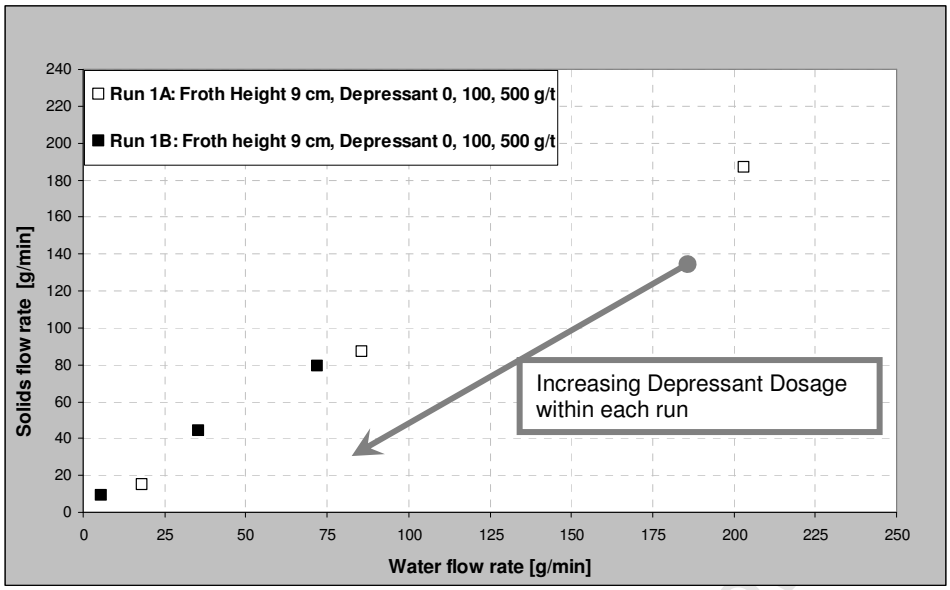

Figure 4. 12: Effect of depressant dosage on concentrate solids and water flow rates (Run 1)

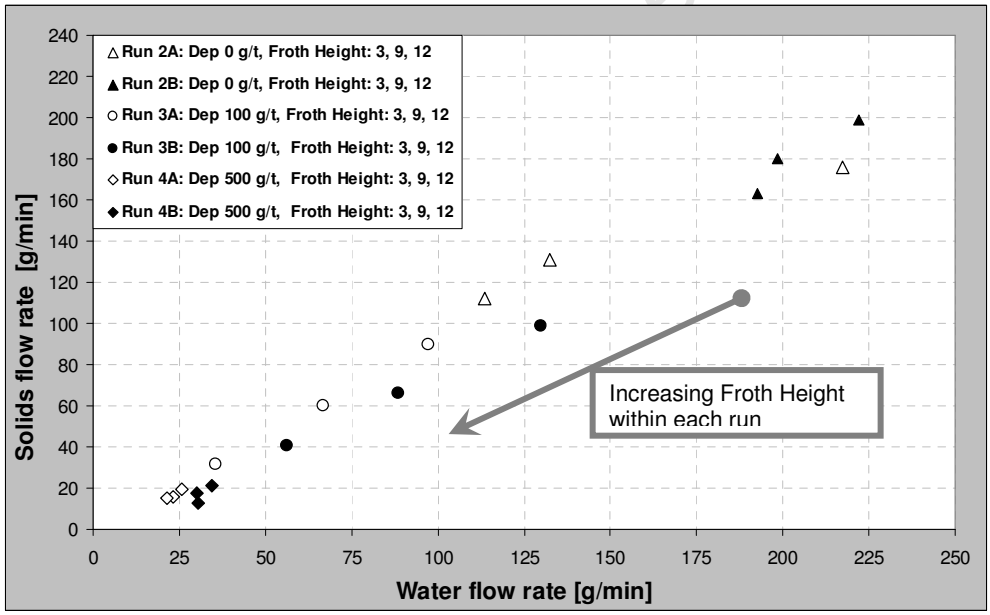

Figure 4. 13: Effect of froth height on concentrate solids and water flow rates (Runs 2, 3 and 4)

Some overall trends are apparent. For example it can be seen that in each of the runs, as the depressant dosage (Figure 4.12) or the froth height (Figure 4.13) was increased, water and total solids recoveries in the concentrates decreased. It can also be seen that the results of duplicate Runs A and B are different in each case, although these runs were performed under similar conditions. This latter

behaviour is probably the result of the combined effect of the differences in mineralogy, size distribution and solids percentage in the feeds as shown in Figures 4.5 to 4.8 above, but a more likely explanation is that the frother dosage was higher during Run 1A. Nevertheless the same trends can be observed.

These results confirm the earlier findings of the laboratory tests (Chapter 3). Runs 1A and 1B (Figure 4.12) investigated the effect of depressant dosage (0, 100 and 500 g/t) at a constant froth height of 9 cm. Increasing the depressant dosage would have led to the removal of floatable gangue minerals from the froth zone, making it less stable and resulting in less water and solids being recovered in the concentrates. This result is similar to that observed during the preliminary laboratory work (see section 3.5.2).

Runs 2, 3 and 4 were carried out at three froth heights (3, 9 and 12 cm) at constant depressant dosages of 0, 100 and 500 g/t, respectively. For each run, as the froth height was increased, the weakly and non-hydrophobic particles would have been subjected to increased drainage, again resulting in less solids and water being recovered in the concentrates. This is in agreement with previous work on the effect of froth height on flotation performance (Engelbrecht and Woodburn, 1975; Tao et al., 2000).

4.3.3 Calculation of entrainment (UCT method)

As discussed in section 2.3.2.7, the UCT methodology allows the calculation of the separate contribution of true flotation and entrainment to the concentrate recovery. The methodology assumes that at high depressant dosage (500 g/t for this project) in PGM flotation, all the gangue minerals are recovered by entrainment only. This methodology was established for column cells in Chapter 3 of this thesis.

The calculation of entrainment in the sections below is based on the following assumptions:

a. The column cell was operated under steady state. Since the samples were taken after three residence times, the column can be considered to have operated under steady state.
b. Mixing was perfect around the pulp/froth interface (concentration under the interface). For this project, the characteristics of the pulp just below the pulp-froth interface are considered to be the same as the feed characteristics, since the feed was injected a few centimeters below the froth zone.
c. All the mineral species have the same entrainability. The entrainability of minerals can be considered to be the same if the particles are very fine, which is the case for this project as was shown in section 4.3.1.

All these assumptions may be regarded as reasonable for the work that was carried out for this thesis.

Figure 4.14 plots the solids versus water flow rates in the concentrate for Runs 4 A and B which were performed at 500 g/t of depressant. Omitting one point from the regression because it was remote from all other data points produces a straight line fit that does not pass through the origin. The correlation coefficient is not very close to unity, because there are few data points and the froth was highly unstable at 500 g/t depressant. It might have been better to use a lower depressant dosage i.e. 300 g/t. Nevertheless, the equation and the curve observed are similar to that shown in Equation 2.12 and Figure 2.5 (section 2.3.2.3). Warren (1985) has shown that the intercept of the regression line represents the recovery by true flotation, while the slope is the entrainment factor.

The result observed in Figure 4.14 is different from the initial assumption that at high depressant dosage, the gangue is recovered by entrainment only (see section 2.3.2.7). Figure 4.14 suggests that even though the tests were performed at 500 g/t of depressant, there were still floatable gangue minerals in the froth.

Nevertheless, following the method of Warren (1985), the slope of the regression line may be taken to represent the degree of entrainment in Runs 4A and B, and hence in all other column tests, as noted in section 2.3.2.3.

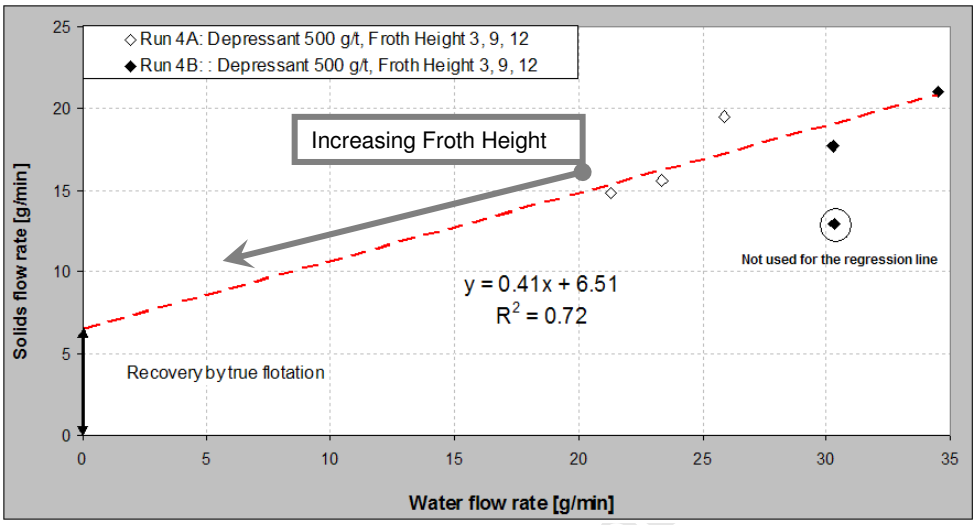

Figure 4. 14: Concentrate solids and water flow rates at 500 g/t of depressant (Run 4)

Following Equation 2.19 (section 2.3.2.6) and using assumption b at the beginning of this section, Anderson (2008) suggested that the X-axis be modified by normalizing it with the ratio of the mass flow rates of solids and water in the feed: $(m_{Solids}/m_w)_{Feed}$. This leads to Figure 4.15 below.

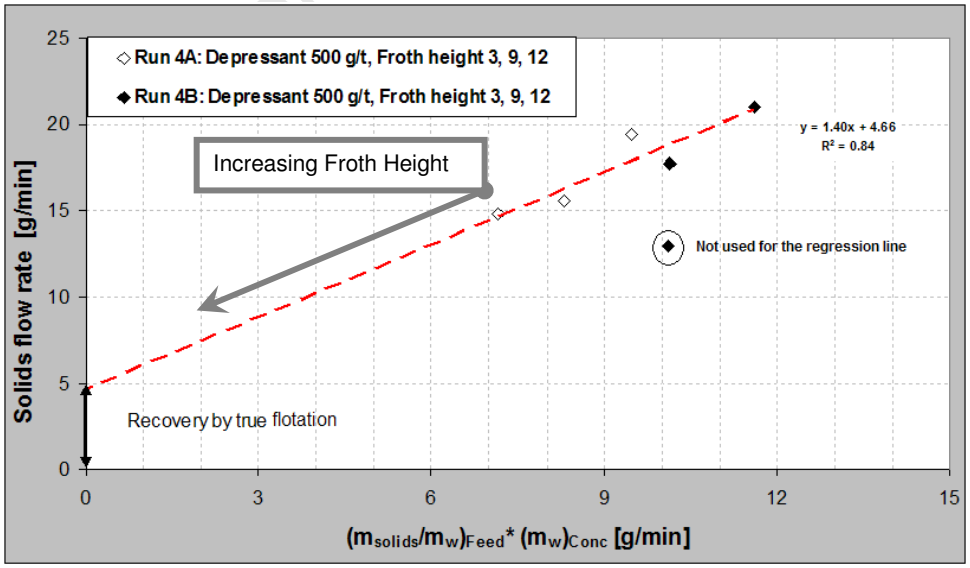

Figure 4. 15: Concentrate solids and water flow rates at 500 g/t of depressant (Run 4)

Figure 4.15 has the advantage of producing a better fit (higher coefficient of correlation), but more importantly the solids and water content of the feed have been taken into account. Therefore for the remainder of this thesis the X-axis will be normalized, as illustrated in Figure 4.15.

4.3.3.1 Calculation of true flotation (UCT Method)

Table 4.4 presents the mass flow rates of the total solids (m_{Conc}) and entrained (m_{Entr}) solids for Runs 1A and B, which were performed at a constant froth height of 9 cm and varying depressant dosage (0, 100 and 500 g/t). The mass flow rates of entrained solids were calculated on the basis of equation 2.12. The degree of entrainment was derived from the linear regression line in Figure 4.15 and is equal to 1.40. The mass flow rate of solids recovered by true flotation (m_{True}) is the difference between the total and the entrained solids flow rates. A sample of calculation is shown below for Test 1 of Run 1A (data in Appendix F):

Table 4. 4 : Flotation data of Test 1 of Run 1A: 0 g/t Depressant, 9 cm Froth Height

$m_{Solids,\ Feed}$ [g/min]	$m_{w,\ Feed}$ [g/min]	$m_{w,\ conc}$ [g/min]	$m_{Solids,\ conc}$ [g/min]
644.62	1332.02	202.97	186.60

$$\left(\frac{m_{Solids}}{m_w}\right)_{Feed} * m_{w,conc} = 98.22\ g/min$$

ENT = 1.40 (refer to Figure 4.15)

The mass flow rate of solids recovered by entrainment,

$$m_{Entr} = ENT * \left(\frac{m_{Solids}}{m_w}\right)_{Feed} * (m_{w,conc}) \quad \textbf{(4. 3)}$$

$$= 1.40 * 98.22\ g/min = 137.51\ g/min$$

The mass flow rate of solids recovered by true flotation is calculated using the following formula

$$m_{True} = m_{Conc} - m_{Entr} \quad \textbf{(4. 4)}$$

$$= 186.60 - 137.51 = 49.09\ g/min$$

Table 4. 5: Total, entrained and true flotation flow rates for Run 1 (UCT method)

Run	Depressant [g/t]	$(m_{Solids}/m_w)_{Feed}*m_{w,conc}$ [g/min]	$m_{w,conc}$ [g/min]	m_{Conc} [g/min]	m_{Entr} [g/min]	m_{True} [g/min]
1A	**0**	98.22	202.97	186.60	137.51	49.09
1A	**100**	35.12	85.67	86.93	49.16	37.77
1A	**500**	6.84	18.20	14.99	9.57	5.42
1B	**0**	26.77	72.08	79.30	37.48	41.82
1B	**100**	13.45	35.53	44.19	18.83	25.36
1B	**500**	1.97	5.44	8.76	2.76	6.01

The data in Table 4.5 are shown graphically in Figure 4.16 for Runs 1A and B. For each run the points on the same vertical line represent the measured total solids flow rate (upper point) and the calculated entrainment flow rate (lower point).

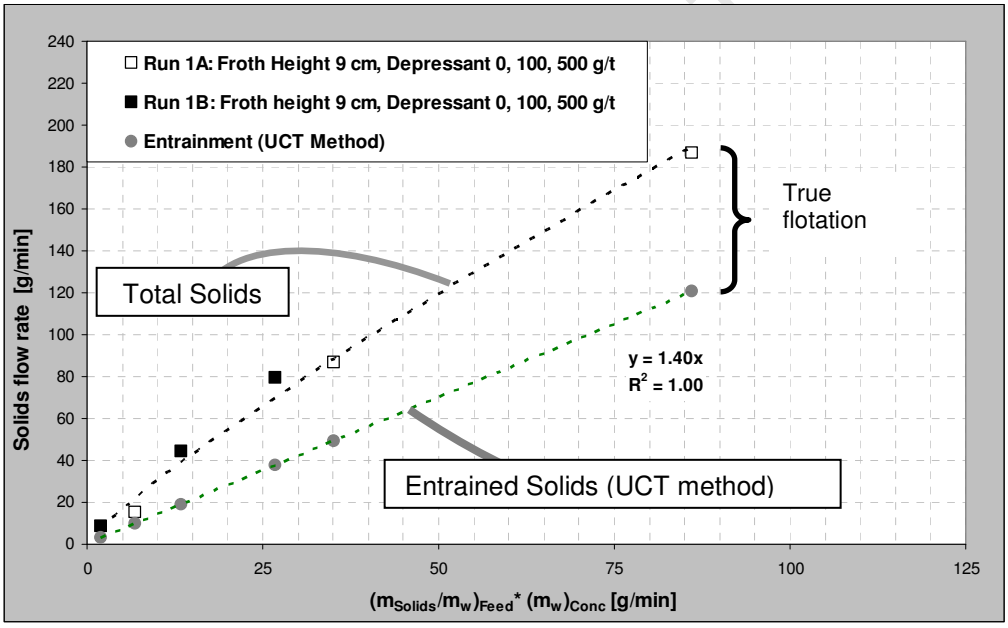

Figure 4. 16: Total, entrained and true flotation flow rates for Run 1 (UCT Method)

Figure 4.16 and Table 4.5 show that as the depressant dosage increased from 0 to 100 and then 500 g/t, the amount of gangue recovered by both entrainment and true flotation decreased appreciably. Although Run 1A and 1B were performed under similar experimental conditions, it can be seen that the solids and water recoveries were much greater for Run 1A than 1B. An explanation of this behaviour can be offered based on the high percentage solids in Run A (Figure 4.8), although the mean particle size was much coarser (figure 4.7).

Table 4.6 presents the details of the entrainment calculations for Runs 2, 3 and, 4, which were carried out at constant depressant dosage (0, 100 and 500 g/t, respectively), but at three different froth heights (3, 9 and 12 cm) within each run. The procedure described above was used to calculate the mass flow rate of solids recovered by entrainment and true flotation in each test. It can be seen that as the froth height increased, the mass flow rate of solids recovered by true flotation decreased. Figure 4.17 shows the same data graphically.

Table 4. 6 : Total, entrained and true flotation flow rates for Runs 2 to 4 (UCT Method)

Runs	Froth Height [cm]	Depressant [g/t]	$(m_{Solids}/ m_w)_{Feed}*m_{w,conc}$ [g/min]	$m_{w,conc}$ [g/min]	m_{conc} [g/min]	m_{Entr} [g/min]	m_{True} [g/min]
2A	3	0	86.22	217.35	175.73	120.70	55.03
2A	9	0	53.35	132.38	130.66	74.69	55.97
2A	12	0	43.86	113.68	112.11	61.40	50.71
2B	3	0	103.77	221.89	198.61	145.28	53.33
2B	9	0	92.68	198.54	179.83	129.76	50.07
2B	12	0	85.08	192.77	163.29	119.12	44.17
3A	3	100	37.49	97.18	89.90	52.49	37.41
3A	9	100	25.37	66.60	60.20	35.52	24.68
3A	12	100	13.21	35.64	31.37	18.50	12.87
3B	3	100	49.57	129.76	98.84	69.40	29.43
3B	9	100	33.54	88.71	65.78	46.96	18.82
3B	12	100	20.38	56.28	40.58	28.54	12.04
4A	3	500	9.48	25.90	19.47	13.27	6.20
4A	9	500	8.30	23.39	15.58	11.62	3.97
4A	12	500	7.17	21.32	14.85	10.03	4.82
4B	3	500	11.60	34.49	21.04	16.23	4.81
4B	9	500	10.14	30.25	17.70	14.20	3.50
4B	12	500	10.10	30.33	12.98	14.15	0[1]

[1] Calculated value < 0, taken as zero

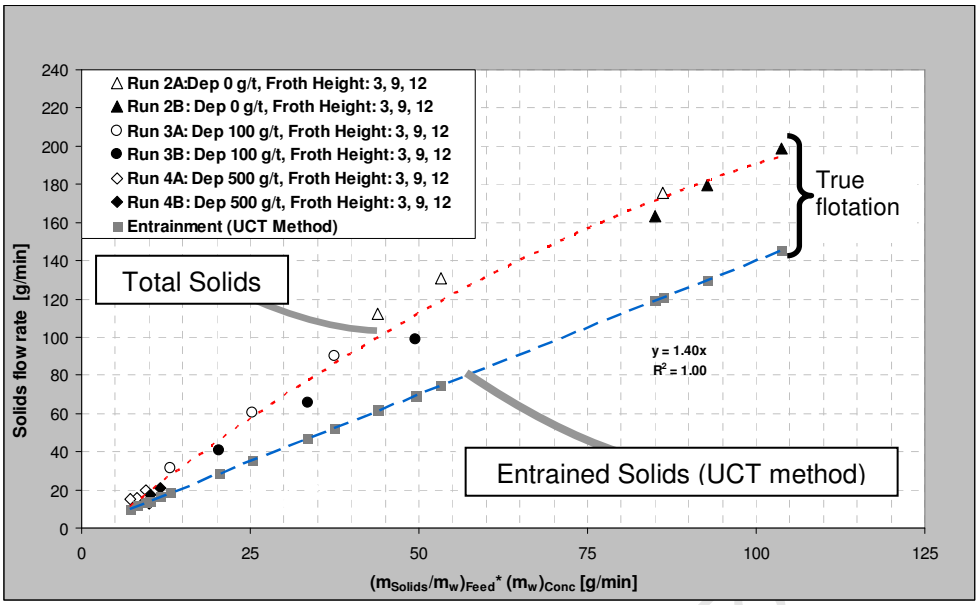

Figure 4. 17: Total, entrained and true flotation flow rates for Runs 2 to 4 (UCT Method)

It can be seen in Table 4.6 that the runs operated at lower depressant dosages generated higher solids flow rates in the concentrate than those carried out at higher depressant dosage, irrespective of the froth height. Thus the runs operated at 500 g/t of depressant (Runs 4A and B) produced the lowest solids flow rates even at the lowest froth depth (3 cm). For the runs carried out at 100 g/t of depressant, the mass flow rates of solids recovered by true flotation decreased appreciably as the froth height was increased. For the runs carried out at 0 g/t depressant, the mass flow rates of solids recovered by true flotation also decreased, but not as appreciably, even though there was a big decrease in the mass flow rates of solids recovered by entrainment. This is probably because the froth was much more stable: even though the water and entrained solids were draining out as the froth height increased, the bubbles were not coalescing, so solids recovery by true flotation remained high.

At 500 g/t of depressant (Runs 4A and 4B) the flow rates of solids recovered by true flotation were close to zero and did not change much with increase in froth height. At 500 g/t of depressant, almost all of the floatable gangue minerals would have been depressed, but there was obviously still a small amount of very

hydrophobic material floating. An increase in froth height did not make a big change in this amount.

The data presented above in Tables 4.5 and 4.6 rely on the extrapolation of the entrainment flow rates beyond the experimental conditions used to derive the linear relationship in Figure 4.15 (Runs 1A and 1B). Additionally, data points used to derive the relationship are limited (5 points). A question therefore arises, as to whether or not it was correct to extrapolate the entrainment data beyond the experimental conditions, as has been done. In order to answer this question an alternative method will be used in the next section to evaluate independently the mass flow rate of solids recovered by entrainment. The result of this evaluation will allow the assessment of the entrainment flow rates predicted by the UCT method.

4.3.4 Calculation of entrainment and true flotation (Savassi Method)

Due to the problem of extrapolation raised above, it was decided evaluate the solids entrainment flow rates using the Savassi method, which is based on the presence of a non-floatable liberated tracer in the feed. In the following sub-section Cr_2O_3 and Al_2O_3 will be studied as indicators (tracers) of entrainability in the tests that were carried out. Cr_2O_3 and Al_2O_3 were selected for potential use as tracers because they both derive from hydrophilic species (Cr_2O_3 and plagioclase, respectively). Other components such as SiO_2 and MgO were not considered because they derive from floatable mineral species (SiO_2 and orthopyroxene, respectively).

4.3.4.1 Investigation of Cr_2O_3 and Al_2O_3 as tracers

Table 4.7 shows the ratios of Cr_2O_3 and Al_2O_3 flow rates to water flow rates in the concentrates of all the tests in which the depressant dosage and the froth height were varied (Runs 1 to 4). It can be seen that the (Cr_2O_3 flow rate / water flow rate) ratio remained practically constant during Runs 2, 3 and 4. This is a strong

indication that the Cr_2O_3 recovery depends only on the water recovery in all the runs, except for Run 1. For Run 1B there is a clear deviation from all other ratios, which will be explored further in the next section[1].

It can also be seen in Table 4.7 that the (Al_2O_3 flow rate / water flow rate) ratios were *not constant* (the standard deviations for Cr_2O_3 are smaller than for Al_2O_3). This suggests that Al_2O_3 cannot be said to be recovered solely by entrainment. Therefore Al_2O_3 will not be considered for use as a tracer in this analysis.

Table 4. 7: Ratios of Cr_2O_3 and Al_2O_3 flow rates to water flow rate in all the tests

	Run 1A: Froth Height : 9 cm				Run 1B Froth Height : 9 cm			
Depressant Dosage [g/t]	0	100	500	STDEV	0	100	500	STDEV
Al_2O_3 Flow rate/water flow rate	0.035	0.036	0.026	0.005	0.038	0.041	0.083	0.025
Cr_2O_3 Flow rate/water flow rate	0.015	0.016	0.011	0.003	0.020	0.020	0.022	0.002
	Run 2A Depressant Dosage: 0 g/t				Run 2B Depressant Dosage: 0 g/t			
Froth Height	3 cm	9 cm	12 cm	STDEV	3 cm	9 cm	12 cm	STDEV
Ratio Al_2O_3 Flow rate/water flow rate	0.035	0.038	0.037	0.001	0.034	0.032	0.031	0.002
Ratio Cr_2O_3 Flow rate/water flow rate	0.012	0.013	0.013	0.000	0.013	0.013	0.012	0.001
	Run 3A Depressant Dosage: 100 g/t				Run 3B Depressant Dosage: 100 g/t			
Froth Height	3 cm	9 cm	12 cm	STDEV	3 cm	9 cm	12 cm	STDEV
Ratio Al_2O_3 Flow rate/water flow rate	0.035	0.033	0.031	0.002	0.036	0.032	0.030	0.003
Ratio Cr_2O_3 Flow rate/water flow rate	0.014	0.013	0.012	0.001	0.014	0.013	0.012	0.001
	Run 4A Depressant Dosage: 500 g/t				Run 4B Depressant Dosage: 500 g/t			
Froth Height	3 cm	9 cm	12 cm	STDEV	3 cm	9 cm	12 cm	STDEV
Ratio Al_2O_3 Flow rate/water flow rate	0.062	0.052	0.037	0.013	0.066	0.060	0.062	0.003
Ratio Cr_2O_3 Flow rate/water flow rate	0.013	0.012	0.012	0.001	0.011	0.011	0.015	0.002

Figure 4.18 plots the flow rates of Cr_2O_3 vs. normalized water flow rates for all the tests. It is obvious that the Cr_2O_3 flow rate is linearly proportional to water flow rate, with a correlation coefficient close to 1, and a Y-intercept close to zero. This confirms that Cr_2O_3 was recovered solely by entrainment. It is important to note that this entrainment relationship is valid for all the Runs, and does not need to be extrapolated to higher water recoveries as in Figure 4.16 and 4.17.

[1] The balanced flow rates of Cr_2O_3 and Al_2O_3 can be found in Appendix D and the water flow rates for all the runs are in Appendix F

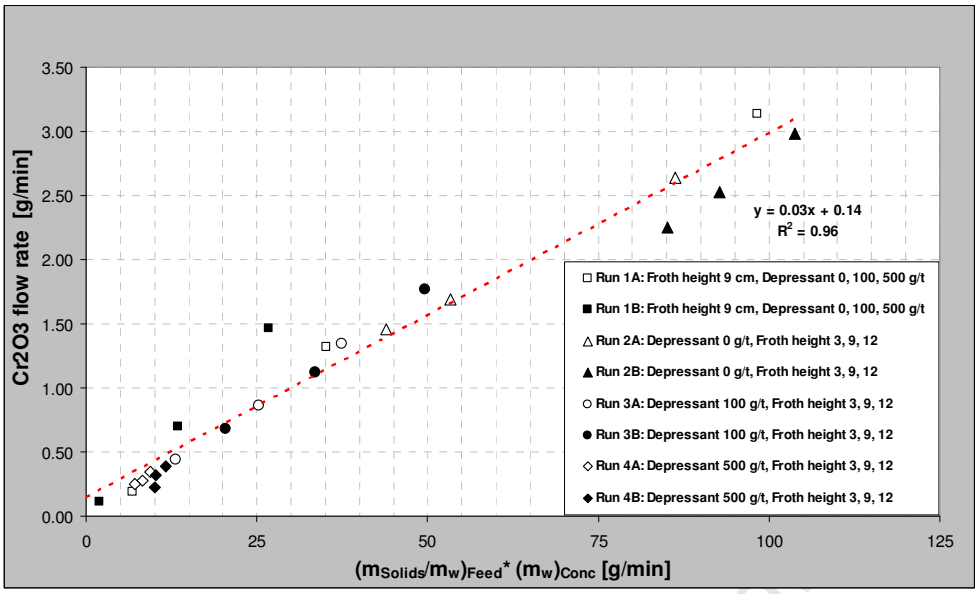

Figure 4. 18: Cr_2O_3 versus water flow rate in all the runs

If Cr_2O_3 was recovered solely by entrainment in the column tests, then Cr_2O_3 recovery can be expected to be representative of the entrainment recovery of all other gangue minerals in the tests. This is in agreement with previous work on the entrainment of hydrophilic minerals (Savassi et al., 1998), which found entrainment to be non-selective (i.e. independent of mineral type). Therefore Cr_2O_3 can be used as a mineral tracer to evaluate entrainment.

4.3.4.2 Calculation of entrainment (Savassi Method)

Now that it has been confirmed that Cr_2O_3 recovery in all the tests is by entrainment only, it may be used as a tracer to establish the recovery of other solids by entrainment. The Savassi method will be used for this purpose. The following relationship, adapted from the work of Savassi (1998), is used to find the degree of entrainment:

$$ENT_{Cr2O3} = \frac{\omega_{Cr2O3,conc}}{\omega_{Cr2O3,feed}} \qquad \textbf{(4. 5)}$$

where ENT_{Cr2O3} = degree of entrainment of Cr_2O_3 based on the feed,

$\omega_{Cr2O3,\ conc}$ = concentration of the tracer (Cr_2O_3) in the concentrate (mass flow rate of Cr_2O_3 in the concentrate / mass flow rate of water in the concentrate)

$\omega_{Cr2O3,\ feed}$ = concentration of the tracer (Cr_2O_3) in the feed (mass flow rate of tracer in the feed / mass flow rate of water in the feed)

Assuming that the degree of entrainment of any other mineral which is in the pulp will be the same as that of Cr_2O_3, the relationship can be rearranged as follows, for the total mass of solids recovered by entrainment:

$$ENT = \frac{\left(m_{Cr2O3}/m_w\right)_{Conc}}{\left(m_{Cr2O3}/m_w\right)_{Feed}} = \frac{\left(m_{Entr}/m_w\right)_{Conc}}{\left(m_{Solids}/m_w\right)_{Feed}} \quad \textbf{(4. 6)}$$

where ENT = degree of entrainment of total solids based on the feed.

m_{Entr} = mass flow rate of total solids recovered by entrainment (in the concentrate)

m_{Solids} = mass flow rate of total solids in the feed

The mass flow rate of solids recovered by entrainment is therefore

$$m_{Entr} = ENT_{Cr2O3}\ x \left(\frac{m_{Solids}}{m_w}\right)_{Feed} x\ (m_w)_{Conc} \quad \textbf{(4. 7)}$$

and for i = another mineral in the feed:

$$m_{Entr,i} = ENT_{Chromite}\ x \left(\frac{m_i}{m_w}\right)_{Feed} x\ (m_w)_{Conc} \quad \textbf{(4. 8)}$$

It should be noted that calculating m_{Entr} of SiO_2 and MgO in this way may not be valid as these components derive from talc and orthopyroxene, respectively, which are known to be floatable.

Table 4.8 shows the details of the calculations for Runs 1 to 4, i.e. how the mass flow rate of solids recovered by entrainment in each tests was calculated based on the degree of entrainment, using equations 4.4 and 4.5. The mass flow rate of

solids recovered by true flotation is also shown, calculated by difference between m_{Conc} and m_{Entr}.

It is apparent that while the degree of entrainment ENT changed within the same run it remained within the same range, with averages ranging from 1.26 to 2.65 and with standard deviations of 0.06 to 0.13. These standard deviations would probably have been smaller if it had been possible to carry out more tests. It can also be seen that as the depressant dosage or the froth depth was increased, m_{Entr}. decreased in all the tests.

Table 4.8 also shows that the average degree of entrainment for Run 1B is higher than all the others. This may be due to the particle size in the feed, which was found to be small in this run (Figure 4.7). This is a further confirmation of the link between the feed characteristics and the flotation performance as explained in section 4.3.1 (Napier-Munn, 1995).

Table 4. 8: Total, entrained and true flotation flow rates in the concentrate (Savassi Method)

Run 1A : Entrainment and true flotation at constant froth height of 9cm							
Depressant [g/t]	ENT	$(m_{Solids}/m_w)_{Feed}$ [g/min]/[g/min]	$m_{w,conc}$ [g/min]	$(m_{Solids}/m_w)_{Feed}*m_{w,conc}$ [g/min]	m_{Entr} [g/min]	m_{Conc} [g/min]	m_{True} [g/min]
0	1.71	0.48	202.97	98.22	168.23	186.60	18.38
100	2.07	0.41	85.67	35.12	72.66	86.93	14.27
500	1.54	0.38	18.20	6.84	10.55	14.99	4.43
Av ENT	1.78	STDEV ENT	0.13				
Run 1B: Entrainment and true flotation at constant froth height of 9cm							
Depressant [g/t]	ENT	$(m_{Solids}/m_w)_{Feed}$ [g/min]/[g/min]	$m_{w,conc}$ [g/min]	$(m_{Solids}/m_w)_{Feed}*m_{w,conc}$ [g/min]	m_{Entr} [g/min]	m_{Conc} [g/min]	m_{True} [g/min]
0	2.36	0.37	72.08	26.77	63.23	79.30	16.06
100	2.52	0.38	35.53	13.45	33.86	44.19	10.33
500	2.95	0.36	5.44	1.97	5.81	8.76	2.95
Av ENT	2.65	STDEV ENT	0.31				
Run 2A : Entrainment and true flotation at constant depressant dosage of 0 g/t							
Froth Height [cm]	ENT	$(m_{Solids}/m_w)_{Feed}$ [g/min]/[g/min]	$m_{w,conc}$ [g/min]	$(m_{Solids}/m_w)_{Feed}*m_{w,conc}$ [g/min]	m_{Entr} [g/min]	m_{Conc} [g/min]	m_{True} [g/min]
3	1.22	0.40	217.35	86.22	105.44	175.73	70.29
9	1.23	0.40	132.38	53.35	65.84	130.66	64.82
12	1.33	0.39	113.68	43.86	58.30	112.11	53.81
Average ENT	1.26	STDEV ENT	0.06				
Run 2B : Entrainment and true flotation at constant depressant dosage of 0 g/t							
Froth Height [cm]	ENT	$(m_{Solids}/m_w)_{Feed}$ [g/min]/[g/min]	$m_{w,conc}$ [g/min]	$(m_{Solids}/m_w)_{Feed}*m_{w,conc}$ [g/min]	m_{Entr} [g/min]	m_{Conc} [g/min]	m_{True} [g/min]
3	1.44	0.47	221.89	103.77	149.71	198.61	48.90
9	1.44	0.47	198.54	92.68	133.77	179.83	46.06
12	1.42	0.44	192.77	85.08	120.75	163.29	42.54
Average ENT	1.44	STDEV ENT	0.01				
Run 3A : Entrainment and true flotation at constant depressant dosage of 100 g/t							
Froth Height [cm]	ENT	$(m_{Solids}/m_w)_{Feed}$ [g/min]/[g/min]	$m_{w,conc}$ [g/min]	$(m_{Solids}/m_w)_{Feed}*m_{w,conc}$ [g/min]	m_{Entr} [g/min]	m_{Conc} [g/min]	m_{True} [g/min]
3	1.77	0.39	97.18	37.49	66.43	89.90	23.47
9	1.67	0.38	66.60	25.37	42.41	60.20	17.79
12	1.79	0.37	35.64	13.21	23.63	31.37	7.73
Average ENT	1.74	STDEV ENT	0.06				
Run 3B : Entrainment and true flotation at constant depressant dosage of 100 g/t							
Froth Height [cm]	ENT	$(m_{Solids}/m_w)_{Feed}$ [g/min]/[g/min]	$m_{w,conc}$ [g/min]	$(m_{Solids}/m_w)_{Feed}*m_{w,conc}$ [g/min]	m_{Entr} [g/min]	m_{Conc} [g/min]	m_{True} [g/min]
3	1.47	0.38	129.76	49.57	72.81	98.84	26.03
9	1.38	0.38	88.71	33.54	46.20	65.78	19.59
12	1.53	0.36	56.28	20.38	31.23	40.58	9.34
Average ENT	1.46	STDEV ENT	0.08				
Run 4A : Entrainment and true flotation at constant depressant dosage of 500 g/t							
Froth Height [cm]	ENT	$(m_{Solids}/m_w)_{Feed}$ [g/min]/[g/min]	$m_{w,conc}$ [g/min]	$(m_{Solids}/m_w)_{Feed}*m_{w,conc}$ [g/min]	m_{Entr} [g/min]	m_{Conc} [g/min]	m_{True} [g/min]
3	1.36	0.37	25.90	9.48	12.91	19.47	6.56
9	1.26	0.35	23.39	8.30	10.49	15.58	5.09
12	1.41	0.34	21.32	7.17	10.10	14.85	4.75
Average ENT	1.34	STDEV ENT	0.07				
Run 4B : Entrainment and true flotation at constant depressant dosage of 500 g/t							
Froth Height [cm]	ENT	$(m_{Solids}/m_w)_{Feed}$ [g/min]/[g/min]	$m_{w,conc}$ [g/min]	$(m_{Solids}/m_w)_{Feed}*m_{w,conc}$ [g/min]	m_{Entr} [g/min]	m_{Conc} [g/min]	m_{True} [g/min]
3	1.58	0.34	34.49	11.60	18.35	21.04	2.69
9	1.38	0.34	30.25	10.14	13.98	17.70	3.73
12	1.01	0.33	30.33	10.10	10.20	12.98	2.78
Average ENT	1.32	STDEV ENT	0.29				

Figure 4.19 shows graphically how the mass recovered by true flotation is found from the total mass flow rate of solids in the concentrate and the mass flow rate

of solids recovered by entrainment, for Runs 1A and 1B, in which the depressant dosage was changed at constant froth height.

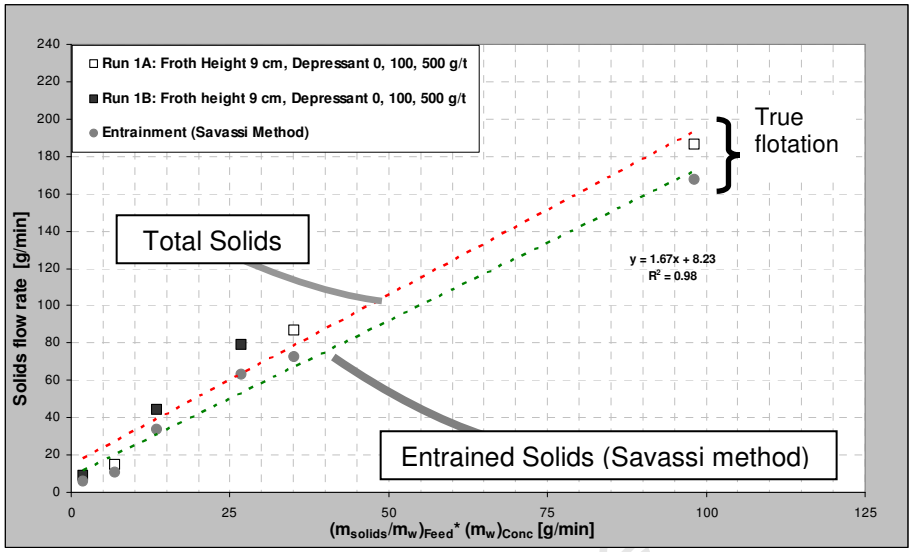

Figure 4. 19: Total, entrained and true flotation flow rates for Run 1 (Savassi Method)

Similarly, Figure 4.20 shows how these values are obtained in Runs 2 to 4 when the froth height was changed. The results are very similar to those found in section 4.3.3.1, using the UCT method. A more systematic comparison between the result obtained using the UCT and the Savassi methods will be performed in the next section.

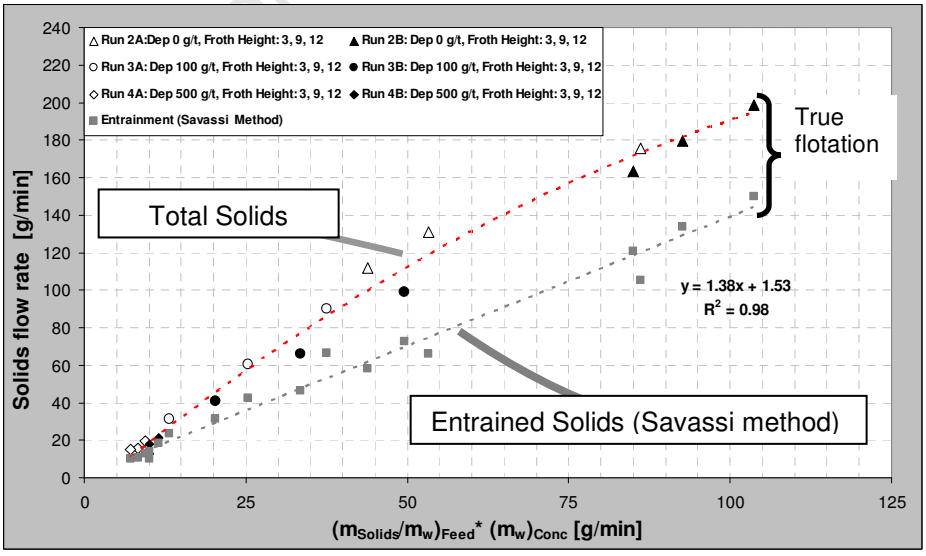

Figure 4. 20: Total and entrained flow rates for Runs 2 to 4 (Savassi Method)

4.3.6 Comparison of the UCT and the Savassi Methods

The aim of this section is to compare statistically the solids entrainment results calculated by the UCT and the Savassi methods. The data to be compared is the observed gradient of Savassi model derived from the Runs 1 to 4 with that predicted by the UCT data, i.e. all the values of m_{Entr} and $(m_{Solids}/ m_w)_{Feed}*m_{w,Conc}$ in Tables 4.5 and 4.7, and Table 4.8.

As with any comparative statistics, the values of interest will be compared on the basis of their means and variances about their means (Napier-Munn, 2003). This comparison is important as it will allow not only the quantification of the accuracy of each of these techniques, but also the identification of any difference between them.

MS Excel was used to obtain the descriptive statistics data for entrainment calculated according to the UCT and the Savassi methods. They are shown in Table 4.9; the full entrainment data can be found in sections 4.3.3.1 and 4.3.4.2 above. Table 4.9 shows that the two entrainment measures are very close: the mean, the standard deviations and medians are not very different. The maximum value shows that the Savassi method provides a slightly higher flow rate than the UCT method.

Table 4. 9: Statistical characteristics of the UCT and Savassi methods

	Solids Entrainment	
Descriptive Statistics	**UCT**	**Savassi**
Mean of Entrainment flow rate	51.55	56.12
Standard Error of Entrainment flow rate	9.39	9.82
Median	36.49	44.30
Standard Deviation	46.03	48.10
Sample Variance	2118.85	2313.55
Minimum	2.76	5.81
Maximum	145.28	168.22

The regression analysis (using MS Excel) of the entrainment values obtained by the UCT method is shown in Table 4.10, where

df is the degrees of freedom

SS is the sum of squares

MS is the mean squares

F is $MS_{regression}/MS_{residual}$

t-Stat is the t-statistic of the standard error. This value can be tested against a t-distribution to determine how probable it is that the true value of the coefficient is zero.

P-value is the Probability that the variances $MS_{regression}$ and $MS_{residual}$ are statistically indistinguishable.

Table 4. 10: Regression analysis of entrainment data obtained using the UCT method

SUMMARY OUTPUT: UCT Method

Regression Statistics	
Multiple R	1
R Square	1
Adjusted R Square	1
Standard Error	8.22146E-15
Observations	24

ANOVA

	df	*SS*	*MS*	*F*	*Significance F*
Regression	1	46070.26826	46070.26826	6.81589E+32	0
Residual	22	1.48703E-27	6.75924E-29		
Total	23	46070.26826			

	Coefficients	*Standard Error*	*t Stat*	*P-value*	*Lower 95%*	*Upper 95%*	*Lower 95.0%*	*Upper 95.0%*
Intercept	2.13163E-14	2.57057E-15	8.292424765	3.23617E-08	1.59852E-14	2.66473E-14	1.59852E-14	2.66473E-14
X Variable 1	1.4	5.36249E-17	2.61073E+16	0	1.4	1.4	1.4	1.4

Table 4.11 shows the same for the Savassi method.

Table 4. 11: Regression analysis of data obtained using the Savassi method

SUMMARY OUTPUT: Savassi Method

Regression Statistics	
Multiple R	0.975814361
R Square	0.952213667
Adjusted R Square	0.950041561
Standard Error	10.75088494
Observations	24

ANOVA

	df	*SS*	*MS*	*F*	*Significance F*
Regression	1	50668.93906	50668.93906	438.3826759	5.10346E-16
Residual	22	2542.793593	115.5815269		
Total	23	53211.73265			

	Coefficients	*Standard Error*	*t Stat*	*P-value*	*Lower 95%*	*Upper 95%*	*Lower 95.0%*	*Upper 95.0%*
Intercept	3.55551697	3.334420142	1.066307429	0.297847411	-3.359647128	10.47068107	-3.359647128	10.47068107
X Variable 1	1.42757187	0.068182244	20.93759002	5.10346E-16	1.286170551	1.568973188	1.286170551	1.568973188

Figure 4.21 presents the data from UCT and Savassi entrainment calculations, their regression lines and their equations.

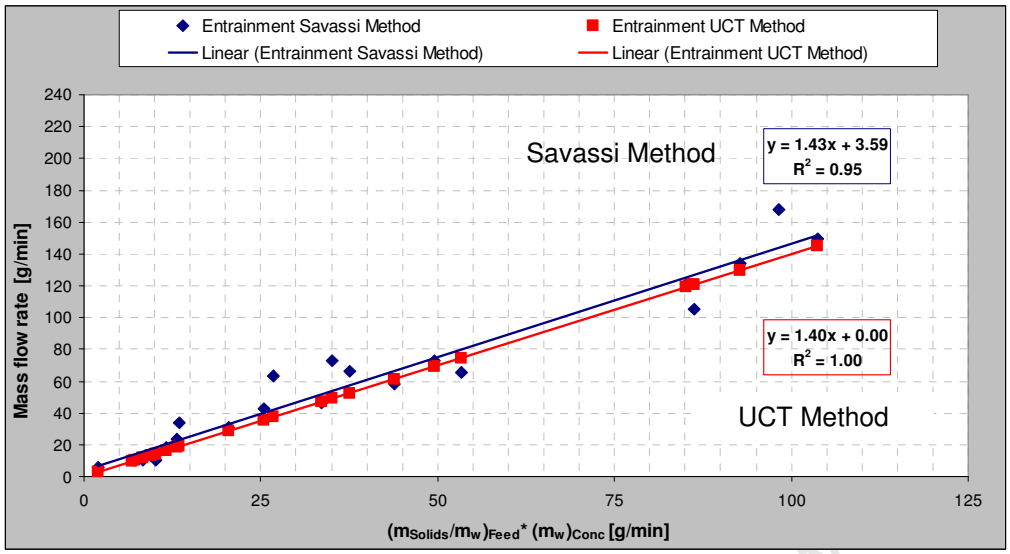

Figure 4. 21: Solids mass flow rates recovered by entrainment using the UCT and Savassi regression lines

From Tables 4.10 and 4.11 it can be seen that the linearity is not in question for either of the UCT and the Savassi methods, as the coefficients of correlation are equal and close to unity (1 and 0.95). A visual observation of the data in Figure 4.21 is a further confirmation of the linear relationship between the mass flow rate of solids recovered by entrainment and the normalized water flow rate (X-axis).

In order to see how close the UCT dataset is to the Savassi dataset, a comparison can be made between the observed gradient of the Savassi data and that predicted by the UCT data. This is a t-test, which can be performed using the following formula[1]:

$$t = \frac{(\text{Savassi Gradient} - \text{UCT Gradient})}{\text{SE of Savassi Gradient}} \qquad \textbf{(4. 9)}$$

where SE is the standard error of Savassi gradient shown in Table 4.13 above. The SE of the UCT data is not included because it is close to nil; this can be seen in Table 4.12. Therefore,

$$t = \frac{(1.4275 - 1.40)}{0.067} = 0.37$$

[1] Napier-Munn, T, 2011. *Personal Communication*

The probability P associated with this value is obtained from the Microsoft Excel function **FDIST (t, df, tails),** where:

t is the value for which the probability is required (Equation 4.9 above)
df is the degree of freedom, which is equal to the number population in the experimental data (Savassi data) minus 2 parameters, which gives 24 - 2 = 22.
tails indicates whether the probability returns one or two-tailed distribution. One (1) is used for a one-tailed distribution and two (2) for a two-tailed distribution. Since a 2-tailed distribution is considered, 2 will be used.

This gives P=TDIST (0.37, 22, 2) = 0.71. This value is not significant at the 95% confidence level. Thus it can be concluded that the Savassi data produced a gradient that is not different from that predicted by the UCT model.

4.3.7 Effect of depressant dosage on froth recovery of gangue minerals

The aim of this thesis is to gain an insight into how the properties of particles entering the froth affect the performance of the froth phase. In platinum ore flotation, gangue minerals are known to have a stabilizing effect on the froth phase (Martinovic et al., 2005); in this thesis, their hydrophobicity was changed by the addition of depressant and the performance of the froth phase was measured in terms of froth recovery.

In order to calculate the froth recovery of the gangue minerals, their recovery by true flotation had first to be determined. For this, data presented in Table 4.8 and Appendix F were used. A sample calculation of the gangue recovery by true flotation is shown below for Test 1 of Run 1A:

Table 4. 12: Flotation data of Test 1 Run 1A: 0 g/t Depressant, 9 cm Froth Height

m_{True} [g/min]	$m_{Solids, Feed}$ [g/min]
18.34	644.62

where m_{True} is the mass flow rate of solids recovered by true flotation (see Table 10)

$m_{Solids,\ Feed}$ is the mass flow rate of solids in the feed (see Appendix F).

The recovery of gangue minerals by true flotation is given by:

$$R_{Solids,True} = 100 * \left(\frac{m_{True}}{m_{Solids,Feed}} \right) \quad \textbf{(4. 10)}$$

$$= 100*(18.34/644.62) = 2.85\ \%$$

Table 4.13 presents the mass flow rates of solids in the feed and the mass flow rates of solids recovered by true flotation for all the tests. The calculated values of gangue recovery by true flotation are also listed for all the tests. It can be seen that for Runs 1, 2 and 3, the gangue recoveries by true flotation decreased as the depressant dosage or froth height increased. However, for Runs 4A and 1B, the gangue recoveries by true flotation did not follow quite the same trend; this shows that the froth was highly unstable at 500 g/t of depressant. It is interesting to note that the gangue recoveries by true flotation were as high as 10 % in the absence of depressant, dropping to less than 1% at 500 g/t, indicating the efficacy of the depressant addition.

Having determined the gangue recovery by true flotation in each test, the froth recovery of gangue minerals in each test can be calculated according to a modification of the froth varying technique (Vera et al., 1999b). The following steps were followed:

1. Plot the gangue (solids) recoveries against froth height[1]. Extrapolate the line to froth height = 0; the intercept gives the collection zone recovery ($R_{c,\ Solids}$) (see Figure 20). The total recovery ($R_{Solids,\ True}$) of the column is given by equation 10 (section 2.5 above):

$$R_{Solids,True} = \frac{R_{c,Solids} R_{f,Solids}}{\left(1 - R_{c,Solids} + R_{c,Solids} R_{f,Solids}\right)} \quad \textbf{(4. 11)}$$

[1] Roger Amelunxen, 2010. *Personal communication*

2. Solve for $R_{f,\ Solids}$

Figure 4.22 shows the gangue recoveries by true flotation plotted against the froth heights for Runs 2, 3 and 4. No values are plotted for Runs 1A and 1B, because these tests were performed at constant froth height. Except for Run 4B, there is a linear relationship between the gangue recovery by true flotation and the froth height, at all the depressant dosages tested.

Table 4. 13: True flotation and froth recoveries of gangue minerals for all the Runs

Run 1A : Constant froth height of 9 cm				
Depressant	$m_{Solids,Feed}$	m_{True}	$R_{Solids,True}$	$R_{f,Solids}$
[g/t]	[g/min]	[g/min]	[%]	[%]
0	644.62	18.38	2.85	*
100	612.43	14.27	2.33	*
500	568.19	4.43	0.78	*
Run 1B : Constant froth height of 9 cm				
Depressant	$m_{Solids,Feed}$	m_{True}	$R_{Solids,True}$	$R_{f,Solids}$
[g/t]	[g/min]	[g/min]	[%]	[%]
0	490.20	16.06	3.28	*
100	551.40	10.33	1.87	*
500	534.92	2.95	0.55	*
Run 2A : Constant depressant dosage of 0 g/t				
Froth Height	$m_{Solids,Feed}$	m_{True}	$R_{Solids,True}$	$R_{f,Solids}$
[cm]	[g/min]	[g/min]	[%]	[%]
3	601.42	70.29	11.69	91.49
9	610.68	64.82	10.61	82.08
12	590.46	53.81	9.11	69.32
Run 2B :Constant depressant dosage of 0 g/t				
Froth Height	$m_{Solids,Feed}$	m_{True}	$R_{Solids,True}$	$R_{f,Solids}$
[cm]	[g/min]	[g/min]	[%]	[%]
3	610.07	48.90	8.02	95.12
9	610.66	46.06	7.54	89.04
12	609.54	42.54	6.98	81.89
Run 3A:Constant depressant dosage of 100 g/t				
Froth Height	$m_{Solids,Feed}$	m_{True}	$R_{Solids,True}$	$R_{f,Solids}$
[cm]	[g/min]	[g/min]	[%]	[%]
3	621.68	23.47	3.78	79.60
9	622.92	17.79	2.86	59.65
12	586.97	7.73	1.32	27.09
Run 3B:Constant depressant dosage of 100 g/t				
Froth Height	$m_{Solids,Feed}$	m_{True}	$R_{Solids,True}$	$R_{f,Solids}$
[cm]	[g/min]	[g/min]	[%]	[%]
3	609.08	26.03	4.27	80.26
9	612.36	19.59	3.20	59.40
12	586.80	9.34	1.59	29.09
Run 4A: Constant depressant dosage of 500 g/t				
Froth Height	$m_{Solids,Feed}$	m_{True}	$R_{Solids,True}$	$R_{f,Solids}$
[cm]	[g/min]	[g/min]	[%]	[%]
3	602.13	6.56	1.09	**
9	594.37	5.09	0.86	**
12	519.99	4.75	0.91	**
Run 4B:Constant depressant dosage of 500 g/t				
Froth Height	$m_{Solids,Feed}$	m_{True}	$R_{Solids,True}$	$R_{f,Solids}$
[cm]	[g/min]	[g/min]	[%]	[%]
3	576.81	2.69	0.47	**
9	576.71	3.73	0.65	**
12	534.81	2.78	0.52	**

NB: * froth recovery was not calculated Runs 1A and B because froth height was constant.
** froth recoveries were not calculated because the froth was unstable, which led to Rf > 100 % in some of the tests.

In Runs 4A and Run 4B the coefficients of correlation are small, showing that the froth was unstable. The high depressant dosage (500 g/t) used in these runs was believed to be the reason for this.

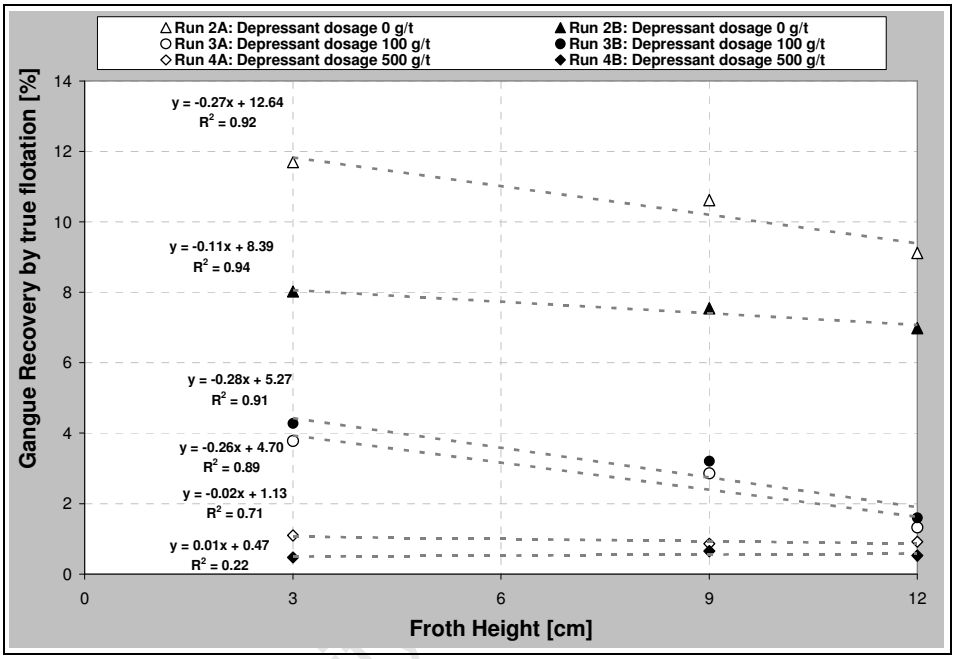

Figure 4. 22: Gangue recovery vs. froth height by true flotation (Runs 2, 3 and 4)

For all the Runs, the collection zone recoveries (Y-axis intercepts in Figure 4.22) were low (less than 15%). This is in agreement with the fact that the feed used in these tests was the concentrate from the primary cleaner second stage, which had lost some of the floatable gangue minerals in the plant feed. As the depressant dosage increased, the collection zone recoveries decreased appreciably. At 0 g/t of depressant, the collection zone recoveries were 12.64 and 8.39 %; these values decreased to 5.27 and 4.70 % at 100 g/t depressant, and to 1.13 and 0.47 % at 500 g/t, showing again the impact of the depressant dosage on the recovery of the gangue minerals by true flotation.

Having found the collection zone recovery of gangue minerals, Equation 4.11 was used to estimate the froth recoveries in each test. A sample calculation is shown below for Test 7 of Run 2A:

Table 4. 14: Flotation data of Test 7 Run 2A: 0 g/t Depressant, 3 cm Froth Height

$R_{c,\ Solids}$ [%]	$R_{Solids,\ True}$ [%]
12.64	11.69

where $R_{C,\ Solids}$ is the collection zone recovery of the gangue minerals (see Figure 4.22)

$R_{Solids,\ True}$ is the gangue recovery by true flotation (see Table 4.8: recovery by true flotation, Savassi method)

Hence $$11.69 = \frac{12.64 * R_{f,Solids}}{(1 - 12.64 + 12.64 * R_{f,Solids})}$$

which gives $R_{f,\ Solids}$ = 91.49 %. The calculated values of froth recovery of gangue minerals are listed in Table 4.13 for all the tests.

Figure 4.23 summarizes the relationship between the froth recovery of gangue minerals and the froth height at 0, 100 g/t of depressant (Runs 2A and B, 3A and B). The froth recoveries for tests operated at 500 g/t (Runs 4A and B) are not shown, because the froth was very unstable. It is apparent that the froth recovery of the floatable gangue minerals decreased approximately linearly with froth height irrespective of the depressant dosage used. Froth recoveries were very high in the absence of depressant, indicating that any floatable gangue entering the froth stood a very good chance of being recovered in the concentrate. Froth recovery then decreased as the depressant dosage increased (100 g/t). The lowest froth recovery was observed for the tests operated at 100 g/t of depressant. It can also be seen that the increase in froth height (3 to 9 cm) caused a greater drop in froth recovery of gangue at 100 g/t depressant than in the absence of depressant. Figure 4.23 shows that increasing the depressant dosage had a greater effect at 12 cm froth height. This result suggests that the combination of the depressant dosage and the froth height was effective in decreasing the recovery of floatable gangue minerals.

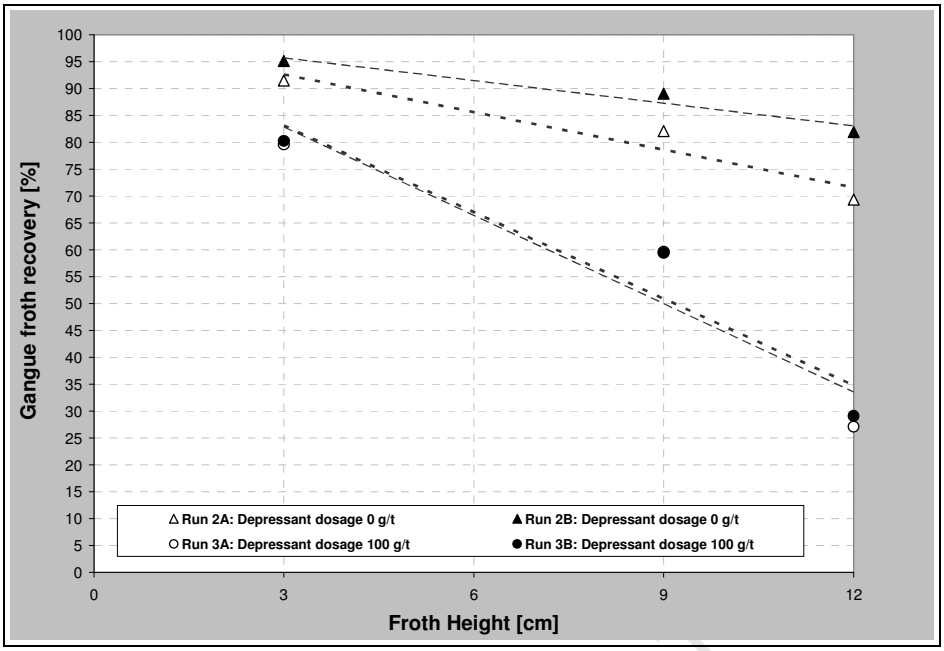

Figure 4. 23: Effect of froth height on froth recovery of gangue minerals (Runs 2 and 3)

4.3.7 Effect of depressant dosage on froth recovery of PGM

The same procedure as used above may be used to examine the effect of depressant dosage on the froth performance of the PGMs.

The first step is to evaluate the recovery of PGMs by entrainment. The entrainment factors calculated in section 4.3.4.2 will be used for this purpose. The estimation of PGM recovery by entrainment is required, because the calculation of the froth recovery requires the knowledge of the separate amount of PGMs recovered by true flotation and entrainment. A sample calculation of the mass flow rates of PGM recovered by true flotation and entrainment is shown below for Test 1 of Run 1A (data in Table 4.8 and Appendix F):

Table 4. 15: PGM flotation data of Test 1 Run 1A: 0 g/t Depressant, 9 cm Froth Height

$m_{PGM, Feed}$ [g/min]	$m_{w, Feed}$ [g/min]	$m_{w, Conc}$ [g/min]	$m_{PGM, Conc}$ [g/min]
0.04866	1332.02	202.97	0.01565

where $m_{PGM, Feed}$ is the mass flow rate of PGM in the feed.

$m_{PGM, Conc}$ is the mass flow rate of PGM in the concentrate.

$m_{w, Feed}$ is the mass flow rate of water the feed.

$m_{w,\,Conc}$ is the mass flow rate of water in the concentrate.

The correction factor to normalise the water flow rate in the concentrate is

$$\left(\frac{m_{PGM}}{m_w}\right)_{Feed} * m_{w,Conc} = 0.00623\ g/min$$

The degree of entrainment is

ENT = 1.71 (refer to Table 4.8)

Hence, the mass flow rate of PGMs recovered by entrainment is

$$m_{PGM,Entr} = ENT * \left(\frac{m_{PGM}}{m_w}\right)_{Feed} * (m_{w,Conc}) \quad \textbf{(4. 12)}$$
$$= 1.71 * 0.00741\ g/min = 0.01270\ g/min$$

The mass flow rate of PGMs recovered by true flotation is calculated using the following formula

$$m_{PGM,True} = m_{PGM,Conc} - m_{PGM,Entr} \quad \textbf{(4. 13)}$$
$$= 0.01652 - 0.01270 = 0.0295\ g/min$$

Finally, the PGM recovery by entrainment is

$$R_{PGM,Entr} = 100 * \left(\frac{m_{PGM,Entr}}{m_{PGM,Feed}}\right) \quad \textbf{(4. 14)}$$

where $m_{PGM,\,Feed}$ is the mass flow rate of PGM in the feed (see Appendix F).

Hence

$$R_{PGM,Entr} = 100 * \left(\frac{0.01270}{0.04866}\right)$$
$$= 26.10\ \%$$

Table 4.16 presents the PGM recoveries by entrainment for all the tests. It can be seen that PGM recoveries by entrainment are quite high at low depressant dosage. For instance at 0 g/t of depressant, the recoveries by entrainment are 26.10 and 12.90 %, respectively, for Runs 1A and 1B (tests performed at constant froth height of 9 cm), which represent 81.16 and 51.42 % of the total PGM recoveries. As shown in section 4.3.2, low depressant dosage is known to

be associated with high froth stability, which results in high recovery by entrainment. As the depressant dosage increases in Runs 1A and B, PGM recovery by entrainment decreases.

Table 4. 16: Mass flow rates of PGM recovered by entrainment and true flotation for all the Runs

Run 1A : PGMs Entrainment and true flotation at constant froth height of 9 cm								
Depressant [g/t]	ENT	Normal*$m_{w,conc}$ [g/min]	m_{Entr} [g/min]	$m_{PGM,Conc}$ [g/min]	$m_{PGM,True}$ [g/min]	$R_{PGM,Entr}$ [%]	$R_{PGM,Total}$ [%]	$R_{PGM,True}$ [%]
0	1.71	0.00741	0.01270	0.01565	0.00295	26.10	32.15	6.06
100	2.07	0.00272	0.00563	0.01570	0.01007	11.86	33.08	21.21
500	1.54	0.00053	0.00081	0.01578	0.01496	1.86	36.07	34.21
Run 1B: PGMs Entrainment and true flotation at constant froth height of 9 cm								
Depressant [g/t]	ENT	Normal*$m_{w,conc}$ [g/min]	m_{Entr} [g/min]	$m_{PGM,Conc}$ [g/min]	$m_{PGM,True}$ [g/min]	$R_{PGM,Entr}$ [%]	$R_{PGM,Total}$ [%]	$R_{PGM,True}$ [%]
0	2.36	0.00190	0.00448	0.00872	0.00424	12.90	25.09	12.19
100	2.52	0.00095	0.00238	0.00767	0.00528	6.14	19.75	13.61
500	2.95	0.00014	0.00042	0.00775	0.00732	1.09	19.85	18.76
Run 2A : PGMs Entrainment and true flotation at constant depressant dosage of 0 g/t								
Froth Height [cm]	ENT	Normal*$m_{w,conc}$ [g/min]	m_{Entr} [g/min]	$m_{PGM,Conc}$ [g/min]	$m_{PGM,True}$ [g/min]	$R_{PGM,Entr}$ [%]	$R_{PGM,Total}$ [%]	$R_{PGM,True}$ [%]
3	1.22	0.00623	0.00761	0.01652	0.00890	17.53	38.04	20.51
9	1.23	0.00472	0.00583	0.01686	0.01103	10.78	31.20	20.41
12	1.33	0.00379	0.00504	0.01502	0.00997	9.87	29.41	19.54
Run 2B : PGMs Entrainment and true flotation at constant depressant dosage of 0 g/t								
Froth Height [cm]	ENT	Normal*$m_{w,conc}$ [g/min]	m_{Entr} [g/min]	$m_{PGM,Conc}$ [g/min]	$m_{PGM,True}$ [g/min]	$R_{PGM,Entr}$ [%]	$R_{PGM,Total}$ [%]	$R_{PGM,True}$ [%]
3	1.44	0.00659	0.00950	0.01786	0.00836	24.54	46.13	21.59
9	1.44	0.00607	0.00876	0.01702	0.00825	21.91	42.54	20.64
12	1.42	0.00560	0.00794	0.01576	0.00781	19.81	39.30	19.49
Run 3A:PGMs Entrainment and true flotation at constant depressant dosage of 100 g/t								
Froth Height [cm]	ENT	Normal*$m_{w,conc}$ [g/min]	m_{Entr} [g/min]	$m_{PGM,Conc}$ [g/min]	$m_{PGM,True}$ [g/min]	$R_{PGM,Entr}$ [%]	$R_{PGM,Total}$ [%]	$R_{PGM,True}$ [%]
3	1.77	0.00241	0.00427	0.01166	0.00739	10.69	29.17	18.49
9	1.67	0.00162	0.00271	0.00873	0.00603	6.81	21.96	15.15
12	1.79	0.00084	0.00151	0.00540	0.00389	4.03	14.40	10.38
Run 3B: PGMs Entrainment and true flotation at constant depressant dosage of 100 g/t								
Froth Height [cm]	ENT	Normal*$m_{w,conc}$ [g/min]	m_{Entr} [g/min]	$m_{PGM,Conc}$ [g/min]	$m_{PGM,True}$ [g/min]	$R_{PGM,Entr}$ [%]	$R_{PGM,Total}$ [%]	$R_{PGM,True}$ [%]
3	1.47	0.00322	0.00472	0.01260	0.00788	11.95	31.88	19.93
9	1.38	0.00213	0.00293	0.00863	0.00570	7.54	22.19	14.64
12	1.53	0.00131	0.00201	0.00655	0.00453	5.32	17.30	11.97
Run 4A: PGMs Entrainment and true flotation at constant depressant dosage of 500 g/t								
Froth Height [cm]	ENT	Normal*$m_{w,conc}$ [g/min]	m_{Entr} [g/min]	$m_{PGM,Conc}$ [g/min]	$m_{PGM,True}$ [g/min]	$R_{PGM,Entr}$ [%]	$R_{PGM,Total}$ [%]	$R_{PGM,True}$ [%]
3	1.36	0.00085	0.00116	0.02855	0.02739	2.03	54.52	52.48
9	1.26	0.00079	0.00100	0.02312	0.02211	1.76	40.63	38.87
12	1.41	0.00057	0.00081	0.01484	0.01404	1.94	33.69	31.75
Run 4B: PGMs Entrainment and true flotation at constant depressant dosage of 500 g/t								
Froth Height [cm]	ENT	Normal*$m_{w,conc}$ [g/min]	m_{Entr} [g/min]	$m_{PGM,Conc}$ [g/min]	$m_{PGM,True}$ [g/min]	$R_{PGM,Entr}$ [%]	$R_{PGM,Total}$ [%]	$R_{PGM,True}$ [%]
3	1.58	0.00126	0.00199	0.02829	0.02630	3.18	45.25	42.06
9	1.38	0.00117	0.00161	0.02193	0.02032	2.42	32.97	30.54
12	1.01	0.00113	0.00114	0.01411	0.01297	1.91	23.61	21.70

N.B.: "*Normal*" in Column 3 above is the normalization factor defined previously.

The runs performed at constant depressant dosage and varying froth heights (Runs 2, 3 and 4) show the same trend: As the depressant dosage increases, PGM recovery by entrainment decreases. It is interesting to note that for all the tests operated at 500 g/t of depressant, the PGM recoveries by entrainment are very low, irrespective of froth height.

The recovery of the PGM by true flotation is based on the total PGM recovery and the recovery of PGM by entrainment. A sample calculation of PGM recovery by true flotation is shown below for Test 1 of Run 1A:

Table 4. 17: Flotation data of Test 1 Run 1A: 0 g/t Depressant, 9 cm Froth Height

$m_{PGM,\ Conc}$ [g/min]	$m_{PGM,\ Feed}$ [g/min]
0.01565	0.04866

$$R_{PGM,Total} = 100 * \left(\frac{m_{PGM,Conc}}{m_{PGM,Feed}} \right) \quad \textbf{(4. 15)}$$

where $R_{PGM,\ Total}$ is the total PGM recovery and is equal to 32.15 %

The PGM recovery by true flotation is calculated using the following formula

$$R_{PGM,True} = R_{PGM,Total} - R_{PGM,Entr} \quad \textbf{(4. 16)}$$
$$= 32.15 - 26.10 = 6.06\ \%$$

The recoveries of PGM by true flotation for all the runs are also shown in Table 4.16. Several trends can be observed. For the runs operated at constant froth height (Runs 1A and 1B) more PGM were recovered by true flotation when the depressant dosage increases. This was not expected: perhaps, as the depressant dosage increases, more PGM particles became available in the froth, due to the fact that gangue minerals were depressed, which led to the increase in PGM recovery by true flotation. For the runs operated in the absence of depressant (Runs 2A and 2B), PGM recoveries by true flotation remained fairly constant, indicating that the froth was stable even at a froth height of 12 cm.

For the other runs (Runs 3 and 4), the recovery of PGM by true flotation decreased as the froth height increased. This indicates that the froth was becoming less stable as the depressant was added, and that more coalescence

and drainage occurred as the froth height increased, resulting in losses in PGM recovery.

Having estimated the recovery of PGM by entrainment and true flotation, the effect of depressant dosage on the froth recovery of PGM can now be calculated. For this purpose, the same procedure is used as described in section 4.3.6 for naturally floatable gangue minerals. In Figure 4.24 the PGM recoveries are plotted against the froth heights for Runs 2, 3 and 4. In each case there is a linear relationship between the PGM recoveries and the froth heights, at all the depressant dosages tested. The coefficients of correlation and the equations of the correlation are shown in Table 4.18. The linear relationship between PGM recovery and the froth height is further confirmed by the coefficients of correlation which are close to 1 for all the runs.

Table 4. 18: Linear correlation parameters of PGM recoveries vs. froth height

Run	Equations	Coefficients of correlation
2A: 0 g/t depressant	y = -0.09x + 20.91	R^2 = 0.65
2B: 0 g/t depressant	y = -0.22x + 22.35	R^2 = 0.94
3A: 100 g/t depressant	y = -0.85x + 21.49	R^2 = 0.92
3B: 100 g/t depressant	y = -0.88x + 22.58	R^2 = 1.00
4A: 500 g/t depressant	y = -2.30x + 59.43	R^2 = 1.00
4B: 500 g/t depressant	y = -2.21x + 49.15	R^2 = 0.99

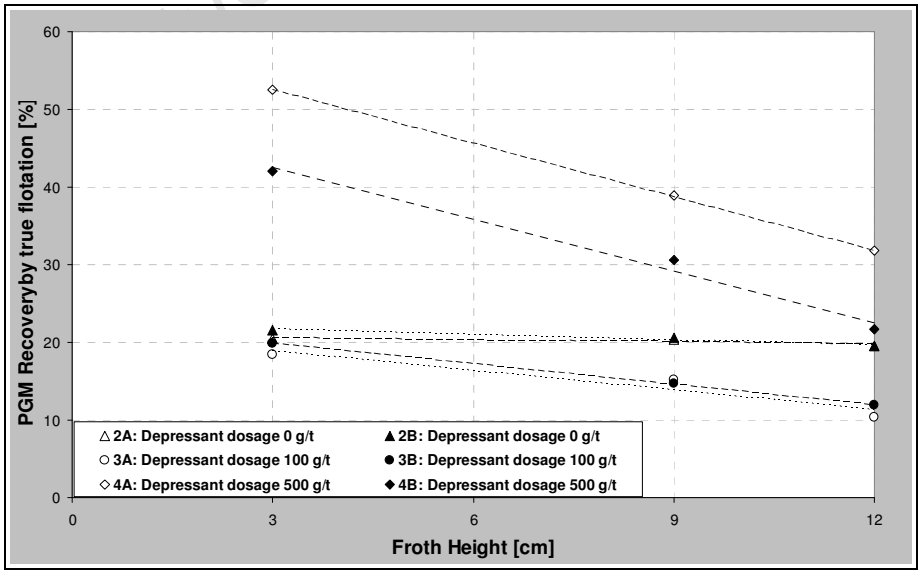

Figure 4. 24: Recovery of PGMs by true flotation vs. froth height (Runs 2, 3 and 4)

The overall trends are similar to those observed for the naturally floatable gangue minerals (Figure 4.22). However, there are some notable differences. The recoveries of gangue minerals are markedly lower than those of the PGM, even at 500 g/t depressant dosage and 3 cm froth height. The recoveries are around 20 % for the PGMs and only around 8 to 12 % for the gangue minerals at 0 g/t depressant. As the depressant dosage and froth height increased to 100 g/t depressant and 9 cm respectively, the recoveries of PGM are around 12 % and < 2% for the gangue minerals. At 500 g/t depressant dosage, the gangue recoveries are even lower (≈ 1 %), but the PGM recoveries are unexpectedly high, going from around 25 % at 3 cm froth height to around 45 % at 12 cm froth height. This increase in PGM recoveries is believed to be the result of the increase in PGM grade in the feed (refer to Table 21 below).

Equation 4.16 which is similar to Equation 4.11 is used to find the froth recoveries of PGM in all the tests. As with the gangue minerals, the intercepts of the straight lines are taken as the collection zone recoveries.

$$R_{PGM,True} = \frac{R_{c,PGM}R_{f,PGM}}{\left(1 - R_{c,PGM} + R_{c,PGM}R_{f,PGM}\right)} \quad \textbf{(4. 17)}$$

Table 4.19 presents the PGM recoveries by true flotation ($R_{PGM,\ True}$), the collection zone ($R_{C,\ PGM}$) and froth zone ($R_{f,\ PGM}$) recoveries, as well as the feed and concentrate PGM grades for Runs 2, 3 and 4. Within the same run (i.e. same depressant dosage) the froth recovery follows the overall recovery trend and decreased as the froth height increases. As would be expected, the grades increase as the froth height increases for all the runs except for Run 4 corresponding to 500 g/t of depressant. In Runs 4A and 4B, the PGM grade in the concentrate was very high at 3 and 9 cm froth height, but dropped with a further increase in the froth height (to 12 cm). This behaviour can be explained by the fact that the froth phase was already unstable in Run 4A and 4B at 9 cm froth height, so an increase in froth height (to 12 cm) would have caused a further destabilization of the froth phase resulting in the drop in grade. It can also be seen that total recovery can be correlated to the feed PGM grade: recoveries are

highest where the feed grades are highest. Napier-Munn (1998) observed the same behaviour on a copper-gold flotation plant.

Table 4. 19: Froth zone recovery of PGM at 0, 100 and 500 g/t of depressant

Run	Froth Height [cm]	Feed Grade [g/t]	Conc Grade [g/t]	R_t [%]	R_c [%]	R_f [%]
2A	**3**	72.21	94.00	20.51	20.91	97.58
0 g/t depressant	**9**	88.51	129.05	20.41	20.91	97.03
	12	86.47	133.94	19.54	20.91	91.84
2B	**3**	63.48	89.94	21.59	22.35	95.64
0 g/t depressant	**9**	65.49	94.62	20.64	22.35	90.35
	12	65.78	96.50	19.49	22.35	84.09
3A	**3**	64.29	129.70	18.49	21.49	78.57
100 g/t depressant	**9**	63.85	145.10	15.15	21.49	54.60
	12	63.86	172.13	10.38	21.49	32.71
3B	**3**	64.88	127.47	19.93	22.58	81.25
100 g/t depressant	**9**	63.53	131.22	14.64	22.58	54.69
	12	64.51	161.35	11.97	22.58	38.81
4A	**3**	94.38	1466.17	52.48	59.43	68.68
500 g/t depressant	**9**	95.72	1483.47	38.87	59.43	35.09
	12	79.84	999.42	31.75	59.43	23.49
4B	**3**	108.39	1344.40	42.06	49.15	73.42
500 g/t depressant	**9**	115.36	1238.84	30.54	49.15	49.59
	12	111.72	1086.99	21.70	49.15	28.52

Figure 4.25 summarizes the relationship between froth recovery and froth height at 0, 100 and 500 g/t of depressant (Runs 2A and B, 3A and B, 4A and B). It is obvious that the froth recovery decreases approximately linearly with froth height irrespective of the depressant dosage used. It can also be seen that froth recovery dropped mostly sharply at high depressant dosage.

At a froth height of 3 cm the froth recovery dropped from 90 % to 70 % as the depressant dosage was increased from 0 to 500 g/t of depressant; at 9 cm froth height, the froth recovery decreased from 80 to around 40 %; and at 12 cm the froth recovery went from 70 to around 25%.

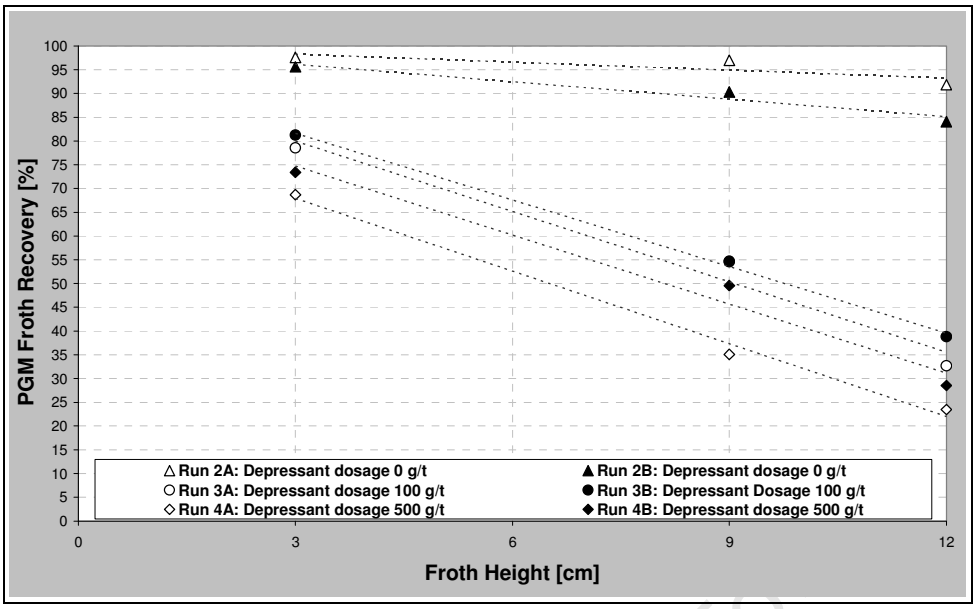

Figure 4. 25: Effect of froth height on froth recovery of PGMs (Runs 2 to 4)

The result shown above may be used to interpret the results of the tests operated at three depressant dosages and a constant froth height of 9 cm (Runs 1A and 1B). Figure 4.26 shows the effect of depressant dosage on PGM grade for these two runs. As can be seen, the grade of PGM increased to 1050 and 882.90 g/t at 500 g/t of depressant dosage. This corresponds to the removal of floatable gangue from the froth, which is supported by the sharp decrease in the mass flow rates of solids upon addition of depressant (see section 4.3.2). It is believed that high depressant dosage caused the boundaries between bubbles in the froth to be thinned, and the bubbles to coalesce. This would cause drainage of dense and/or less hydrophobic particles.

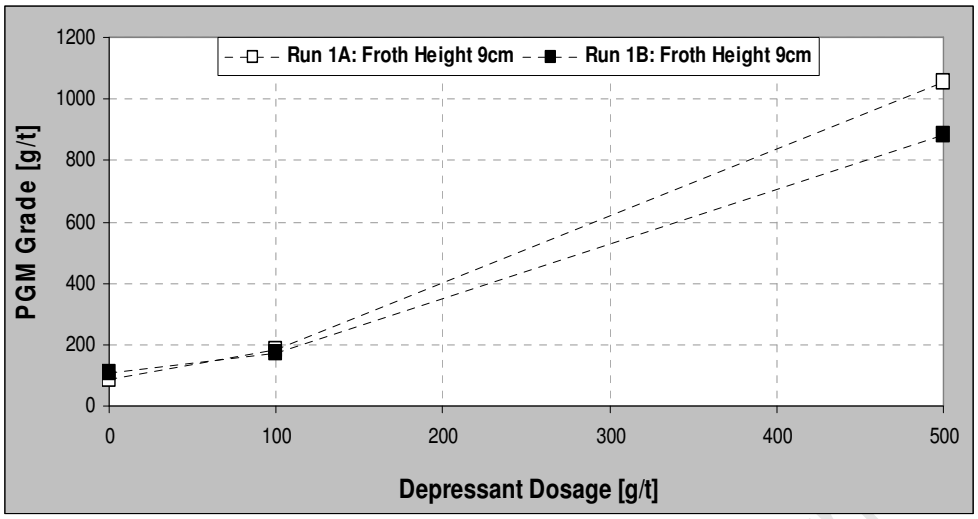

Figure 4. 26: Effect of depressant dosage on PGM grade (Runs 1A and 1B)

The effect of depressant dosage on total PGM recovery is shown in Figure 4.27 for Runs 1A and 1B. It can be seen that in Run 1B the recovery decreased from 0 to 100 g/t of depressant, but then remained constant. In Run 1A, the PGM recovery increased slightly as the depressant dosage increased from 0 to 100 and 500 g/t. This result shows that on average there was no significant loss in PGM recovery despite an increase in grade, which usually implies loss in recovery. The PGM recoveries are believed to be the result of the low air rate[1], at which all the tests were operated. Low to moderate air rate is known to generate high bubble loading, which is indicative of a more selective separation. High bubble loading promoted a more stable froth. It appears that this was sufficient to counteract the destabilizing effect of increasing depressant dosage. This is consistent with work by previous workers (Barbian et al., 2005).

[1] Refer to section 3.1

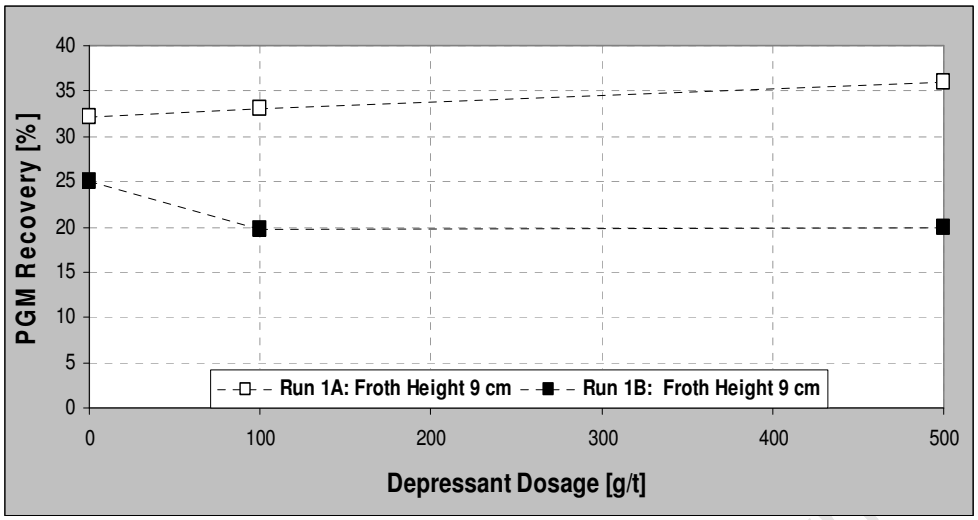

Figure 4. 27: Effect of depressant dosage on PGM recovery (Runs 1A and 1B)

4.4 SUMMARY OF THE SITE WORK

This Chapter had two main objectives: firstly, to determine separately the recovery of minerals by true flotation and entrainment and, secondly, to evaluate the effect of depressant dosage on froth performance. The column cell was used in the final cleaning application of the UG2 ore (K3 flotation plant / Lonmin). These objectives had been met.

While providing an opportunity to work with a reasonable solids percentage, the site tests brought the inconvenience of having very little control over the feed material. This was in terms of feed variability as well as dosages of reagent, which were added upstream of the column operation.

Nevertheless, the UCT method was used successfully to predict separately the amount of gangue recovered by true flotation and entrainment. Furthermore, Cr_2O_3 was used as a tracer to evaluate entrainment in the UG2 Platinum ore, which allowed the accuracy of the UCT method in predicting entrainment recovery (and hence true flotation) to be confirmed.

The froth varying technique was used to evaluate the effect of depressant dosage on the PGM froth recovery. The results (found) suggest that there was a

linear relationship between the froth recoveries and the froth height for both gangue minerals and PGM, which is in agreement with previous work on froth recovery. However true recoveries of gangue decreased, while recoveries of PGMs remained high.

CHAPTER FIVE: CONCLUSIONS AND RECOMMENDATIONS

5.1 CONCLUSION

This project has investigated the effect of depressant dosage on flotation performance, as measured by recovery, grade and froth recovery of naturally floatable gangue and PGM. This was done using a continuously-operated column flotation cell. The purpose of the current study was:

1. To develop a test procedure to study the interaction between the pulp and froth phases.
2. To see whether or not the "UCT method" can be implemented on a continuously-run column cell. The UCT method was initially developed on laboratory batch flotation cells to find separately the amount of gangue recovered by true flotation and entrainment.
3. To gain insight into how the properties of the solids in the pulp phase (as modified by depressant addition) affect the froth performance.

In laboratory tests, an experimental procedure was developed which allows the study of the interaction between the froth and the pulp phases. In this procedure, the column is run continuously while changing the flotation conditions. This procedure allows the study of the effect of any flotation parameter (e.g. collector type and dosage, depressant type, feed size...) on flotation performance. Work done in the laboratory and on site showed that the UCT method can be used on a continuously run column flotation cell.

The site tests were carried out to investigate the effect of depressant dosage on the froth performance in the flotation of PGM. The UCT method was used to predict recovery by entrainment. A second technique using Cr_2O_3 as a tracer was employed to assess the accuracy of the UCT entrainment predictions. The results obtained confirmed those the entrainment predictions of the UCT method are very close to that measured by the tracer method. This is a significant finding

as, previously, the UCT method had not been applied on a continuously-run column flotation cell.

One of the more significant findings to emerge from this study is that froth recovery of both gangue minerals and PGMs is linearly proportional to froth height. This was consistent with findings by previous workers (Vera et al., 2002), who observed a linear relationship between the overall rate constant and the froth height. Froth zone recovery R_f was found to be strongly linked to particle properties entering the froth: when the depressant dosage was increased, froth recoveries of both gangue minerals and PGM were affected negatively. This confirms work by previous researchers that particle properties (depressant) critically affect froth stability, which was found to be proportional to floatable solids content in the froth phase.

In froth flotation, an increase in grade is generally known to result in loss in recovery. This project showed that working at moderate air rate resulted in very high PGMs grade, while avoiding a loss in recovery. A possible reason for this is the low air flow rates employed in these tests, because of the phenomenon of pulp/froth interface vanishing, as described in section 3.1 above. This result is useful and should be investigated further in future tests.

This project also showed that as the PGM feed grade increased (due to plant variability), the grade increased proportionally, suggesting a correlation between the feed characteristics and the flotation performance. This is in agreement with previous work (Napier-Munn, 1995).

An important outcome of this project is the remarkable difference in the recoveries of the gangue minerals and the PGMs, at the different conditions studied. The combined effect of increasing the depressant dosage and the froth height caused the recoveries of the gangue minerals to drop to below 1%, while

the PGM recoveries remained high, even at 500 g/t depressant dosage and 12 cm froth height.

5.2 RECOMMENDATIONS AND LIMITATIONS

1. Build a smaller column to allow test work to be done in the laboratory at various conditions. It was found that while site tests were good for an unrestricted access to pulp, this came with a price: the scope for investigating a wide range of parameters was very limited. For instance, frother could not be added to the feed, because there was already too much in the circuit. In addition, the exact dosage used on site could not be accounted for accurately. This was also true for other reagents such as the collector and the depressant. A smaller column flotation cell will also requires less ore per test, allowing more test work to be done.
2. Due to higher frother content in the pulp, the tests performed on site were done at low superficial gas rate. The volumetric air rate used was determined by visual observation of the pulp interface froth / interface. This lacked accuracy. It is recommended that in future tests, the column flotation cell be fitted with a device (e.g. pressure gauge) to allow the determination of the working range of the superficial gas rate.
3. Site tests could have provided more insight if they were performed at different solids percentage. Entrainment has been found to depend strongly on pulp dilution (Lynch et al., 1981). Therefore it is recommended that in future work the solids percentage be considered as an important parameter.
4. During site tests, it was noted that, as the level of the pulp decreased in the feed tank, the mixing deteriorated. This translated into a decrease to the feed solids percentage in the column cell even within the same run. It is recommended that improving mixing characteristics of the feed tank be included in future work.

REFERENCES

Aktas, Z., Cilliers, J.J. and Banford, A.W., 2008. *Dynamic froth stability: Particle size, airflow rate and conditioning time effects.* International Journal of Mineral Processing, 87: 65-71.

Alexander, D.J., Franzidis, J.P. and Manlapig, E.V, 2003. *Froth recovery measurement in plant scale flotation cells.* Minerals Engineering 16: 1197–1203.

Alexander, D.J., Runge, K.C., Franzidis, J.P. and Manlapig, E.V., 2000. *The application of multicomponent floatability models to full scale flotation circuits*, 7th Mill Operators Conference, Aus. IMM Kalgoorlie, Australia, 167-178.

Anderson, C.J., 2008. *Flotation in a Novel Oscillatory Baffled Column.* PhD *Thesis*, Centre for Minerals Research, University of Cape Town.

Anderson, C.J., Harris, M.C. and Deglon, D.A., 2009. *Flotation in a novel oscillatory baffled column.* Minerals Engineering 22: 1079–1087.

Ata, S., Ahmed, N., Jameson, G.J., 2004. *The effect of hydrophobicity on the drainage of gangue minerals in flotation froths*. Minerals Engineering, 17: 897-901.

Banford, A.W., Aktas, Z., Woodburn E.T., 1998. *Interpretation of the effect of froth structure on the performance of froth flotation using image analysis.* Powder Technology, 98: 51-73.

Barbian, N., Hadler, K. and J.J. Cilliers, J.J, 2006. *The froth stability column: measuring froth stability at an industrial scale*. *Minerals Engineering* 19 (6–8): 713–718.

Barbian, N., Ventura-Medina E. and Cilliers, J.J., 2005. *Mineral attachment and bubble bursting in flotation froths*. In: Proceedings of the Centenary of Flotation Symposium, Brisbane, Australia.

Barbian, N., Hadler, K; Ventura-Medina, K. E., Cilliers, J.J., 2005. *The froth stability column: linking froth stability and flotation performance*. Minerals Engineering 18: 317–324.

Barbian, N., Ventura-Medina, E. and Cilliers, J.J., 2003. *Dynamic froth stability in froth flotation*. Minerals Engineering 16: 1111–1116.

Becker, M, Harris, P.J., Wiese, J.G and Bradshaw, D.J., 2009. *Mineralogical characterization of naturally flotable gangue in Merensky Reef ore flotation*. International Journal of Mineral Processing, 93: 246 - 255.

Bikerman, J.J.; 1973. *Foams.* Applied Physics and Engineering, 10, Springer-Verlag, Berlin.

Bisshop, J. P. and White, M. E., 1976. *A Study of Particle Entrainment in Flotation Froths.* Trans IMM, 85, C191-C194.

Bradshaw, D.J., 2009. *Introduction to minerals processing and assessment of flotation performance, Lecture 7, Process Mineralogy Course*. University of Cape Town, Cape Town, South Africa.

Bradshaw, D.J, Harris, P.J., and O'Connor, C.T, 2005a. *The Effect of Collectors and Their Interactions with Depressants on the Behaviour of the Froth Phase in Flotation*, in Centenary of Flotation Symposium, Brisbane, 329-333.

Bradshaw, D.J., Oostendorp, B., Harris, P.J., 2005b. *Development of methodologies to improve the assessment of reagent behaviour in flotation with particular reference to collectors and depressants.* Minerals Engineering 18: 239–246.

Bulatovic, S.M., 2007. *Handbook of Flotation Reagents, 1*. Elsevier, Amsterdam, 446 pp

Cawthorn, R. G., 2011. *Geological interpretations from the PGE distribution in the Bushveld Merensky and UG2 chromitite reefs*. The Journal of the Southern African Institute of Mining and Metallurgy. Vol. 111, pp 67 - 79.

Cilliers, J, 2006. *Understanding froth behaviour with CFC.* Fifth International Conference on CFD in the Process Industries CSIRO, Melbourne, Australia 13-15 December.

Cutting, G.W., Watson, D., Whitehead, *A.,* Barber, S.P., 1981. *Froth Structure in* Continuous Flotation Cells. International Journal of Mineral Processing; 7: 347 – 369.

Dahlke, R., Gomez, C.O. and Finch, J.A., 2005. *Operating range of a flotation cell determined from gas holdup vs. gas rate*. Minerals Engineering 18 (9), 977–980.

de Jager, G, Hatfield, D P, Bradshaw, D J; Francis, J J and Morar, S H, 2004. *A method and a control system for extracting valuable minerals from mined ore*, 'SmartFroth', Adams & Adams Patent Attorneys, Pretoria, A&A Ref: v16148 (1-9), Provisional patent.

Del Villar, R, Gomez, C.O., Finch, J.A. and Espinosa, R.G., 1989. *Flotation Column Amenability and Scale-up Parameter Estimation Tests*, 28th Annual Conference of Metallurgists of C.I.M., Halifax, Canada, August.

Dippenaar, A., 1982a. *The destabilization of froth by solids. I. The mechanism of film rupture*. International Journal of Mineral Processing, 9: 1-14.

Dippenaar, A., 1982b. *The destabilization of froth by solids.II The rate-determining step*. International Journal of Mineral Processing, 9: 15-22.

Ekmekçi, Z, Bradshaw, D.J., P.J. Harris, P.J. and Buswell, A.M., 2006. *Interactive effects of the type of milling media and CuSO4 addition on the flotation performance of sulphide minerals from Merensky ore Part II: Froth stability*. International Journal of Mineral Processing, 78: 164 – 174.

Engelbrecht, J.A. and Woodburn, E.T., 1975. *The effect of froth height, aeration rate and gas precipitation on flotation*. J. S. Afr. Inst. Min. Metall. 10: 125–132.

Falutsu, M. and Dobby, G.S., 1989. *Direct measurement of froth drop back and collection zone recovery in a laboratory flotation column*. Minerals Engineering 2 (3), 377–386.

Feteris, S.M., Frew, J.A. and Jowett, A., 1987. *Modelling the Effect of Froth Depth, In Flotation. International Journal of Mineral Processing,* 20: 121-135.

Finch, J. A. and Dobby, G. S., 1990. *Column Flotation*, Pergamon Press.

Finch, J. A. and Dobby, G., 1985. *Mixing Characteristics of Industrial Flotation Column*. Chemical Engineering Science 40 (7): 1068 – 1068.

Finch, J. A.; Yianatos, J.; Dobby, G., 1989 Column Froths Mineral Processing and Extractive Metallurgy Review: An International Journal 5: 281 - 305.

Finch, J, Cilliers, J, Yianatos, J, 2007. *Column Flotation.* 681 - 737 in *Froth Flotation. A Century of Innovation.* Edited by Fuerstenau M. C., Jameson, G. and Yoon, R-H, 2007. Society for Mining, Metallurgy and Exploration, Colorado.

Forbes, G., 2005. *Texture and Bubble Size Measurements for Modelling Concentrate Grade in Flotation Froth Systems*, Ph.D. thesis, University of Cape Town.

Francis, J., 2001. *Machine vision for froth flotation*, Ph.D. thesis, University of Cape Town.

Fuerstenau, 2007. *Developments in the Chemistry of Flotation Processing*. 3 – 64 in *Froth Flotation. A Century of Innovation.* Edited by Fuerstenau M. C., Jameson, G. and

George, P., Nguyen, A.V. and Jameson, G. J., 2004. *Assessment of true flotation and entrainment in the flotation of submicron particles by fine bubbles.* Minerals Engineering 17: 847–853.

Goodall, C.M. and O'Connor, C.T., 1991. Residence Time Distribution Studies in a Flotation Column*. Part 1: The Modeling of Residence Time Distributions in a Laboratory Column Flotation Cell.* International Journal of Mineral Processing, 31(1-2), 97–113*.*

Gupta, A. and Yan, D. S. Y, 2005. *Mineral processing design and operation: an introduction.* Elsevier, Amsterdam.

Hadler, K, Smith, C.D, Cilliers, J.J., 2010. *Recovery vs. mass pull: The link to air recovery.* Minerals Engineering 23: 994–1002.

Harris, P.J, 1982. *Frothing phenomena and frothers*. In: R.P. King, Editor, Principles of Flotation, South African Institute of Mining and Metallurgy, Johannesburg (1982), pp. 237–250.

Hatfield, D P., Bradshaw, D J. and de Jager, G, 2003. *The relationship between concentrate yield and descriptors from a machine vision system in platinum flotation application*, in Proceedings: XXII International Mineral Processing Congress, pp 929-936.

Havre H., 1952. *Préparation mécanique et concentration des minerais par flotation et sur liqueurs denses.* Librairie Polytechnique Béranger, Paris.

Heinrich, G, 2003. *An investigation into the use of froth colour as sensor for metallurgical grade in a copper system*. Master's thesis, University of Cape Town.

Hemmings, C.E., 1980. *An alternative viewpoint on flotation behaviour of ultrafine particles*. Trans. Inst. Min. Metall. (Sect. C Miner. Process. Extract. Metall.), 89: C113-C120.

Huls B.J., Lachance C.D. and Dobby G.S., 1989. *Gas rate and froth depth effects on performance of a Cu-Ni separation flotation column*, in Processing of Complex Ores(Dobby and Rao, eds.), Pergamon Press, CIM 28th Annual Conf. of Metallurgists, Halifax, Nova Scotia.

Jasieniak, M. and Smart,R. St. C., 2010. *Surface chemical mechanisms of inadvertent recovery of chromite in UG2 ore flotation: Residual layer identification using statistical ToF-SIMS analysis.* International Journal of Mineral Processing, Vol. 94: 1-2.

JKMRC/Amira International, 2004. *Amira Project P9M Volume II Flotation Module 2000 – 2003*.

Johansson, G. I., and Pugh, R. J., 1992. *The influence of particle size and hydrophobicity on the stability of mineralized froths*. International Journal of Mineral Processing, 34: 1-21.

Johnson, N.W., McKee, D.J and Lynch, A.J, 1974. *Flotation rates of nonsulphide minerals in chalcopyrite flotation processes*. Trans. A.I.M.E**.** 256**:** 204–209.

Kelly E.G. and Spottiswood D.J., 1989. *Introduction to mineral processing*. Wiley Interscience, Australia.

Klassen, V.I. and Mokrousov, V.A., 1963. *An Introduction to the Theory of Flotation*, Butterworths, London.

Kohmuench, J. N., 1998. *Precombustion removal of hazardous air pollutant precursors*. Msc thesis, Virginia Polytechnic Institute and State University.

Laskowski, J.S., 2008. *Surface chemistry of disperse systems*. Short Course: Centre for Minerals Research. University of Cape Town.

Liddell, K.S., McRae; L.B. and Dunne, R.C., 1986. *Process routes for beneficiation of noble metals from Merensky and UG-2 ores*, Mintek Review, no.4.

Luttrell, G.H., 2010. *Techbal. Flow sheet Mass Balance Spreadsheet*. http://www.coalprepsociety.org/Toolbox/tabid/115/Default.aspx, August 31 2010

Lynch, A.J., Johnson, N.W., Manlapig, E.V., Thorne, C.G., 1981. *Developments in Mineral Processing - Mineral and Coal Flotation Circuits*. Elsevier Scientific Publishing Co., New York, pp 31.

Lynch, A.J., Johnson, N.W., McKee, D.J. and Thorne, C.G., 1974. *The behaviour of minerals in sulphide processes, with reference to simulation and control*. Journal of South African Institute of Mining and Metallurgy, Johannesburg.

Martinovic, J., et al, 2005. *Investigation of surface properties of gangue minerals in platinum bearing ores*. Journal of the South African Institute of Mining and Metallurgy, Vol.105 No.3.

Morar, H., Hatfield, D.P., Barbian, N., Bradshaw, D.J., Cilliers, J.J. and Triffett, B. 2006. *A comparison of flotation froth stability measurements and their use in the prediction of concentrate grade*. In G. Onal, et al. (eds), Proceedings of the XXIII International Mineral Processing Congress, 3-8 September 2006, Istanbul, Turkey, 739-744. ISBN 975-7946-27-3.

Morar, S H, Forbes, G, Heinrich, G S, Bradshaw, D J., King, D; Adair, B J I and Esdaile, L, 2005. *The Use of a Colour Parameter in a Machine Vision System, SmartFroth, to Evaluate Copper Flotation Performance at Rio Tinto's Kennecott Utah Copper Concentrator in Flotation*, in Centenary of Flotation Symposium, Brisbane, 147-151.

Moudgil, B. M. and Somasundaran, P, 1988. *Reagents in Mineral Technology*. New York: Marcel Dekker.

Naik, S. and van Drunick, W., 2005. *Anglo research (AR) experience with integrated comminution and flotation plant modelling*. Journal of the South African Institute of Mining and Metallurgy, Vol. 107.

Napier-Munn, T.J. 2003. *An Introduction to Comparative Statistics and Experimental Design for Minerals Engineering*. University of Queensland (JKMRC).

Napier-Munn, T.J., 1998. Analysing plant trials by comparing recovery-grade regression lines. Minerals Engineering 11 (10): 949–958.

Napier-Munn, T.J., 1995. *Detecting performance improvements in trials with time-varying mineral processes -three case studies*. Minerals Engineering 8 (8): 843–858.

Neethling, S. J., Lee, H. T. and Cilliers, J. J., 2003. *Simple relationships for predicting the recovery of liquid from flowing foams and froths*. Minerals Engineering 16: 1123–1130.

Nguyen, A.V. and Schulze, H. J., 2004. *Colloidal Science of Flotation*, Marcel Dekker, Inc., New York.

Oostendorp, B, Harris P., Bradshaw, D., 2005a. *Research Report: Development of a methodology for determining the entrainment factor in batch flotation*. Unpublished Research Report, Mineral Processing Research Unit, Department of Chemical Engineering. University of Cape Town.

Oostendorp, B, Harris P. and Bradshaw, D., 2005b. *Development of methodologies to improve the assessment of reagent behaviour in flotation with particular reference to collectors and depressants*. Minerals Engineering 18: 239–246.

Opobou-Lando, S.D., 2010. *Mineralogical characterisation of chromite in the UG2 Reef from Waterval Mine, Western Bushveld: Implications for minerals processing*. Master's thesis, University of Stellenbosch.

Pearse, M.J., 2004. *An overview of the use of chemical reagents in mineral processing*. Minerals Engineering 18: 139–149.

Penberthy, C.J., Oosthuyzen, E.J. and Merkle, R.K.W, 2000. *The recovery of platinum-group elements from the UG-2 chromitite, Bushveld Complex—a mineralogical perspective*. Mineralogy and Petrology 68: 213–222.

Pugh, J., 2005. *Experimental techniques for studying the structure of foams and froths,* Advances in Colloid and Interface Science, 114-115: 239-251.

Rahal, K., Manlapig, E. and Franzidis, J.P., 2001. *Effect of frother type and concentration on the water recovery.* Minerals and Metallurgical Processing, 18: 138-141.

Ross, V.E. and Van Deventer, J.S.J., 1988. *In: Sastry, K. (Ed.), Column Flotation '88* -Proceedings of an International Symposium. SME Inc., Littleton, pp. 383–386.

Ross, V.E., 1990. *Flotation and entrainment of Particles during batch flotation tests*. Mineral Processing, 3: 245–256.

Ross, V.E., 1991. *Comparison of methods for evaluation of true flotation and entrainment*. Transactions of the Institution of Mining and Metallurgy (Section C: Mineral Processing and Extractive Metallurgy) 100: 121–126.

Savassi, O.N., Alexander, D.J., Franzidis, J.-P. and Manlapig, E.V., 1998. *An empirical model for entrainment in industrial flotation plants*. Minerals Engineering 11 (3): 243–256.

Seaman, D.R, Manlapig, E.M and J.P. Franzidis, 2006. *Selective transport of attached particles across the pulp–froth interface*. *Minerals Engineering*, 19: 841–851.

Seaman, D.R., Franzidis, J.P and Manlapig, E.M, 2004. *Bubble load measurement in the pulp zone of industrial flotation machines—a new device for determining the froth recovery of attached particles*. International Journal of Mineral Processing, 74: 1–13.

Schouwstra, R.P and E.D. Kinloch, E.D., 2000. *A short geological review of the Bushvelt complex.* Platinum Minerals Review 44: 33–39.

Schwarz, S., 2004. *The relationship Between Froth Recovery and Froth Structure*, *PhD Thesis*, Ian Wark Research Institute, University of South Australia.

Shah, Y.T., Kelkar, B.G., Godbole, S.P. and Deckwer, W.D., 1982. *Design parameters estimations for bubble column reactors.* AIChE J.28: 353–380.

Solomon, N, 2010. *Effect of HPGR on Platinum Bearing Ores and the Flotation Response.* Master's thesis, University of Cape Town.

Somasundaran, P. and Moudgil, B.M., 1988. *Reagents in Mineral Technology*. Marcel Dekker, New York.

Sweet, C., 2000. *The application of a machine vision system to relate to froth surface characteristics to the metallurgical performance of a PGM flotation process*. Master's thesis, University of Cape Town.

Sweet, C., van Hoogstraten, J., Harris, M.C. and Laskowski, J.S., 1997. *The effects of frothers on bubble size and frothability of aqueous solutions*. In: Finch, J.A., Holubec, I. (Eds.), Processing of Complex Ores – Proceedings of 2nd UBC-McGill Symposium. CIM, Montreal, pp. 235–246.

Tao, D., Luttrell, G. H., Yoon, R. -H., 2006. *A parametric study of froth stability and its effect on column flotation of fine particles.* International Journal of Mineral Processing, 59: 25 - 43.

Trahar, W.J. and Warren, L.J., 1976. *The floatability of very fine particles–a review*. International Journal of Mineral Processing 3: 103–131.

Tsatouhas, G., Grano, S.R. and Vera, M., 2006. *Case studies on the performance and characterisation of the froth phase in industrial flotation circuits.* Minerals Engineering 19: 774–783.

Ventura-Medina, E.; Barbian, N. and Cilliers, J.J., 2003. *Froth stability and flotation performance. IMPC 2003 Proceedings*, Cape Town, South Africa.

Ventura-Medina, E. and Cilliers, J.J., 2002. *A model to describe flotation performance based on physics of foams and froth image analysis*. International Journal of Mineral Processing 67, 79–99.

Ventura-Medina, E.; Barbian, E and Cilliers, J.J, 2004. *Solids loading and grade on mineral froth bubble lamellae*. *International* Journal of Mineral Processing, 74:1-4.

Vera, M. A.; Franzidis, J. P. And Manlipig, E. V., 1999a. *The JKMRC high bubble surface area flux flotation cell*. Minerals Eng., 12: 477-484.

Vera, M.A., Franzidis, J.-P and Manlapig, E.V., 1999b. *Simultaneous determination of collection zone rate constant and froth zone recovery in a mechanical flotation environment*. Minerals Engineering 12 (10): 1163–1176.

Vera, M.A, Mathe, Z.T; Franzidis, J.P; Harris, M.C.; Manlapig, E.V and O'Connor, C.T, 2002. *The modelling of froth zone recovery in batch and continuously operated laboratory flotation cells. International* Journal of Mineral Processing 64: 135–151.

Vianna, S.M., 2004. *The Effect of Particle Size, Collector Coverage and Liberation on the Floatability of Galena Particles in an Ore* (Ph.D. thesis). University of Queensland.

Warren, L. J., 1985. *Determination of the Contributions of True Flotation and Entrainment in Batch Flotation Test.* International Journal of Mineral Processing, 14: 33.

Welsby, S.D.D., Vianna, S M.S. and Franzidis, J-P. (2010). *The significance of internal recycle in froth flotation*. In: XXV International Mineral Processing Congress - IMPC 2010 'Smarter processing for the future. International Mineral Processing Congress 2010, Brisbane, Qld, Australia, (2543-2550). 6-10 September, 2010.

Wesseldijk, QI; Bradshaw, DJ; Harris, PJ and Reuter, MA, 1999. *The flotation behaviour of chromite with respect to the beneficiation of UG2 ore*, Minerals Engineering, 12 (10): 1177-1184.

Wiese, J.G., Harris, P., Bradshaw, D.J., 2006a. *The role of the reagent suite in optimizing pentlandite recoveries from the Merensky reef.* Minerals Engineering 19: 1290–1300.

Wiese, J.G., Becker, M, Bradshaw, D J and Harris, J.P., 2006b. *Interpreting the role of reagents in the flotation of platinum bearing Merensky ores*. International Platinum Conference 'Platinum Surges Ahead'. The Southern African Institute of Mining and Metallurgy.

Wiese, J.G., Harris, P. and Bradshaw, D.J., 2007. *The response of sulphide and gangue minerals in selected Merensky ores to increased depressant dosages.* Minerals Engineering 20: 986–995.

Wiese, J.G., Harris, H., Bradshaw, D.J., 2005. *Investigation of the role and interactions of a dithiophosphate collector in the flotation of sulphides from the Merensky reef*. Minerals Engineering. 18(8):791-800.

Wiese, J.G., Harris, P., Bradshaw; D.J., 2010. T*he effect of increased frother dosage on froth stability at high depressant dosages*. Mineral Engineering 23: 1010–1017.

Wills, B.A and Napier-Munn, T., 2006. *Mineral Processing Technology: An Introduction to the Practical Aspects of Ore Treatment and Mineral Recovery*, 7th edition, Pergamon Press.

Xu, M., Quinn, P.; Stratton-Crawley, R., 1996. *A feed-line aerated flotation column part 1: Batch and continuous testwork*. Minerals Engineering, 9(5), 499–507.

Xu, M., Uribe-Salas, A., Finch, J.A. and Gomez, C.O, 1989. *Gas rate limitation in flotation column*. In: G.S. Dobby and S.R. Rao, Editors, *Processing of Complex Ores, Proceedings of 28th Annual Conference of Metallurgists of CIM*, Pergamon Press, New York, p. 397.

Yianatos, J.B., 2007. *Fluid flow and kinetic modelling in flotation related processes: columns and mechanically agitated cells*. *Chemical Engineering Research and Design* 85 (A12): 1–13.

Yianatos, J.B., 1989. *Column flotation modelling and technology.* In Developments in Froth Flotation, International Colloquium. In: *The South African Inst. Min. and Met.* Vol.2: 1–30 Cape Town, South Africa.

APPENDICES

APPENDIX A: SPREADSHEET PRELIMINARY TESTS

BALANCED DETAILS OF PRELIMINARY WORK
(DEPRESSANT DOSAGE AND FROTH HEIGHT CHANGES)

Run A: Frother Dosage 5 ppm

Test 1 (Run A): Depressant dosage 0 g/t

Sample	Mass Flow [g/min]	Water Flow [g/min]	Copper Grade [%]	Copper Mass [g/min]	Copper Recovery [%]	Nickel Grade [%]	Nickel Mass [g]	Nickel Recovery [%]	Sulphur Grade [%]	Sulphur Mass [g]	Sulphur Recovery [%]
C1	16.69	27.81	0.49	0.08	67.08	0.45	0.07	32.68	1.54	0.26	47.13
C2	18.75	27.75	0.46	0.09	69.85	0.54	0.10	35.31	1.81	0.34	48.36
C3	20.89	29.09	0.47	0.10	71.05	0.54	0.11	38.52	1.92	0.40	52.99
C4	20.45	29.62	0.50	0.10	72.76	0.56	0.11	42.34	1.94	0.40	55.38
C5	10.62	16.16	0.69	0.07	65.53	0.75	0.08	56.18	2.86	0.30	48.16
C6	9.37	17.49	1.24	0.12	75.02	1.17	0.11	39.19	5.40	0.51	60.82
F1	194.37	3378.73	0.09	0.17							
F2	183.52	3332.07	0.09	0.16							
T1	157.53	3227.97	0.04	0.04		0.10	0.15		0.18	0.29	
T2	194.83	3520.45	0.03	0.04		0.09	0.18		0.19	0.36	
T3	177.01	3206.59	0.03	0.04		0.10	0.18		0.20	0.36	
T4	162.27	3003.81	0.03	0.04		0.10	0.16		0.20	0.32	
T5	161.92	2949.79	0.03	0.04		0.04	0.06		0.20	0.33	
T6	170.64	2896.87	0.03	0.04		0.10	0.17		0.19	0.33	

Test 2 (Run A): Depressant dosage 100 g/t

Sample	Mass Flow [g/min]	Water Flow [g/min]	Copper Grade [%]	Copper Mass [g/min]	Copper Recovery [%]	Nickel Grade [%]	Nickel Mass [g]	Nickel Recovery [%]	Sulphur Grade [%]	Sulphur Mass [g]	Sulphur Recovery [%]
C1	10.55	20.96	1.23	0.13	65.32	1.41	0.15	45.94	5.02	0.53	62.19
C2	9.83	20.46	1.18	0.12	64.06	1.41	0.14	44.71	5.18	0.51	62.07
C3	9.66	19.38	1.12	0.11	62.58	1.41	0.14	45.15	4.97	0.48	63.27
C4	10.02	20.39	1.17	0.12	62.51	1.36	0.14	44.33	4.80	0.48	61.75
C5	8.89	18.35	0.95	0.08	57.35	1.31	0.12	42.58	4.94	0.44	60.37
T1	180.44	3046.16	0.04	0.07		0.11	0.20		0.21	0.38	
T2	175.04	2954.53	0.04	0.07		0.10	0.17		0.18	0.32	
T3	179.85	2986.19	0.04	0.07		0.10	0.17		0.17	0.31	
T4	169.85	2805.92	0.04	0.06		0.10	0.17		0.16	0.28	
T5	180.52	3072.05	0.04	0.07		0.09	0.17		0.17	0.30	

Test 3 (Run A): Depressant dosage 300 g/t

Sample	Mass Flow [g/min]	Water Flow [g/min]	Copper Grade [%]	Copper Mass [g/min]	Copper Recovery [%]	Nickel Grade [%]	Nickel Mass [g]	Nickel Recovery [%]	Sulphur Grade [%]	Sulphur Mass [g]	Sulphur Recovery [%]
C1	5.01	11.74	1.78	0.09	63.40	1.68	0.08	40.25	6.46	0.32	61.55
C2	5.66	11.91	1.76	0.10	67.40	2.66	0.15	55.98	7.93	0.45	68.57
C3	5.36	12.49	1.87	0.10	66.60	2.86	0.15	54.28	8.60	0.46	68.50
C4	5.72	10.93	1.87	0.11	70.35	3.07	0.18	56.07	10.70	0.61	71.44
C5	4.58	10.58	1.76	0.08	63.60	3.40	0.16	52.57	10.90	0.50	66.33
T1	128.71	2547.08	0.04	0.05		0.10	0.12		0.16	0.20	
T2	127.68	2511.91	0.04	0.05		0.09	0.12		0.16	0.21	
T3	123.96	2541.61	0.04	0.05		0.10	0.13		0.17	0.21	
T4	121.12	2485.40	0.04	0.05		0.11	0.14		0.20	0.24	
T5	120.79	2410.51	0.04	0.05		0.12	0.14		0.21	0.25	

Run B: Frother Dosage 16 ppm

Test 1 (Run B): Depressant dosage 0 g/t

Sample	Mass Flow [g/min]	Water Flow [g/min]	Copper Grade [%]	Copper Mass [g/min]	Copper Recovery [%]	Nickel Grade [%]	Nickel Mass [g]	Nickel Recovery [%]	Sulphur Grade [%]	Sulphur Mass [g]	Sulphur Recovery [%]
C1	29.69	43.98	0.45	0.13	64.05	0.40	0.12	34.67	1.50	0.45	52.90
C2	30.66	43.27	0.46	0.14	62.47	0.43	0.13	32.29	1.68	0.52	48.14
C3	35.45	44.48	0.44	0.16	64.19	0.49	0.17	38.62	1.80	0.64	52.93
C4	36.41	45.01	0.46	0.17	65.77	0.50	0.18	39.47	1.88	0.68	55.48
C5	18.86	29.36	0.47	0.09	50.60	0.46	0.09	23.76	1.89	0.36	40.18
F1	332.63	3705.63	0.07	0.25		0.12	0.40		0.00	0.00	
F2	361.27	3554.39	0.08	0.28		0.13	0.46			0.00	
T1	250.96	3380.36	0.03	0.08		0.09	0.22		0.16	0.40	
T2	299.91	3630.43	0.03	0.09		0.09	0.27		0.19	0.55	
T3	297.09	3569.60	0.03	0.09		0.09	0.27		0.19	0.57	
T4	293.71	3612.39	0.03	0.09		0.09	0.28		0.19	0.55	
T5	293.16	3581.65	0.03	0.09		0.09	0.28		0.18	0.53	

Test 2 (Run B): Depressant dosage 100 g/t

Sample	Mass Flow [g/min]	Water Flow [g/min]	Copper Grade [%]	Copper Mass [g/min]	Copper Recovery [%]	Nickel Grade [%]	Nickel Mass [g]	Nickel Recovery [%]	Sulphur Grade [%]	Sulphur Mass [g]	Sulphur Recovery [%]
C1	19.42	26.21	0.89	0.17	65.34	0.98	0.19	39.45	4.44	0.86	62.49
C2	15.93	24.33	1.01	0.16	65.48	1.14	0.18	37.87	5.11	0.81	58.46
C3	15.18	23.26	0.92	0.14	61.52	1.57	0.24	44.09	5.41	0.82	58.24
C4	18.87	26.86	0.91	0.17	67.02	1.43	0.27	45.02	4.93	0.93	61.13
C5	16.46	24.81	0.88	0.14	62.30	0.96	0.16	33.64	4.17	0.69	56.81
F1											
F2											
T1	315.55	3557.21	0.03	0.09		0.09	0.29		0.16	0.52	
T2	316.08	3548.01	0.03	0.08		0.09	0.30		0.18	0.58	
T3	311.48	3530.56	0.03	0.09		0.10	0.30		0.19	0.59	
T4	309.63	3557.43	0.03	0.08		0.11	0.33		0.19	0.59	
T5	320.16	3651.69	0.03	0.09		0.10	0.31		0.16	0.52	

Test 3 (Run B): Depressant dosage 300 g/t

Sample	Mass Flow [g/min]	Water Flow [g/min]	Copper Grade [%]	Copper Mass [g/min]	Copper Recovery [%]	Nickel Grade [%]	Nickel Mass [g]	Nickel Recovery [%]	Sulphur Grade [%]	Sulphur Mass [g]	Sulphur Recovery [%]
C1	12.03	20.44	1.11	0.13	59.44	1.22	0.15	34.24	5.09	0.61	56.28
C2	11.10	23.24	1.29	0.14	61.74	1.12	0.12	32.77	5.60	0.62	60.85
C3	13.96	27.44	1.30	0.18	69.80	1.56	0.22	47.90	6.04	0.84	69.70
C4	11.69	24.00	1.45	0.17	69.75	1.59	0.19	45.55	6.60	0.77	69.69
C5	10.79	21.44	1.46	0.16	68.40	1.94	0.21	49.22	7.03	0.76	69.96
F1											
F2											
T1	306.81	3486.67	0.03	0.09		0.09	0.28		0.16	0.48	
T2	300.61	3381.97	0.03	0.09		0.08	0.26		0.13	0.40	
T3	281.97	3288.33	0.03	0.08		0.08	0.24		0.13	0.37	
T4	268.47	3154.16	0.03	0.07		0.08	0.22		0.13	0.34	
T5	262.67	3111.00	0.03	0.07		0.08	0.22		0.12	0.33	

Test 4 (Run B): Depressant dosage 500 g/t

Sample	Mass Flow [g/min]	Water Flow [g/min]	Copper Grade [%]	Copper Mass [g/min]	Copper Recovery [%]	Nickel Grade [%]	Nickel Mass [g]	Nickel Recovery [%]	Sulphur Grade [%]	Sulphur Mass [g]	Sulphur Recovery [%]
C1	7.60	16.30	1.84	0.14	67.61	2.00	0.15	41.91	10.01	0.76	78.96
C2	6.88	15.18	2.15	0.15	70.02	2.31	0.16	43.35	11.40	0.78	82.45
C3	9.15	15.00	1.74	0.16	72.30	2.51	0.23	53.24	10.90	1.00	84.45
C4	5.57	12.45	2.49	0.14	69.44	2.16	0.12	36.48	12.20	0.68	75.24
C5	6.82	14.95	3.02	0.21	80.92	2.25	0.15	48.95	12.20	0.83	84.13
F1											
F2											
T1	259.56	3069.03	0.03	0.07		0.08	0.21		0.08	0.20	
T2	243.71	2988.19	0.03	0.06		0.09	0.21		0.07	0.17	
T3	255.12	3066.47	0.02	0.06		0.08	0.20		0.07	0.18	
T4	256.20	3039.08	0.02	0.06		0.08	0.21		0.09	0.22	
T5	200.47	2601.60	0.02	0.05		0.08	0.16		0.08	0.16	

Run C: Frother Dosage 20 ppm

Test 1 (Run C): Depressant dosage 0 g/t

Sample	Mass Flow [g/min]	Water Flow [g/min]	Copper Grade [%]	Copper Mass [g/min]	Copper Recovery [%]	Nickel Grade [%]	Nickel Mass [g]	Nickel Recovery [%]	Sulphur Grade [%]	Sulphur Mass [g]	Sulphur Recovery [%]
C1	32.00	47.00	0.50	0.16	62.45	0.42	0.14	33.68			
C2	32.86	47.50	0.50	0.16	63.93	0.44	0.14	33.61			
C3	31.95	46.84	0.51	0.16	62.63	0.45	0.15	33.74			
C4	32.53	48.05	0.49	0.16	62.21	0.45	0.15	33.22			
C5	30.42	47.52	0.56	0.17	62.01	0.50	0.15	31.99			
F1	513.08	5680.40	0.03	0.16		0.12	0.61				
F2	573.28	5652.36	0.03	0.17		0.13	0.73				
T1	301.54	3721.34	0.03	0.10		0.09	0.27				
T2	309.44	3697.26	0.03	0.09		0.09	0.28				
T3	310.16	3710.48	0.03	0.10		0.09	0.29				
T4	312.24	3736.48	0.03	0.10		0.09	0.30				
T5	347.60	4103.84	0.03	0.10		0.09	0.33				

Test 2 (Run C): Depressant dosage 100 g/t

Sample	Mass Flow [g/min]	Water Flow [g/min]	Copper Grade [%]	Copper Mass [g/min]	Copper Recovery [%]	Nickel Grade [%]	Nickel Mass [g]	Nickel Recovery [%]	Sulphur Grade [%]	Sulphur Mass [g]	Sulphur Recovery [%]
C1	16.40	31.52	0.88	0.14	57.23	0.87	0.14	30.19			
C2	16.89	34.92	0.88	0.15	60.11	0.87	0.15	32.02			
C3	14.96	31.10	1.06	0.16	62.93	0.87	0.13	30.28			
C4	15.76	35.83	0.98	0.15	62.47	0.90	0.14	33.81			
C5	16.00	37.23	1.09	0.17	65.38	1.14	0.18	38.22			
F1											
F2											
T1	336.72	3889.78	0.03	0.11		0.10	0.33				
T2	339.80	3879.52	0.03	0.10		0.09	0.31				
T3	320.66	3676.90	0.03	0.09		0.09	0.30				
T4	313.28	3680.22	0.03	0.09		0.09	0.28				
T5	316.82	3580.14	0.03	0.09		0.09	0.30				

Test 3 (Run C): Depressant dosage 300 g/t

Sample	Mass Flow [g/min]	Water Flow [g/min]	Copper Grade [%]	Copper Mass [g/min]	Copper Recovery [%]	Nickel Grade [%]	Nickel Mass [g]	Nickel Recovery [%]	Sulphur Grade [%]	Sulphur Mass [g]	Sulphur Recovery [%]
C1	6.00	20.00	1.01	0.06	69.16	0.94	0.06	17.92			
C2	5.50	20.00	0.96	0.05	68.14	0.90	0.05	16.65			
C3	5.00	22.00	1.22	0.06	69.97	0.97	0.05	16.12			
C4	6.00	21.00	0.98	0.06	68.60	1.02	0.06	19.07			
C5	6.00	19.00	0.95	0.06	68.47	1.03	0.06	19.56			
F1											
F2											
T1	283.70	3346.86	0.03	0.03		0.09	0.26				
T2	292.62	3406.90	0.03	0.02		0.08	0.25				
T3	287.60	3304.48	0.03	0.03		0.09	0.25				
T4	288.32	3326.38	0.03	0.03		0.09	0.26				
T5	283.00	3180.38	0.03	0.03		0.09	0.25				

Test 4 (Run C): Depressant dosage 500 g/t

Sample	Mass Flow [g/min]	Water Flow [g/min]	Copper Grade [%]	Copper Mass [g/min]	Copper Recovery [%]	Nickel Grade [%]	Nickel Mass [g]	Nickel Recovery [%]	Sulphur Grade [%]	Sulphur Mass [g]	Sulphur Recovery [%]
C1	5.00	15.00	1.15	0.06	68.52	1.15	0.06	38.53			
C2	4.30	14.00	1.19	0.05	65.25	1.19	0.05	35.84			
C3	4.60	15.00	1.45	0.07	71.76	1.47	0.07	43.07			
C4	4.30	16.00	1.35	0.06	68.06	1.70	0.07	46.05			
C5	4.50	15.00	1.45	0.07	71.17	1.84	0.08	48.80			
F1											
F2											
T1	289.04	3306.32	0.03	0.03		0.08	0.09				
T2	300.40	3383.36	0.03	0.03		0.09	0.09				
T3	418.24	3265.68	0.02	0.03		0.08	0.09				
T4	265.88	3296.66	0.02	0.03		0.08	0.09				
T5	267.56	3368.36	0.02	0.03		0.08	0.09				

Run C: Frother Dosage 25 ppm

Test 1 (Run D): Depressant dosage 0 g/t

Sample	Mass Flow [g/min]	Water Flow [g/min]	Copper Grade [%]	Copper Mass [g/min]	Copper Recovery [%]	Nickel Grade [%]	Nickel Mass [g]	Nickel Recovery [%]	Sulphur Grade [%]	Sulphur Mass [g]	Sulphur Recovery [%]
C1	37.69	68.28	0.37	0.14	65.23	0.28	0.10	33.48	0.88	0.33	57.37
C2	37.22	67.42	0.38	0.14	57.36	0.30	0.11	28.95	0.84	0.31	52.65
C3	38.71	68.88	0.40	0.15	63.44	0.34	0.13	35.18	0.77	0.30	48.67
C4	37.92	68.16	0.40	0.15	60.50	0.39	0.15	35.43	0.97	0.37	56.51
C5	38.45	69.22	0.40	0.15	61.13	0.39	0.15	37.30	1.08	0.42	60.43
F1	156.96	3193.50	0.09	0.13		0.13	0.20		0.00	0.00	
F2	261.00	3029.31	0.07	0.18		0.11	0.28			0.00	
T1	248.85	3285.00	0.03	0.08		0.08	0.21		0.10	0.25	
T2	309.33	2722.83	0.03	0.11		0.09	0.27		0.09	0.28	
T3	295.83	2925.96	0.03	0.09		0.08	0.24		0.11	0.31	
T4	304.74	2800.20	0.03	0.10		0.09	0.27		0.09	0.28	
T5	284.70	2787.54	0.03	0.10		0.09	0.25		0.10	0.27	

Test 2 (Run D): Depressant dosage 100 g/t

Sample	Mass Flow [g/min]	Water Flow [g/min]	Copper Grade [%]	Copper Mass [g/min]	Copper Recovery [%]	Nickel Grade [%]	Nickel Mass [g]	Nickel Recovery [%]	Sulphur Grade [%]	Sulphur Mass [g]	Sulphur Recovery [%]
C1	22.51	52.94	0.67	0.15	59.62	0.66	0.15	33.17	2.04	0.46	64.29
C2	21.51	51.98	0.71	0.15	63.70	0.70	0.15	36.01	2.60	0.56	61.87
C3	21.09	52.27	0.74	0.16	61.36	0.74	0.16	36.57	2.65	0.56	70.33
C4	21.21	51.93	0.71	0.15	58.95	0.75	0.16	35.65	2.39	0.51	66.76
C5	20.83	52.40	0.74	0.15	62.84	0.75	0.16	37.55	2.61	0.54	70.91
F1											
F2											
T1	316.89	3685.89	0.03	0.10		0.09	0.30		0.08	0.26	
T2	304.98	3523.26	0.03	0.09		0.09	0.27		0.11	0.34	
T3	283.77	3329.40	0.03	0.10		0.09	0.27		0.08	0.24	
T4	319.44	3787.56	0.03	0.10		0.09	0.29		0.08	0.25	
T5	296.61	3491.58	0.03	0.09		0.09	0.26		0.08	0.22	

Test 3 (Run D): Depressant dosage 300 g/t

Sample	Mass Flow [g/min]	Water Flow [g/min]	Copper Grade [%]	Copper Mass [g/min]	Copper Recovery [%]	Nickel Grade [%]	Nickel Mass [g]	Nickel Recovery [%]	Sulphur Grade [%]	Sulphur Mass [g]	Sulphur Recovery [%]
C1	17.81	40.00	0.71	0.13	61.53	0.70	0.13	33.01	2.21	0.39	67.76
C2	18.64	43.00	0.68	0.13	61.38	0.81	0.15	38.87	2.79	0.52	67.79
C3	18.62	39.00	0.65	0.12	62.39	0.81	0.15	40.19	2.90	0.54	74.02
C4	19.42	42.00	0.63	0.12	63.86	0.88	0.17	44.31	2.76	0.54	75.89
C5	19.46	41.00	0.62	0.12	65.01	0.85	0.16	44.25	2.78	0.54	74.67
F1											
F2											
T1	264.12	3248.37	0.03	0.08		0.10	0.25		0.07	0.19	
T2	269.43	3185.67	0.03	0.08		0.09	0.24		0.09	0.25	
T3	263.31	3015.69	0.03	0.07		0.09	0.22		0.07	0.19	
T4	254.55	2935.92	0.03	0.07		0.08	0.21		0.07	0.17	
T5	233.19	2852.79	0.03	0.06		0.09	0.21		0.08	0.18	

Test 4 (Run D): Depressant dosage 500 g/t

Sample	Mass Flow [g/min]	Water Flow [g/min]	Copper Grade [%]	Copper Mass [g/min]	Copper Recovery [%]	Nickel Grade [%]	Nickel Mass [g]	Nickel Recovery [%]	Sulphur Grade [%]	Sulphur Mass [g]	Sulphur Recovery [%]
C1	6.00	22.00	0.71	0.04	62.53	0.83	0.05	15.88	2.96	0.18	43.93
C2	6.20	23.00	0.74	0.05	63.71	0.83	0.05	20.09	2.95	0.18	52.83
C3	5.60	20.00	0.77	0.04	62.42	0.89	0.05	18.08	2.84	0.16	46.73
C4	6.00	25.00	0.79	0.05	63.07	0.92	0.06	19.72	3.57	0.21	51.13
C5	5.50	21.00	0.81	0.04	62.93	0.87	0.05	19.29	2.64	0.15	43.61
F1											
F2											
T1	290.19	3419.01	0.03	0.03		0.09	0.26		0.08	0.23	
T2	238.44	3580.02	0.26	0.03		0.09	0.21		0.07	0.16	
T3	251.85	3578.25	0.26	0.03		0.09	0.23		0.07	0.18	
T4	234.54	3670.08	0.03	0.03		0.10	0.22		0.09	0.20	
T5	239.82	3602.28	0.03	0.03		0.08	0.20		0.08	0.19	

APPENDIX B: EXAMPLE OF TECHBAL MASS BALANCE OPERATION

(Run 1A)

UCT Methodology (Depressant Dosage change): Run 1A Test 1

TECHBAL - MATERIAL BALANCE SPREADSHEET

Author: G. H. Luttrell
Department: Mining & Minerals Engineering
Address: Virginia Polytechnic Institute and State University
Blacksburg, Virginia USA 24061-0258

CIRCUIT: Column Cell Cleaning Application:0g/t depressant dosage Run 1A Test 1

	Node											
Stream	Test 1										Sum	Circuit
Float Feed	1										1	feed
Float Conc	-1										-1	product
Float Tail	-1										-1	product
Junction	0										0	
Separator	1										1	

(1=In,-1=Out,0=No Effect)

Number of feed streams: 1
Number of product streams: 2
Number of internal streams: 0
Minimum required samples: 3

TECHBAL - MATERIAL BALANCE SPREADSHEET

Author: G. H. Luttrell
Department: Mining & Minerals Engineering
Address: Virginia Polytechnic Institute and State University
Blacksburg, Virginia USA 24061-0258

CIRCUIT: Column Cell Cleaning Application:0g/t depressant dosage Run 1A Test 1

	Measured Values						Estimated Values					
Stream	Mass	PGM [g/t]	Cr [%]	Mass Fraction of Solids	SiO2 [%]	Al2O3 [%]	Mass	PGM [g/t]	Cr [%]	Mass Fraction of Solids	SiO2 [%]	Al2O3 [%]
Float Feed	600.00	78.35	2.41	0.30	50.06	5.34	644.62	75.49	1.87	0.33	49.48	4.74
Float Conc	207.77	82.92	1.61	0.50	52.27	3.72	186.60	83.85	1.68	0.48	52.45	3.81
Float Tail	461.10	70.44	1.74	0.28	47.90	4.78	458.02	72.08	1.94	0.26	48.28	5.12

Total WSSQ: 37.29

TECHBAL - MATERIAL BALANCE SPREADSHEET

Author: G. H. Luttrell
Department: Mining & Minerals Engineering
Address: Virginia Polytechnic Institute and State University
Blacksburg, Virginia USA 24061-0258

CIRCUIT: Column Cell Cleaning Application:0g/t depressant dosage Run 1A Test 1

	Relative Standard Deviations (%)						Relative Change in Measured Value (%)					
Stream	Mass	PGM [g/t]	Cr [%]	Fraction of	SiO2 [%]	Al2O3 [%]	Mass	PGM [g/t]	Cr [%]	Fraction of	SiO2 [%]	Al2O3 [%]
Float Feed	10.00	5.00	5.00	10.00	5.00	5.00	7.44	-3.65	-22.48	8.71	-1.14	-11.20
Float Conc	10.00	5.00	5.00	10.00	5.00	5.00	-10.19	1.12	4.36	-4.20	0.34	2.26
Float Tail	10.00	5.00	5.00	10.00	5.00	5.00	-0.67	2.33	11.54	-5.77	0.78	7.13

Total WSSQ: 37.29

TECHBAL - MATERIAL BALANCE SPREADSHEET

Author: G. H. Luttrell
Department: Mining & Minerals Engineering
Address: Virginia Polytechnic Institute and State University
Blacksburg, Virginia USA 24061-0258

CIRCUIT:

	Standard Deviations						Weighted Square Differences					
Stream	Test 1						Test 1					
Float Feed	60.00	3.92	0.12	0.03	2.50	0.27	0.55	0.53	20.21	0.76	0.05	5.02
Float Conc	20.78	4.15	0.08	0.05	2.61	0.19	1.04	0.05	0.76	0.18	0.00	0.20
Float Tail	46.11	3.52	0.09	0.03	2.40	0.24	0.00	0.22	5.33	0.33	0.02	2.03
						WSSQ:	1.60	0.80	26.30	1.27	0.08	7.25
											Total WSSQ:	37.29

TECHBAL - MATERIAL BALANCE SPREADSHEET

Author: G. H. Luttrell
Address: Virginia Polytechnic Institute and State University
Department: Mining & Minerals Engineering
Blacksburg, Virginia USA 24061-0258

CIRCUIT:

Unit Matrix: **Mass**

	Node										
Stream	Test 1										Sum
Float Feed	644.6	0.0	0.0	0.0	0.0	0.0	0.0	0.0	0.0	0.0	644.6
Float Conc	-186.6	0.0	0.0	0.0	0.0	0.0	0.0	0.0	0.0	0.0	-186.6
Float Tail	-458.0	0.0	0.0	0.0	0.0	0.0	0.0	0.0	0.0	0.0	-458.0
	0.0	0.0	0.0	0.0	0.0	0.0	0.0	0.0	0.0	0.0	0.0
	0.0	0.0	0.0	0.0	0.0	0.0	0.0	0.0	0.0	0.0	0.0
Sum	0.0	0.0	0.0	0.0	0.0	0.0	0.0	0.0	0.0	0.0	0.0

TECHBAL - MATERIAL BALANCE SPREADSHEET

Author: G. H. Luttrell
Address: Virginia Polytechnic Institute and State University
Department: Mining & Minerals Engineering
Blacksburg, Virginia USA 24061-0258

CIRCUIT:

Unit Matrix: **PGM [g/t]**

	Node										
Stream	Test 1										Sum
Float Feed	48661.8	0.0	0.0	0.0	0.0	0.0	0.0	0.0	0.0	0.0	48661.8
Float Conc	-15646.6	0.0	0.0	0.0	0.0	0.0	0.0	0.0	0.0	0.0	-15646.6
Float Tail	-33015.2	0.0	0.0	0.0	0.0	0.0	0.0	0.0	0.0	0.0	-33015.2
	0.0	0.0	0.0	0.0	0.0	0.0	0.0	0.0	0.0	0.0	0.0
Sum	0.0	0.0	0.0	0.0	0.0	0.0	0.0	0.0	0.0	0.0	0.0

TECHBAL - MATERIAL BALANCE SPREADSHEET

Author: G. H. Luttrell
Address: Virginia Polytechnic Institute and State University
Department: Mining & Minerals Engineering
Blacksburg, Virginia USA 24061-0258

CIRCUIT:

Unit Matrix: **Cr [%]**

	Node										
Stream	Test 1										Sum
Float Feed	1202.9	0.0	0.0	0.0	0.0	0.0	0.0	0.0	0.0	0.0	1202.9
Float Conc	-313.9	0.0	0.0	0.0	0.0	0.0	0.0	0.0	0.0	0.0	-313.9
Float Tail	-889.0	0.0	0.0	0.0	0.0	0.0	0.0	0.0	0.0	0.0	-889.0
	0.0	0.0	0.0	0.0	0.0	0.0	0.0	0.0	0.0	0.0	0.0
	0.0	0.0	0.0	0.0	0.0	0.0	0.0	0.0	0.0	0.0	0.0
Sum	0.0	0.0	0.0	0.0	0.0	0.0	0.0	0.0	0.0	0.0	0.0

TECHBAL - MATERIAL BALANCE SPREADSHEET

Author: G. H. Luttrell
Address: Virginia Polytechnic Institute and State University
Department: Mining & Minerals Engineering
Blacksburg, Virginia USA 24061-0258

CIRCUIT:

Unit Matrix: **Mass Fraction of Solids**

	Node										
Stream	Test 1										Sum
Float Feed	210.2	0.0	0.0	0.0	0.0	0.0	0.0	0.0	0.0	0.0	210.2
Float Conc	-89.4	0.0	0.0	0.0	0.0	0.0	0.0	0.0	0.0	0.0	-89.4
Float Tail	-120.8	0.0	0.0	0.0	0.0	0.0	0.0	0.0	0.0	0.0	-120.8
	0.0	0.0	0.0	0.0	0.0	0.0	0.0	0.0	0.0	0.0	0.0
Sum	0.0	0.0	0.0	0.0	0.0	0.0	0.0	0.0	0.0	0.0	0.0

TECHBAL - MATERIAL BALANCE SPREADSHEET

Author: G. H. Luttrell
Department: Mining & Minerals Engineering
Address: Virginia Polytechnic Institute and State University
Blacksburg, Virginia USA 24061-0258

CIRCUIT:

Unit Matrix: SiO2 [%]

	Node										
Stream	Test 1										Sum
Float Feed	31898.6	0.0	0.0	0.0	0.0	0.0	0.0	0.0	0.0	0.0	31898.6
Float Conc	-9787.7	0.0	0.0	0.0	0.0	0.0	0.0	0.0	0.0	0.0	-9787.7
Float Tail	-22110.9	0.0	0.0	0.0	0.0	0.0	0.0	0.0	0.0	0.0	-22110.9
	0.0	0.0	0.0	0.0	0.0	0.0	0.0	0.0	0.0	0.0	0.0
	0.0	0.0	0.0	0.0	0.0	0.0	0.0	0.0	0.0	0.0	0.0
Sum	0.0	0.0	0.0	0.0	0.0	0.0	0.0	0.0	0.0	0.0	0.0

TECHBAL - MATERIAL BALANCE SPREADSHEET

Author: G. H. Luttrell
Department: Mining & Minerals Engineering
Address: Virginia Polytechnic Institute and State University
Blacksburg, Virginia USA 24061-0258

CIRCUIT:

Unit Matrix: Al2O3 [%]

	Node										
Stream	Test 1										Sum
Float Feed	3057.9	0.0	0.0	0.0	0.0	0.0	0.0	0.0	0.0	0.0	3057.9
Float Conc	-710.6	0.0	0.0	0.0	0.0	0.0	0.0	0.0	0.0	0.0	-710.6
Float Tail	-2347.3	0.0	0.0	0.0	0.0	0.0	0.0	0.0	0.0	0.0	-2347.3
	0.0	0.0	0.0	0.0	0.0	0.0	0.0	0.0	0.0	0.0	0.0
	0.0	0.0	0.0	0.0	0.0	0.0	0.0	0.0	0.0	0.0	0.0
Sum	0.0	0.0	0.0	0.0	0.0	0.0	0.0	0.0	0.0	0.0	0.0

APPENDIX C: TECHBAL SITE WORK DATA

(DEPRESSANT DOSAGE AND FROTH HEIGHT CHANGES

C.1 UCT Methodology (Depressant Dosage change): Run 1A Test 1

TECHBAL - MATERIAL BALANCE SPREADSHEET

Author: G. H. Luttrell
Department: Mining & Minerals Engineering
Address: Virginia Polytechnic Institute and State University, Blacksburg, Virginia USA 24061-0258

CIRCUIT: Column Cell Cleaning Application:0g/t depressant dosage Run 1A Test 1

	Measured Values						Estimated Values					
Stream	Mass	PGM [g/t]	Cr [%]	Mass Fraction of Solids	SiO2 [%]	Al2O3 [%]	Mass	PGM [g/t]	Cr [%]	Mass Fraction of Solids	SiO2 [%]	Al2O3 [%]
Float Feed	600.00	78.35	2.41	0.30	50.06	5.34	644.62	75.49	1.87	0.33	49.48	4.74
Float Conc	207.77	82.92	1.61	0.50	52.27	3.72	186.60	83.85	1.68	0.48	52.45	3.81
Float Tail	461.10	70.44	1.74	0.28	47.90	4.78	458.02	72.08	1.94	0.26	48.28	5.12

Total WSSQ: 37.29

C.2 UCT Methodology (Depressant Dosage change): Run 1A Test 2

TECHBAL - MATERIAL BALANCE SPREADSHEET

Author: G. H. Luttrell
Department: Mining & Minerals Engineering
Address: Virginia Polytechnic Institute and State University, Blacksburg, Virginia USA 24061-0258

CIRCUIT: Column Cell Cleaning Application:100 g/t depressant dosage Run 1A Test 2

	Measured Values						Estimated Values					
Stream	Mass	PGM [g/t]	Cr [%]	Mass Fraction of Solids	SiO2 [%]	Al2O3 [%]	Mass	PGM [g/t]	Cr [%]	Fraction of	SiO2 [%]	Al2O3 [%]
Float Feed	600.00	78.35	2.00	0.30	50.06	5.34	612.43	77.50	1.81	0.29	48.92	4.90
Float Conc	88.28	180.00	1.50	0.50	49.20	3.72	86.93	180.59	1.51	0.50	49.35	3.75
Float Tail 1	529.40	60.00	1.74	0.25	48.00	4.78	525.49	60.45	1.86	0.26	48.85	5.09

Total WSSQ: 10.54

C.3 UCT Methodology (Depressant Dosage change): Run 1A Test 3

TECHBAL - MATERIAL BALANCE SPREADSHEET

Author: G. H. Luttrell
Department: Mining & Minerals Engineering
Address Virginia Polytechnic Institute and State University, Blacksburg, Virginia USA 24061-0258

CIRCUIT: Column Cell Cleaning Application:500 g/t depressant dosage Run 1A Test 3

	Measured Values						Estimated Values					
Stream	Mass	PGM [g/t]	Cr [%]	Mass Fraction of Solids	SiO2 [%]	Al2O3 [%]	Mass	PGM [g/t]	Cr [%]	Mass Fraction of Solids	SiO2 [%]	Al2O3 [%]
Float Feed	600.00	78.35	2.41	0.30	50.06	5.34	568.19	76.98	1.83	0.27	49.95	4.82
Float Conc	14.73	1050.20	1.29	0.45	25.42	3.20	14.99	1052.64	1.29	0.45	25.42	3.21
Float Tail 1	538.40	50.00	1.60	0.25	50.51	4.50	553.21	50.55	1.85	0.27	50.62	4.86

Total WSSQ: 40.67

C.4 UCT Methodology (Depressant Dosage change): Run 1B Test 1

TECHBAL - MATERIAL BALANCE SPREADSHEET

Author: G. H. Luttrell
Department: Mining & Minerals Engineering
Address: Virginia Polytechnic Institute and State University, Blacksburg, Virginia USA 24061-0258

CIRCUIT: Column Cell Cleaning Application:0 g/t depressant dosage Run 1B Test 1

	Relative Standard Deviations (%)						Relative Change in Measured Value (%)					
Stream	Mass	PGM [g/t]	Cr [%]	Fraction of	SiO2 [%]	Al2O3 [%]	Mass	PGM [g/t]	Cr [%]	Fraction of	SiO2 [%]	Al2O3 [%]
Float Feed	10.00	5.00	5.00	10.00	5.00	6.00	-8.32	-2.85	0.00	12.84	-4.64	14.45
Float Conc	10.00	5.00	5.00	10.00	5.00	6.00	4.86	1.90	0.00	-4.76	0.73	-1.59
Float Tail	10.00	5.00	99.00	10.00	5.00	6.00	-2.17	2.21		-11.21	3.53	-18.35

Total WSSQ: 21.38

C.5 UCT Methodology (Depressant Dosage change): Run 1B Test 2

TECHBAL - MATERIAL BALANCE SPREADSHEET

Author: G. H. Luttrell
Department: Mining & Minerals Engineering
Address: Virginia Polytechnic Institute and State University, Blacksburg, Virginia USA 24061-0258

CIRCUIT: Column Cell Cleaning Application:100 depressant dosage Run 1B Test 2

	Measured Values						Estimated Values					
Stream	Mass	PGM [g/t]	Cr [%]	Mass Fraction of Solids	SiO2 [%]	Al2O3 [%]	Mass	PGM [g/t]	Cr [%]	Mass Fraction of Solids	SiO2 [%]	Al2O3 [%]
Float Feed	534.70	72.98	3.50	0.24	54.61	5.12	551.40	70.39	2.07	0.27	54.61	5.12
Float Conc	44.56	172.31	1.56	0.57	50.52	3.33	44.19	173.47	1.58	0.55	50.52	3.33
Float Tail	520.00	59.80	1.77	0.30			507.21	61.40	2.11	0.25	54.97	5.28

Total WSSQ: 87.71

C.6 UCT Methodology (Depressant Dosage change): Run 1B Test 3

TECHBAL - MATERIAL BALANCE SPREADSHEET

Author: G. H. Luttrell
Department: Mining & Minerals Engineering
Address: Virginia Polytechnic Institute and State University, Blacksburg, Virginia USA 24061-0258

CIRCUIT: Column Cell Cleaning Application:500 depressant dosage Run 1B Test 3

	Measured Values						Estimated Values					
Stream	Mass	PGM [g/t]	Cr [%]	Mass Fraction of Solids	SiO2 [%]	Al2O3 [%]	Mass	PGM [g/t]	Cr [%]	Mass Fraction of Solids	SiO2 [%]	Al2O3 [%]
Float Feed	534.00	72.98	2.32	0.24	54.61	5.12	534.92	72.98	1.96	0.27	54.61	5.12
Float Conc	8.80	882.93	1.30	0.62	28.58	5.14	8.76	884.27	1.30	0.62	28.58	5.14
Float Tail			1.77	0.30			526.16	59.47	1.97	0.26	55.04	5.12

Total WSSQ: 17.73

C.7 Froth Height change: Run 2A Test 1

TECHBAL - MATERIAL BALANCE SPREADSHEET

Author: G. H. Luttrell
Department: Mining & Minerals Engineering
Address: Virginia Polytechnic Institute and State University, Blacksburg, Virginia USA 24061-0258

CIRCUIT: Column Cell Cleaning Application: Depressant Constant 0 g/t at 3 cm Froth Height : 2A Test 1

	Measured Values						Estimated Values					
Stream	Mass	PGM [g/t]	Cr [%]	Mass Fraction of Solids	SiO2 [%]	Al2O3 [%]	Mass	PGM [g/t]	Cr [%]	Mass Fraction of Solids	SiO2 [%]	Al2O3 [%]
Float Feed	574.45	86.52	2.50	0.26	51.07	4.97	601.42	72.21	2.50	0.28	51.07	4.97
Float Conc	172.78	89.52	1.50	0.47	49.64	4.36	175.73	94.00	1.50	0.45	49.64	4.36
Float Tail	458.55	58.57		0.23			425.68	63.21	2.91	0.22	51.66	5.22

Total WSSQ: 16.65

C.8 Froth Height change: Run 2A Test 2

TECHBAL - MATERIAL BALANCE SPREADSHEET

Author: G. H. Luttrell
Department: Mining & Minerals Engineering
Address: Virginia Polytechnic Institute and State University, Blacksburg, Virginia USA 24061-0258

CIRCUIT: Column Cell Cleaning Application: Depressant Constant 0 g/t at 9 cm Froth Height: 2A Test 2

	Measured Values						Estimated Values					
Stream	Mass	PGM [g/t]	Cr [%]	Mass Fraction of Solids	SiO2 [%]	Al2O3 [%]	Mass	PGM [g/t]	Cr [%]	Mass Fraction of Solids	SiO2 [%]	Al2O3 [%]
Float Feed	574.45	86.52	2.50	0.26	51.07	4.97	610.68	88.51	2.57	0.29	51.07	4.25
Float Conc	136.09	130.03	1.30	0.52	50.45	3.78	130.66	129.05	1.30	0.50	50.45	3.87
Float Tail	501.25	78.77	3.00	0.25		3.99	480.03	77.47	2.92	0.23	51.24	4.35

Total WSSQ: 15.57

C.9 Froth Height change: Run 2A Test 3

TECHBAL - MATERIAL BALANCE SPREADSHEET

Author: G. H. Luttrell
Department: Mining & Minerals Engineering
Address: Virginia Polytechnic Institute and State University
Blacksburg, Virginia USA 24061-0258

CIRCUIT: Column Cell Cleaning Application: Depressant Constant 0 g/t at 12 cm Froth Height: Run 2A Test 3

	Measured Values						Estimated Values					
Stream	Mass	PGM [g/t]	Cr [%]	Mass Fraction of Solids	SiO2 [%]	Al2O3 [%]	Mass	PGM [g/t]	Cr [%]	Mass Fraction of Solids	SiO2 [%]	Al2O3 [%]
Float Feed	574.45	86.52	2.50	0.26	51.07	4.97	590.46	86.47	2.50	0.28	51.07	4.97
Float Conc	113.99	133.94	1.30	0.51	51.38	3.71	112.11	133.94	1.30	0.50	51.38	3.71
Float Tail	488.95	75.32		0.24			478.35	75.35	2.78	0.23	51.00	5.27
											Total WSSQ:	1.00

C.10 Froth Height change: Run 2B Test 1

TECHBAL - MATERIAL BALANCE SPREADSHEET

Author: G. H. Luttrell
Department: Mining & Minerals Engineering
Address: Virginia Polytechnic Institute and State University
Blacksburg, Virginia USA 24061-0258

CIRCUIT: Column Cell Cleaning Application: Depressant Constant 0 g/t at 3 cm Froth Height : Run 2B Test 1

	Measured Values						Estimated Values					
Stream	Mass	PGM [g/t]	Cr [%]	Mass Fraction of Solids	SiO2 [%]	Al2O3 [%]	Mass	PGM [g/t]	Cr [%]	Mass Fraction of Solids	SiO2 [%]	Al2O3 [%]
Float Feed	539.40	78.70	1.99	0.29	51.91	4.89	610.07	63.48	1.99	0.32	51.91	4.89
Float Conc	194.90	84.26	1.50	0.50	51.53	3.78	198.61	89.94	1.50	0.47	51.53	3.78
Float Tail	522.75	47.04		0.26			411.46	50.71	2.23	0.24	52.09	5.43
											Total WSSQ:	27.13

C.11 Froth Height change: Run 2B Test 2

TECHBAL - MATERIAL BALANCE SPREADSHEET

Author: G. H. Luttrell
Department: Mining & Minerals Engineering
Address: Virginia Polytechnic Institute and State University
Blacksburg, Virginia USA 24061-0258

CIRCUIT: Column Cell Cleaning Application: Depressant Constant 0 g/t at 9 cm Froth Height : Run 2B Test 2

	Measured Values						Estimated Values					
Stream	Mass	PGM [g/t]	Cr [%]	Mass Fraction of Solids	SiO2 [%]	Al2O3 [%]	Mass	PGM [g/t]	Cr [%]	Mass Fraction of Solids	SiO2 [%]	Al2O3 [%]
Float Feed	539.40	78.70	2.50	0.29	51.91	4.89	610.66	65.49	1.89	0.32	50.68	5.45
Float Conc	175.35	89.58	1.35	0.50	42.00	3.59	179.83	94.62	1.40	0.48	42.24	3.50
Float Tail	558.20	49.63	1.85	0.27	53.28	7.11	430.83	53.33	2.09	0.25	54.20	6.27
											Total WSSQ:	66.24

C.12 Froth Height change: Run 2B Test 3

TECHBAL - MATERIAL BALANCE SPREADSHEET

Author: G. H. Luttrell
Department: Mining & Minerals Engineering
Address: Virginia Polytechnic Institute and State University
Blacksburg, Virginia USA 24061-0258

CIRCUIT: Column Cell Cleaning Application: Depressant Constant 0 g/t at 12 cm Froth Height : Run 2B Test 3

	Measured Values						Estimated Values					
Stream	Mass	PGM [g/t]	Cr [%]	Mass Fraction of Solids	SiO2 [%]	Al2O3 [%]	Mass	PGM [g/t]	Cr [%]	Mass Fraction of Solids	SiO2 [%]	Al2O3 [%]
Float Feed	539.40	78.70	2.50	0.29	51.61	4.89	609.54	65.78	1.86	0.31	50.86	5.13
Float Conc	163.18	91.79	1.33	0.47	41.38	3.68	163.29	96.50	1.38	0.46	41.51	3.64
Float Tail	544.65	50.63	1.80	0.26	53.69	5.94	446.26	54.54	2.04	0.25	54.29	5.68
											Total WSSQ:	55.25

C.13 Froth Height change: Run 3A Test 1

TECHBAL - MATERIAL BALANCE SPREADSHEET

Author: G. H. Luttrell
Department: Mining & Minerals Engineering
Address: Virginia Polytechnic Institute and State University
Blacksburg, Virginia USA 24061-0258

CIRCUIT: Column Cell Cleaning Application: Depressant Constant 0 g/t at 3 cm Froth Height: 3A Test 1

	Measured Values						Estimated Values					
Stream	Mass	PGM [g/t]	Cr [%]	Mass Fraction of Solids	SiO2 [%]	Al2O3 [%]	Mass	PGM [g/t]	Cr [%]	Mass Fraction of Solids	SiO2 [%]	Al2O3 [%]
Float Feed	583.50	65.64	2.03	0.26	53.13	5.13	621.68	64.29	2.03	0.28	53.13	5.13
Float Conc	90.46	128.95	1.50	0.49	48.42	3.83	89.90	129.70	1.50	0.48	48.42	3.83
Float Tail	570.70	52.49		0.26			531.78	53.23	2.12	0.24	53.93	5.35
											Total WSSQ:	2.07

C.14 Froth Height change: Run 3A Test 2

TECHBAL - MATERIAL BALANCE SPREADSHEET

Author: G. H. Luttrell
Department: Mining & Minerals Engineering
Address: Virginia Polytechnic Institute and State University
Blacksburg, Virginia USA 24061-0258

CIRCUIT: Column Cell Cleaning Application: Depressant Constant 0 g/t at 9 cm Froth Height : Run 3A Test 2

	Measured Values						Estimated Values					
Stream	Mass	PGM [g/t]	Cr [%]	Mass Fraction of Solids	SiO2 [%]	Al2O3 [%]	Mass	PGM [g/t]	Cr [%]	Mass Fraction of Solids	SiO2 [%]	Al2O3 [%]
Float Feed	583.50	65.64	2.03	0.26	53.13	5.13	622.92	63.85	2.03	0.28	53.13	5.13
Float Conc	60.09	144.39	1.43	0.48	49.20	3.60	60.20	145.10	1.43	0.47	49.20	3.60
Float Tail	584.65	54.06		0.27			562.73	55.16	2.09	0.25	53.55	5.29
											Total WSSQ:	1.78

C.15 Froth Height change: Run 3A Test 3

TECHBAL - MATERIAL BALANCE SPREADSHEET

Author: G. H. Luttrell
Department: Mining & Minerals Engineering
Address: Virginia Polytechnic Institute and State University
Blacksburg, Virginia USA 24061-0258

CIRCUIT: Column Cell Cleaning Application: Depressant Constant 0 g/t at 12 cm Froth Height: Run 3A Test 3

	Measured Values						Estimated Values					
Stream	Mass	PGM [g/t]	Cr [%]	Mass Fraction of Solids	SiO2 [%]	Al2O3 [%]	Mass	PGM [g/t]	Cr [%]	Mass Fraction of Solids	SiO2 [%]	Al2O3 [%]
Float Feed	583.50	65.64	2.03	0.26	53.13	5.13	586.97	63.86	1.88	0.27	53.48	5.99
Float Conc	30.73	171.48	1.41	0.47	50.51	3.54	31.37	172.13	1.41	0.47	50.49	3.52
Float Tail	571.60	56.50	1.79	0.27	54.00	8.21	555.60	57.75	1.90	0.26	53.65	6.13
											Total WSSQ:	41.79

C.16 Froth Height change: Run 3B Test 1

TECHBAL - MATERIAL BALANCE SPREADSHEET

Author: G. H. Luttrell
Department: Mining & Minerals Engineering
Address: Virginia Polytechnic Institute and State University
Blacksburg, Virginia USA 24061-0258

CIRCUIT: Column Cell Cleaning Application: Depressant Constant 100 g/t at 3 cm Froth Height: 3B Test 1

	Measured Values						Estimated Values					
Stream	Mass	PGM [g/t]	Cr [%]	Mass Fraction of Solids	SiO2 [%]	Al2O3 [%]	Mass	PGM [g/t]	Cr [%]	Mass Fraction of Solids	SiO2 [%]	Al2O3 [%]
Float Feed	590.00	65.70	2.43	0.26	57.05	5.51	609.08	64.88	2.43	0.28	57.05	5.51
Float Conc	99.86	127.04	1.79	0.44	50.14	4.68	98.84	127.47	1.79	0.43	50.14	4.68
Float Tail	522.75	52.49		0.26			510.25	52.76	2.55	0.25	58.39	5.67
											Total WSSQ:	0.96

C.17 Froth Height change: Run 3B Test 2

TECHBAL - MATERIAL BALANCE SPREADSHEET

Author: G. H. Luttrell
Department: Mining & Minerals Engineering
Address: Virginia Polytechnic Institute and State University
Blacksburg, Virginia USA 24061-0258

CIRCUIT: Column Cell Cleaning Application: Depressant Constant 0 g/t at 9 cm Froth Height: 3B Test 2

	Measured Values						Estimated Values					
Stream	Mass	PGM [g/t]	Cr [%]	Mass Fraction of Solids	SiO2 [%]	Al2O3 [%]	Mass	PGM [g/t]	Cr [%]	Mass Fraction of Solids	SiO2 [%]	Al2O3 [%]
Float Feed	590.00	65.70	2.43	0.26	57.05	5.51	612.36	63.53	2.42	0.27	55.61	5.99
Float Conc	65.04	130.31	1.70	0.43	50.65	4.60	65.78	131.22	1.70	0.43	50.78	4.56
Float Tail	558.20	54.06	2.50	0.27	55.00	6.81	546.58	55.38	2.51	0.26	56.19	6.16
											Total WSSQ:	8.61

C.18 Froth Height change: Run 3B Test 3

TECHBAL - MATERIAL BALANCE SPREADSHEET

Author: G. H. Luttrell
Department: Mining & Minerals Engineering
Address: Virginia Polytechnic Institute and State University
Blacksburg, Virginia USA 24061-0258

CIRCUIT: Column Cell Cleaning Application: Depressant Constant 100 g/t at 12 cm Froth Height: 3B Test 3

	Measured Values						Estimated Values					
Stream	Mass	PGM [g/t]	Cr [%]	Mass Fraction of Solids	SiO2 [%]	Al2O3 [%]	Mass	PGM [g/t]	Cr [%]	Mass Fraction of Solids	SiO2 [%]	Al2O3 [%]
Float Feed	590.00	65.70	2.43	0.26	57.05	5.51	586.80	64.51	2.19	0.27	49.96	5.16
Float Conc	40.73	160.86	1.68	0.42	48.10	4.14	40.58	161.35	1.69	0.42	48.43	4.15
Float Tail	544.65	56.50	2.07	0.26	45.81	4.97	546.22	57.31	2.23	0.25	50.08	5.23
											Total WSSQ:	18.95

C.19 Froth Height change: Run 4A Test 1

TECHBAL - MATERIAL BALANCE SPREADSHEET

Author: G. H. Luttrell
Department: Mining & Minerals Engineering
Address: Virginia Polytechnic Institute and State University
Blacksburg, Virginia USA 24061-0258

CIRCUIT: Column Cell Cleaning Application: Depressant Constant 500 g/t at 3 cm Froth Height: 4A Test 1

	Measured Values						Estimated Values					
Stream	Mass	PGM [g/t]	Cr [%]	Mass Fraction of Solids	SiO2 [%]	Al2O3 [%]	Mass	PGM [g/t]	Cr [%]	Mass Fraction of Solids	SiO2 [%]	Al2O3 [%]
Float Feed	575.90	92.96	2.50	0.26	51.83	4.66	602.13	94.38	2.69	0.27	49.79	4.09
Float Conc	22.96	1479.62	1.79	0.43	19.47	8.21	22.52	1466.17	1.79	0.43	19.48	8.28
Float Tail	597.25	41.36	3.00	0.27	49.20	3.60	579.61	41.09	2.73	0.26	50.97	3.93
											Total WSSQ:	16.79

C.20 Froth Height change: Run 4A Test 2

TECHBAL - MATERIAL BALANCE SPREADSHEET

Author: G. H. Luttrell
Department: Mining & Minerals Engineering
Address: Virginia Polytechnic Institute and State University
Blacksburg, Virginia USA 24061-0258

CIRCUIT: Column Cell Cleaning Application: Depressant Constant 500 g/t at 9 cm Froth Height: 4A Test 2

	Measured Values						Estimated Values					
Stream	Mass	PGM [g/t]	Cr [%]	Mass Fraction of Solids	SiO2 [%]	Al2O3 [%]	Mass	PGM [g/t]	Cr [%]	Mass Fraction of Solids	SiO2 [%]	Al2O3 [%]
Float Feed	575.90	92.96	2.60	0.26	51.83	4.66	594.37	95.72	2.60	0.26	51.83	4.66
Float Conc	16.40	1502.33	1.75	0.40	20.10	7.75	15.58	1483.47	1.75	0.40	20.10	7.75
Float Tail	570.75	59.45		0.26			578.78	58.35	2.62	0.26	52.68	4.58
											Total WSSQ:	0.93

C.21 Froth Height change: Run 4A Test 3

TECHBAL - MATERIAL BALANCE SPREADSHEET

Author: G. H. Luttrell
Department: Mining & Minerals Engineering
Address: Virginia Polytechnic Institute and State University
Blacksburg, Virginia USA 24061-0258

CIRCUIT: Column Cell Cleaning Application: Depressant Constant 500 g/t at 12 cm Froth Height: 4A Test 3

	Measured Values						Estimated Values					
Stream	Mass	PGM [g/t]	Cr [%]	Mass Fraction of Solids	SiO2 [%]	Al2O3 [%]	Mass	PGM [g/t]	Cr [%]	Mass Fraction of Solids	SiO2 [%]	Al2O3 [%]
Float Feed	575.90	92.96	2.50	0.26	51.83	4.66	519.99	79.84	2.50	0.25	51.83	4.66
Float Conc	13.00	959.50	1.70	0.41	31.62	5.34	14.85	999.42	1.70	0.41	31.62	5.34
Float Tail	550.00	49.23		0.24			505.14	52.80	2.52	0.25	52.42	4.64

Total WSSQ: 14.59

C.22 Froth Height change: Run 4B Test 1

TECHBAL - MATERIAL BALANCE SPREADSHEET

Author: G. H. Luttrell
Department: Mining & Minerals Engineering
Address: Virginia Polytechnic Institute and State University
Blacksburg, Virginia USA 24061-0258

CIRCUIT: Column Cell Cleaning Application: Depressant Constant 500 g/t at 3 cm Froth Height: 4B Test 1

	Measured Values						Estimated Values					
Stream	Mass	PGM [g/t]	Cr [%]	Mass Fraction of Solids	SiO2 [%]	Al2O3 [%]	Mass	PGM [g/t]	Cr [%]	Mass Fraction of Solids	SiO2 [%]	Al2O3 [%]
Float Feed	530.75	105.94	2.12	0.24	50.83	6.50	576.81	108.39	2.12	0.25	48.74	7.24
Float Conc	22.19	1349.83	1.85	0.38	20.94	8.18	21.04	1344.40	1.85	0.38	20.95	8.14
Float Tail	580.85	62.41	2.50	0.26	48.00	8.39	555.77	61.59	2.13	0.25	49.80	7.20

Total WSSQ: 16.38

C.23 Froth Height change: Run 4B Test 2

TECHBAL - MATERIAL BALANCE SPREADSHEET

Author: G. H. Luttrell
Department: Mining & Minerals Engineering
Address: Virginia Polytechnic Institute and State University
Blacksburg, Virginia USA 24061-0258

CIRCUIT: Column Cell Cleaning Application: Depressant Constant 500 g/t at 9 cm Froth Height: 4B Test 2

	Measured Values						Estimated Values					
Stream	Mass	PGM [g/t]	Cr [%]	Mass Fraction of Solids	SiO2 [%]	Al2O3 [%]	Mass	PGM [g/t]	Cr [%]	Mass Fraction of Solids	SiO2 [%]	Al2O3 [%]
Float Feed	530.75	105.94	2.12	0.24	50.83	6.50	576.71	115.36	2.28	0.25	48.81	7.17
Float Conc	20.64	1281.12	1.80	0.37	19.00	8.00	17.70	1238.84	1.80	0.37	19.01	7.97
Float Tail	544.20	85.76	2.50	0.26	48.00	8.18	559.00	79.78	2.29	0.25	49.75	7.15

Total WSSQ: 25.61

C.24 Froth Height change: Run 4B Test 3

TECHBAL - MATERIAL BALANCE SPREADSHEET

Author: G. H. Luttrell
Department: Mining & Minerals Engineering
Address: Virginia Polytechnic Institute and State University
Blacksburg, Virginia USA 24061-0258

CIRCUIT: Column Cell Cleaning Application: Depressant Constant 500 g/t at 12 cm Froth Height: 4B Test 3

	Measured Values						Estimated Values					
Stream	Mass	PGM [g/t]	Cr [%]	Mass Fraction of Solids	SiO2 [%]	Al2O3 [%]	Mass	PGM [g/t]	Cr [%]	Mass Fraction of Solids	SiO2 [%]	Al2O3 [%]
Float Feed	530.75	105.94	2.00	0.24	50.83	6.50	534.81	111.72	2.22	0.25	48.89	5.82
Float Conc	13.65	1099.15	1.75	0.30	17.00	7.11	12.98	1086.99	1.75	0.30	17.01	7.13
Float Tail	503.40	91.70	2.60	0.26	48.00	5.34	521.83	87.47	2.23	0.25	49.69	5.79

Total WSSQ: 23.94

APPENDIX D: MEASURED AND MASS BALANCE FLOW RATES AND PERCENTAGE SOLIDS

Run 1A: Measured and Balanced Flow and Solids percentage

Sample	Meas. PGM [g/h]	Bal. PGM [g/h]	Meas. Cr [kg/h]	Bal. Cr [kg/h]	Meas. Solids [%]	Bal. Solids [%]	Meas. Al2O3 [g/min]	Bal. Al2O3 [g/min]	Depressant Dosage [g/t]
F1	2.82	2.92	86.65	72.17	30.00	32.61	32.05	30.58	0
C1	1.03	0.94	20.10	18.83	50.00	47.90	7.74	7.11	0
T1	1.95	1.98	48.14	53.34	28.00	26.38	22.06	23.47	0
F2	2.82	2.85	72.00	66.60	30.00	29.07	32.05	30.00	100
C2	0.95	0.94	7.95	7.90	50.00	50.37	3.29	3.26	100
T2	1.91	1.91	55.27	58.70	25.00	25.55	25.33	26.74	100
F3	2.82	2.62	86.65	62.47	30.00	27.31	32.05	27.38	500
C3	0.93	0.95	1.14	1.16	45.00	45.16	0.47	0.48	500
T3	1.62	1.68	51.69	61.31	25.00	26.82	24.23	26.90	500

Run 1B: Measured and Balanced Flow and Solids percentage

Sample	Meas. PGM [g/h]	Bal. PGM [g/h]	Meas. Cr [kg/h]	Bal. Cr [kg/h]	Meas. Solids [%]	Bal. Solids [%]	Meas. Al2O3 [g/min]	Bal. Al2O3 [g/min]	Depressant Dosage [g/t]
F1	2.34	2.09	74.43	68.24	24.00	27.08	27.38	28.73	0
C1	0.49	0.52	8.39	8.80	55.00	52.38	2.64	2.72	0
T1	1.56	1.56	0.00	59.43	25.00	22.20	32.55	26.00	0
F2	2.34	2.33	112.29	68.33	24.00	27.46	27.38	28.23	100
C2	0.46	0.46	4.17	4.20	57.00	55.43	1.48	1.47	100
T2	1.87	1.87	55.22	64.14	30.00	25.02	0.00	26.76	100
F3	2.34	2.34	74.33	63.01	24.00	26.60	27.34	27.39	500
C3	0.47	0.46	0.69	0.68	62.00	61.72	0.45	0.45	500
T3	0.00	1.88	0.00	62.33	30.00	26.01	0.00	26.94	500

Run 2A: Measured and Balanced Flow and Solids percentage

Sample	Meas. PGM [g/h]	Bal. PGM [g/h]	Meas. Cr [kg/h]	Bal. Cr [kg/h]	Meas. Solids [%]	Bal. Solids [%]	Meas. Al2O3 [g/min]	Bal. Al2O3 [g/min]	Froth Height [cm]
F1	2.98	2.61	86.17	90.21	26.00	28.40	28.55	29.89	3
C1	0.93	0.99	15.55	15.82	47.00	44.71	7.53	7.66	3
T1	1.61	1.61	0.00	74.40	23.00	21.67	0.00	22.23	3
F2	2.98	3.24	86.17	94.23	26.00	28.72	28.55	25.96	9
C2	1.06	1.01	10.62	10.16	52.00	49.67	5.14	5.06	9
T2	2.37	2.23	90.23	84.07	25.00	23.02	20.00	20.90	9
F3	2.98	3.06	86.17	88.57	26.00	27.84	28.55	29.35	12
C3	0.92	0.90	8.89	8.74	51.00	49.65	4.23	4.16	12
T3	2.21	2.16	0.00	79.83	24.00	22.73	0.00	25.19	12

Run 2B: Measured and Balanced Flow and Solids percentage

Sample	Meas. PGM [g/h]	Bal. PGM [g/h]	Meas. Cr [kg/h]	Bal. Cr [kg/h]	Meas. Solids [%]	Bal. Solids [%]	Meas. Al2O3 [g/min]	Bal. Al2O3 [g/min]	Froth Height [cm]
F1	2.55	2.32	64.40	72.84	29.00	31.86	26.38	29.83	3
C1	0.99	1.07	17.54	17.88	50.00	47.23	7.37	7.51	3
T1	1.48	1.25	0.00	54.97	26.00	24.45	0.00	22.32	3
F2	2.55	2.40	80.91	69.09	29.00	31.83	26.38	33.30	9
C2	0.94	1.02	14.20	15.14	50.00	47.53	6.30	6.29	9
T2	1.66	1.38	61.96	53.96	27.00	25.27	39.69	27.01	9
F3	2.55	2.41	80.91	68.16	29.00	30.62	26.38	31.29	12
C3	0.90	0.95	13.02	13.50	47.00	45.86	6.01	5.95	12
T3	1.65	1.46	58.82	54.66	26.00	25.05	32.35	25.34	12

Run 3A: Measured and Balanced Flow and Solids percentage

Sample	Meas. PGM [g/h]	Bal. PGM [g/h]	Meas. Cr [kg/h]	Bal. Cr [kg/h]	Meas. Solids [%]	Bal. Solids [%]	Meas. Al2O3 [g/min]	Bal. Al2O3 [g/min]	Froth Height [cm]
F1	2.30	2.40	71.07	75.72	26.00	27.84	29.93	31.89	3
C1	0.70	0.70	8.14	8.09	49.00	48.05	3.46	3.44	3
T1	1.80	1.70	0.00	67.63	26.00	24.42	0.00	28.45	3
F2	2.30	2.39	71.07	75.87	26.00	27.58	29.93	31.96	9
C2	0.52	0.52	5.16	5.17	48.00	47.48	2.16	2.17	9
T2	1.90	1.86	0.00	70.71	27.00	25.46	0.00	29.79	9
F3	2.30	2.25	71.07	66.09	26.00	27.05	29.93	35.15	12
C3	0.32	0.32	2.60	2.66	47.00	46.82	1.09	1.10	12
T3	1.94	1.93	61.39	63.43	27.00	25.93	46.93	34.05	12

Run 3B: Measured and Balanced Flow and Solids percentage

Sample	Meas. PGM [g/h]	Bal. PGM [g/h]	Meas. Cr [kg/h]	Bal. Cr [kg/h]	Meas. Solids [%]	Bal. Solids [%]	Meas. Al2O3 [g/min]	Bal. Al2O3 [g/min]	Froth Height [cm]
F1	2.33	2.37	86.02	88.80	26.00	27.64	32.51	33.55	3
C1	0.76	0.76	10.72	10.62	44.00	43.24	4.67	4.62	3
T1	1.65	1.62	0.00	78.19	26.00	24.62	0.00	28.93	3
F2	2.33	2.33	86.02	88.97	26.00	27.44	32.51	36.67	9
C2	0.51	0.52	6.63	6.71	43.00	42.58	2.99	3.00	9
T2	1.81	1.82	83.73	82.25	27.00	25.61	38.01	33.66	9
F3	2.33	2.27	86.02	77.20	26.00	26.59	32.51	30.28	12
C3	0.39	0.39	4.11	4.11	42.00	41.89	1.69	1.69	12
T3	1.85	1.88	67.65	73.09	26.00	25.45	27.07	28.59	12

Run 4A: Measured and Balanced Flow and Solids percentage

Sample	Meas. PGM [g/h]	Bal. PGM [g/h]	Meas. Cr [kg/h]	Bal. Cr [kg/h]	Meas. Solids [%]	Bal. Solids [%]	Meas. Al2O3 [g/min]	Bal. Al2O3 [g/min]	Froth Height [cm]
F1	3.21	3.41	86.39	97.36	26.00	26.80	26.84	24.63	3
C1	2.04	1.98	2.47	2.41	43.00	42.92	1.89	1.86	3
T1	1.48	1.43	107.51	94.94	27.00	26.17	21.50	22.76	3
F2	3.21	3.41	89.84	92.72	26.00	26.19	26.84	27.70	9
C2	1.48	1.39	1.72	1.64	40.00	39.99	1.27	1.21	9
T2	2.04	2.03	0.00	91.08	26.00	25.82	0.00	26.49	9
F3	3.21	2.49	86.39	78.00	26.00	25.16	26.84	24.23	12
C3	0.75	0.89	1.33	1.51	41.00	41.06	0.69	0.79	12
T3	1.62	1.60	0.00	76.48	24.00	24.69	0.00	23.44	12

Run 4B: Measured and Balanced Flow and Solids percentage

Sample	Meas. PGM [g/h]	Bal. PGM [g/h]	Meas. Cr [kg/h]	Bal. Cr [kg/h]	Meas. Solids [%]	Bal. Solids [%]	Meas. Al2O3 [g/min]	Bal. Al2O3 [g/min]	Froth Height [cm]
F1	3.37	3.75	67.51	73.40	24.00	25.16	34.50	41.75	3
C1	1.80	1.70	2.46	2.34	38.00	37.89	1.81	1.71	3
T1	2.18	2.05	87.13	71.06	26.00	24.68	48.72	40.04	3
F2	3.37	3.99	67.51	78.73	24.00	25.11	34.50	41.36	9
C2	1.59	1.32	2.23	1.91	37.00	36.92	1.65	1.41	9
T2	2.80	2.68	81.63	76.83	26.00	24.74	44.50	39.95	9
F3	3.37	3.59	63.69	71.30	24.00	24.99	34.50	31.13	12
C3	0.90	0.85	1.43	1.36	30.00	29.96	0.97	0.92	12
T3	2.77	2.74	78.53	69.94	26.00	24.87	26.89	30.21	12

APPENDIX E: SITE TESTS Feed size distribution analyses

(DEPRESSANT DOSAGE AND FROTH HEIGHT CHANGES

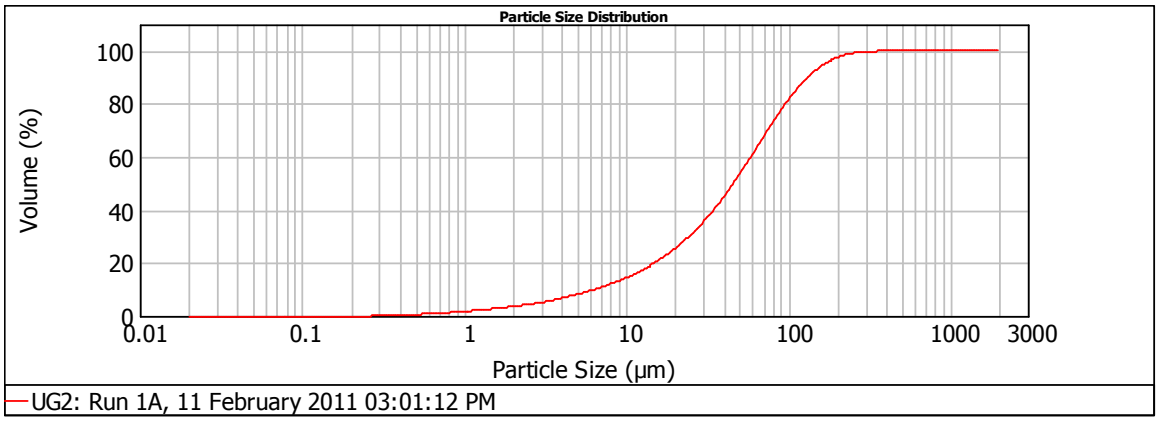

Figure 0.1: PSD of the Feed run 1A Depressant change

Table 1: PSD of the Feed run 1A Depressant change

	Volume In %	Size (µm)	Volume In %	Size (µm)	Volume In %	Size (µm)	Volume In %	Size (µm)	Volume In %	Size (µm)	Volume In %
0.010	0.00	0.105	0.00	1.096	0.31	11.482	1.87	120.226	3.65	1258.925	0.00
0.011	0.00	0.120	0.00	1.259	0.34	13.183	2.11	138.038	2.86	1445.440	0.00
0.013	0.00	0.138	0.00	1.445	0.37	15.136	2.39	158.489	2.13	1659.587	0.00
0.015	0.00	0.158	0.00	1.660	0.41	17.378	2.70	181.970	1.48	1905.461	0.00
0.017	0.00	0.182	0.00	1.905	0.47	19.953	3.06	208.930	0.97	2187.762	0.00
0.020	0.00	0.209	0.00	2.188	0.53	22.909	3.45	239.883	0.57	2511.886	0.00
0.023	0.00	0.240	0.01	2.512	0.60	26.303	3.87	275.423	0.31	2884.032	0.00
0.026	0.00	0.275	0.07	2.884	0.68	30.200	4.31	316.228	0.14	3311.311	0.00
0.030	0.00	0.316	0.10	3.311	0.77	34.674	4.75	363.078	0.08	3801.894	0.00
0.035	0.00	0.363	0.14	3.802	0.86	39.811	5.17	416.869	0.01	4365.158	0.00
0.040	0.00	0.417	0.17	4.365	0.95	45.709	5.52	478.630	0.00	5011.872	0.00
0.046	0.00	0.479	0.20	5.012	1.04	52.481	5.77	549.541	0.00	5754.399	0.00
0.052	0.00	0.550	0.22	5.754	1.14	60.256	5.87	630.957	0.00	6606.934	0.00
0.060	0.00	0.631	0.24	6.607	1.24	69.183	5.79	724.436	0.00	7585.776	0.00
0.069	0.00	0.724	0.26	7.586	1.36	79.433	5.51	831.764	0.00	8709.636	0.00
0.079	0.00	0.832	0.27	8.710	1.50	91.201	5.04	954.993	0.00	10000.000	
0.091	0.00	0.955	0.29	10.000	1.67	104.713	4.39	1096.478	0.00		
0.105		1.096		11.482		120.226		1258.925			

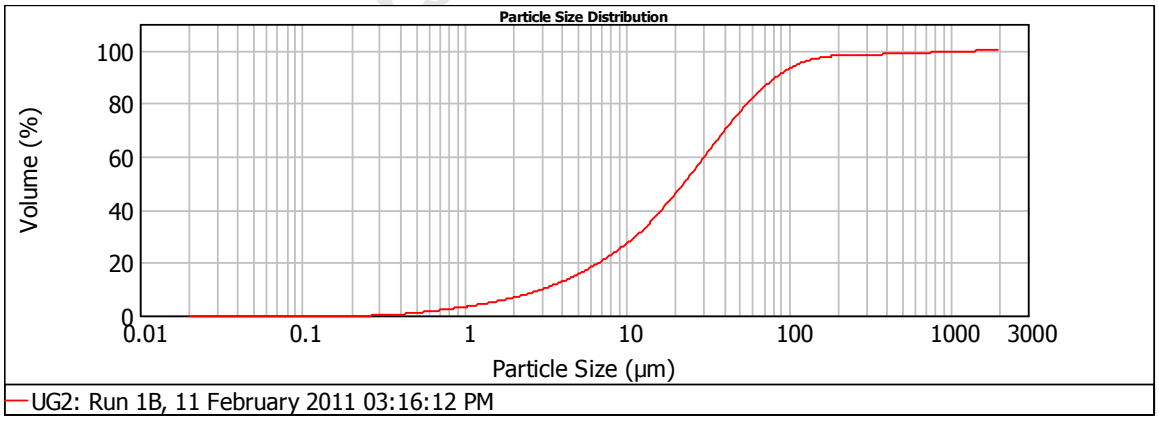

Figure 0.2: PSD of the Feed run 1B Depressant change

Table 2: PSD of the Feed run 1B Depressant change

Size (µm)	Volume In %	Size (µm)	Volume In %	Size (µm)	Volume In %	Size (µm)	Volume In %	Size (µm)	Volume In %	Size (µm)	Volume In %
0.010	0.00	0.105	0.00	1.096	0.58	11.482	3.32	120.226	1.19	1258.925	0.10
0.011	0.00	0.120	0.00	1.259	0.64	13.183	3.65	138.038	0.79	1445.440	0.07
0.013	0.00	0.138	0.00	1.445	0.72	15.136	3.97	158.489	0.49	1659.587	0.04
0.015	0.00	0.158	0.00	1.660	0.80	17.378	4.28	181.970	0.28	1905.461	0.01
0.017	0.00	0.182	0.00	1.905	0.91	19.953	4.54	208.930	0.15	2187.762	0.00
0.020	0.00	0.209	0.00	2.188	1.03	22.909	4.74	239.883	0.09	2511.886	0.00
0.023	0.00	0.240	0.03	2.512	1.16	26.303	4.85	275.423	0.07	2884.032	0.00
0.026	0.00	0.275	0.13	2.884	1.31	30.200	4.86	316.228	0.07	3311.311	0.00
0.030	0.00	0.316	0.20	3.311	1.46	34.674	4.78	363.078	0.09	3801.894	0.00
0.035	0.00	0.363	0.26	3.802	1.62	39.811	4.60	416.869	0.11	4365.158	0.00
0.040	0.00	0.417	0.31	4.365	1.78	45.709	4.34	478.630	0.13	5011.872	0.00
0.046	0.00	0.479	0.36	5.012	1.94	52.481	4.00	549.541	0.15	5754.399	0.00
0.052	0.00	0.550	0.40	5.754	2.10	60.256	3.61	630.957	0.17	6606.934	0.00
0.060	0.00	0.631	0.43	6.607	2.28	69.183	3.16	724.436	0.17	7585.776	0.00
0.069	0.00	0.724	0.46	7.586	2.49	79.433	2.67	831.764	0.17	8709.636	0.00
0.079	0.00	0.832	0.50	8.710	2.73	91.201	2.17	954.993	0.16	10000.000	
0.091	0.00	0.955	0.54	10.000	3.01	104.713	1.66	1096.478	0.13		
0.105		1.096		11.482		120.226		1258.925			

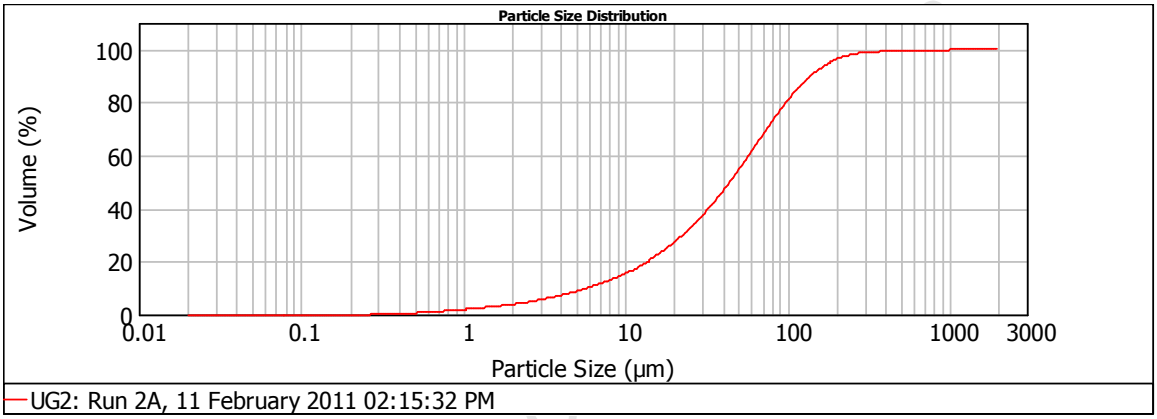

Figure 0.3: PSD of the Feed run 2A Depressant change

Table 3: PSD of the Feed run 2A Depressant change

Size (µm)	Volume In %	Size (µm)	Volume In %	Size (µm)	Volume In %	Size (µm)	Volume In %	Size (µm)	Volume In %	Size (µm)	Volume In %
0.010	0.00	0.105	0.00	1.096	0.33	11.482	2.00	120.226	3.54	1258.925	0.00
0.011	0.00	0.120	0.00	1.259	0.36	13.183	2.25	138.038	2.86	1445.440	0.00
0.013	0.00	0.138	0.00	1.445	0.40	15.136	2.53	158.489	2.21	1659.587	0.00
0.015	0.00	0.158	0.00	1.660	0.45	17.378	2.84	181.970	1.61	1905.461	0.00
0.017	0.00	0.182	0.00	1.905	0.50	19.953	3.16	208.930	1.11	2187.762	0.00
0.020	0.00	0.209	0.00	2.188	0.57	22.909	3.51	239.883	0.70	2511.886	0.00
0.023	0.00	0.240	0.02	2.512	0.65	26.303	3.87	275.423	0.41	2884.032	0.00
0.026	0.00	0.275	0.08	2.884	0.73	30.200	4.23	316.228	0.22	3311.311	0.00
0.030	0.00	0.316	0.12	3.311	0.82	34.674	4.57	363.078	0.12	3801.894	0.00
0.035	0.00	0.363	0.15	3.802	0.92	39.811	4.89	416.869	0.08	4365.158	0.00
0.040	0.00	0.417	0.19	4.365	1.01	45.709	5.16	478.630	0.08	5011.872	0.00
0.046	0.00	0.479	0.21	5.012	1.11	52.481	5.34	549.541	0.09	5754.399	0.00
0.052	0.00	0.550	0.23	5.754	1.21	60.256	5.42	630.957	0.10	6606.934	0.00
0.060	0.00	0.631	0.25	6.607	1.32	69.183	5.35	724.436	0.11	7585.776	0.00
0.069	0.00	0.724	0.27	7.586	1.45	79.433	5.12	831.764	0.10	8709.636	0.00
0.079	0.00	0.832	0.29	8.710	1.61	91.201	4.72	954.993	0.08	10000.000	
0.091	0.00	0.955	0.31	10.000	1.79	104.713	4.18	1096.478	0.07		
0.105		1.096		11.482		120.226		1258.925			

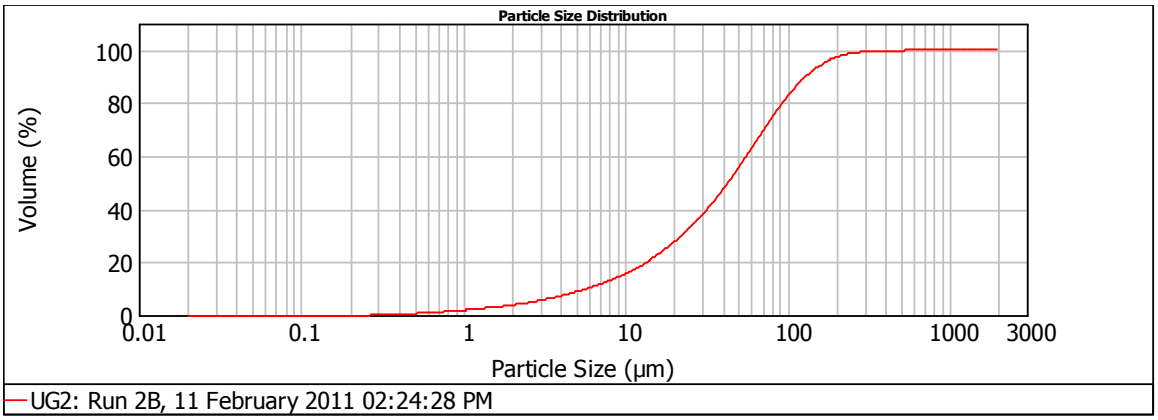

Figure 0.4: PSD of the Feed run 2B Depressant change

Table 4: PSD of the Feed run 2B Depressant change

Size (µm)	Volume In %	Size (µm)	Volume In %	Size (µm)	Volume In %	Size (µm)	Volume In %	Size (µm)	Volume In %	Size (µm)	Volume In %
0.010	0.00	0.105	0.00	1.096	0.33	11.482	2.05	120.226	3.39	1258.925	0.00
0.011	0.00	0.120	0.00	1.259	0.36	13.183	2.29	138.038	2.66	1445.440	0.00
0.013	0.00	0.138	0.00	1.445	0.40	15.136	2.57	158.489	1.98	1659.587	0.00
0.015	0.00	0.158	0.00	1.660	0.45	17.378	2.88	181.970	1.39	1905.461	0.00
0.017	0.00	0.182	0.00	1.905	0.50	19.953	3.21	208.930	0.92	2187.762	0.00
0.020	0.00	0.209	0.00	2.188	0.57	22.909	3.57	239.883		2511.886	0.00
0.023	0.00	0.240	0.01	2.512	0.65	26.303	3.94	275.423	0.33	2884.032	0.00
0.026	0.00	0.275	0.08	2.884	0.74	30.200	4.33	316.228	0.18	3311.311	0.00
0.030	0.00	0.316	0.12	3.311	0.83	34.674	4.70	363.078	0.11	3801.894	0.00
0.035	0.00	0.363	0.15	3.802	0.93	39.811	5.05	416.869	0.09	4365.158	0.00
0.040	0.00	0.417	0.19	4.365	1.03	45.709	5.34	478.630	0.08	5011.872	0.00
0.046	0.00	0.479	0.21	5.012	1.13	52.481	5.54	549.541	0.07	5754.399	0.00
0.052	0.00	0.550	0.23	5.754	1.24	60.256	5.60	630.957	0.04	6606.934	0.00
0.060	0.00	0.631	0.25	6.607	1.35	69.183	5.50	724.436	0.00	7585.776	0.00
0.069	0.00	0.724	0.27	7.586	1.49	79.433	5.21	831.764	0.00	8709.636	0.00
0.079	0.00	0.832	0.29	8.710	1.65	91.201	4.73	954.993	0.00	10000.000	0.00
0.091	0.00	0.955	0.31	10.000	1.83	104.713	4.10	1096.478	0.00		
0.105	0.00	1.096		11.482		120.226		1258.925	0.00		

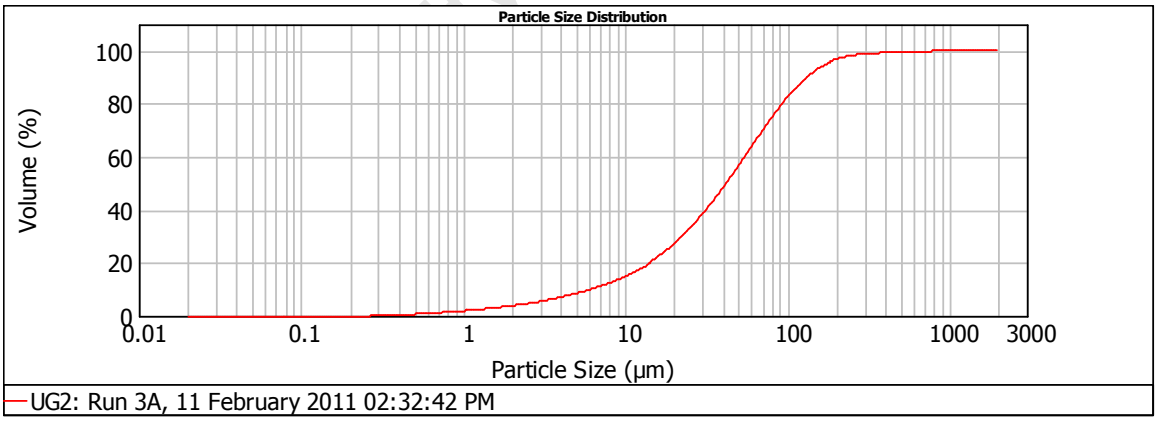

Figure 0.5: PSD of the Feed run 3A Depressant change

Table 5: PSD of the Feed run 3B Depressant change

Size (µm)	Volume In %	Size (µm)	Volume In %	Size (µm)	Volume In %	Size (µm)	Volume In %	Size (µm)	Volume In %	Size (µm)	Volume In %
0.010	0.00	0.105	0.00	1.096	0.32	11.482	2.06	120.226	3.22	1258.925	0.00
0.011	0.00	0.120	0.00	1.259	0.35	13.183	2.37	138.038	2.54	1445.440	0.00
0.013	0.00	0.138	0.00	1.445	0.38	15.136	2.71	158.489	1.92	1659.587	0.00
0.015	0.00	0.158	0.00	1.660	0.42	17.378	3.09	181.970	1.36	1905.461	0.00
0.017	0.00	0.182	0.00	1.905	0.48	19.953	3.47	208.930	0.92	2187.762	0.00
0.020	0.00	0.209	0.00	2.188	0.54	22.909	3.86	239.883	0.58	2511.886	0.00
0.023	0.00	0.240	0.02	2.512	0.61	26.303	4.24	275.423	0.35	2884.032	0.00
0.026	0.00	0.275	0.09	2.884	0.69	30.200	4.59	316.228	0.21	3311.311	0.00
0.030	0.00	0.316	0.13	3.311	0.78	34.674	4.90	363.078	0.15	3801.894	0.00
0.035	0.00	0.363	0.16	3.802	0.87	39.811	5.16	416.869	0.13	4365.158	0.00
0.040	0.00	0.417	0.19	4.365	0.96	45.709	5.35	478.630	0.13	5011.872	0.00
0.046	0.00	0.479	0.22	5.012	1.05	52.481	5.45	549.541	0.13	5754.399	0.00
0.052	0.00	0.550	0.24	5.754	1.15	60.256	5.43	630.957	0.12	6606.934	0.00
0.060	0.00	0.631	0.26	6.607	1.26	69.183	5.27	724.436	0.11	7585.776	0.00
0.069	0.00	0.724	0.27	7.586	1.40	79.433	4.95	831.764	0.07	8709.636	0.00
0.079	0.00	0.832	0.29	8.710	1.58	91.201	4.48	954.993	0.00	10000.000	
0.091	0.00	0.955	0.30	10.000	1.80	104.713	3.88	1096.478	0.00		
0.105	0.00	1.096		11.482		120.226		1258.925			

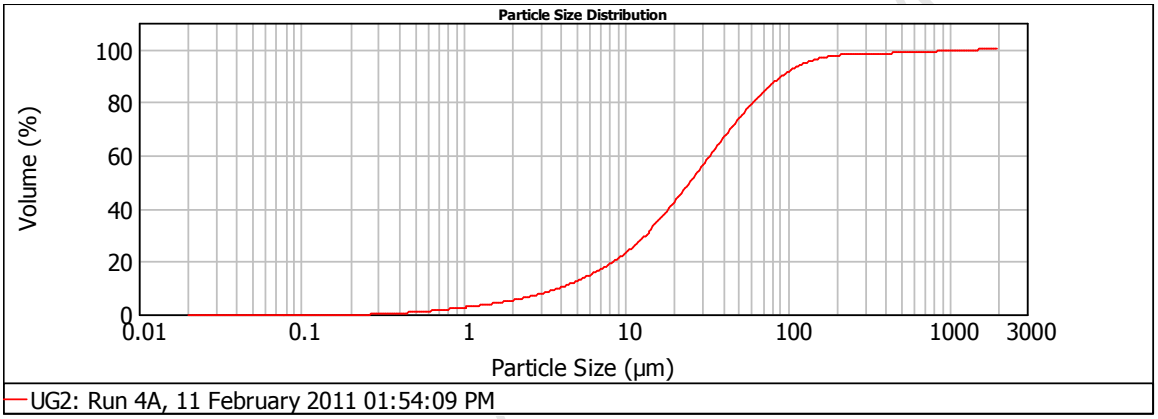

Figure 0.6: PSD of the Feed run 4A Depressant change

Table 6: PSD of the Feed run 4B Depressant change

Size (µm)	Volume In %	Size (µm)	Volume In %	Size (µm)	Volume In %	Size (µm)	Volume In %	Size (µm)	Volume In %	Size (µm)	Volume In %
0.010	0.00	0.105	0.00	1.096	0.45	11.482	3.37	120.226	1.47	1258.925	0.13
0.011	0.00	0.120	0.00	1.259	0.50	13.183	3.74	138.038	1.04	1445.440	0.09
0.013	0.00	0.138	0.00	1.445	0.56	15.136	4.08	158.489	0.69	1659.587	0.05
0.015	0.00	0.158	0.00	1.660	0.63	17.378	4.39	181.970	0.44	1905.461	0.01
0.017	0.00	0.182	0.00	1.905	0.71	19.953	4.64	208.930	0.27	2187.762	0.00
0.020	0.00	0.209	0.00	2.188	0.81	22.909	4.82	239.883	0.16	2511.886	0.00
0.023	0.00	0.240	0.02	2.512	0.92	26.303	4.91	275.423	0.11	2884.032	0.00
0.026	0.00	0.275	0.11	2.884	1.05	30.200	4.92	316.228	0.09	3311.311	0.00
0.030	0.00	0.316	0.17	3.311	1.19	34.674	4.85	363.078	0.09	3801.894	0.00
0.035	0.00	0.363	0.21	3.802	1.34	39.811	4.70	416.869	0.10	4365.158	0.00
0.040	0.00	0.417	0.25	4.365	1.50	45.709	4.48	478.630	0.12	5011.872	0.00
0.046	0.00	0.479	0.29	5.012	1.68	52.481	4.20	549.541	0.14	5754.399	0.00
0.052	0.00	0.550	0.31	5.754	1.88	60.256	3.86	630.957	0.17	6606.934	0.00
0.060	0.00	0.631	0.34	6.607	2.11	69.183	3.45	724.436	0.18	7585.776	0.00
0.069	0.00	0.724	0.36	7.586	2.38	79.433	2.99	831.764	0.19	8709.636	0.00
0.079	0.00	0.832	0.39	8.710	2.68	91.201	2.49	954.993	0.18	10000.000	
0.091	0.00	0.955	0.42	10.000	3.02	104.713	1.97	1096.478	0.16		
0.105	0.00	1.096		11.482		120.226		1258.925			

APPENDIX F: SPREAD SHEET BALANCED DETAILS OF SITEWORK

(DEPRESSANT DOSAGE AND FROTH HEIGHT CHANGES)

Test 1, 2 and 3 (Run 1A): Depressant dosage change

Sample	Solids Flow [g/min]	PGM Grade [g/t]	PGM Recovery %	PGM Flow rate [g/h]	Cr_2O_3 Grade [%]	Cr_2O_3 Flow rate [Kg/h]	Cr_2O_3 Recovery [%]	Solids Percentage [%]	Water Flow rate [g/min]
C1	186.60	83.85	32.15	0.939	1.68	18.83	26.10	47.90	202.97
C2	84.13	178.66	32.03	0.902	1.51	7.45	10.72	50.38	82.87
C3	14.99	1052.64	36.07	0.947	1.29	1.16	2.05	45.16	18.20
F1	644.62	75.49		2.920	1.87	72.17		32.61	1332.02
F2	609.61	76.98		2.816	1.90	69.50		29.01	1491.62
F3	568.19	76.98		2.624	1.66	56.74		27.31	1512.72
T1	458.02	72.08		1.981	1.94	53.34		26.38	1277.99
T2	525.48	60.70		1.914	1.97	62.06		25.59	1527.88
T3	553.21	50.55		1.678	1.67	55.58		26.82	1509.36

Test 4, 5 and 6 (Run 1B): Depressant dosage change

Sample	Solids Flow [g/min]	PGM Grade [g/t]	PGM Recovery %	PGM Flow rate [g/h]	Cr_2O_3 Grade [%]	Cr_2O_3 Flow rate [Kg/h]	Cr_2O_3 Recovery [%]	Solids Percentage [%]	Water Flow rate [g/min]
C1	79.30	109.95	25.09	0.52	1.85	8.80	12.90	52.38	72.08
C2	44.19	173.47	19.75	0.46	1.58	4.17	6.50	55.43	35.53
C3	8.76	884.27	19.85	0.46	1.30	0.68	1.09	61.72	5.44
F1	490.20	70.90		2.09	2.32	68.24		27.08	1319.94
F2	551.41	70.39		2.33	1.94	64.21		27.46	1456.59
F3	534.92	72.98		2.34	1.96	63.01		26.60	1476.40
T1	410.90	63.37		1.56	2.41	59.43		22.20	1440.19
T2	520.00	61.40		1.92	1.97	61.56		25.02	1558.04
T3	526.16	59.47		1.88	1.97	62.33		26.01	1496.70

Tests 7, 8 and 9 (Run 2A): Froth Height change

Sample	Mass Flow [g/min]	PGM Grade [g/t]	PGM Recovery %	PGM Flow rate [g/h]	Cr_2O_3 Grade [%]	Cr_2O_3 Flow rate [Kg/h]	Cr_2O_3 Recovery [%]	Percentage Solids [%]	Water Flow rate [g/min]
C1	175.73	94.00	38.04	0.991	1.50	15.82	17.53	44.71	217.35
C2	130.66	129.05	31.20	1.012	1.30	10.16	10.78	49.67	132.38
C3	112.11	133.94	29.41	0.901	1.30	8.74	9.87	49.65	113.68
F1	601.42	72.21		2.606	2.50	90.21		28.40	1516.14
F2	610.68	88.51		3.243	2.57	94.23		28.72	1515.37
F3	590.46	86.47		3.064	2.50	88.57		27.84	1530.39
T1	425.68	63.21		1.615	2.91	74.40		21.67	1538.70
T2	480.03	77.47		2.231	2.92	84.07		23.02	1605.07
T3	478.35	75.35		2.163	2.78	79.83		22.73	1626.26

Tests 10, 11 and 12 (Run 2B): Froth Height change

Sample	Mass Flow [g/min]	PGM Grade [g/t]	PGM Recovery %	PGM Flow rate [g/h]	Cr_2O_3 Grade [%]	Cr_2O_3 Flow rate [Kg/h]	Cr_2O_3 Recovery [%]	Percentage Solids [%]	Water Flow rate [g/min]
C1	198.61	89.94	46.13	1.07	1.50	17.88	22.20	47.23	221.92
C2	179.83	94.62	42.54	1.02	1.40	15.14	21.91	47.53	198.54
C3	163.29	96.50	39.30	0.95	1.38	13.50	19.81	45.86	192.77
F1	610.07	63.48		2.32	1.99	80.53		31.86	1304.53
F2	610.66	65.49		2.40	1.89	69.09		31.83	1308.12
F3	609.54	65.78		2.41	1.86	68.16		30.62	1381.04
T1	411.46	50.71		1.25	2.54	62.65		24.45	1271.57
T2	430.83	53.33		1.38	2.09	53.96		25.27	1273.96
T3	446.26	54.54		1.46	2.04	54.66		25.05	1335.50

Tests 13, 14 and 15 (Run 3A): Froth Height change

Sample	Mass Flow [g/min]	PGM Grade [g/t]	PGM Recovery [%]	PGM Flow rate [g/h]	Cr_2O_3 Grade [%]	Cr_2O_3 Flow rate [Kg/h]	Cr_2O_3 Recovery [%]	Percentage Solids [%]	Water Flow rate [g/min]
C1	89.90	129.70	29.17	0.700	1.50	8.09	10.69	48.05	97.18
C2	60.20	145.10	21.96	0.524	1.43	5.17	6.81	47.48	66.60
C3	31.37	172.13	14.40	0.324	1.41	2.66	4.03	46.82	35.64
F1	621.68	64.29		2.398	2.03	75.72		27.84	1611.23
F2	622.92	63.85		2.386	2.03	75.87		27.58	1635.31
F3	586.97	63.86		2.249	1.88	66.09		27.05	1583.21
T1	531.78	53.23		1.698	2.12	67.63		24.42	1645.45
T2	562.73	55.16		1.862	2.09	70.71		25.46	1647.79
T3	555.60	57.75		1.925	1.90	63.43		25.93	1587.01

Tests 16, 17 and 18 (Run 3B): Froth Height change

Sample	Mass Flow [g/min]	PGM Grade [g/t]	PGM Recovery %	PGM Flow rate [g/h]	Cr_2O_3 Grade [%]	Cr_2O_3 Flow rate [Kg/h]	Cr_2O_3 Recovery [%]	Percentage Solids [%]	Water Flow rate [g/min]
C1	98.84	127.47	31.88	0.76	1.79	10.62	11.95	43.24	129.76
C2	65.78	131.22	22.19	0.52	1.70	6.71	7.54	42.58	88.71
C3	40.58	161.35	17.30	0.39	1.69	4.11	5.32	41.89	56.28
F1	609.08	64.88		2.37	2.43	88.80		27.64	1594.27
F2	612.36	63.53		2.33	2.42	88.97		27.44	1619.49
F3	586.80	64.51		2.27	2.19	77.20		26.59	1620.14
T1	510.25	52.76		1.62	2.55	78.19		24.62	1561.98
T2	546.58	55.38		1.82	2.51	82.25		25.61	1587.25
T3	546.22	57.31		1.88	2.23	73.09		25.45	1599.88

Tests 19, 20 and 21 (Run 4A): Froth Height change

Sample	Mass Flow [g/min]	PGM Grade [g/t]	PGM Recovery [%]	PGM Flow rate [g/h]	Chrome Grade [%]	Chrome Flow rate [Kg/h]	Chromium Recovery [%]	Percentage Solids [%]	Water Flow rate [g/min]
C1	19.47	1466.17	54.52	1.713	1.79	2.09	2.14	42.92	25.90
C2	15.58	1483.47	40.63	1.387	1.75	1.64	1.76	39.99	23.39
C3	14.85	999.42	33.69	0.890	1.70	1.51	1.94	41.06	21.32
F1	602.13	94.38		3.410	2.69	97.36		26.80	1644.79
F2	594.37	95.72		3.413	2.60	92.72		26.19	1675.22
F3	519.99	79.84		2.491	2.50	78.00		25.16	1546.62
T1	579.61	41.09		1.429	2.73	94.94		26.17	1635.04
T2	578.78	58.35		2.026	2.62	91.08		25.82	1663.11
T3	505.14	57.82		1.753	2.52	76.39		24.69	1540.45

Tests 22, 23 and 24 (Run 4B): Froth Height change

Sample	Mass Flow [g/min]	PGM Grade [g/t]	PGM Recovery [%]	PGM Flow rate [g/h]	Chrome Grade [%]	Chrome Flow rate [Kg/h]	Chromium Recovery [%]	Percentage Solids [%]	Water Flow rate [g/min]
C1	21.04	1344.40	45.25	1.70	1.85	2.34	3.18	37.89	34.49
C2	17.70	1238.84	32.97	1.32	1.80	1.91	2.01	36.92	30.25
C3	12.98	1086.99	23.61	0.85	1.75	1.36	1.76	29.96	30.33
F1	576.81	108.39		3.75	2.12	73.40		25.16	1715.34
F2	576.71	115.36		3.99	2.28	78.73		25.11	1719.96
F3	534.81	111.72		3.59	2.22	71.30		24.99	1605.30
T1	555.77	61.59		2.05	2.13	71.06		24.68	1695.88
T2	559.00	79.78		2.68	2.29	76.83		24.74	1700.81
T3									